Development of a microfluidic immunoassay platform for the rapid quantification of low-picomolar concentrations of protein biomarkers

Marc Herrmann, M.Sc.

Biomedical Engineering Department
McGill University
Montreal, Canada

Submitted June 2008

A thesis submitted to McGill University, Faculty of Graduate and Postdoctoral Studies, in partial fulfilment of the requirements of the degree of doctor of philosophy.

Je dédis cette thèse en premier lieu à mes parents, qui m'ont toujours soutenu indéfectiblement dans mes choix et m'ont donné une éducation privilégiée sans laquelle je n'aurais pu aboutir à un tel accomplissement.

A mes grand parents, Edgar et Mariette, Marcel et Liliane, et à Mameman.

A mon frère Sébastien, qui a toujours été et continue d'être un exemple pour moi au travail comme dans la vie.

A tous un grand merci, avec toute mon affection.

ABSTRACT

The sensitive and specific detection of proteins is at the center of many routine analyses in fundamental research, medical diagnosis, food quality control and environmental safety. The current gold standard for these applications remains the laborious and costly microwell plate ELISA. Over the last decade, new miniaturized devices have emerged: microfluidic systems that can drastically reduce the costs and the time of analysis. Many approaches and designs have been proposed. However, some recurrent difficulties remain that prevent the achievement of a system with the necessary balance between scientific performance, cost-effectiveness and user friendliness. These limitations include the complexity to maintain a constant flow rate in a simple and repeatable fashion, to mix solutions in a laminar flow regime, to control undesired surface effects, and to connect the chip to external pumping instruments.

This thesis describes a novel microfluidic immunoassay platform that addresses the aforementioned issues while also achieving highly sensitive parallel measurements for the rapid quantification of protein biomarkers. The development of this platform followed three consecutive stages: (i) the establishment of an initial design for the simple manipulation of solutions in stop-flow mode, and the elaboration of strategies for mixing and for the simultaneous detection of parallel reactions, (ii) the introduction of the concept of Dual Network system, which removes the need for channel passivation against the non-specific adsorption of proteins, and (iii) the optimization of the critical assay parameters for the quantification of the cytokine TNF-alpha.

The main attributes of the developed platform are also presented: the straightforward fabrication process, the simplified flow control, the enzymatically generated fluorescent signal, and the multi-purpose use of magnetic beads. These microbeads were utilized as functionalized substrate to capture the analyte, but also to induce mixing during incubation phases and to transfer the immune-complexes into the *clean* channels before the immunodetection step. Finally, a standard curve for the quantification of TNF-alpha in serum within the low-picomolar concentration range was obtained in less than 1 hour, confirming the potential of the platform for diagnostic purposes.

RÉSUMÉ

La détection sensible et spécifique de protéines se trouve au cœur d'analyses de routine dans la recherche fondamentale, le diagnostique médical, le contrôle qualité de la nourriture et la sûreté environnementale. Le standard actuel pour ces applications est toujours le coûteux et laborieux test ELISA en micropuits. Au cours de la dernière décennie, de nouveaux dispositifs miniaturisés ont fait leur apparition : des systèmes microfluidiques pouvant réduire de manière drastique les coûts et les temps d'analyse. Plusieurs approches et designs ont été proposés. Cependant, certaines difficultés récurrentes entravent toujours l'avènement d'un système possédant l'équilibre nécessaire entre la performance scientifique, le maintient de coûts bas, et la facilité d'utilisation. Ces limitations incluent la complixité de fixer une vitesse de flot constante de façon simple et reproductible, de mixer des solutions en régime laminaire, de contrôler les effets de surfaces indésireux, et de connecter la puce à des instruments de pompage externes.

Cette thèse décrit une nouvelle plateforme d'immunoessais microfluidiques, qui adresse les problèmes mentionnés tout en réalisant des mesures hautement sensibles et en parallèle pour la quantification de biomarqueurs protéiques. Son développement a suivi trois étapes consécutives : (i) l'établissement d'un design initial pour la manipulation aisée de solutions en mode stop-flow, l'élaboration de stratégies de mixage et de détection simultanée de réactions parallèles, (ii) l'introduction du concept de système Dual Network, qui supprime la nécessité de passiver les canaux contre l'adsorption non-spécifique de protéines, et (iii) l'optimisation des paramètres critiques de l'essai pour la quantification de la cytokine TNF-alpha.

Les attribues principaux de la plateforme sont également présentés : le procédé de fabrication rapide, le contrôle du flot simplifié, le signal fluorescent généré par une enzyme, mais aussi l'utilisation multiple de billes magnétiques comme surfaces fonctionnalisées pour la capture de l'analyte, pour induire un mixage pendant les périodes d'incubation, et pour transférer les complexes immuns dans les canaux *propres* avant l'étape d'immuno-détection. Une courbe standard pour la quantification de TNF-alpha dans le sérum à des concentrations de l'ordre du picomolaire a été obtenue en moins d'une heure, confirmant le potentiel de la plateforme pour des applications diagnostiques.

ACKNOWLEDGEMENTS

Firstly, I would like to gratefully thank my supervisors, Dr. Maryam Tabrizian and Dr. Teodor Veres for providing me with an excellent research environment, cutting edge laboratory equipments and precious advice on managing my project and career. Moreover, they generously gave me the opportunity to travel and share my work at many international conferences.

I would also like to acknowledge several other professors, in particular Dr. Ciriaco Piccirillo (Department of Microbiology and Immunology) for his availability and for being a much appreciated member of my committee; Dr. Henrietta Galiana and Dr. Satya Prakash (Department of Biomedical Engineering) for their useful comments and guidance during my PhD committee meetings.

Francois Normandin, from Industrial Materials Institute, also deserves all my thanks for giving me priceless technical advice and building the bead manipulation device. I would also like to express my appreciation to Nadia Morrone, Pina Sorrini and Lina Vuch for providing expert technical assistance, and that always with a refreshing smile. A well deserved *thank you* also to Dr. Anna Hillberg and Dr. Marcel Roberts for contributing willingly to the sometimes difficult task of editing my prose.

Last but not least, I would like to thank all my former and present co-workers in Dr. Tabrizian's and Dr. Veres' laboratories. In particular, my co-PhD fellow from the very first day, Xuyen Hoa, who has accompanied me and supported me during these last 4 years every step of the way; and Dr. Emmanuel Roy for being my personal fabrication expert (and always a great partner for historical, political and philosophical discussions). To them and all my friends from both labs, whose names would be too long to enumerate here: thank you for creating such a great working environment and a place fun to live in!

Finally, I would like to acknowledge the funding sources that made this work possible: the Canadian Institute for Health Research (CIHR), the National Research Council of Canada (CNRC), the Fonds Québécois de la Recherche de la Nature et des Technologies (FQRNT) through the Centre for Biorecognition and Biosensors (CBB), and NanoQuebec.

TABLE OF CONTENTS

LIST OF FIGURES

LIST OF TABLES

GLOSSARY OF TERMS

β-Gal	Beta-galactosidase
Ab	Antibody
AP	Alkaline phosphatase
BSA	Bovine serum albumin
CE	Capillary electrophoresis
COC	Cyclic olefin copolymer
COT	Channel outgas technique
CV	Coefficient of variation
Cy3/5	Cyanine 3/5
DMEM	Dulbecco's modified Eagle's medium
DNA	Deoxyribonucleic acid
EIA	Enzyme immunoassay
ELISA	Enzyme linked immuno-sorbent assay
EOF	Electro osmotic flow
EWOD	Electro-wetting on dieletric
FBS	Fetal bovine serum
FDP	Fluorescein diphosphate
FITC	Fluorescein isothiocyanate
FRET	Fluorescence resonance energy transfer
HRP	Horseradish peroxidase
IA	Immunoassay
IF	Immunofluorescence
IgG	Immunoglobulin G
LIF	Laser induced fluorescence
LIGA	Lithography (Lithographie), Electroplating (Galvanoformung), and Molding (Abformung)
LOC	Lab-on-a-chip
LOD	Limit of detection
NSA	Non specific adsorption
PBS	Phosphate buffer saline
PC	Polycarbonate
PCR	Polymerase chain reaction
PDMS	Poly(dimethyl)siloxane
PEG	Polyethylenglycol
PEO	Polyethylenoxide
PMMA	Poly(methyl methacrylate)
PS	Polystyrene
QCM	Quartz crystal microbalance
QD	Quantum dot
RIA	Radio immunoassay
SAW	Surface acoustic wave
SPR	Surface plasmon resonance
TBS	Tris buffer saline
TNF	Tumor necrosis factor

CONTRIBUTIONS OF AUTHORS

This thesis is presented as a collection of manuscripts written by the candidate with the collaboration of the co-authors. All the fabrications and the experimentations presented in this thesis have been performed by the candidate. The manuscripts are based on experimental data generated from experiments designed and executed by the candidate, who was also responsible for data collection and analysis. Both supervisors appear as co-authors on manuscripts to reflect their supervisory role during the execution of the work and their involvement in the manuscript preparation. On the second paper, Dr. Emmanuel Roy appears as a co-author to acknowledge his contribution in helping to achieve the design and the fabrication of the Dual Network system's master mold.

OUTLINES

This thesis is divided into ten chapters:

Chapter 1 introduces the motivations behind the development of microfluidic immunoassays. Several advantages inherent to this technology are presented along with the main difficulties associated with the use of microfluidic systems.

Chapter 2 describes the rationale for the project before clearly stating the objectives of this thesis.

Chapter 3 provides the background knowledge related to the two technologies at the center of this work. First, standard immunoassay techniques, their principles, diverse formats, different detection methodologies and evolutionary trends are presented. Second, the latest developments in microfluidics for the manipulation of minute volumes of solution and various strategies for pumping, mixing and directing a flow are examined. The methods of fabrication for such microfluidic chips are also briefly described in this chapter with a particular emphasis on the technique known as rapid prototyping.

Chapter 4 presents an overview of the field of microfluidic immunoassays and discusses the state-of-the-art with respect to several important characteristics of these systems. In the first section, the choice of material, the implemented detection methods and the performance of microfluidic immunoassays as published in the literature are catalogued in tables. Each of these aspects is then analyzed in the following section with more emphasis on the advantages and disadvantages of the different techniques. To conclude this chapter, three significant examples of microfluidic immunoassay platforms are reported.

Chapter 5 describes the three main axes which, combined, confer its originality to the developed microfluidic immunoassay platform. The experimental approach and successive developmental stages are also presented in order to introduce the next three chapters, forming the results and discussion part of this thesis.

Chapter 6 focuses on the initial developmental step, which aims at establishing a design for the simple manipulation of consecutively injected solutions in stop-flow mode, and developing the mixing strategy and the simultaneous detection of parallel reactions

on-chip. These preliminary advancements were published in **Lab-on-a-chip** (Herrmann M. *et al.*, 2006, 6(4):555-560).

Chapter 7 describes the original concept at the center of this thesis work: the Dual Network system. This new method was created to eliminate the high background noise due to non-specific adsorption of proteins without the need for pre-treating the microfluidic channels. The Dual Network system combines an expanded design based on the initial developments, featuring embedded pressure valves and the displacement of magnetic microbeads in order to physically separate the immune-complex building phase and the detection phase. The proof-of-concept was published in **Lab-on-a-chip** (Herrmann M. *et al.*, 2006, 7(11):1546-1552).

Chapter 8 corresponds to the last step of this project aiming at the characterization and optimization of the Dual Network platform. The purpose was to demonstrate the platform's potential for applications in point-of-care diagnosis. As an example, a standard curve for the quantification of the cytokine TNF-alpha, a known biomarker of sepsis, was established in pure serum. These last results are currently *in press* in **Analytical Chemistry**.

Chapter 9, the conclusion, discusses the extent of completion of the preset objectives and the future developments that could be undertaken in order to further improve the platform.

Chapter 10 provides a cumulative list of all references cited in this manuscript.

In the appendices, reprints of all published material are included, with permission. A review on the current state of intellectual property in microfluidic nucleic acid analysis, published in **Recent Patents on Engineering** (Malic L., Herrmann M., Hoa X. *et al.*, 2007, 1:71-88), is also included at the end of this manuscript.

Chapter 1
Introduction

1.1 Motivations behind the development of microfluidic immunoassays

Biological assays are implanted in many aspects of our society and continue to expand with a marked impact on our lifestyle and economy. Applications vary from point-of-care diagnosis, environmental or food safety, security, and for screening purposes in the biotechnology or pharmacology industries. Therefore, the ability to rapidly detect and quantify a specific species within a complex biological or environmental sample is becoming increasingly critical. Because of the growing number of samples to be tested and information to be analyzed, novel constraints in terms of cost- and time-efficiency, portability, throughput, multiplexing, but also simplicity and versatility of use are rising in addition to evermore stringent scientific requirements.

In the last decades, immunoassays in particular have tremendously evolved from complex and time-consuming bench-top experimentations to miniaturized, parallel, integrated and automated systems. By doing so, the large consumption of precious samples and costly reagents can be avoided, while similar operations can be performed in only a fraction of the time by an untrained individual. In the trend toward miniaturization, two main strategies have emerged. At one end, microarrays, already widely used for DNA and protein analysis, soon to be available for cell and tissue examination, have appeared first. These chips are typically composed of a large number of probes immobilized on a surface area a centimetre square or less in size, and capable of screening a relatively small volume of sample for thousands of potential markers or threats. A very high density of information can be obtained in a relatively short amount of time with the use of microarrays. Unfortunately, this technology is limited to industrial and highly specialized laboratory environments as it still requires expensive and large apparatus for reading and sorting useful data. At the other end, miniaturized systems, often called lab-on-a-chip (LOC), have been devised. They are mainly intended for point-of-care diagnosis, on-field analysis or for the realization of a series of laboratory

protocols. These systems are generally targeted on a particular function, and prioritize integration, portability, low costs and user friendliness over the density of data obtained. Although the end goal and practical requirements of both strategies can slightly vary, they are often complementary and have been brought together in a variety of different cases.

Common to both microarrays and LOC is the need for manipulating minute volumes of solution and the integration of several functionalities such as separating, mixing and diluting the flow in a confined space. All these operations are typically performed in micro-sized channels fabricated in glass or plastic substrates known as microfluidic systems. Due to their exceptional potential for biomedical applications and newly adapted fabrication techniques, microfluidic systems have recently exploded in scientific publications and issued patents, giving rise to a large number of dynamic and successful companies (Figure 1.1).[1] The possibilities and opportunities offered by this technology are truly remarkable. Also, its ease of use and low fabrication costs can foster the implantation of such high-tech medical devices in settings with limited resources as well as in developing countries.[2]

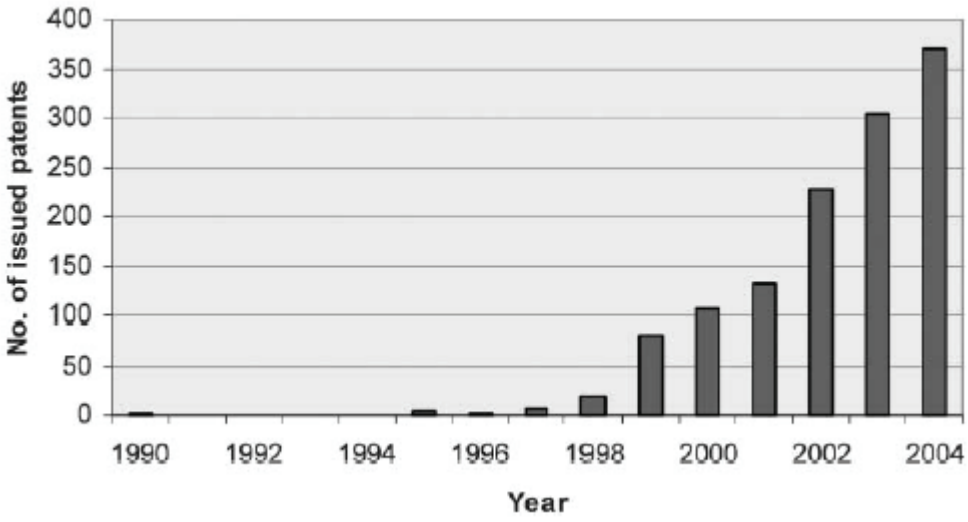

Figure 1.1: Number of microfluidic patents issued per year in the United-States for biochemical, environmental and diagnostic applications [*Lab Chip*, 2006, **6**, 1118-1121] – *Reproduced by permission of The Royal Society of Chemistry* – http://dx.doi.org/10.1039/b610250f

1.2 Microfluidic immunoassay: between dream and reality

The ideal platform for immunoassays should present a variety of characteristics that can be grouped in three main categories: (i) the *fabrication procedures*, such as the simplicity, rapidity and associated costs for production, and integration possibilities; (ii) the *user friendliness*, including the ease of operating the platform and the assay time, as well as multiplexing, high throughput and automation possibilities; and (iii) the *performance*, comprising the sensitivity, dynamic range, reproducibility and specificity of an immunoassay.

Microfluidic devices deliver a significant number of advantages as compared to traditional bench-top assays. The small size of channels reduces considerably the volumes of solution used, and decreases the reaction times due to the shorter diffusion distances. Likewise, the density of channels that can be produced on a smaller area enables researchers to attain medium to high throughput with no additional costs in fabrication. The precise manipulation of solutions inside the microscopic channels also allows for a better control of the experimental conditions, which often contributes to increase the reproducibility between assays.

Still, the reality in the field of microfluidic immunoassays is different. Some recurrent limitations remain, such as the difficulty to maintain a constant flow rate during and between assays, to mix solutions in a laminar flow regime, to control undesired surface effects (hydrophobicity and non-specific adsorption), as well as to connect the chip to external pumping instruments. More importantly, the main difficulty remains the integration of all elementary components into a fully functional platform.

In definitive, there is no ideal platform for immunoassays. The three aspects listed above are often contradictory and some level of trade-off is almost always necessary. Consequently, each system must be defined by the balance achieved between user friendliness, cost-effectiveness, and the scientific performance required for a specific application.

Chapter 2
Rationale and Objectives

2.1 Rationale

Sepsis is responsible for over 120 000 deaths each year in the United States.[3] The main reason of such a high number of cases, even in the world's best intensive care units, is the late diagnosis of the potentially lethal infection. Bacterial cultures can take days and physical symptoms only appear at an advanced state of the infection. Therefore, biochemical tools that can quickly diagnose sepsis and allow the doctors to give an appropriate and timely treatment are still an urgent need. Thanks to small sample volumes and short analyses times, microfluidic immunoassays are very good candidates for this type of application.

However, the timely diagnosis of sepsis is not an easy task to achieve. Ideally, several biomarkers, mainly small circulating proteins called cytokines, should be monitored at regular intervals of the order of an hour. Also, the concentration thresholds for these protein biomarkers are situated within the low-picomolar range and precise quantification is often an absolute necessity. These demands are very challenging in terms of scientific performance, and push the limits of even the current gold-standard of immunoassays, the ELISA test. Because of the stringent time and performance requirements, the large majority of microfluidic immunoassays described to date have failed to provide a platform adapted for such a challenging application. In this thesis, we propose a novel platform for microfluidic immunoassays, based on original concepts and designs, and demonstrate its potential for the diagnosis of sepsis.

2.2 Objectives

The overall objective of this project is to develop a functional platform based on microfluidic technology adapted for fast and reliable point-of-care diagnosis based on the quantification of protein biomarkers.

The detailed objectives are:

1- Conceive a versatile platform for immunoassays with the following characteristics:

   a. Design a microfluidic chip that is simple and economical to fabricate.

   b. Maintain the versatility and ease of use, and the potential for automation and integration.

   c. Achieve low density parallelization adapted for point-of-care diagnosis while maintaining the possibility of further increasing the throughput.

   d. Equal or surpass the performance of standard bench-top immunoassays while decreasing the time and cost of analysis.

2- Demonstrate the potential of the developed platform to perform a rapid and sensitive test for a relevant biomedical application such as the quantification of the cytokine TNF-alpha in the context of sepsis diagnosis.

Chapter 3
Background Knowledge

3.1 Principle of immunoassays

By definition, immunoassays rely primarily on the binding properties of an antibody to its specific target, the antigen, in order to selectively extract it from a complex biological or environmental sample for analysis. *In vivo*, antibodies are the keystone proteins of the immune system, acting as the link between the recognition event and the effective phase of the immune response. For *in vitro* assays, their natural bipolarity is utilized to bind a molecule of interest, called the analyte, while attached to a solid substrate or coupled to a molecule providing a detectable signal. The structure of the subclass of antibodies most frequently used in immunoassays, the immunoglobulin of the G isotype (IgG), is divided into two main units: (i) the $F(ab')_2$ fragment, composed of two identical F(ab'), each terminated by a variable domain specific to a unique antigen and (ii) the Fc fragment, common to all antibodies produced in a same animal species. Each fragment is composed of two heavy and two light amino-acid chains, brought together by several disulfide linkages, hence forming the typical tertiary structure of IgG often represented as a "Y" shape.[4] Depending on the extent of the selection process, one can distinguish polyclonal antibodies composed of an entire population of many different antibodies, or clones, purified from an animal serum and directed against a unique antigen. Also determined are monoclonal antibodies, which corresponds to only one specific clone purified from a polyclonal population. Polyclonal antibodies recognize the same analyte but bind to different sites with various specificities, whereas monoclonal antibodies are extremely uniform and selected for their well-characterized binding properties.

The performance of an immunoassay is assessed on several parameters, namely the sensitivity, the specificity, the range of detection and the reproducibility. The sensitivity refers to the *efficiency* with which the signal can be discriminated from the background noise. More precisely, the sensitivity is calculated by running solutions of decreasing amounts of an analyte, plotting a standard curve of the signal with respect to the analyte concentration. The sensitivity then corresponds to the concentration value at three times

the standard deviation obtained from at least five repetitions of the negative control. The specificity represents the *accuracy* with which the signal can be discriminated from the background noise generated by non-specific adsorption or from false-positive signal created by the non-selective binding of a similar molecule on the antibody. The specificity can vary with many experimental factors, such as the type of buffer solution, the presence or absence of detergent, and the washing procedure. It also largely depends on the intrinsic specificity of the antibody-antigen couple. Both the sensitivity and specificity are usually improved by the use of monoclonal antibodies. The range of detection delimits a minimum and a maximum concentration between which the amount of the analyte can be correlated to variation in the measured signal. Frequently, only the linear portion is kept for quantification of the analyte. The intra- and the inter-assay reproducibility are expressed by their respective coefficients of variation (CV) as defined by the ratio of the standard deviation to the mean signal intensity at a given concentration of the analyte.

3.1.1 Different formats of immunoassays

Over the last 50 years, immunoassays have spread into many fields of research and industries. They have been customized in a variety of formats adapted to particular applications and experimental procedures. A first important distinction originates in the necessity to isolate the specific signal from the noise after the binding event has occurred. In some formats, referred to as homogeneous immunoassays, the method of detection does not require the separation of the immune-complex (the analyte bound to a detection molecule), from unbound detection molecules. This is the case for techniques such as fluorescence polarization[5], fluorescence resonance energy transfer (FRET)[6], capillary electrophoresis immunoassay[7], and agglutination assay[8]. In other formats, described as heterogeneous immunoassays, the method of detection imposes the initial separation of the immune-complex from the unbound probes. The immune-complex is bound to a solid support, permitting the retention of the molecules of interest while the unbound entities are washed out of the system. The solid support can take the form of a polymeric surface, a membrane, a chromatographic resin or micro-sized beads. Heterogeneous assays, although longer and more complex to perform, are more versatile, more sensitive and

more specific. The use of a solid support however creates recurrent issues, in particular the necessity to bind the capture entity to the surface without loss of activity[9,10] and to block (or passivate) the uncovered parts of the support against non-specific adsorption.

In the heterogeneous format, competitive and non-competitive assays are available (Figure 3.1). In a competitive assay, the analyte in the test sample is measured by its ability to compete and remove a labelled antigen externally provided to the system. The detected signal is *inversely* proportional to the concentration of the analyte. Conversely, in a non-competitive assay, no external antigen is provided to the system. The analyte is bound on a free capture site and its concentration in the test sample is *directly* proportional to the intensity of the signal measured. Because the non-competitive format measures directly the quantity of bound analyte rather than estimating a difference between two large quantities, which potentially introduces large errors, this type of assay offers higher accuracy.[11] The detection of small amounts of analyte in this case is however limited by the sensitivity of the detection device or the signalling label itself.

Additionally, one-site and two-site assays can be performed. In a one-site immunoassay, only one specific antibody is necessary to capture the analyte. If the detection method requires it, all proteins in the sample can be non-specifically labelled prior to the start of the experiment. In a two-site or sandwich immunoassay, a pair of non-overlapping antibodies (binding to two different sites of the analyte) is used. Typically, the first one is called the capture antibody; the second one is the detection antibody. The detection antibody can generate the signal directly, or it can be further recognized by a "generic" secondary labelled entity. This method permits to improve the sensitivity by increasing the number of labels corresponding to the capture of a single analyte. The use of a pair of antibodies, while more costly and not always available especially for small analyte molecules, also enhances the overall specificity of the assay. In this project, we have developed a heterogeneous non-competitive sandwich immunoassay, thus the following parts of this thesis will put more emphasis on this type of assay format.

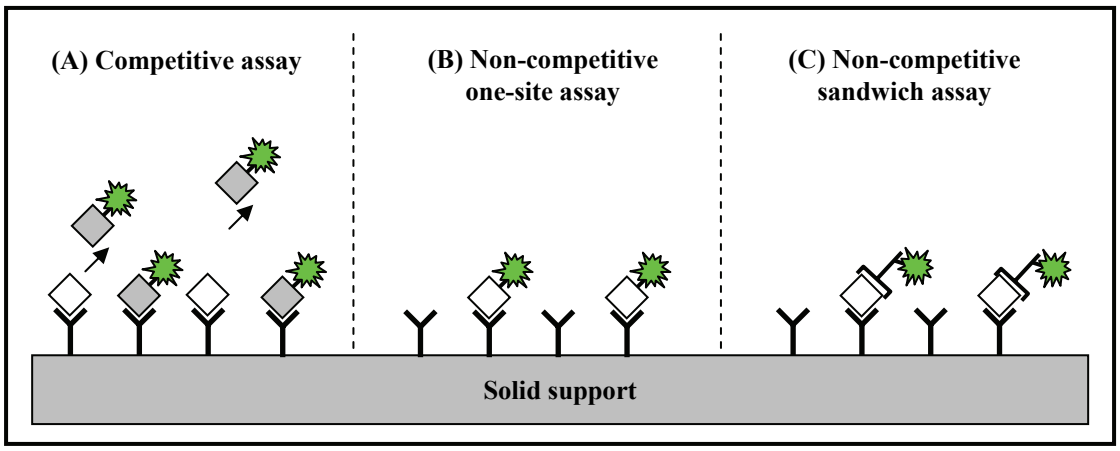

Figure 3.1: Formats of heterogeneous immunoassays. The different molecules are pictured as follow: the black **Y**- and **T**-shapes represent the antibodies; the white square the analyte; the grey square the externally provided antigen and the star-shape the detection label.

3.1.2 Different detection methodologies for immunoassays

In the early days of immunoassays, radioactive-labelled proteins were often used in a simple one-site competitive approach (RIA) (Figure 3.2).[12] For safety reasons, the labels of choice have shifted towards organic fluorescent molecules such as fluorescein (FITC), rhodamine or cyanine dyes (Cy3 and Cy5). These molecules offer high fluorescence intensities and narrow peaks at both the excitation and emission wavelengths. This translates into highly sensitive immuno-fluorescent assays (IF) with interesting multiplexing possibilities. More recently, organic fluorescent dyes tend to be replaced by nano-sized inorganic particles, called Quantum Dots (QD), which display even greater fluorescent intensity and better stability when exposed to light (no photo-bleaching).[13] QD are also characterized by a wide excitation wavelength and a narrow size-dependent emission wavelength. They have a great potential as labels for *in-vitro* immunoassays, even if toxicity issues have yet to be solved for *in-vivo* applications. In the recent years, direct measurement techniques such as surface plasmon resonance (SPR) or quartz crystal microbalance (QCM) have gained increasing interest. These methods do not require the use of external labels, therefore they exhibit simpler methodologies and shorter times of analysis.[14] However these techniques have not yet reached equivalent

sensitivities as compared to fluorescent sandwich immunoassays and are less specific due to the use of only one antibody. The detection of low molecular weight analytes is made particularly difficult with these techniques as they are based on the sensing of a mass change.

Simultaneous to the progress of fluorescent labels, enzymatic immunoassays (EIA) have been developed that often enhance the sensitivity of an assay by several orders of magnitude. Enzymes such as the horseradish peroxydase (HRP), the alkaline phosphatase (AP) or to a lesser extend, the β-galactosidase (β-GAL) and glucose oxydase (GO), are the most popular alternatives for this type of assays. The choice of the enzyme usually depends on the conditions under which the assay is performed, taking into account possible issues such as low stability at elevated temperatures or potential chemical inhibitions.[15] Many different enzymatic substrates exist for colorimetric, fluorescent, electrochemical and bioluminescent detection.

Among all possible formats, the Enzyme-Linked Immuno-Sorbent Assay (ELISA) remains the most sensitive and most versatile form of immunoassays. Typically, the ELISA is performed in a microwell plate, running in parallel up to 96 independent reactions or more with an automated system. The main advantage of this methodology rests in the enzymatic amplification of the signal, which provides an exceptionally high sensitivity. The detection antibody can be directly coupled with an enzyme or can be recognized by a secondary antibody (or coupled to a biotin-streptavidin system) carrying the enzyme. After the immune-complex has been formed, an enzymatic substrate is added to the wells, starting the reaction and steadily accumulating the colorimetric or fluorescent product. When the signal reaches the appropriate level, the reaction is stopped by the addition of a stopping buffer and the plate is read in a spectrophotometer or fluorometer. For decades, ELISA has been the most commonly used technique in research and medical laboratories, as well as in the biotechnology and pharmacology industries. Despite many benefits, this method is limited by the consumption of large volumes of costly reagents and precious samples, and by the requirement for several hour-long incubation times.

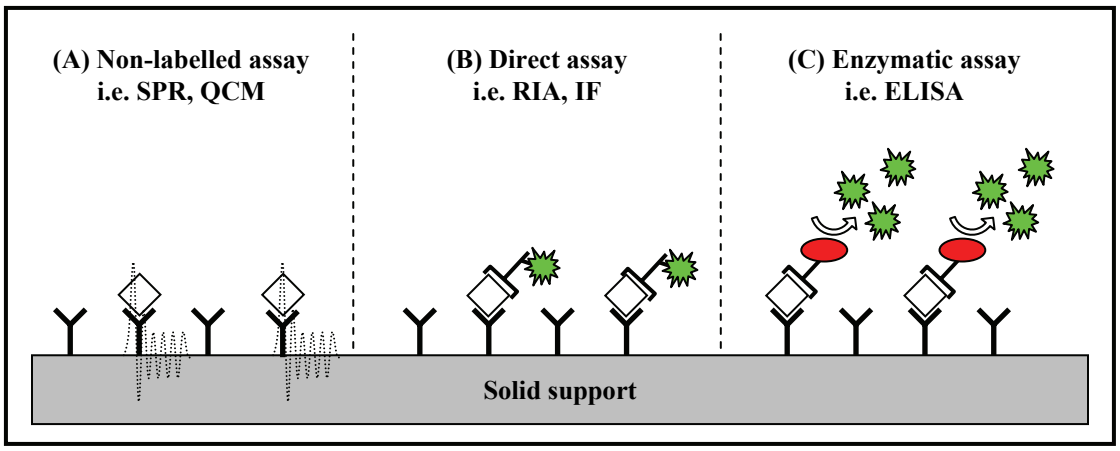

Figure 3.2: Methodologies for heterogeneous immunoassays. The different molecules are pictured as previously. The doted sinusoidal line represents the signal used in non-labelled detection methods; the oval represents an enzyme.

3.1.3 Current trends in immunoassays

A major difficulty in protein assays arises from the absence of a technique, equivalent to the polymerase chain reaction (PCR) for DNA, which could amplify specifically a target analyte within a complex mixture of proteins. Instead, enhancement strategies for the detection of protein have to rely on the amplification of the signal rather than on the multiplication of the target, as it is the case in the ELISA. In this regard, a number of new labelling techniques have recently initiated the emergence of "ultra-sensitive" immunoassays.[16] Some of these techniques utilize natural molecules, for instance fluorescent-loaded liposomes, DNA probes coupled to the detection antibody in a variety of derived protocols (immuno-PCR, proximity ligation assay or rolling circle amplification) or DNA probes for direct recognition (aptamers). Some other techniques take advantages of the recent advances in micro- and nano-technologies to implement bio-barcode assay, electrochemical assay with carbon nanotubes or Surface-Enhanced Raman Scattering of gold nano-particles. Some of these new techniques have been shown to provide a several fold increase in sensitivity compared to the corresponding ELISA.

Moreover, the last decade has witnessed the exponential development of miniaturized assays, driven by the ever growing need for higher throughput and multiplexing. Derived from DNA technologies, protein microarrays can resolve several thousands of capture

probes on a very restricted area, to the point of testing a sample for the entire human proteome on a single chip. In the so-called planar microarray format, direct fluorescence is the most commonly used method of detection, although enzymatic amplification and label-free techniques have been implemented with success as well.[17] Despite being an attractive tool for protein analysis, some issues remain in the preparation and the operation of protein microchips, such as (i) the difficulty of patterning uniform spots of a capture entity without loss of activity, (ii) the presence of a high number of proteins and antibodies in a same solution, increasing the occurrence of cross-talk and the appearance of false-positive signals, (iii) the high costs involved in the production of the antibody-loaded chips, and (iv) the need for expensive scanners and software to handle the overwhelming process of data acquisition and analysis.

To address some of these challenges, another type of protein microarray has been developed based on the use of functionalized microbeads. The bead-based microarray format offers several advantages over a planar chip, trading some of the multiplexing capabilities for a less complex procedure and lower associated costs. The number of analytes simultaneously measured is usually no more than a few tens. The use of microbeads however facilitates the attachment of the antibodies on chemically active surfaces and increases the total capture area in the entire sample volume.[18-20] Yet, discriminating between the various analytes requires the encoding of the differentially functionalized beads. Typically achieved through fluorescence labelling, the current encoding strategies limit the multiplexing capabilities of the bead-based format, as the label must not interfere with the quantitative signal in flow cytometry.

Lastly, the recent transfer of microfabrication procedures from the semi-conductor industry into biology laboratories has revolutionized the field of immunoassays. Due to this technological transfer, the development of microfluidic immunoassays has expanded tremendously within the last few years. The vast potential of these systems to provide biosensors and tools adapted for rapid and economical diagnostic applications is of particular interest. Microfluidic immunoassays being the main focus of this thesis, they will be discussed in more detail in the next chapter.

3.2 Principle of microfluidics

The term *microfluidics* refers to the manipulation of liquids or gas at the micrometer scale. Inside microchannels, some forces become dominant that can be otherwise neglected in macrosize settings. The properties of microfluidic flow, fabrication techniques, and methods to generate and control the flow are explained in this section.

3.2.1 Properties of microfluidic flow

In general fluidics, the flow regime is characterized by the Reynolds number (Re), a non-dimensional number that evaluates the relative influence of inertial forces to viscous forces. The Reynolds number is defined by:

$$\mathrm{Re} = \frac{\rho \upsilon D_h}{\mu} \qquad (1)$$

where ρ [kg/m^3] is the fluid density, υ [m/s] is the characteristic velocity of the fluid, μ [Ns/m^2] is the fluid viscosity and D_h [m] is the hydraulic diameter.

Because Re is directly dependent on the diameter (or section) of the fluidic path, low Re values are experienced in microfluidic channels, well below the transition from laminar to turbulent regime for internal flows at Re = 2300.[21] As a result, the flow in microfluidic devices is almost always laminar. As opposed to the chaotic turbulent flow, laminar flow follows a predictable velocity pattern. One major consequence in microfluidic channels is that two streams following each other, or running next to each other, will not mix except through a slow process of diffusion.

When considering a channel of a virtual radius r_v, its surface area decreases with $1/r_v^2$ while its volume drops with $1/r_v^3$. As a result, the surface-to-volume ratio is rapidly increased at microscopic values of r_v, thus strongly amplifying surface effects.

Among these effects, the fluidic resistance plays an important role in microfluidics. When a constant pressure difference ΔP is applied, the average flow rate Q can be defined as $Q = \Delta P / R_h$, where R_h is the hydraulic resistance. This resistance mainly depends on the geometry of the channel and the viscosity of the solution. By solving the Navier-Stokes equation for a channel with a rectangular cross-section (as it is often the

case in microfluidic devices), R_h can be described as (2). As a result, elongating the channel, or decreasing its width or height, significantly increases the fluidic resistance in microfluidic channels.

$$R_h = \frac{12\mu L}{wh^3\left(1 - 0.63\frac{h}{w}\right)} \tag{2}$$

where L [m] is the channel length, w [m] is its width and h [m] its height.

Surface tension is another force that becomes significant in microfluidics. This effect mostly depends on the nature of the solution and the material used for the fabrication of the microfluidic chip, and their mutual affinity. This affinity can be modified for instance by adding a surfactant in the solution or by treating the surface by chemical or physical means, impacting the resulting contact angle and in turn, the surface tension. In some cases, the high surface tension and the small size of microfluidic channels are sufficient for capillary effects to create a flow through the total length of the channel.

Both the laminar flow regime and the high surface-to-volume ratio provide remarkable possibilities for the design of microfluidic devices and integrated functionalities. However, these two aspects of the flow in microchannels can be either advantageous or detrimental depending on the targeted application. Some of the related issues will be discussed in more details later in this section.

3.2.2 Fabrication of microfluidic devices

In the early days of microfluidics, fabrication techniques were essentially inspired from the microelectronic industry. Processes such as micromachining, photolithography followed by wet or dry etching, electroforming (LIGA) or electron beam lithography have been utilized for the production of microchannels in silicon or glass.[22] These so-called *hard* techniques however require the use of costly equipment and dedicated cleanroom facilities. Furthermore, microfluidic devices for biomedical applications are almost always disposable chips in order to avoid sample contamination. For this reason,

these chips must be easily fabricated in large numbers and at low cost to be relevant for large-scale realistic applications.

In recent years, *soft* fabrication techniques more adapted for this kind of applications have emerged. They allow for the rapid production of a large number of microfluidic devices at lower costs and with methods that can be exported out of the specialized cleanrooms. This new generation of microfluidic devices are predominantly fabricated in polymeric materials of different types. Hard thermoplastics, such as polymethylmethacrylate (PMMA), polycarbonate (PC), polystyrene (PS) or cyclic olefin copolymers (COC) can be thermoformed against a master mold by micro-embossing or injection molding. Because of the thermal and pressure constraints that are applied on the mold, the latter must be manufactured in a strong material using classical hard-lithography techniques. Another *soft* technique, developed in the late 90s by G.M. Whitesides and collaborators has marked the beginning of a new era in the field of biomedical microfluidics. This method, called replica molding, enables the rapid prototyping of microfluidic devices by producing high fidelity replicates in elastomeric polydimethylsiloxane (PDMS) on standard Su-8 molds (Figure 3.3).[23] Because of the simple fabrication method and some advantageous properties of PDMS, replica molding has become since the most favoured technique for the prototyping and testing of biomedical microdevices.[24,25]

PDMS is optically transparent and displays very low background fluorescence in the green and red light spectra. It is also chemically resistant to strong acids and bases, stable at high temperatures, permeable to gas and biocompatible. Due to its elastomeric nature, PDMS conforms to relatively flat surfaces, hence achieving a water-tight bonding with another sheet of PDMS, glass or silicon. The bonding is reversible but can be made permanent by treating beforehand both surfaces with oxygen plasma. The connection of external pumping devices to the microfluidic channels is also facilitated by the soft elastomeric nature of PDMS. PDMS is an extremely hydrophobic material with a tendency to adsorb rapidly any sort of biological substance. Various treatments are available, which modify the surface properties of PDMS to make it hydrophilic, chemically functional, or resistant to non-specific adsorption. These surface treatments

and their limitations are of particular importance for microfluidic immunoassays, therefore they will be discussed with greater details in the next chapter.

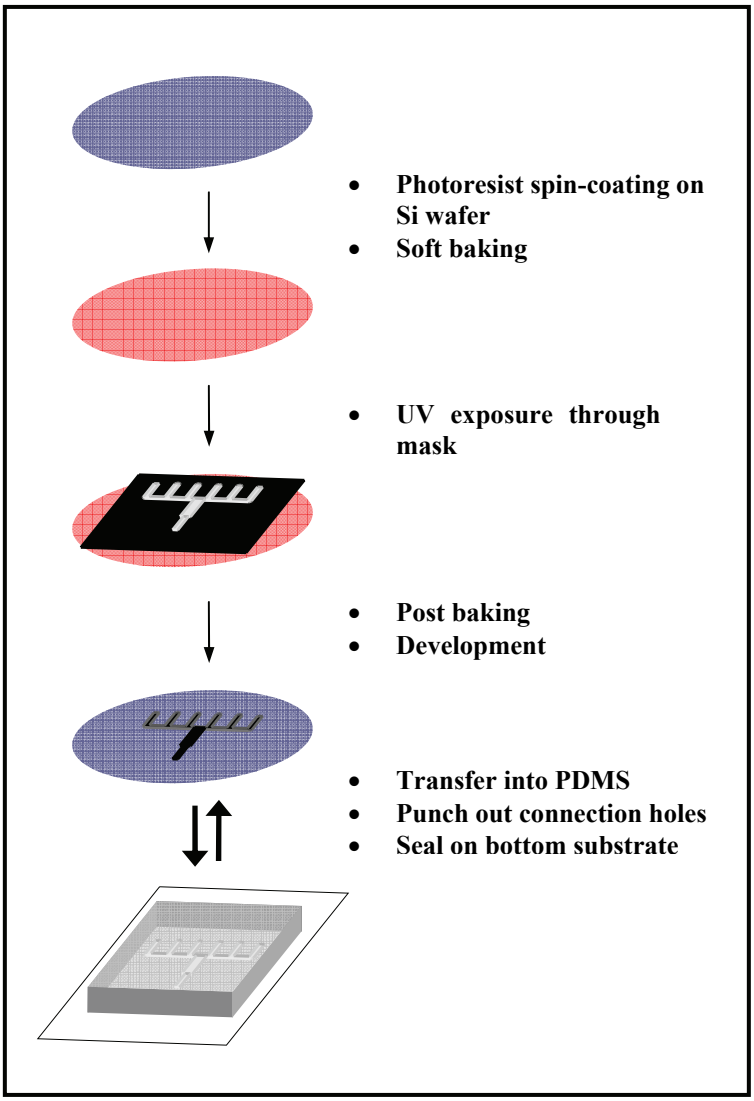

Figure 3.3: Rapid prototyping by replica molding of microfluidic channels in polydimethylsiloxane (PDMS).

3.2.3 Generation of a microfluidic flow

The most straightforward method to generate a flow inside a microfluidic channel is to rely on capillarity.[26] Due to the small section of a typical microfluidic channel, and its high surface-to-volume ratio, a solution with a high enough affinity for the substrate material can travel long distances driven by capillarity only. No bulky devices or external power sources are required. This method however depends largely on the contact angle formed between a solution and the substrate material, which can be only tuned to some extent. Also, relying on capillarity does not permit the real-time control of the flow rate inside microchannels. For these reasons, other methods have been developed, which provide more flexibility in the control of the flow.

Pressure driven flow, for instance, uses a mechanical pump to generate a pressure difference at one end of a channel.[27] The resulting movement of solution behaves as a Hagen-Poiseuille flow, displaying a parabolic shaped solution front with its greatest velocity at the center of the channel (Figure 3.4A). The flow can be generated either by applying a positive pressure at the entrance port, the inlet, in which case the pump is worked in *infusion* mode, or by applying a negative pressure at the exit port, the outlet, in *withdrawal* mode. Such pumps are precisely calibrated and can be used on a wide range of flow rates. However, working at a slow flow rate can become problematic because of the large fluidic resistance inside microchannels. Likewise, it is often necessary to proceed to the initial filling of the microchannel, also called priming, using a more affine solution in order to facilitate the subsequent flow and avoid the formation of air bubbles. Finally, tight connections have to be secured in order to avoid any pressure loss or leakage. This can often be cumbersome and challenging to achieve. Despite the inconvenience, this technique is relatively simple to setup and exhibits low dependency to the nature of the substrate and the solution. As a result, it is the most frequent approach used to this day in microfluidic immunoassay systems.

Another common approach to generate a flow in microfluidic channels is electro-osmotic flow (EOF).[28-30] This technique relies on moving ions at the surface of the channel (Figure 3.4B). It requires that the inner surface of the channel be charged, either naturally or through a specific treatment, so that the counter-ions present in the solution migrate to the surface and form an electric double layer. When an electric field is applied

in the plan of the channel through electrodes placed in the inlets and outlets, the ions condensed at the surface move toward the complementary electrode, dragging along the solution. Unlike pressure driven flow, the solution front in EOF is flat with equal velocities at any positions of the channel cross-section. This phenomenon has been used for instance to create plugs of solution in capillary electrophoresis as it generates a non-deformed smooth fluidic movement at very slow flow rates. However, the limitation in the choice of the substrate material and the necessary high voltage render this technique non-economical and non-safe. It also creates overheating that can be detrimental to biological species present in solution and induces bubble formation.

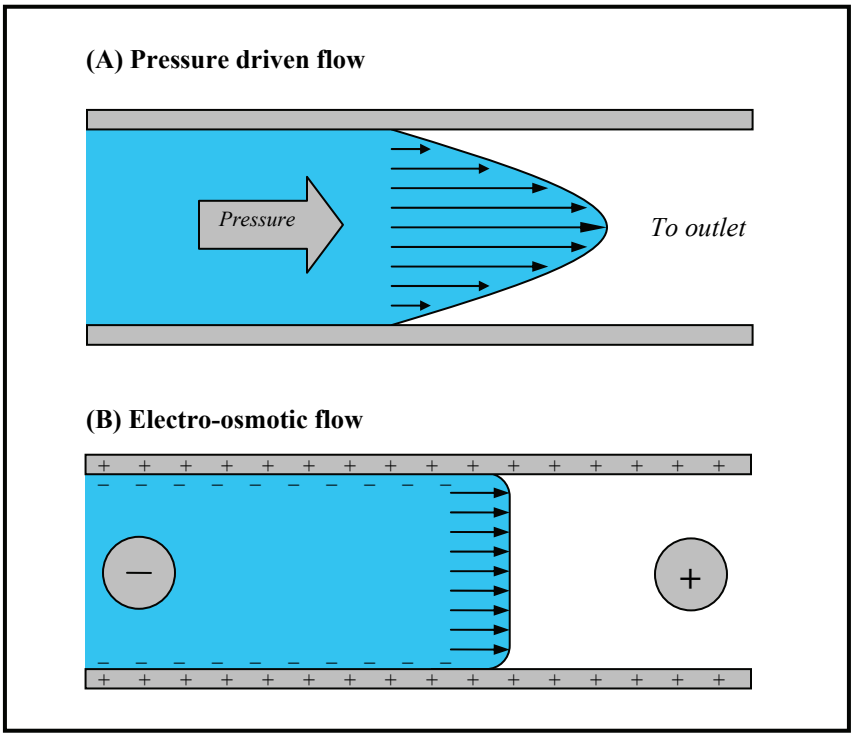

Figure 3.4: Two main approaches for the generation of a flow in a microfluidic channel.

Controlled evaporation, absorption-induced flow and gravity flow are examples of alternative methods that have been used to generate flow in conventional microfluidic devices.[31] Some less conventional microfluidic designs take advantage of their inherent possibilities to generate a flow. CD-based microfluidics for instance uses centrifugal force,[29,32,33] whereas digital microfluidics manipulates droplets of solution using electro-wetting on dielectric (EWOD) or surface acoustic waves (SAW).

3.2.4 Mixing in microfluidics

One of the main characteristic of a microfluidic flow is its laminar behaviour. This singular property has been employed advantageously in a variety of applications, for instance in the separation of particles with the H-filter system or in the analysis of interactions at the interface between two adjacent solutions.[34] Despite its potential usefulness, a constant laminar flow also creates unusual difficulties when it comes to induce rapid chemical or biological reactions. In this regime, the transfer of mass is governed strictly by diffusion without the presence of chaotic mixing. Although lateral distances are short in microfluidic channels, a long flow path is needed before significant interactions can occur though diffusion only.

A first strategy to induce mixing inside microfluidic channels relies on designing *passive mixers* based exclusively on variations in the channel geometry (Figure 3.5A).[35] The simplest design consists in elongating the channel in a serpentine shape to increase the contact time between the two adjacent solutions. Other forms of passive mixers have been described, some in 2D, for instance by forcing the flow into secondary side channels,[36] some in 3D, by adding grooves[37,38] or 3D-serpentine channels.[39] The main advantage of passive mixers is that they are integrated into the fluidic design, and that no additional manipulations are necessary to actuate the mixing over the total volume of the flowed solutions. The drawback is that they are static and thus require the solutions to be moving across the length of channel to be effective.

For mixing stationary solutions, *active mixers* featuring moving elements placed inside the channel have been developed (Figure 3.5B). Several approaches have been designed using magnetic micro-particles, such as plugs of beads being moved in the axis of the flow by alternative electromagnets flanking the channel,[40] lateral chains of

particles rotating around their base,[41] and magnetic particles in CD-shake mode.[32,42] In a more sophisticated approach, a micro-magnetic stir-bar has been fabricated as a part of a microfluidic channel and used both for propulsion and mixing of adjacent solutions.[43]

Several alternative strategies have also been described, such as overlapping an electro-osmotic flow in the direction opposite to the main pressure-driven flow,[44,45] or inserting gas bubbles, which can afterwards be vented downstream of the mixing area.[46,47]

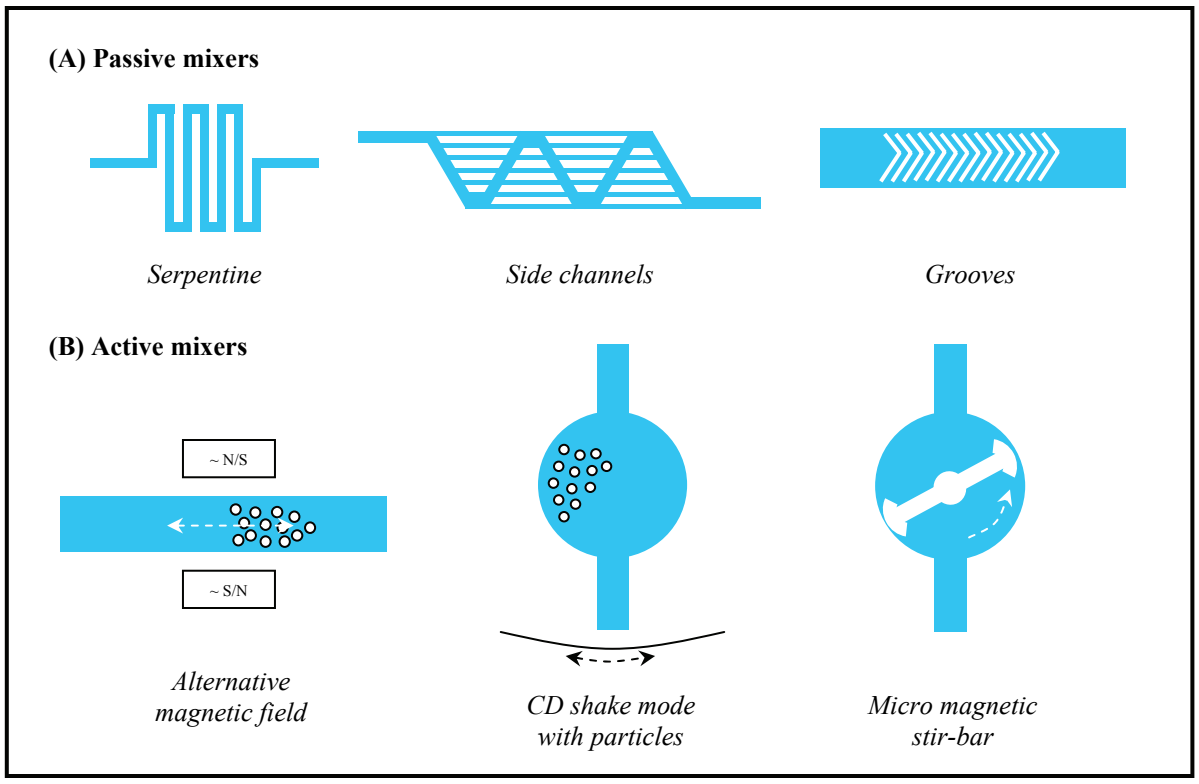

Figure 3.5: Examples of various strategies for mixing in microfluidic channels.

3.2.5 Valving in microfluidics

Pumping and mixing are the elementary functionalities required to perform the most basic reactions in a microfluidic device. In more complex experimental designs, it can be critical that one or many solutions be addressed and controlled individually in a precise

manner through the engineering of valves. The ability to interrupt or direct the flow at strategic positions and times allows for the integration of functions such as injecting sequential solutions, switching the flow direction, isolating a particular section of a microfluidic network and opening or closing fluidic loops.

Some valves are non-reversible and fabricated for single use only (Figure 3.6A). This is the case of Laplace valves based on the modulation of the capillary action. For instance, the abrupt expansion of a channel width and/or height can stop the capillary advancement of a solution. Applying an external pressure forces the liquid through the stoppage zone and subsequently resumes the flow.[48,49] A local change in the surface wettability of the substrate material can produce a similar effect. Such a modification can be included in the fabrication process by chemically patterning hydrophobic zones on the substrate material, thus stopping the capillary flow without modifying the channel geometry.[50] Although Laplace valves can be readily incorporated in a fluidic design, their functionality depends strongly on the geometry of the channel, the surface properties and the nature of the flowed solution. Another category of non-reversible valves utilize a plug of a disposable heterogeneous material such as paraffin[51] or ferrowax,[52] obstructing the channel, that can be subsequently melted to liberate the flow path.

For more complex fluidic manipulations, it is often necessary for a valve to be reversibly actuated. Electrowetting-based valves, a variation of the chemically-modified Laplace valves, uses microfabricated electrodes in order to transiently increase the surface wettability at the surface of a fluidic channel.[53] Similar to the use of paraffin, hydrogels with adapted shrinking and expanding properties have also been incorporated inside microfluidic channels (Figure 3.6B).[54,55] A final kind of actuated valves employs vertical pressure to mechanically compress and close an underlying channel. The necessary pressure can be delivered by external apparatus such as actuated fingers[56] or pneumatic valves,[57] or manually through a system of screws as in the recently described TWIST valves.[58]

Among the variety of actuated valves, another kind, the PDMS pressure valves developed by the team of S.R. Quake in Stanford University have been the most popular alternative implemented in recently reported microfluidic systems. Its success originates from the simple fabrication process using exclusively PDMS, and allowing the parallel

integration of a large number of these valves in a single procedure.[59,60] PDMS pressure valves have been implemented for various applications (only one example of immunoassay), as well as used in series to create microfabricated mixers and pumps.[61-67]

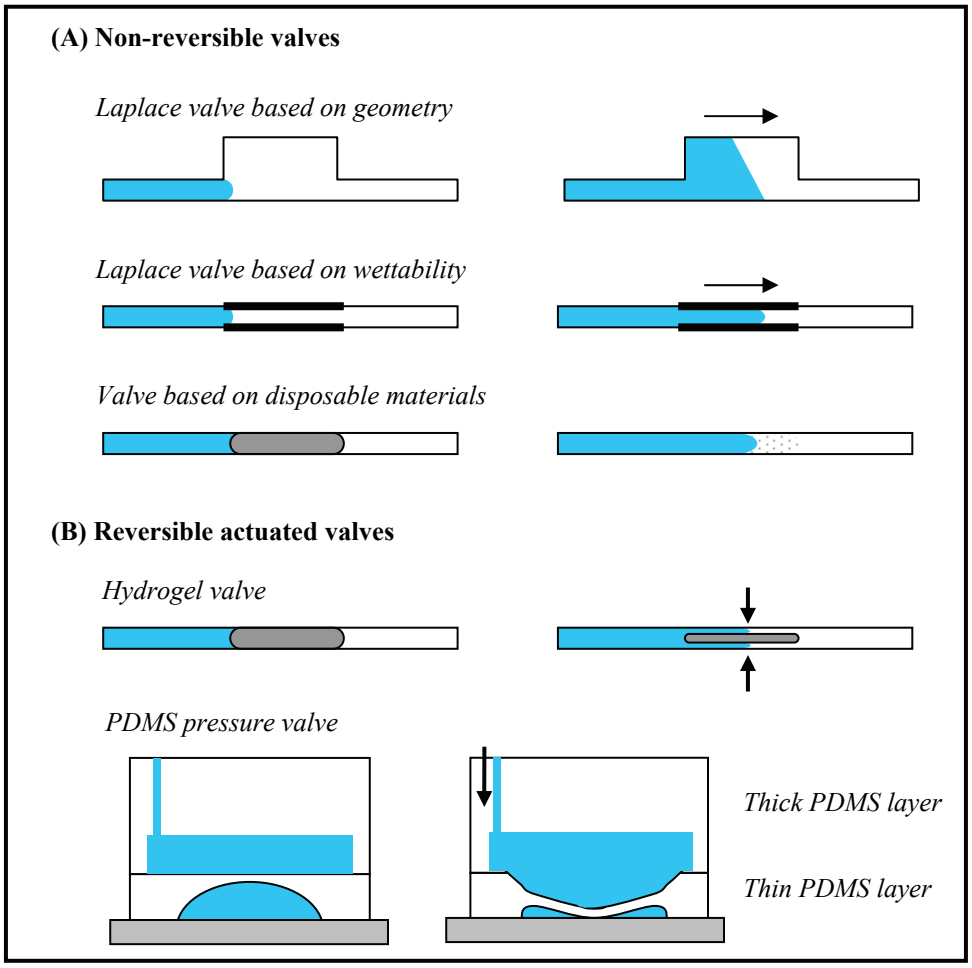

Figure 3.6: Examples of valves in microfluidic devices.

Chapter 4
Microfluidic Immunoassays: State-of-the-art

Over the past 10 years, an exponentially increasing number of microfluidic immunoassays have been described in the literature. While all systems are converging toward the fast, inexpensive, and sensitive detection of protein biomarkers, the most striking observation when first reviewing the field is the large variety of implemented formats, designs and methodologies.[68-70]

Similar to bench-top immunoassays, two main formats can be identified. First are the homogeneous immunoassays, essentially composed of variations of the T-sensor and the capillary electrophoresis (CE) designs (Figure 4.1A). Second, heterogeneous immunoassays have been developed, comprising a majority of planar assays with functionalized channels as substrates, as well as a significant number of bead-based assays using either magnetic, polymer or glass beads (Figure 4.1B).

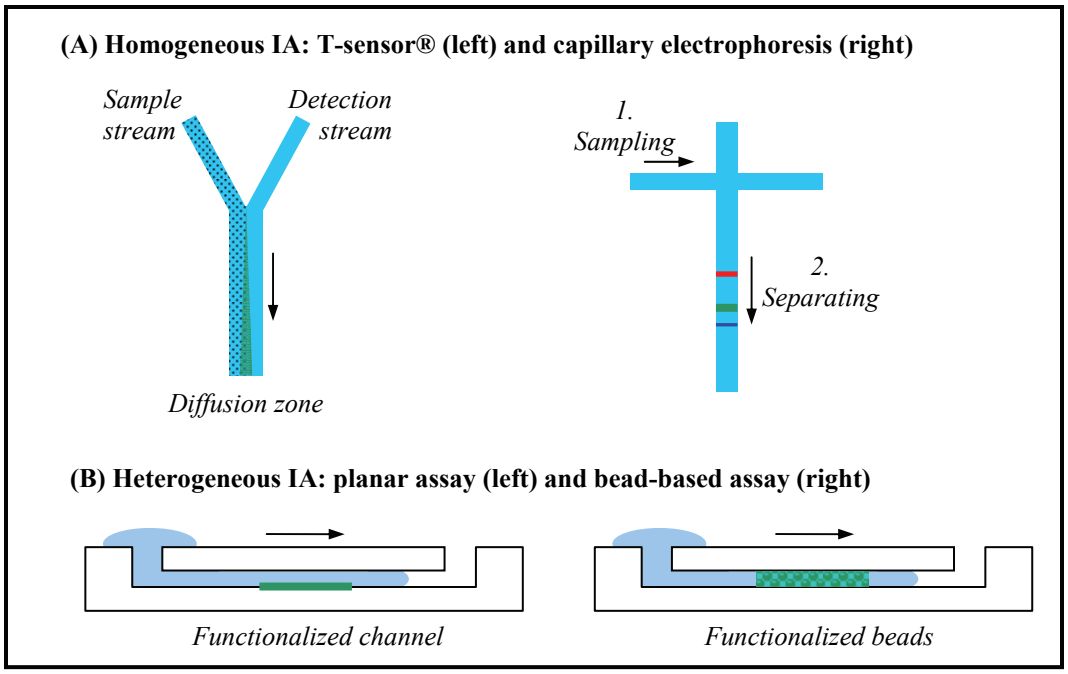

Figure 4.1: Main formats and designs of microfluidic immunoassays.

Beyond the microfluidic design itself, other important aspects play a critical role in the conception of a microfluidic immunoassay platform. The first of these aspects is the chosen material for the fabrication of the microchannels. Evidently, the nature of the material has a direct impact on the procedures used to fabricate the microfluidic chip. Also, it determines the necessity and possibilities for surface treatments, and sets the range of thermal and optical spectrum within which the platform can be operated. The second aspect, closely related to the previous one, is the choice of the detection method.

The first section of this chapter reviews the microfluidic immunoassays described in the literature, classified along their respective formats and methodologies. For each of these assays, the most critical characteristics are provided in the corresponding table. The second section analyses more specifically the materials and associated surface treatments, as well as implemented detection methods. Subsequently, the performances of the listed assays are discussed with regard to these two fundamental aspects. In the last section, three significant examples of fully-achieved platforms for microfluidic immunoassays are presented.

4.1 Literature review of the field of microfluidic immunoassays

In order to facilitate the analysis of such a diversified field, four tables are provided in this section classifying microfluidic immunoassays into different groups with respect to their format (homogeneous or heterogeneous planar/bead-based assay), and the methodology used for the generation of the signal (direct or through an enzymatic reaction). Table 4.1 presents the homogeneous and planar immunoassays with direct detection, table 4.2 the bead-based immunoassays with direct detection, table 4.3 the homogeneous and planar immunoassays with enzymatic detection, and finally table 4.4 the bead-based immunoassays with enzymatic detection. For each one of the listed microfluidic immunoassays, the design, the channel material, the detection method, the sensitivity and dynamic range for a specific analyte, the assay time and the flow type are reported.

Table 4.1: Homogeneous and planar immunoassays with direct detection.

Analyte	Design*	Material	Detection	Sensitivity – range	Assay time	Flow	Ref.
Phenytoin	T sensor	Glass	Fluorescence	430 pM	1 min	pressure	71
TNF-alpha, CRP	Micromosaic (11 x 11 channels)	Si – gold	Fluorescence	20 pg/mL (1 pM) 30 ng/ml	1 hour	Capillary pumps – evaporation	72,73
Rabbit IgG HIV (anti-gp41)	Single channel	PDMS	Gold nanoparticles – silver enhancement	89 pM	< 1 hour	Pressure	74
E coli lysate Ag, H. pylori Ab	H channel	PDMS	Fluorescence	3 µg/mL 20 ng/mL (135 pM)	< 1 hour 22 min	EOF	28,30,75
AFP, IL-6, CEA	CD (104)	Polymer	Fluorescence	150 fM 1.25 pM 1.31 pM	50 min	Centrifugal	76
HIV	Single channel (6)	PDMS	Fluorescence	1.7 nM	< 15 min	Pressure	77
Anti-Hu IgG	Y channel	PDMS	Aggregation – gold nanoparticles	10 ng/mL – 10 µg/mL	2 hours	Pressure	78
Staphylococcus enterotoxin B	Single channel	PDMS	Fluorescence	500 pg/ml – 1000 µg/mL	?	Pressure	79
CRP, PCA, VEGF	Complex with chambers and valves (10)	PDMS	Fluorescence	10 pM	?	Pressure	66
Insulin	CE (4)	Glass	Fluorescence	10 nM	Sampling every 6 sec	EOF	80
Phenytoin	Single channel	Mylar – PDMS glass – gold	SPR imaging	50 nM	5 min	Pressure	81
MMP-8, TNF-alpha, IL-6, CRP	CE with filter	Glass	Fluorescence	130 ng/mL 100 pM 1 nM 20 pM	< 10 min	EOF	82,83
Penytoin	Single channel	PMMA glass – gold	Laminar diffusion – SPR	75 – 1000 nM	10 min	Pressure	84
Streptavidin Anti-PVA IgG, WNV antigens	Single channel	Dialysis membranes	Magnetic beads – dark field microscopy	200 fM 700 viral particles	< 10 min	Pressure	85
T4, CRP, BSA-NT	Micromosaic (12 x 12 channels)	PDMS – silicon nitride	Fluorescence	7.7 – 257.2 nM 0.3 – 4.2 µg/mL 0.03 – 22.3 µg/mL	45 min	Capillarity	86

* The number of on-chip parallel reactions is indicated in parenthesis

Table 4.2: Bead-based immunoassays with direct detection.

Analyte	Design	Material	Detection	Sensitivity – range	Assay time	Flow	Ref.
PTH, IL-5	Single channel	Fused silica capillaries	Fluorescence	2 ng/mL	?	Pressure	87
IFN	Single channel	PDMS	Gold particles – thermal lens microscopy	1 ng/mL (60 pM) – gold particles	< 1 hour	Pressure	88
PSA	Single channel with serpentine and valves	PDMS	Biobare code – silver staining	500 aM	< 1 hour	Pressure	89
Ms IgG	Single channel	Glass – PET	Fluorescence	10 ng/ml – 10 μg/mL (67 pM)	40 min	Pressure	90
Myoglobin, TnT, TnI, CK-MB	CE	PDMS	Cleavable tags – fluorescence	30 – 200 ng/mL 25 – 250 pg/mL 3 – 30 ng/mL 3 – 15 ng/mL	> 4 hours**	EOF	91
IgE	Single channel	PDMS	Magnetophoretic deflection velocity	300 fM	> 4 hours**	Pressure	92
Anti-Ms IgG, anti BSA	Y channel	PDMS	Light scattering – QD	50 ng/mL (330 pM)	< 2 hours	Pressure	93
Ms IgG	Single channel	Glass	Fluorescence	1 ng/mL (7pM)	20 min	Pressure	94

** On-chip detection only

Table 4.3: Homogeneous and planar immunoassays with enzymatic detection.

Analyte	Design*	Material	Detection	Sensitivity – range	Assay time	Flow	Ref.
Sheep IgM	Single channel	PDMS	Fluorescence	15 ng/mL	> 2 hours	Pressure	95
Rat IgG	CD (4)	PMMA	Fluorescence	5 μg/mL (31 nM)	1 hour	Centrifugal	96
BNP	T channel	Glass – gold PDMS	ACh. Esterase – SPR	5 pg/mL – 100 ng/mL (1.5 pM)	30 min	Pressure	97
CRP	Single channel	Cyclic polyolefin	Chemiluminescence	1.85 - 13.8 μg/mL	26 min	Pressure	98
Folic acid	Single channel (8)	Polyimide	Electrochemical	2 – 30 ng/mL	5 min	Pressure	99,100
Ms IgG	2x2 separation and 2x2 convergence (8)	Polyester – screen printing	Electrochemical	10 ng/mL (67 pM)	> 2 hours	Pressure	101

* The number of on-chip parallel reactions is indicated in parenthesis

Table 4.4: Bead-based immunoassays with enzymatic detection.

Analyte	Design	Material	Detection	Sensitivity – range	Assay time	Flow	Ref.
Ms IgG	Single channel	Glass	Electrochemical	50 – 500 ng/mL	20 min	Pressure	102
Botulinum	Complex with filters and hydrogel valves	Polycarbonate – PDMS	Colorimetric	1 μg/mL	2 hours	Pressure	103
FK506 *(drug)*	Single channel	PDMS	Fluorescent	10 pg/mL	15 min	Pressure	104
IFN	Single channel	PDMS	TOOS HRP substrate – thermal lens microscopy	100 pg/mL (6 pM)	< 1 hour	Pressure	105
Ms IgG	Single channel – magnetic microarray	COC	Electrochemical	16.4 ng/mL (110 pM)	35 min	Pressure	106
AFP	Single channel	PDMS	Electrochemical – silver staining	1 ng/mL (15 pM)	1 hour	Pressure	107

4.2 Analyses of the field of microfluidic immunoassays

As an initial remark, it should be noted that a large number of systems published in the literature feature a single straight channel in order to establish a proof-of-concept of a specific aspect of the platform (fabrication procedure, technique for surface treatment or detection method for instance). Less than a quarter of the listed systems have so far proven capabilities for multiplexing or parallelization, although it is an essential requirement to achieve the precise quantification of biomarkers. This section analyses the information contained in the tables, with a particular emphasis on the materials, the surface treatments, and the detection methods implemented in microfluidic immunoassays.

4.2.1 Materials and surface treatments

As mentioned in section 3.2.1, one of the main physical properties of microfluidic channels is their high surface-to-volume ratio. For planar-based immunoassays, this characteristic is advantageous as it facilitates the immobilization of a large number of capture molecules on the surface, while the short diffusion distances accelerate the binding of the analyte. However, this same property of microchannels also implies that a non-optimally covered surface is prone to strong non-specific adsorption (NSA), potentially causing an elevated background noise. In particular, systems using a bead-based approach must be carefully passivated against NSA on the full length of the microchannel. The treatments of glass and silicon channels are mostly achieved through the silanization of surface groups with chemically-active or protein-repellent molecules such as polyethylenoxide (PEO) or Polyethylenglycol (PEG). The treatments of plastics materials can vary greatly depending on the available functionalized groups at the surface of the material.

For PDMS channels, the material used in the majority of the reviewed systems, many techniques have been developed. Active molecules or proteins are rapidly adsorbed on PDMS due to its highly native hydrophobic nature.[108] The most frequent approach to prevent NSA on PDMS employs the direct absorption of large quantities of bovine serum albumin (BSA).[109] This simple technique is however time-consuming as it must be

performed immediately prior to the realization of the assay. Moreover, the quality of the passivation displays high variations in efficacy from assay to assay. The addition of a surfactant such as Tween-20 helps to further reduce NSA by forming a protective film at the surface of the hydrophobic channel.[110,111] Commonly, PDMS can also be treated by oxygen plasma prior to use to facilitate the fluidic flow and diminish NSA. The oxygen plasma treatment induces a dramatic change at the surface of PDMS, drastically changing the water contact angle from 110º to about 20º (Figure 4.2). However, hydrophobic recovery, a phenomenon specific to PDMS, causes important instability at the surface only a few minutes after the completion of the treatment. If left unprotected, the total reversion of the contact angle happens within only a few hours. Hydrophobic recovery is not yet fully understood, but it is partially explained by the migration of short non-polymerized chains accumulating at the surface of PDMS from its bulk. This effect occurs through micro-cracks appearing in the very brittle glassy layer formed by the oxygen plasma treatment. The rate of recovery can be decelerated by permanently keeping the treated PDMS in an aqueous solution. Furthermore, the surface transformation of PDMS into a thin layer of silicon can be utilized for covalently attaching protein resistant groups such as PEG on the microchannel walls by silanization.[112-114]

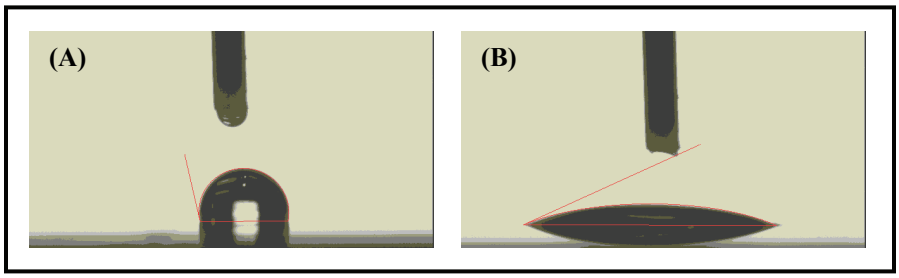

Figure 4.2: Contact angle of water on native and treated PDMS. (A) Untreated PDMS and (B) oxygen plasma treated PDMS.

Despite the relative efficacy of these two techniques, a large variety of surface modification methods have been developed in an attempt to increase PDMS resistance to NSA, and enhance its stability over a long period of time. A non-exhaustive list of these treatments includes the use of lipid bi-layers,[79,115-117] polyelectrolyte layer-by-layer protective films,[118-120] amphiphilic block copolymer,[121,122] chemical vapour deposition,[123-125] atom-transfer radical polymerization,[126] ultraviolet graft polymerization,[127-129] and sol-gel modification of PDMS.[130] In the end, the multitude of these techniques mainly points to the present lack of a convenient, strong and stable method to achieve the efficient passivation of PDMS microchannels.

4.2.2 Detection methods for microfluidic immunoassays

The method of detection chosen for the development of a new immunoassay dictates many of the aspects of the future platform, from the channel design to the chip material.[131] By analogy with bench-top immunoassays, and because of the diversity and sensitivity of commercially available labels and detection devices, fluorescence has been adopted in almost half of the listed systems. Both the detection of surface-bounded labelled antibodies (IF type)[28,30,66,72,73,75,79,80,82,83,86,87,90,94] and fluorescent molecules in solution (ELISA type)[95,96,104,132,133] have been achieved with the use of standard scanners, fluoro-spectrophotometers or fluorescence microscopes (Figure 4.3A). Many strategies have been described to miniaturize and integrate fluorescent detection in a lab-on-chip technology.[32,134-139] Similarly, several enzymatic microfluidic immunoassays have incorporated chemiluminescent detection, despite the limited possibilities for multiplexing compared to fluorescence (Figure 4.3B).[98,140] More optical-based methods have been developed using, for instance, gold nano-particles as labels for aggregation detection,[78] thermal lens microscopy[88,105] or silver reduction.[74,89] Magnetic beads also have been employed with dark field microscopy[85] or magnetophoretic detection,[92,141] as well as latex microspheres combined with QD for targeted light scattering.[93] Finally, microfluidic immunoassays employing non-labelled detection methods, in particular surface plasmon resonance (SPR), have also been reported.[81,84,97]

After fluorescence, electrochemistry is the second most used detection method in microfluidic immunoassays (Figure 4.3C). This technique benefits greatly from the size

reduction of the system.[100,101,106,107,142-144] Among the main electrochemical techniques, voltammetry displays the most significant improvement in performance with the reduction of the electrodes into the low micrometer size range. At this scale, non-planar diffusion occurs, which enhances the collection efficiency of the electroactive species.[145] This effect is further improved by the physical proximity imposed by the small size of microchannels. Another advantage of electrochemistry is the convenient microfabrication processes similar to the ones used for the production of the microfluidic chip itself. Simple electrodes, or more advanced detection devices such as the interdigitated array electrode (IDA), can be mass-produced at low costs, conferring compactness and portability to the system. The decrease in current due to miniaturization however requires improved electronics and shielding materials in order to achieve stable and accurate measurements.

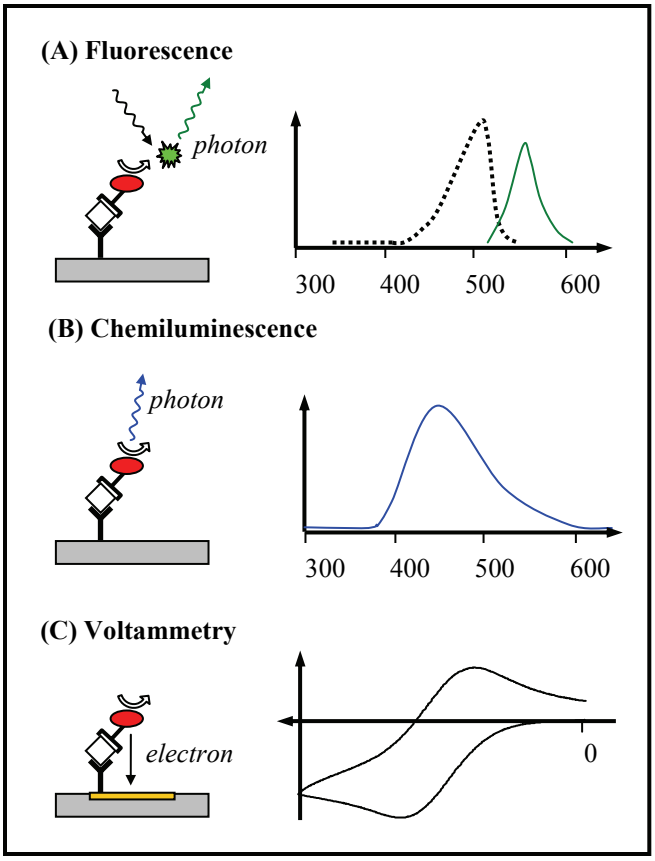

Figure 4.3: Most common methods for enzymatic detection in microfluidic immunoassays.

4.2.3 Performance of microfluidic immunoassays

With regard to the sensitivity, which is the often the only performance data being reported, the most crucial objective is to reach the discriminating threshold related to a given application. If a biomarker is to be quantified for a medical diagnosis, the targeted sensitivity of the immunoassay depends on the concentration of the analyte present in a healthy individual relative to the symptomatic concentrations. These threshold concentrations can vary on several orders of magnitude given a particular analyte and application. As a comparison, standard bench-top ELISA routinely achieve low picomolar sensitivities (1-10 pM), which for an average protein of about 50 kDA, correspond to a concentration of 500 pg/mL. Among the 40 references listed in the tables, about only a quarter of microfluidic immunoassays have reported results in a similar range of sensitivity. Among them, 3 systems have reported sensitivities below 1 pM, in the fentomolar and even atomolar range. These assays however rely largely on their unique detection methods, namely dark field microscopy on magnetic microbeads,[85] magnetophoretic deviation[92] and biobar-code coupled with silver staining.[89] Their implementation in a full scale parallel system remains to be proven. The remaining 6 platforms feature in majority direct fluorescent detection,[66,72,76,94] with the exception of 2 non-fluorescent enzymatic immunoassays, the first one coupled with SPR detection,[97] the second with thermal lens microscopy.[105] Interestingly, only 2 among the 6 lastly cited systems are made exclusively of PDMS.

The average assay time to complete at least one test is about an hour. Most systems described in the literature feature only one channel, which gives an appreciation of the platform possibilities but avoid all complications that might arise from reaction parallelization. Multiplying the number of independent tests is however an inescapable requirement to achieve precise protein quantification, along with running the necessary controls. Direct detection tends to decrease the assay time as compared to enzymatic assays. About a quarter of the systems using direct detection achieved protein detection in 15 minutes or less. Also, because only one binding step is required, homogeneous assays have the potential to be much faster than surface-based assays, displaying turn-over times of less than a minute.[80] They are however generally significantly less sensitive and less specific than heterogeneous assays.

4.3 Significant examples of microfluidic immunoassay systems

Three significant examples of particularly achieved system have been identified and are presented in this section: (i) the micromosaic immunoassay, originally developed by Delamarche's team at IBM Zurich, (ii) the Gyros Bioaffy by Gyros AB and (iii) the Immunochip by Diagnoswiss SA.

(i) The micromosaic immunoassay is one of the most attractive systems developed to date. This relatively simple approach consists in patterning straight lines of capture antibodies on a flat piece of untreated PDMS, using channels embedded in oxygen plasma treated PDMS. Because 3 walls of the channels are made hydrophilic, the solutions are flowed by capillary action only. After the washing and blocking steps are realized, another piece of PDMS with treated channels is placed perpendicularly to the patterned lines, and the samples and detection antibodies are successively flowed to complete the immune-complex formation. The signal generated by the labelled detection antibodies are then analyzed on a fluorescent scanner. This simple approach has led to the development of rapid, low-cost, user-friendly parallel immunoassays with moderate sensitivities.[73,86]

Using this technique, Cesaro-Tadic *et al.* achieved the quantification of the cytokine TNF-alpha in cell culture medium with a detection limit of 20 pg/mL (1.14 pM) (Figure 4.4).[72] The range of quantification is about 2 to 3 orders of magnitude; the time of completion is less than an hour to perform 11 independent assays. However, in order to reach performances comparable to those of a bench-top ELISA, compromises had to be made in the fabrication procedures and the complexity of the assay protocol. Similar to the earlier systems, the capture antibodies were adsorbed on a flat block of PDMS. The microfluidic channels however were fabricated in glass, covered with a layer of gold and passivated with HS-PEG. Two of these chips had to be prepared and utilized for each micromosaic assay. Furthermore, the flow rates were tightly controlled through a system of capillary pumps and induced slow evaporation. Although the sensitivity has been drastically enhanced, these changes significantly increase the costs and complexity of the micromosaic assay. Additionally, several manual manipulations of the chip itself are required to complete the assay, potentially limiting the possibilities for automation.

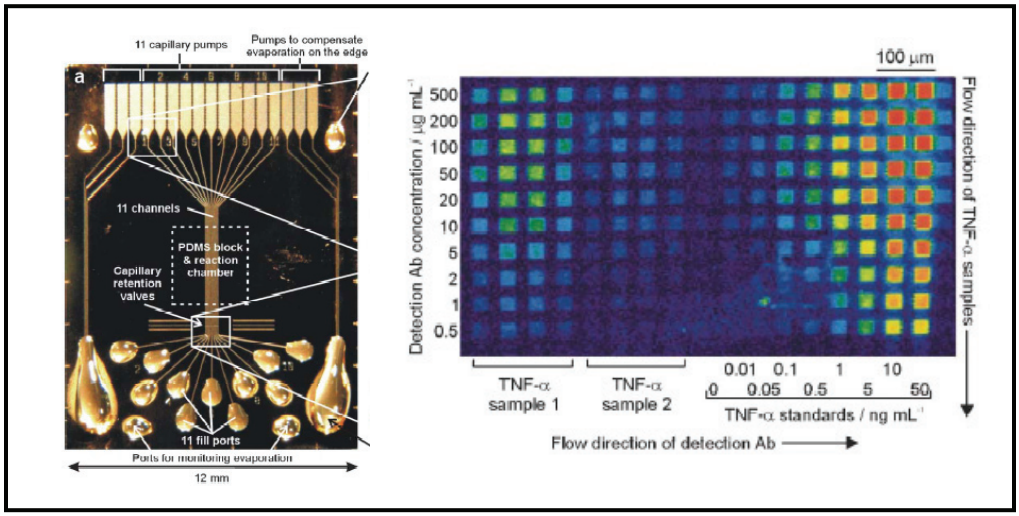

Figure 4.4: Silicon-gold microfabricated chip for the highly sensitive quantification of TNF-alpha by a micromosaic immunoassay [*Lab Chip*, 2004, **4**, 563-569] – *Reproduced by permission of The Royal Society of Chemistry* – http://dx.doi.org/10.1039/b610250f

(ii) Commercialized by Gyros AB, the Gyrolab Bioaffy is another good example of a fully achieved platform for microfluidic immunoassay (Figure 4.5). Slightly more than 100 assays can be completed simultaneously with low-picomolar sensitivity in less than an hour.[76] The system is completely automated, with pre-loaded solutions and integrated self-metering capabilities. The channels are fabricated in a polymeric CD, which allows for the selective release of different solutions by gradually increasing the rotation velocity of the disk. The fluorescent detection is realized on-line by laser induced fluorescence incorporated in the quite large bench-top Gyrolab Workstation LIF.

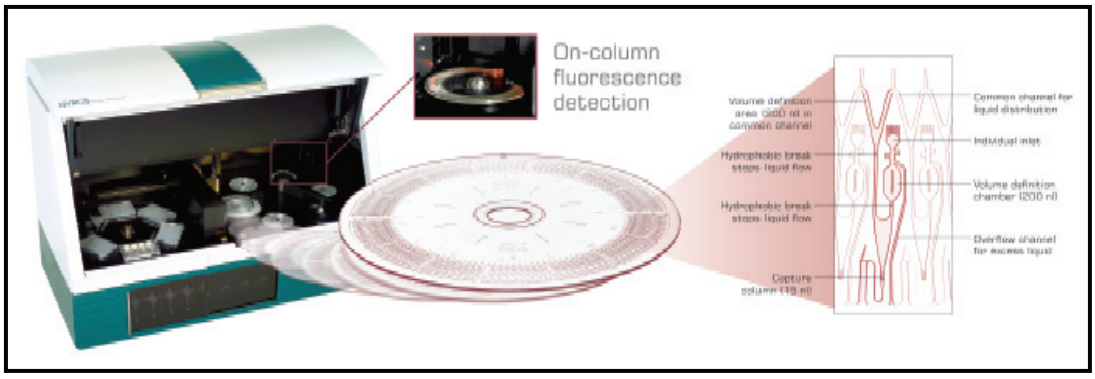

Figure 4.5: The Gyrolab Bioaffy® and the Gyrolab Workstation LIF®.
(http://www.touchbriefings.com/pdf/890/PT04_gyros.pdf)

(iii) Less sensitive but very attractive for its simplicity, the Immunochip developed in Rossier's laboratory is another excellent example of a successfully integrated microfluidic immunoassay platform (Figure 4.6).[99] This system exploits the advantages of electrochemical detection to realize 8 parallel assays in less than 10 minutes. All fluidic and detection components are integrated into a relatively small workstation, featuring independent peristaltic pumps, pressure valves and a heating element. The microfluidic chip itself takes the form of a pocket-sized cartridge. Based on the same detection technology, the so-called GRAVI-Chip is presently commercialized by Diagnoswiss SA. In the latter system, the fluidic workstation is replaced by on-chip functionalized magnetic beads and gravitational flow capabilities.

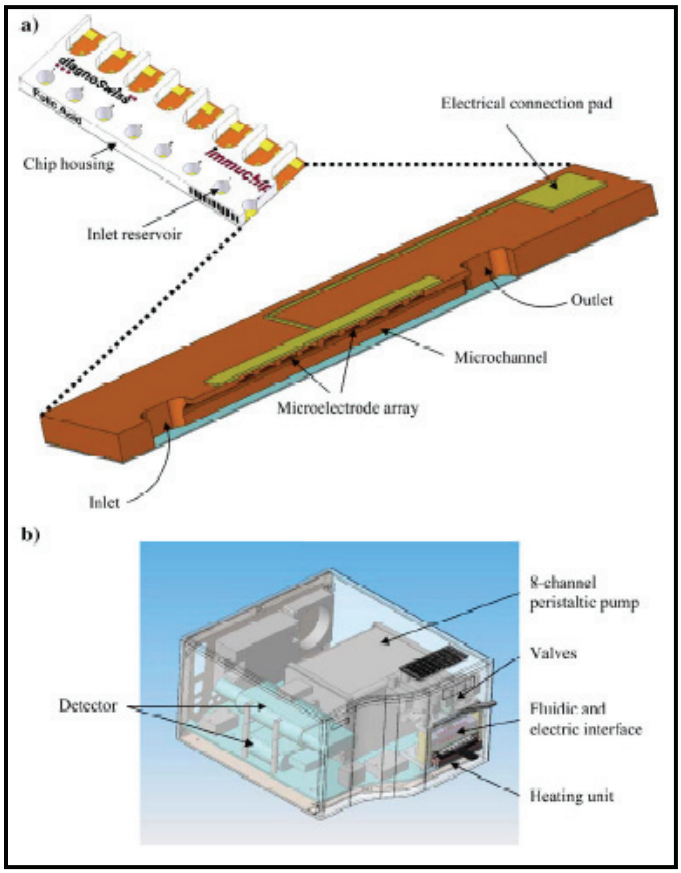

Figure 4.6: The Immunochip and its workstation. (A) Electrochemical immunochip for the realization of 8 parallel microfluidic immunoassays. (B) Immunochip workstation comprising a heating unit, integrated valves and peristaltic pumps and detector [*Anal Bioanal Chem*, 2007, **387**, 267-275] – *Reproduced by permission of Springer*.

Chapter 5
System Description and Originality

5.1 System description

Based on the analysis of the field of microfluidic immunoassays provided in the previous chapter, and the recurrent limitations observed in these systems, the platform described in this thesis was developed around 3 main axes:

1- **An original microfluidic design**:

The final design of the microfluidic chip was conceived to adapt the two novel concepts introduced in this thesis: the stop-flow and Dual Network systems. In a first iteration of the chip, the channel layout was adjusted to perform in stop-flow mode, rather than in continuous flow conditions. In stop-flow mode, the channels are quickly filled with a given solution before the flow is stopped. After a period of incubation, the next solution is injected, replacing the previous one without mixing due to the laminar flow. This method was expected to increase the potential analyte exploitation rate as the system shifts from a reaction limited regime to a transport limited regime (Figure 5.1). In this mode, the performance of the system is independent of the flow rate, allowing simple connection and pumping schemes. Additionally, the volume of solution used for the assay is defined by the volume of the channel itself, rather than by the volume of solution manually pipetted and flowed through the system. For these reasons, working in stop-flow mode should contribute to increase the reproducibility between independent assays.

Based on the initial layout, the concept of Dual Network system was later introduced. This novel concept relies on the physical separation of the immune complex formation phase and the enzymatic reaction phase into two distinct networks of channels. The independence of the two networks, ensured by PDMS pressure valves, permits the realization of the final immuno-detection step in an environment free of non-specifically adsorbed proteins. Through reducing the noise, this method was expected to increase the assay performance. Also, it removes the necessity of passivating channels before use, leading to the development of a faster, less expensive and less complex protocol.

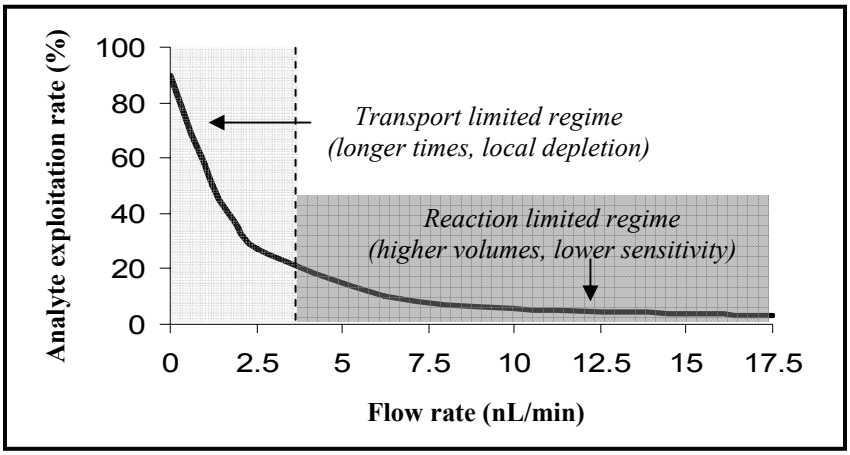

Figure 5.1: Modeling of the analyte exploitation rate versus the flow rate in heterogeneous surface-based microfluidic immunoassays. Adapted from Zimmermann *et al.*[109]

2- **The multi-purpose use of magnetic microbeads**:

Microbeads have been used previously in microfluidic immunoassays. Most frequently, they serve as functionalized substrates to support the formation of the immune complex. Microbeads, both in conventional and microfluidic immunoassays, increase the active surface area and provide specific chemistries used to attach the capture entity with an adequate orientation and a preserved binding activity. A large amount of microbeads can be functionalized in advance and placed in long-term storage without significant loss of activity. This permits the system to be more versatile, with no functionalization necessary prior the beginning of an experiment, and also contributes to reducing the overall assay time and complexity. In other systems, non-functionalized microbeads have been used to induce mixing inside microfluidic channels.

In this work, magnetic microbeads were utilized to achieve both purposes simultaneously. During the incubation periods in stop-flow mode, local depletion of the analyte might occur. To prevent this effect, the beads were magnetically displaced inside a limited portion of the fluidic channel, homogenizing the solution, while capturing the analyte molecules inside a well-defined volume. This technique was expected to accelerate the analyte exploitation rate in stop-flow mode. Additionally, the magnetic beads were also used in combination with the Dual Network design as vessels to transfer the newly formed immune-complexes into the yet unused reaction network.

3- **The enzymatically amplified fluorescence signal**:

Fluorescent detection was implemented in order to achieve high quality measurements for protein quantification. To this date, fluorescence remains one of the most used detection method as it is highly sensitive and offers multiplexing and imaging possibilities. Besides, powerful devices such as microscopes and scanners are already in place in most laboratories, lowering the investments associated with the acquisition of a new technology.

The fluorescent signal was generated and amplified through an enzymatic reaction, accumulating the fluorescent molecules in a time-dependant manner. Simultaneous detection of parallel independent assays was achieved thanks to the adapted design at the detection site. The fluorescent signal intensities were measured away from the reactive beads in order to physically stop all parallel reactions at the same instant, and avoid scattering interferences or background noise induced by the bead's polystyrene shell.

5.2 System originality

The design of stop-flow microfluidic ELISA with parallel fluorescent detection, the conception and implementation of the Dual Network system, and the multi-purpose use of magnetic microbeads are the principal aspects contributing to the originality of the present work. The Dual Network platform is fully functional and allows for every step of a protein quantification experiment to be completed on a single PDMS chip. In the remaining part of this thesis, the initial developments leading to the proof-of-concept for the Dual Network system are first presented. Second, the performance of the platform as characterized through the optimization of important assay parameters for the rapid quantification of TNF-alpha are described. By doing so, the use of the platform in research applications, as well as its potential for the fast and cost-effective diagnosis of sepsis were demonstrated. The original contribution of this work was recognized and published in three peer-reviewed articles presented in this thesis as chapters 6, 7 and 8.

Chapter 6
Initial Microfluidic Design and Detection Method

This first paper, published in *Lab-on-a-Chip*, established the initial microfluidic design adapted for the enzymatic generation and the simultaneous detection of the fluorescent signal of parallel assays in stop-flow mode.

Several technical elements were addressed, such as the shapes and sizes of the different portions of the microfluidic channels, the connection and pumping schemes, and the magnetic mixing strategy. A general protocol for the generation and the detection of the fluorescent signal was also established.

In this first iteration of the platform, only the enzymatic reaction and detection were performed *on-chip*. The first part of the assay, which consists in the formation of the immune-complexes on the functionalized magnetic beads, was realized *off-chip* in standard reaction tubes. This approach avoided completely the issue of elevated background noise caused by non-specific adsorption of proteins on the channel walls.

Reproduced by permission of The Royal Society of Chemistry - http://dx.doi.org/10.1039/b707883h

Enzymatically-generated fluorescent detection in micro-channels with internal magnetic mixing for the development of parallel microfluidic ELISA

M. Herrmann,[a] T. Veres[b] and M. Tabrizian[a]

[a]Biomedical Engineering Department, McGill University

[b]Industrial Materials Institute, National Research Council of Canada

6.1 Abstract

The Enzyme-Linked Immuno-Sorbent Assay, or ELISA, is commonly utilized to quantify small concentrations of specific proteins for a large variety of purposes, ranging from medical diagnosis to environmental analysis and food safety. However, this technique requires large volumes of costly reagents and long incubation periods. The use of microfluidics permits one to specifically address these drawbacks by decreasing both the volume and the distance of diffusion inside the micro-channels. Existing microfluidic systems are limited by the necessary control of extremely low flow rates to provide sufficient time for the molecules to interact with each other by diffusion only. In this paper, we describe a new design of micro-channels for the realization of parallel ELISA in stop-flow conditions. Magnetic beads were used both as a solid phase to support the formation of the reactive immune complex and to achieve a magnetic mixing inside the channels. In order to test the detection procedure, the formation of the immune complex was performed off-chip before the reactive beads were injected into the reaction chamber. Anti-streptavidin antibodies were quantified with low picomolar sensitivity (0.1 – 6.7 pM), a linear range of 2 orders of magnitude and good reproducibility. This work represents the first step toward a microfluidic platform for simple, highly effective and parallel microfluidic ELISA.

6.2 Introduction

The sensitive detection of specific proteins is an important analysis for applications in biotechnology, biomedical diagnosis, food and environmental safety. Label-free methods, such as Surface Plasmon Resonance (SPR) or Quartz Crystal Microbalance (QCM), provide simple and real-time measurements, but they are yet limited by a lack of sensitivity.[146] Alternatively, sandwich immunoassays allow the detection of a specific protein with greater sensitivity at the cost of a more complex procedure. In particular, the Enzyme-Linked Immuno-Sorbent Assay (ELISA), in which the enzymatic amplification of the signal greatly lowers the limit of detection, is the current standard for protein quantification. However, this method requires large volumes of reagents as well as long incubation times due to the high volume-to-surface ratio. The use of microfluidic to perform sandwich immunoassays permits one to specifically address these drawbacks. The low scale of these devices reduces the volumes and diffusion distances inside the micro-channels, therefore decreasing the duration of the successive incubation periods.

Many microfluidic platforms have been described using various methods of detection such as indirect fluorescence,[77,87,147,148] electro-chemistry[100,102,143] or fluorescence generated through an enzymatic reaction.[95,96,132,149] Fluorescence is a popular technique as it provides powerful detection tools, increasing sensitivity and gives the possibility of imaging numerous sites on a restricted area.[73,150] Interestingly, optical fibers and diodes (LED) have been successfully incorporated in some microfluidic platforms in order to miniaturize and integrate the fluorescent detection device.[136,137] To date, the highest sensitivity achieved in a microfluidic immunoassay has been reported for the quantification of the cytokine TNFα with a detection limit of 20 pg/mL (1.14 pM).[72] This system is however restricted by the number of necessary manipulations and the requirement for sophisticated equipments, which increase the complexity and the cost of the assay. Moreover, it has been demonstrated that one of the main challenges to perform highly sensitive microfluidic immunoassays is related to the fine tuning of the flow velocity.[151] When the flow velocity is high, the kinetic of capture of the analyte is reaction-limited. In this regime, the exploitation of the analyte present in the solution is only about 5%. Conversely, when the flow velocity is extremely slow, or even stopped, the analyte exploitation reaches values up to 90%. The regime is then transport-limited as

the incubation time required to attain such high exploitation rates is extended due to the absence of mixing.

Micro-beads have been used for more than a decade in immunoassays as a means of concentrating specific molecules and of increasing the available surface area supporting the formation of the immune complex.[88,104,152] In particular, paramagnetic micro-beads can be easily manipulated by applying variable magnetic fields with permanent magnets or electromagnets. Magnetic beads are for instance commonly utilized in macroscopic automated system such as the immunoassay analyzer Elecsys.[153] In microfluidic systems, they have been employed to capture specific molecules[154-160] as well as to produce mixing inside micro-channels or microfluidic chambers.[40,42]

Based on these observations, we designed a system to perform microfluidic ELISA in stop-flow rather than in continuous flow conditions. In stop-flow conditions, the channel is first rapidly filled with the desired solution. The flow is then stopped for a defined incubation period. This approach has two major advantages, (i) the volume of solution in the system is precisely defined by the volume of the channel, thus avoiding imprecision due to pipetting and (ii) the assay is not limited by the complex control of extremely low flow rates. The outcome of the assay is hence not dependent on the flow rate but only on the incubation time corresponding to the stop period. The issue of transport limitation is circumvented by using magnetic micro-beads both as a solid phase to support the formation of the immune complex and as a means to create an internal mixing.

This paper is divided in two parts. First, an original microfluidic design to perform parallel ELISA in stop-flow conditions is described. Then, the enzymatic amplification and detection of the fluorescent signal was tested on-chip following the off-chip formation of the immune complex. Rapid prototyping in PDMS, manipulation of magnetic beads and epifluorescence microscopy have been combined in order to achieve the detection and quantification of anti-streptavidin antibodies.

6.3 Material and methods

6.3.1 Fabrication method

Micro-channels were molded in Poly(dimethylsiloxane) (PDMS) (Dow Corning, MI) by the technique of replica modeling. A negative photo-resist (SU-8 2035, MicroChem, MA) was spin-coated on to a silicon wafer to achieve a homogenous layer of 50 μm. The patterns were exposed with UV-light (I-liner, 365nm) through a high-definition transparent mask and then developed to obtain a negative master of the channel network. PDMS was prepared by mixing the elastomer and the curing solutions in a 10:1 ratio and baked in an oven at 80°C for 2 hours or more. The PDMS was then pealed off the wafer and the connection holes were pierced before assembling.

Both the PDMS block and a 5 cm x 7.5 cm glass slide were cleaned and carefully dried under a nitrogen flow before they were brought into contact to form a tight waterproof reversible bond. The platform was then placed onto the homemade trapping/mixing device. The channels were primed with ethanol to prevent the formation of air bubbles and then connected to a syringe pump (Model 210, Lomir biomedical, NY) via a single outlet. The fluidic tests were carried out with a buffer solution mixed with a red food dye for visualization.

6.3.2 Bead preparation and formation of the immune-complex

Phosphate Buffer Saline (PBS), Trizma Base (TRIS), Tween-20, glycine and Bovine Serum Albumin (BSA) were obtained from Sigma-Aldrich (Oakville, ON). Magnesium chloride was purchased from ACP Chemicals (Montreal, QC).

The desired amount of streptavidin-coated beads (Dynabeads® MyOneTM Streptavidin, Dynal Biotech, NY) was diluted 10 times in PBS 0.05% Tween-20 (PBS-T). The beads were washed 3 times in PBS-T and separated into different eppendorf tubes. They were then incubated for 30 minutes with the anti-streptavidin IgG (Rockland Immunochemicals, PA) diluted at the appropriate concentration in a solution of PBS 1% BSA, under constant mixing. A volume of 10 μL of the protein solution per μL of beads was used (equivalent to 1 assay). Following the incubation, the beads were washed 3 times in PBS-T. They were then incubated another 30 minutes in a 1 $\mu g.mL^{-1}$ solution of

anti-rabbit IgG coupled with Alkaline Phosphatase (AP) (Rockland Immunochemicals, PA) diluted in PBS 1% BSA. Finally, the beads were washed 3 times and kept in PBS-T at 4°C until use.

6.3.3 Procedure for on-chip signal generation and enzymatic amplification

The channels were rinsed twice with 10 µL of PBS-T. The remaining solutions trapped at the bottom of each inlet were rapidly withdrawn with a pipette between each run to avoid cross-contamination of the sequentially injected solutions inside the inlets. The beads were then injected into the channel and trapped by an external rare earth magnet in the reaction chamber, forming a loose bed that can be moved by displacing the magnet back and forth along the direction of the channel. The beads were washed twice with 10 µL of TRIS buffer pH = 9, 10 mM $MgCl_2$, 10 mM Glycine (TRIS). The solution containing the enzymatic substrate, namely 20 µM Fluorescein Di-Phosphate (FDP) (Biotum, CA) in TRIS, was subsequently flowed into the channels and incubated for 5 minutes with 30 seconds mixing every minute.

6.3.4 Detection method and data processing

An inverted microscope (TE2000-U, Nikon), a stereoscopic zoom microscope (SMZ1500, Nikon) and a digital camera (DXM1200F, Nikon) operated with the ACT-1 software were used to acquire pictures of the channels. For fluorescence imaging, the microscope is equipped with a high pressure mercury lamp (C-SHG1, Nikon) and with the appropriate set of filters for fluorescein (FITC) excitation and emission wavelengths. The intensity of fluorescence in each channel was measured with ImageJ (software for image processing and analysis in Java) over the total section of the captured channel (100x magnifications). All data were normalized by subtracting the intensity obtained in the negative control.

6.4 Results and discussion

6.4.1 Microfluidic design

Employing the technique of replica molding,[23] the network of 3 walled micro-channels was fabricated in PDMS. After cleaning and drying, the PDMS block was placed on the surface of a microscope glass slide, closing the channels and creating a reversible watertight seal. The original design of the system enables the simple parallelization of individual ELISA on a single chip. Fig. 6.1 presents a photograph of the entire platform, along with close-ups at various strategic locations. The system comprises eight independent micro-channels for the realization of parallel simultaneous measurements with identical experimental conditions. Each channel is composed of 3 different sections: (a) an independent inlet linked to a wide channel acting as a diffusion barrier, (b) a reaction chamber where the generation of the signal and the magnetic mixing are realized, and (c) a smaller channel where the intensity of the fluorescent signal is measured before the solution is discarded via the single outlet of the system.

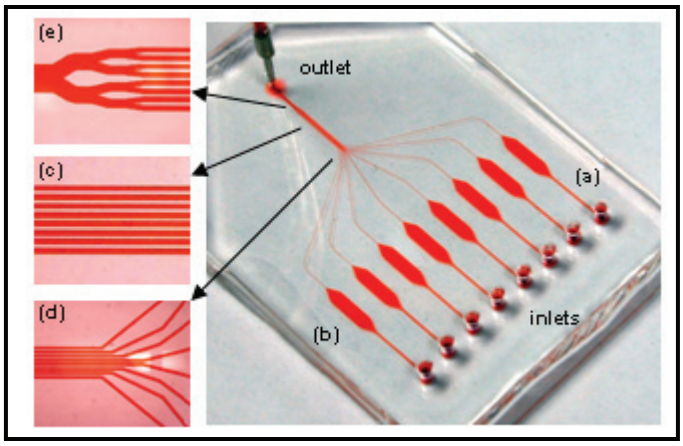

Figure 6.1: PDMS chip for the realization of simultaneous microfluidic ELISA: (a) individual channel with a cross-section of 200 x 50 µm acting as a diffusion barrier; (b) reaction chamber with dimensions of 6 mm x 2 mm x 50 µm (L x W x H); (c) network of channels with a cross-section of 50 x 50 µm referred as the detection area; (d) gathering of the independent channels; (e) merging of the channels into a unique outlet channel connected to a syringe pump in withdrawal mode.

Section (a), linking the inlet to the reaction chamber, is formed by a rectangular segment of 200 μm in width and 50 μm in height. Its relatively large dimension slows down the diffusion of liquid from the inlet into the rest of the system when the flow is stopped, thus acting as a diffusion barrier between the sequentially injected solutions. In addition, it allows for a better lateral distribution of the beads and the various solutions, which flow through the gradual opening into the wider reaction chamber.

Section (b), or reaction chamber, is 2 mm wide, 6 mm long and 50 μm high. These dimensions keep the fluid regime in the laminar domain, where solutions injected sequentially follow each other with only minimal mixing at the interface. The reaction chamber is terminated with two symmetrical cone-shaped ends, opening and closing over a 2 mm long path. The gradual change of width leads the solutions from and to the narrower channels with no apparent dead-volumes or liquid retention in the corners. The reaction chamber defines a volume of 600 nL, which has been demonstrated to be suitable in achieving the highly sensitive detection of TNF-alpha in a dendritic cell culture medium.[72] The larger dimension of the chamber also contributes to decrease the linear flow velocity, thus reduces the hydrodynamic forces that are applied on the beads. As a result, the magnetic force necessary to capture and hold the beads at the desired location is also diminished.

However, as the flow is laminar within the entire system, turbulent mixing does not spontaneously occur inside the micro-channels. Additionally, when working in stop-flow conditions, fresh solution is not continuously transported toward the capture area. As a result, it is necessary to actively produce an internal mixing in order to promote binding events of complementary proteins, increase enzymatic substrate availability and homogenize the generated fluorescent signal. For our microfluidic platform, a prototype device was fabricated in order to efficiently trap and manipulate the magnetic beads inside the micro-channels. The microfluidic chip is placed on the top of the device, bringing the external rare earth magnet in close contact with the bottom of the glass slide used to seal the channels. The magnet can be manually displaced from one end of the reaction chamber to the other entraining the beads along in its course. The displacement of the external magnet moves the beads in a synchronized way, causing the fluid to circulate around them and mixing the surrounding solution. With about 10^6 beads of 1

μm in diameter trapped in the chamber (equivalent of 1 μL of Dynabeads concentrated solution), only a few seconds were necessary to initiate the mixing, and moving the magnet for less than 2 minutes was enough time to ensure the good homogeneity of the solution in the entire reaction chamber (Fig. 6.2).

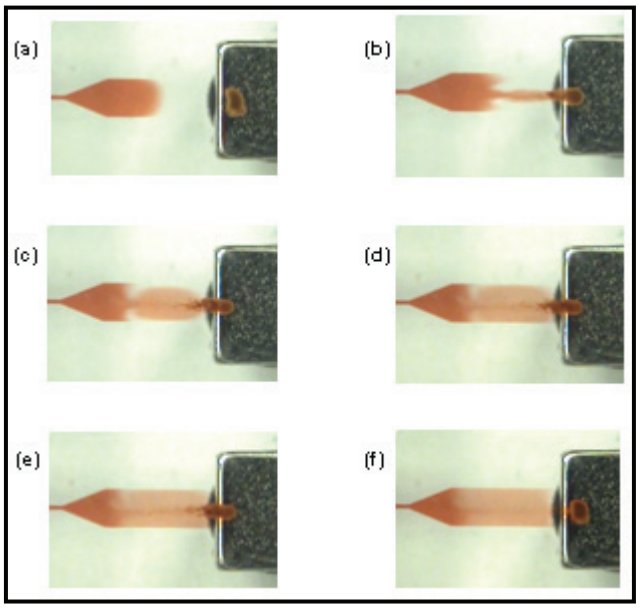

Figure 6.2: Magnetic mixing inside the reaction chamber: (a) about 10^6 beads of 1 μm in diameter are injected and trapped by an external permanent magnet. The reaction chamber is half-filled with a solution of red-food dye and left aside for 1 minute to ensure that the colored solution is not advancing anymore; mixing of the solution after (b) 5 seconds (c) 30 seconds (d) 60 seconds (e) 90 seconds (f) 120 seconds.

Section (c), or detection area, corresponds to the portion of the system where the eight independent 50 μm wide channels gather (section (d)) to form a network with a 100 μm pitch. The total width of the detection area is about 750 μm, which allows the simultaneous observation and acquisition of the signal from all channels in one single shot. At the end of the detection area, the channels merged into one larger channel leading to the single outlet connected to a syringe pump in withdrawal mode (section (e)). This particular design necessitates the utilization of only one source of vacuum, simultaneously driving the solution into multiple channels, thereby facilitating the parallelization and the synchronization of individual reactions.

6.4.2 Fluorescent signal generation and detection

In order to demonstrate the efficiency of the microfluidic platform for protein quantification, a generic detection scheme has been utilized that can be adapted for potentially any desired applications. In addition, the chip does not require that it be pre-coated with either capture proteins or antibodies, thus it can be used for a specific application without the need for any further modifications. The analytical concept of the system is described in Fig. 6.3. Paramagnetic beads of 1 µm in diameter, coated with a layer of streptavidin, were used as a support for the formation of the immune complex. In that experiment, streptavidin was not used for its affinity for biotynilated molecules, but rather as a target protein to be recognized by anti-streptavidin polyclonal antibodies. The streptavidin-coated beads were first incubated with various concentrations of anti-streptavidin antibody, followed by a solution of secondary antibody coupled with alkaline phosphatase (AP). The enzymatic substrate Fluorescein-diphosphate (FDP) was subsequently used to generate the fluorescent signal. FDP is a very efficient fluorogenic enzymatic substrate for alkaline phosphatase, which has been previously utilized both for enzymatic assays and ELISA.[161,162] The enzymatic reaction generates fluorescein, a strongly green fluorescent molecule, through the hydrolysis of the two phosphate groups of the colorless and non-fluorescent fluorescein-diphosphate.

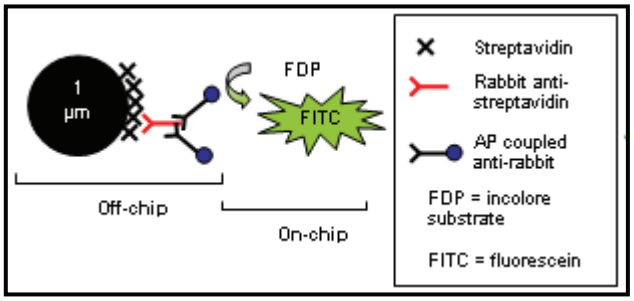

Figure 6.3: Analytical concept for the quantification of anti-streptavidin antibodies: the formation of the immune complex is performed off-chip by incubating the streptavidin-coated micro-beads first with rabbit anti-streptavidin antibodies and then with 1 $\mu g.mL^{-1}$ of secondary anti-rabbit antibodies coupled with Alkaline Phosphatase. The beads are then injected into the micro-channels and both signal generation and detection are performed on-chip.

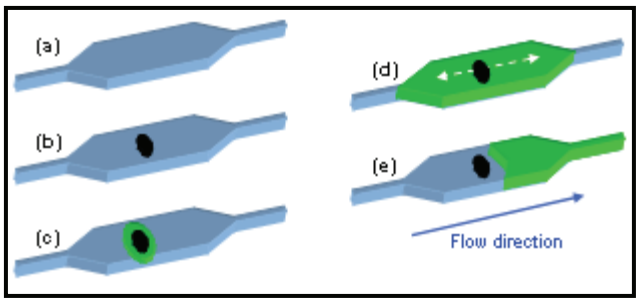

Figure 6.4: Schematic presentation of the procedure for the on-chip generation of fluorescein and signal detection in the downstream channels: (a) filling and washing with PBS-T; (b) injection of about 10^6 beads, trapping in the reaction-chamber and washing with PBS-T and TRIS buffer; (c) introduction of the substrate solution (20 µM FDP in TRIS buffer), 5 minutes incubation with (d) alternate magnetic mixing and (e) detection. The total procedure takes about 10 minutes to be completed.

As the beads aggregate to form a loose bed, the reactive surface with the AP-coupled-antibodies becomes extremely concentrated and localized into the reaction chamber (Fig. 6.4). The reaction then occurs very rapidly around the bead bed but the rest of the enzymatic substrate solution is left unreacted. Moving the beads and mixing the solution thus improve the substrate availability and the resulting signal homogeneity. The transformation of FDP into fluorescein is processed at a steady rate into the reaction chamber, yielding to a final fluorescent intensity which depends both on the duration of the incubation period and the number of immobilized enzymes. As a result, when the incubation period is fixed, the intensity of the fluorescent signal is only dependent on the number of immobilized enzymes, which itself is directly proportional to the quantity of anti-streptavidin antibodies bound on the surface of the streptavidin-coated beads. After 5 minutes of incubation and alternate mixing, the reacted solution is simply driven away from the magnetic beads, physically stopping all reactions at the same time, and giving a precise control over the duration of the multiple individual enzymatic reactions. The relatively large volume of the reaction chamber permits the downstream detection channel to be entirely filled up without the need for an extremely precise control of the flow.

Figure 6.5 shows the fluorescent image obtained for multiple reactions performed in parallel on a single chip. No beads were introduced in the first and last channels. They

served as controls to ensure that the solution of FDP did not exhibit auto-fluorescence due to deterioration of the substrate molecule during the storage period. From the top to the bottom, the second channel corresponds to the negative control where beads have been incubated with the secondary AP-antibody only. The weak signal obtained in this channel represents the background signal due to the unspecific binding of AP-coupled antibodies to the streptavidin-coated beads. Channels 3 to 7 correspond to increasing concentrations of anti-streptavidin antibodies, ranging from 12.5 $pg.mL^{-1}$ (0.1 pM) to 1 $ng.mL^{-1}$ (6.7 pM). The same experiment was repeated 3 times and a standard curve for the quantification of anti-streptavidin antibodies was plotted. The linear range of quantification for this model was approximately of 2 orders of magnitude ($R^2 = 0.987$). The low picomolar sensitivity showed promising potential with regards to the performance of the optimized immunoassay for TNF-alpha (1.14 pM).[72] A 3 to 4 folds increase in sensitivity was observed with systems using indirect fluorescence (1 nM).[77] The sensitivity was also enhanced by at least a factor of 10 when compared to previously described microfluidic ELISA (17 pM to 31 nM).[95,96,132] The standard deviations varied from 3% to 15% of the highest fluorescent intensity. The inter-assay coefficient of variation, which is defined by the ratio between the standard deviation and the mean fluorescence intensity, was about 15% for concentrations above 500 $pg.mL^{-1}$ (3.3 pM). Similarly, Fig. 6.6 displays a fluorescent picture where all channels, except for the negative control in channel 3, were filled with beads incubated with a solution of 500 $pg.mL^{-1}$ of anti-streptavidin antibodies. The measured intra-assay coefficient of variation was 15.1%. Both inter- and intra-assay variability were comparable to those recently obtained by Honda et al. using indirect fluorescence on a compact disk-shaped microfluidic device.[163] Additionally, the automation of the assay procedure is currently under development, which is expected to further reduce the variability of the system.

Employing streptavidin-coated micro-beads as the solid phase, the formation of the immune complex was realized off-chip. With this method, the issue of non-specific adsorption of proteins on the channel walls has been circumvented, thus largely eliminating the potential background noise for the enzymatic reaction that can cause a damageable loss in sensitivity.

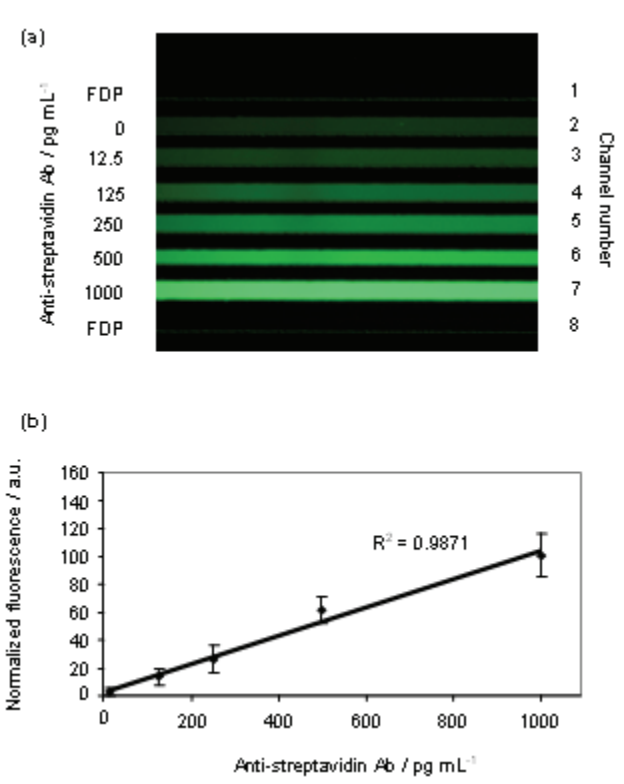

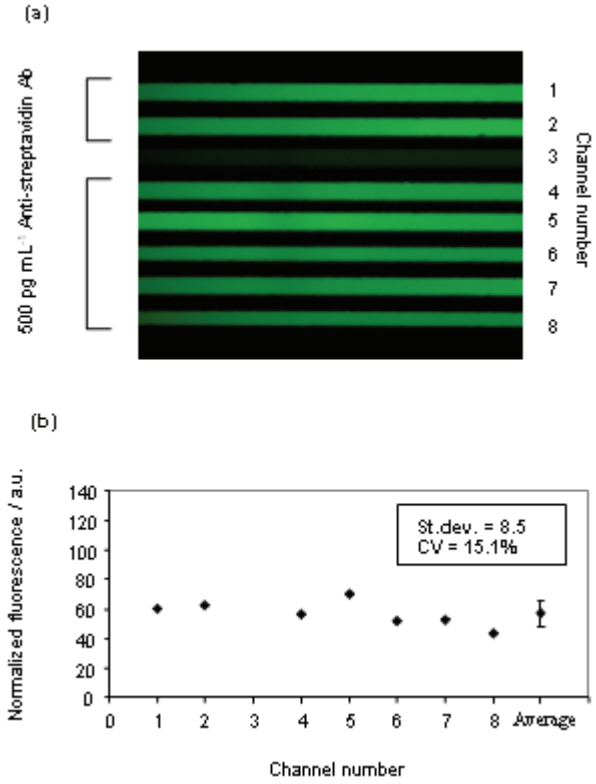

Figure 6.5 (left): Standard curve for the quantification of anti-streptavidin antibodies: (a) fluorescent imaging of the downstream channels after 5 minutes incubation with concentrations of anti-streptavidin antibodies varying from 12.5 pg.mL^{-1} to 1000 pg.mL^{-1} (100x); (b) linear range of quantification for anti-streptavidin antibodies. The averages and error bars were calculated from 3 independent assays.

Figure 6.6 (right): Determination of the intra-assay coefficient of variation: all channels were filled with beads previously incubated with a solution of 500 pg.mL^{-1} anti-streptavidin antibodies and secondary AP-coupled antibodies, except for channel 3 where the beads were incubated with the secondary antibody only. The average fluorescent intensity after normalization was 56.3 a.u., the associated standard deviation was 8.5 a.u., which represented a coefficient of variation of 15.1%.

However, this approach slightly increases the quantity of reagents used, as sub-microliter volumes are not conveniently manipulated outside the chip. The overall duration of the assay is also augmented. Therefore, current efforts are focused on the realization of the entire assay on-chip, including the formation of the immune complex. This next stage of development has been so far limited by the difficulty of obtaining effectively passivated surfaces to avoid random adsorption of proteins on the channel walls.[108,114]

6.5 Conclusion

As a first step toward a microfluidic platform for parallel ELISA in stop-flow conditions, we have developed a system featuring micro-channels molded in PDMS, manipulation of paramagnetic micro-beads and fluorescence detection. The original microfluidic design enables one to conveniently work in stop-flow conditions. The magnetic beads are used both as a solid phase to support the formation of the reactive immune complex and as a means to produce an internal mixing of the solution. In order to test the amplification and detection of the signal inside the microfluidic system, the formation of the immune complex was performed off-chip before the reactive beads were injected into the reaction chamber. A standard curve for the quantification of anti-streptavidin antibodies was realized, exhibiting low picomolar sensitivity, a dynamic range of quantification of 2 orders of magnitude, and inter- and intra- coefficients of variation of about 15%. Current developments include the optimization of the fluidic network, the automation of the magnetic mixing and the treatment of internal surfaces to proceed to the on-chip formation of the immune complex, as well as the quantification of bio-medically relevant proteins.[164] Finally, we believe that the design of the system could allow further integration into a portable biosensor using a miniaturized pump and electromagnets.

Chapter 7
The Dual Network System: Proof-of-concept

This second paper, also published in *Lab-on-a-Chip*, followed up on the previous article by describing a means to realize the immune-complex formation *on-chip* in addition to the generation and the detection of the signal. The entire immunoassay was performed on a single chip, using two interdigitated networks of channels similar to the one developed initially. It is therefore referred to as the Dual Network system. This original method was hereby proved to replace efficiently common physical or chemical treatments used to block non-specific adsorption on PDMS in the presented immunoassay.

With the development of the Dual Network chip, the microfluidic design had to be adjusted, in particular the size and position of the fluidic bridges linking the two networks. Certain challenges related to the fabrication and the operation of the pressure valves had to be overcome.

A specific chip-holder was conceived in order to align the chip on the moving magnets and to secure the tight connection to the valves. A computer-controlled mixing device was also developed in order to provide more freedom and precision for the manipulations of the magnetic beads. The latter was especially necessary for achieving the bead transfer between the two networks of channels prior to the enzymatic reaction phase. This paper establishes the proof-of-concept of the finalized prototype of the Dual Network platform.

Reproduced by permission of The Royal Society of Chemistry - http://dx.doi.org/10.1039/b516031f

Microfluidic ELISA on non-passivated PDMS chip using magnetic bead transfer inside Dual Networks of channels

M. Herrmann,[ab] E. Roy,[b] T. Veres[b] and M. Tabrizian[a]

[a]Biomedical Engineering Department, McGill University
[b]Industrial Materials Institute, National Research Council of Canada

7.1 Abstract

Achieving efficient passivation of micro-channels against non-specific adsorption of biomolecules is a critical aspect of the development of microfluidic ELISA systems. Usual surface treatments such as pre-coating of the channels with serum albumin, exposure to oxygen plasma, poly-ethylene glycol grafting however exhibit a lack of long-term stability, with procedures that can be time-consuming, complex or associated with costly materials and instruments. In this paper, we present a new fluidic design combined with an original strategy of manipulating magnetic beads in order to reduce assay noise in bead-based microfluidic ELISA without the need for prior channel pre-treatment. The novelty of the system relies on the physical separation of the immune complex formation phase and the enzymatic reaction phase into two independent networks of channels. These networks are linked by fluidic bridges, whose openings are controlled by pressure valves, and through which the beads are magnetically transferred. A standard curve for the quantification of a model antibody was obtained within 30 minutes. A detection limit of 100 $pg.mL^{-1}$ (660 fM) and good linearity of the signal up to 4 $ng.mL^{-1}$ were observed.

7.2 Introduction

For more than a decade, microfluidics has been employed to adapt standard bench-work bioassays into time- and cost-effective devices. As a result, techniques such as immunoassays are being increasingly used in clinical diagnostics, food safety and environmental applications.[74,92,99,165] In particular, various platforms for the realization of microfluidic Enzyme-Linked Immuno-Sorbent Assay (ELISA) have been proposed in an effort to reduce the use of large volumes of expensive reagents and hour-long incubation periods, whilst preserving the specificity and the sensitivity of the original assay.[68]

In conjunction with improvement in design and functionality, an important part of the development of microfluidic-based systems has focused on creating bio-functional surfaces and, alternatively, on finding means to efficiently passivate microchannels against non-specific adsorption (NSA) of biomolecules. The latter is especially critical in microfluidic ELISA systems, as the large surface-to-volume ratio greatly amplifies the undesired surface effects that generate noise and lower sensitivity. Many research groups have investigated chemical surface modifications of various polymeric materials to limit the effects of NSA.[166-172] In particular, surface modifications of poly(dimethylsiloxane) (PDMS) have been extensively explored as it is currently the preferred polymer for biochip fabrication.[79,108,119,121,124,173-176] Despite many advantages, PDMS is notorious for its high native hydrophobicity and its tendency to rapidly adsorb biological materials.[177] Usual surface treatments such as pre-coating of the channels with serum albumin, exposure to oxygen plasma and poly-ethylene glycol grafting lack long-term stability, and require procedures that are often time-consuming, complex or associated with costly materials and instruments.

In a previous publication, we proposed an innovative concept of stop-flow microfluidic ELISA in which functionalized magnetic beads were used both as a solid-support to sustain the reactive immune complex formation and as a mean to increase mixing of the surrounding solution during incubation steps.[133] In order to establish the fluidic design and protocol for the enzymatic amplification and fluorescent detection, the reactive immune complex was formed off-chip at the surface of the beads, before the reactive beads were injected inside the microfluidic system. With this method, the enzymatic reaction occurred in unused protein-free channels thus considerably limiting

the assay noise. The necessity to passivate the PDMS chip was then avoided, which represented a substantial reduction in both the time and the complexity of the assay.

In this paper, we describe the next generation of the system, which combines an original fluidic design and the manipulation of magnetic beads to reduce the noise in bead-based microfluidic immunoassays and realize microfluidic ELISA entirely on-chip, without prior channel passivation. This new approach relies on the physical separation of the immune complex formation phase and the enzymatic reaction phase. Two independent networks of channels are used (dual networks), linked by fluidic bridges through which the beads are magnetically transferred. Pressure valves embedded in bi-layered PDMS[59] have been engineered which seal the fluidic bridges when pressure is applied, thus ensuring the complete isolation of the networks and avoiding contamination. Using this new fluidic design and an adapted protocol, a standard curve for the quantification of a model antibody was obtained within 30 minutes. A detection limit of 100 $pg.mL^{-1}$ (660 fM) and good linearity up to a concentration of 4 $ng.mL^{-1}$ were observed.

7.3 Material and methods

7.3.1 Fabrication of the bi-layer PDMS microfluidic ELISA chip

The master for the control layer was fabricated by standard SU-8 photo-lithography. SU-8 1070 photo-resist (Microchem, Newton, MA) was spin-coated on a silicon wafer to achieve a homogenous layer of 40 μm. The patterns were exposed through a high-definition transparent mask (Fineline Imaging, Colorado Springs, CO) with UV-light and developed, resulting in channels with rectangular cross-sections. The features on the control mask were designed at a 101.6% ratio of the desired dimensions to compensate for the shrinkage of PDMS before alignment. For the fabrication of the master corresponding to the fluidic level, a similar method was applied to construct the two networks of channels. The fluidic bridges were fabricated using AZ 50xt positive resist (AZ Electronic Materials, Branchburg, NJ) and aligned on an aligner EVG 6200 (EV Group, Schaerding, Austria). After development, the master was treated with Trichloro(1H,1H,2H,2H-perfluorooctyl)-silane (Sigma-Aldrich, St. Louis, MO) to obtain

a hydrophobic surface and facilitate the release of cured PDMS. The surface treatment was followed by reflow of the positive resist for 10 minutes at 120°C resulting in fluidic bridges with semi-circular cross-sections.

The two layers of PDMS Sylgard184 (Dow Corning, Midland, MI) were cured separately on their respective masters as established by Quake et al.[59] For the control layer, PDMS 5:1 (elastomer base:curing agent) was mixed, degassed at room temperature and poured to obtain a thickness of about 4 mm. For the fluidic layer, PDMS 20:1 was prepared and spin-coated on the fluidic master at a thickness of about 70 μm, forming a 10 μm thick membrane above the 60 μm high fluidic bridges. After a 30 minutes pre-curing step in an oven at 80°C aimed at minimally hardening both layers of PDMS, the control layer was released from its master and the control inlet punched out. It was then aligned on top of the fluidic layer. The bi-layer assembly was further cured at 80°C for at least 2 hours to achieve permanent thermal bonding. Finally, the bi-layer PDMS device was pealed off the fluidic master and the inlets and outlets were punched out. The system was then reversibly sealed on a glass slide and ready for use.

7.3.2 Microfluidic ELISA with dual networks of channels

Trizma Base, Tween-20 and glycine were obtained from Sigma-Aldrich (St. Louis, MO) and magnesium chloride from ACP Chemicals (Slough, UK). The streptavidin-coated magnetic beads (Dynabeads® M-280 Streptavidin) were purchased from Invitrogen (Burlington, ON) and the rabbit anti-streptavidin IgG from Rockland Immunochemicals (Gilbertsville, PA). The secondary alkaline phosphatase (AP) anti-rabbit antibodies and the enzymatic substrate fluorescein diphosphate (FDP) were purchased from Anaspec (San Jose, CA). All protein dilutions and washing steps were performed in 0.1 M Tris, 150 mM NaCl, 0.02% Tween-20, pH = 7.4 (TBS-T). FDP was diluted to a final concentration of 4 μM in the reaction buffer consisting of 0.1 M Tris, 10 mM MgCl2, 10 mM Glycine, pH = 9.0.

Before mounting the PDMS chip on the mixing platform and securing the valve connection, both the fluidic and the control channels were filled with TBS-T using the Channel Outgas Technique (COT).[178] Unless specified otherwise, the protocol for completion of the microfluidic ELISA was performed as reported in table 7.1. For each

step, a few microliters of solution (5-15 μL) were deposited in the inlets and flowed through the channels by connecting the appropriate outlet to a peristaltic pump in withdrawal mode. After each run, the residual solution trapped at the bottom of the inlets was aspirated to avoid cross-contamination of the sequentially injected solutions.

7.3.3 Fluorescent signal detection

An inverted microscope (TE2000-U, Nikon), a stereoscopic zoom microscope (SMZ1500, Nikon) and a digital camera (DXM1200F, Nikon) operated with the ACT-1 software were used to acquire pictures of the channels. For fluorescence imaging, the microscope is equipped with a high-pressure mercury lamp (C-SHG1, Nikon) and with the appropriate set of filters for fluorescein (FITC) excitation and emission wavelengths. The intensity of fluorescence in each channel was measured with ImageJ (software for image processing and analysis in Java, http://rsb.info.nih.gov/ij/). All data were normalized by subtracting the fluorescence intensity obtained in the negative control.

7.4 Results and discussion

7.4.1 Design of microfluidic ELISA with dual networks of channels

The concept of microfluidic ELISA with dual networks of channels relies on the physical separation of the immune complex formation phase and the enzymatic reaction phase (Fig. 7.1a). A first network of channels (complexation network) is used to achieve the formation of the immune complex, consisting of binding consecutive antibodies and antigens to the surface of the magnetic beads. During this phase, several complex solutions are successively pumped through the network, resulting in the non-specific adsorption of proteins on the channel walls, especially secondary antibodies that would normally cause an elevation in the assay noise. Instead, a second network of channels (reaction network), so far unused and thus free of non-specifically adsorbed proteins, is employed to carry on the enzymatic reaction at the surface of the beads that generates the fluorescent signal. Both networks are independent, linked only by fluidic bridges through which the reactive beads are magnetically transferred.

The complexation network is composed of eight inlets connected by 500 µm wide channels, acting as diffusion barrier, to the same number of complexation chambers. Each chamber forms a 480 nL volume in which the beads are magnetically trapped and displaced to prevent local depletion of proteins and homogenize the surrounding solution during incubation periods. Outlet channels connect the eight complexation chambers to a single outlet from which the successive solutions can be flowed using a peristaltic pump in withdrawal mode.

The reaction network is very similar to the complexation one. Inlets, diffusion barriers and chambers, referred to as reaction chambers, are laid out in an identical manner, parallel to those of the complexation network. The outlet section is however different as the eight independent channels converge to form the detection area. Upstream of the detection area, the outlet channels are adjusted to the same length in order to ensure identical flowing conditions. Downstream to the detection area, the outlet channels merged into a second outlet.

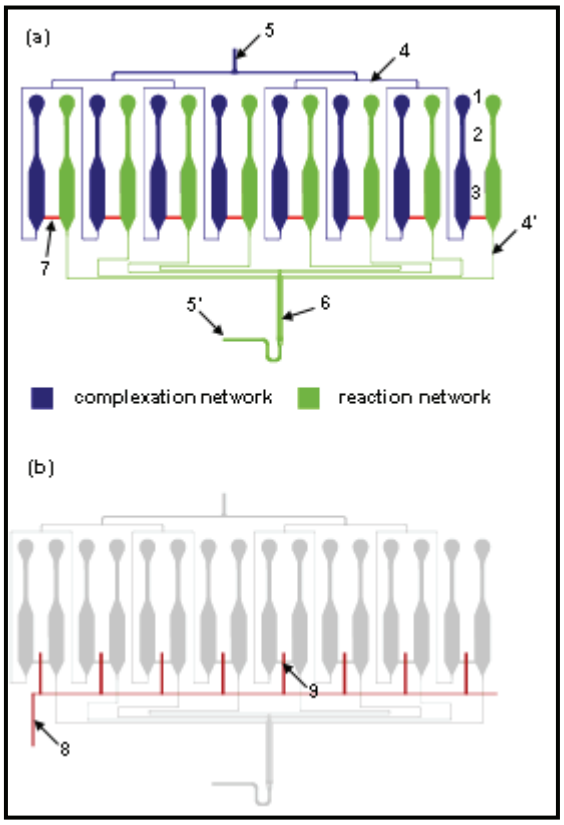

Figure 7.1: Layout of the bi-layer PDMS microfluidic ELISA chip. *(a) Fluidic level*: the solutions are injected into the inlets (1), connected to the complexation/reaction chambers (3) through large channels acting as diffusion barriers (2). In the complexation network, outlet channels (4) of equal length link the complexation chambers to the upper outlet (5). In the reaction network, outlet channels (4') adjusted to the same length come closer to form the detection area (6) and then gather into a larger channel connected to the lower outlet (5'). The two networks are linked by the fluidic bridges (7). *(b) Control level*: the control level is composed of a single closed channel (8) fanning into eight branches to form the pressure valves (9) on the top of the fluidic bridges. The fluidic level is represented in light grey to display the overlap of the control channel on the top of the fluidic channels.

7.4.2 Engineering of pressure valves

In order to avoid contamination of the reaction chambers, pressure valves were engineered to close the fluidic bridges and completely isolate the two networks from one another. The valves are opened to allow the passage of the beads into the reaction network and then closed again to perform the final steps of the assay.

Due to the design of the fluidic network, the control line for the valves necessarily overlaps fluidic channels in order to reach the bridges (Fig. 7.1b). As fluidic bridges should be able to close when pressure is applied without disrupting the flow inside the outlet channels, the width of both the fluidic and control channels were tuned as established by Studer et al.[60] They have demonstrated that as the widths of the overlapping channels increased, less pressure was required to close the valves. In our design, the overlap for operational valves features a 300 x 300 μm area. Non-functional crossings display a limited area of only 50 x 50 μm, thus enabling the selective closing of the bridges.

For the same reason, the fluidic bridges were given a semi-circular cross-section, as opposed to the outlet channels which display a rectangular cross-section.[59] Yet, semi-circular channels are difficult to obtain using a negative resist such as SU-8. They are preferably produced by reflow of a positive resist. Consequently, the fluidic master was fabricated in three consecutive steps (Fig. 7.2). First, all the fluidic features but the bridges were realized in SU-8 at a 40 μm thickness. Next, the fluidic bridges, realized in positive resist at a thickness of 50 μm, were aligned so to connect the pairs of chambers. A final baking step at elevated temperature allowed for the positive resist to reflow giving the bridges their final semi-circular shapes.

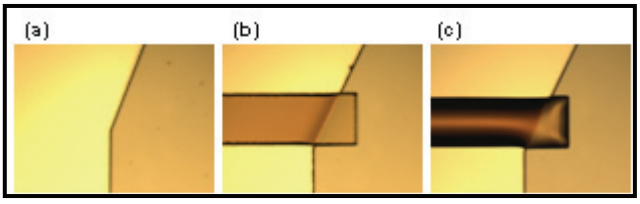

Figure 7.2: Fabrication steps for the fluidic master. (a) The two independent networks of channels are fabricated in the negative resist SU-8. (b) The fluidic bridges are made using the positive resist AZ 50xt. (c) The master is post-baked, hardening the SU-8 and inducing the reflow of fluidic bridges.

Using the fabricated fluidic master, bi-layer PDMS microfluidic ELISA chips were produced in large quantities with high reproducibility of the valve functionality. The pressure necessary to close the valves is supplied by connecting the control channel to a screw syringe with a blunt-ended needle. To prevent leakage at the connection site, the modified needle is passed through a tight piece of rubber and strongly held down together with the PDMS device. A pressure of about 20 PSI in the control line was found to be appropriate to completely and reversibly close the eight valves without disrupting the flow in the outlet channels (Fig. 7.3). The pressure valves proved to be operational for at least several hours, without observable leakage, pressure drop or contamination between the pairs of chambers.

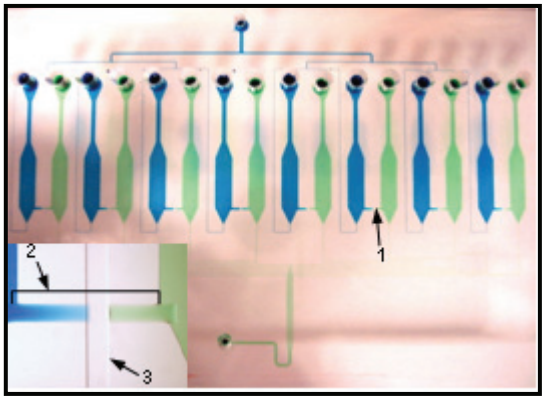

Figure 7.3: Photograph of the PDMS microfluidic ELISA device showing the two independent networks of channels. The complexation network is filled with a blue dye solution; the detection network is filled with green. All eight pressure valves (1) are closed resulting in the complete isolation of the two networks. The insert provides a close-up view of an interrupted fluidic bridge (2) crossed by the control channel (3).

7.4.3 Proof-of-concept: quantification of a model antibody

The operational setup for the realization of the microfluidic ELISA is described in figure 7.4. After priming the channels, the PDMS chip is inserted into its support and the connection for the control channel is secured. A blunt-ended needle, which tightly fits the outlets of the system, is adapted at the end of a tube linked to a peristaltic pump. The pump is then used to flow the diverse solutions through the channels at the required flow rate. The needle can be reversibly and easily switched from one outlet to the other depending on which network is to be operated. Round permanent magnets of 3 mm in

diameter are disposed directly under the PDMS-glass chip. Eight magnets, one for each of the complexation chamber, are precisely aligned and held together by a plastic piece in which holes the size of the magnets have been drilled. The plastic piece is attached to a mixing platform, which can be moved in all directions with micrometer precision in a pre-determined sequence via a Labview software developed in-house.

In order to demonstrate the concept of dual networks to reduce the noise in bead-based microfluidic ELISA, a standard curve for the quantification of a model antibody was realized without prior channel passivation. For this purpose, commercially available magnetic beads coated with a layer of streptavidin, the model antigen, were used to detect anti-streptavidin antibodies, the model analyte (Fig. 7.5). The protocol for the realization of the microfluidic ELISA is presented in Table 7.1. The total assay time was about 30 minutes, mostly due to many pipetting steps, and could be further reduced in a fully automated system. About 10^6 beads were injected and trapped in each of the eight complexation chambers. During the several incubation periods, the beads were continuously displaced from end to end of the chambers at a velocity of 400 $\mu m.sec^{-1}$. The velocity and distance of the magnet to the beads were adjusted so they formed a loose bed that was dragged behind the magnet, thus facilitating the penetration and diffusion of solutions between the beads. After both incubation steps with the analyte antibody and the AP-coupled secondary antibody, the beads were washed twice with TBS-T and transferred to the reaction chambers via the fluidic bridges with transiently opened valves. No pre-treatment of the PDMS chip or glass was performed. As a control experiment, the whole assay was also performed in a single network with identical experimental conditions.

Table 7.1: Protocol for the realization of the microfluidic ELISA with dual networks

Step nb.	Complexation network	Manipulation	Reaction network
1		Close valves	
2	Inject beads		
3	Wash (1x)		
4	Inject primary antibody (antigen)	5 min incubation with mixing	
5	Wash (1x)		
6	Inject AP-coupled secondary antibody	5 min incubation with mixing	
7	Wash (2x)		
8		Open valves	
9	Wash (1x)		
10		Transfer beads	
11		Close valves	
12		5 min incubation with mixing	Inject FDP solution
13			Move reacted solution to the detection area

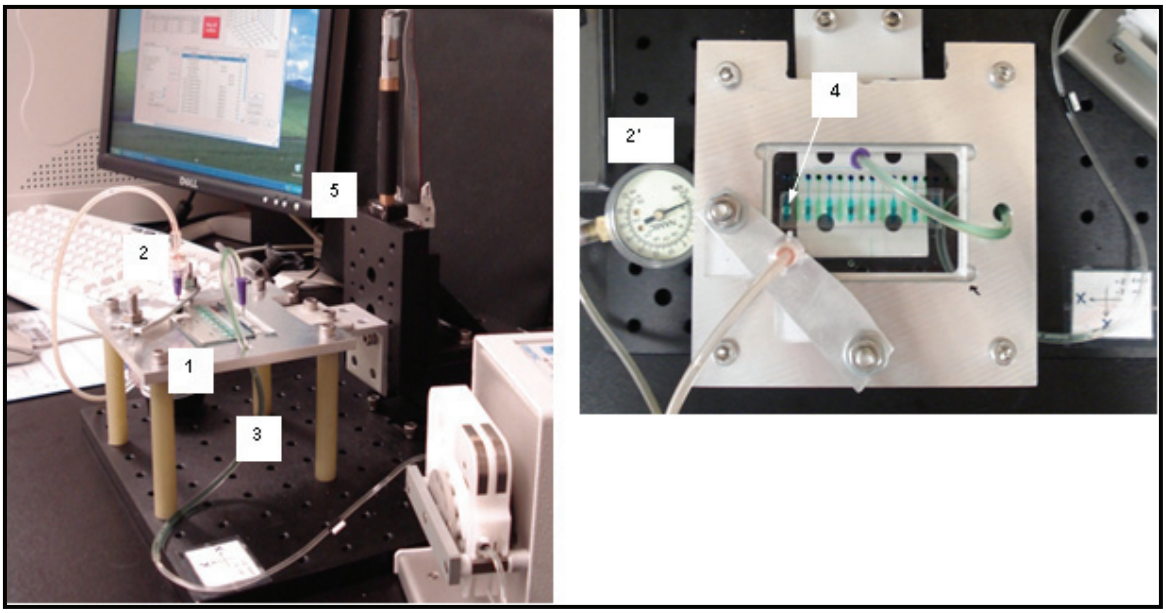

Figure 7.4: Operational platform for microfluidic ELISA: the microfluidic chip is inserted into its support (1). The control channel (2) is connected to a manometer syringe (2') and secured to avoid leakage. One of the fluidic outlets is connected to a peristaltic pump in withdrawal mode (3). Below the chip, the eight permanent magnets (4), mounted on the mixing device (5), are aligned with the complexation chambers.

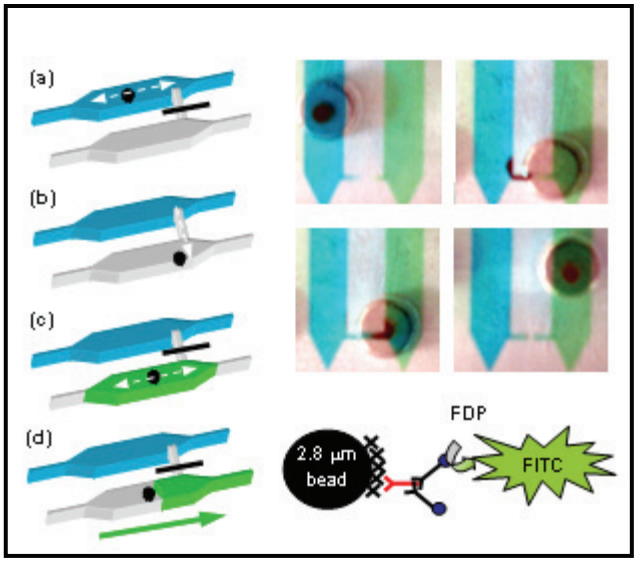

Figure 7.5: Schematic of the immune complex formation and detection procedure: (a) About 10^6 streptavidin-coated magnetic beads are trapped inside the complexation chamber. The anti-streptavidin antibody (analyte) binds specifically to the streptavidin (antigen)-coated beads during a five minutes incubation period with mixing. Similarly, the AP-coupled secondary antibody is added to form the reactive immune complex. (b) The valve is transiently opened and the reactive beads are magnetically transferred into the reaction chamber. (c) The enzyme processes the FDP substrate into the fluorescent molecule FITC. While the reaction takes place, the solution is homogenized by displacing the beads. (d) The reacted solution is then pushed into the detection area.

From the fluorescent microscopy images (Fig. 7.6a), it is striking that the level of noise caused by NSA on the channel walls is greatly reduced in the dual network system. Some residual noise is noticeable when comparing channels 1 and 2 in the dual network system (respectively corresponding to un-reacted FDP solution and the negative control, where only the analyte was omitted from the reaction), which might be due to very low NSA at the surface of the beads, however much less than for the same reactions in the single network system.

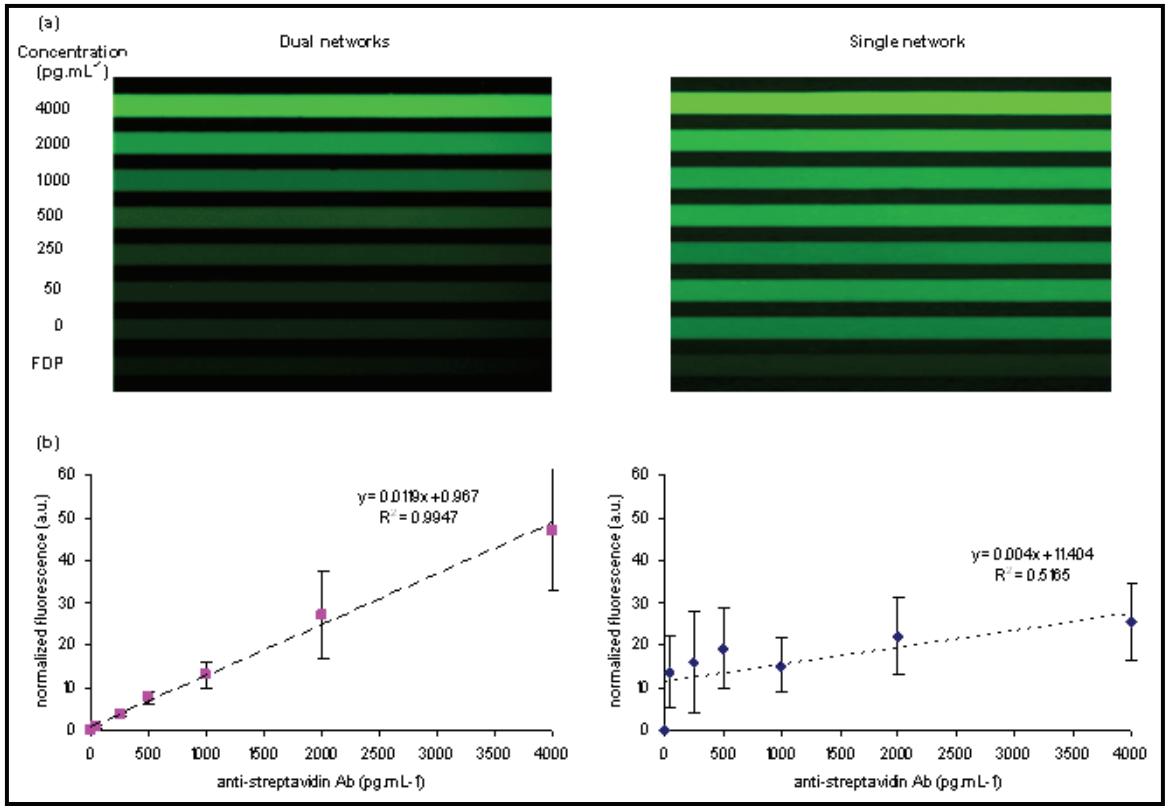

Figure 7.6: Comparative results for microfluidic ELISA without pre-treatment against NSA using a single network and dual networks of channels. (a) Simultaneous fluorescent detection in all eight channels of the device. (b) Standard curves for the quantification of anti-streptavidin antibodies. Each point represents the average obtained on 4 separate experiments.

The reported data are the average of four independent experiments for each of the curves (Fig. 7.6b). To facilitate inter-assay comparison, all values have been normalized by subtracting the signal obtained for the negative control on the same chip. With the dual network protocol, a limit of detection (LOD) of 100 $pg.mL^{-1}$, corresponding to a molarity of about 660 fM (MW = 150 kDa) and good linearity up to 4 $ng.mL^{-1}$ were observed for the tested anti-streptavidin antibody. The LOD was taken as 3 times the standard deviation of 5 negative control replicas. For the two highest concentrations, the standard deviations are quite elevated due to the variation in the reaction kinetics from assay to assay performed on separate chips. This variation could surely be minimized in a platform with automated injection and a better control of external conditions such as temperature and ambient light.

When comparing the assays of the single network to the dual networks, both the sensitivity and linearity are significantly improved for the dual network system. While the absolute values are generally higher in the single network experiment, the normalization to the negative control highlights the weaker contrast in this setup between the lowest and the highest concentrations due to the elevated noise that quickly saturates the signal. The sudden increase between the negative control and the lowest concentration of 50 $pg.mL^{-1}$ can be explained by the fact that several secondary antibodies can bind a non-specifically adsorbed analyte thereby amplifying the noise as compared to directly non-specifically adsorbed secondary antibodies.

The results achieved with the dual network system are close to those obtained in the first iteration of our system where the immune complex was formed off-chip. The decrease in sensitivity, from about 70 fM previously to 660 fM, can be explained by the lesser dispersion of the beads and shorter incubation periods of the on-chip procedure. However, the reduction of the sample size (by a factor of 5) and the shorter total assay time (from several hours to 30 minutes) represent a strong improvement to the global performance of the assay. Moreover, improving bead dispersion and compromising on the incubation times would increase the sensitivity of the assay significantly. Nevertheless, even with the current protocol, the dual network system is among the most sensitive microfluidic immunoassays reported to date,[66,72,76,77,80,89,90,92,95,99,100,105,132,179] without the use of costly, complex and time-consuming pre-treatments.

7.5 Conclusion

In this paper, the novel concept of dual networks of channels was presented. This approach permits to reduce noise in bead-based microfluidic ELISA without the need for prior channel passivation. The original design features two independent networks linked by fluidic bridges, whose openings are controlled by pressure valves. Following the formation of the immune complex, the reactive beads are magnetically transferred through the bridges before performing the final steps of the assay in unused protein-free channels. A three-step lithography process was developed for the fabrication of the fluidic master, on which the bi-layer PDMS device was produced in large quantities with constant functionality. The pressure valves were tested and proved to be operational for at least several hours, without observable leakage, pressure drop or contamination between the dual chambers. A protocol was established, which has permitted to obtain standard curves for the quantification of a model antibody in about 30 minutes. A detection limit of 100 $pg.mL^{-1}$ (660 fM) and good linearity up to 4 $ng.mL^{-1}$ were observed. These data are comparable to the performance of the most sensitive microfluidic immunoassays reported to date without the need for channel pre-treatment.

Chapter 8
Characterization of the Platform's Performances for the Quantification of the Cytokine TNF-alpha

This third and last paper, published in *Analytical Chemistry*, established the potential of the Dual Network microfluidic ELISA platform developed previously for its use in biomedical applications. In particular, the cytokine TNF-alpha was chosen as a model of protein biomarker for two reasons: (i) to facilitate the comparison with commercial ELISA and microfluidic immunoassays systems targeting the same analyte, and (ii) to evaluate the potential of the platform for challenging biomedical applications such as the diagnosis of sepsis.

In this paper, the Dual Network platform was characterized through the optimization of four critical parameters, namely the concentration of the detection antibody, the bead displacement velocity, the incubation times and the detection time. For each of these parameters, a standard curve for the quantification of TNF-alpha was carefully plotted with at least three repetitions of the same experiment. Each condition was discussed and the optimal parameters for this particular analyte were set.

The influence of the solution for the dilution of TNF-alpha was also investigated. The complexity of the surrounding solution was increased from the buffer solution used for the optimization step, to a cell culture medium to pure serum. As a result, a last standard curve for the quantification of TNF-alpha in serum was established, enabling the evaluation of the performance of the Dual Network platform in realistic conditions related to the diagnosis of sepsis.

Quantification of low-picomolar concentrations of TNF-alpha in serum using the Dual Network microfluidic ELISA platform

M. Herrmann,[ab] T. Veres[b] and M. Tabrizian[a]

[a]Biomedical Engineering Department, McGill University

[b]Industrial Materials Institute, National Research Council of Canada

8.1 Abstract

For both research and diagnostic purposes, the ability to detect low levels of proteins in a cost- and time-effective manner is essential. In this study, the cytokine TNF-alpha, a widely used protein indicator of inflammatory response, was chosen to demonstrate the ability of the Dual Network microfluidic ELISA platform developed by the authors to quantify rapidly low concentrations of this biomarker in serum. Through the optimization of several experimental parameters, the system was shown to meet the requirements for fundamental and applied studies, while also relevant for challenging clinical applications such as the diagnosis of septic patients. A sensitivity of 45 pg/mL (2.6 pM) in both culture medium and serum, with inter- and intra-variations of less than 15% were attained for the quantification of human TNF-alpha to a concentration of up to 500 pg/mL. The overall time for completion of the assay in eight parallel reactions was less than an hour.

8.2 Introduction

Tumor Necrosis Factor-alpha (TNF-alpha) is a biomarker frequently assayed for diverse research and diagnostic purposes. It is a small circulating protein of the cytokine family (17.4 kDa), secreted primarily by monocytes and macrophages as a mediator in the early stage of the inflammatory and immune functions.[180] Alone or in combination with other

proteins, TNF-alpha is used as an indicator to follow cellular reactions to external stimuli or to detect certain pathological conditions. Among other applications, TNF-alpha secretion is commonly assessed in immunological studies,[181] and its level measured to determine the biocompatibility of various types of materials and implants.[182] In these studies, the accepted relevant concentrations of TNF-alpha range in the 100 pg/mL bracket. For diagnostic purposes, TNF-alpha is used as an early indicator of inflammatory reactions. When such a reaction occurs, the fine balance between pro- and anti-inflammatory cytokines has to be monitored and maintained in the patient's blood.[3] The up-regulation of pro-inflammatory cytokines, in particular TNF-alpha, can lead to acute inflammatory reactions, tissue injuries or in the instance of a severe infection, to a dangerous state of septic shock. The concentration of TNF-alpha in septic patients typically ranges from 20 to 100 pg/mL, rendering the diagnosis of sepsis particularly challenging even for the most sensitive immunoassays currently in use. Elevated levels of TNF-alpha have also been associated with chronic inflammatory syndromes such as rheumatic arthritis or Crohn's disease.[183]

Conventional immunoassays are time- and resource-consuming, particularly when extensive automation is not economically beneficial or when portability becomes a predominant requirement. Consequently, there has been a sustained effort in the past decade to develop reliable diagnostic tools while reducing the complexity and associated costs of such assays. The miniaturization of immunoassays using microfluidics has been with no contest one of the most popular techniques, as it permits to significantly reduce reagent volumes and incubation times.[28,68,74,82,88,96,132,184] However to date, few microfluidic systems have achieved fast, parallel and highly sensitive detection of biomedically relevant proteins using a single fully functional microfluidic chip.[72,76,89] The Dual Network microfluidic ELISA platform developed in our laboratory has displayed promising characteristics as to achieve that goal.[185] Its original concept relies on the physical separation of the immune complex formation phase and the enzymatic reaction phase into two independent networks of channels. These two networks are linked only by fluidic bridges whose openings are controlled by embedded pressure valves through which the reactive beads are magnetically transferred before the final immunodetection step is performed. As a result, the background noise originated from non-specific

adsorption of protein on the channel walls was eliminated, thereby removing the need for long, costly or unstable pre-treatments.

In this paper, we demonstrate that the Dual Network microfluidic ELISA can be successfully tuned in order to quantify low levels of biomarkers in both cell culture medium and serum, through the adjustment of its most critical assay parameters. The variables regulated were the amount of detection antibody, the bead displacement velocity and the duration of the incubation and detection periods. By doing so, low picomolar concentrations of TNF-alpha were detected in eight parallel reactions with good reproducibility in less than an hour, thus confirming the potential use of this system for biomedical applications in research or for the diagnosis of septic patients in clinical conditions.

8.3 Material and methods

8.3.1 Proteins and reagents

Trizma Base (Tris), Tween-20 and glycine were obtained from Sigma-Aldrich and magnesium chloride from ACP Chemicals. Tosylactivated paramagnetic microbeads (Dynabeads® M-280 Tosylactivated) were purchased from Invitrogen, as well as the pair of capture (AHC 3712) and biotin-labelled detection (AHC 3419) monoclonal antibodies against TNF-alpha. The human recombinant TNF-alpha was obtained from Preprotech and the alkaline phosphatase coupled streptavidin, alkaline phosphatase coupled anti-rabbit and anti-mouse antibodies from Rockland Immunochemicals. The enzymatic substrate fluorescein diphosphate (FDP) was purchased from Anaspec. The washing buffer, also used for priming of the channels, was a Tris buffer saline (0.1 M Tris, 150 mM NaCl, pH = 7.4) supplemented with 0.02% Tween-20 (TBS-T). All proteins were diluted in TBS-T 0.1% BSA as carrier protein, unless mentioned otherwise. The enzymatic substrate FDP was diluted to a final concentration of 4 μM in the reaction buffer consisting of 0.1 M Tris, 10 mM $MgCl_2$, 10 mM Glycine, pH = 9.0.

8.3.2 Tosylactivated beads functionalization

Dynabeads M-280 Tosylactivated were functionalized according to the manufacturer's instructions. Briefly, 200 µL of beads (40.10^7 beads) were thoroughly washed in a 0.1 M borate buffer pH 9.5. The beads were then incubated overnight at 37°C with slow tilt rotation in a solution of the same borate buffer containing the mouse monoclonal capture antibody at a ratio of 3 µg of antibody / 10^7 beads. Subsequently, the beads were washed twice in PBS buffer, pH 7.4, 0.1% BSA at 4°C, once in 0.2 M Tris, pH 8.5, 0.1% BSA for 4 hours at 37°C for blocking the free tosyl-groups and a last time with the PBS buffer at 4°C. The beads were resuspended and stored in 200 µL of PBS, pH 7.4, 0.1% BSA supplemented with 0.02% sodium azide as preservative. Following the above procedure, the functionalized beads were tested to ensure the successful binding of the capture antibodies. On a Dual Network microfluidic ELISA chip featuring eight independent pairs of channels, two were used as negative controls in the presence of non-functionalized beads, three for incubation of the functionalized beads with an alkaline phosphatase coupled anti-rabbit antibody, and the remaining three for incubation of the same beads with an alkaline phosphatase coupled anti-mouse antibody. The results of such a test are provided as supporting information (figure S-8.1).

8.3.3 Protocol for Dual Network microfluidic ELISA with TNF-alpha

Before mounting the chip on the mixing platform and securing the valve connection, both the fluidic and the control channels were filled with TBS-T using the Channel Outgas Technique (COT).[178] The concept of Dual Network and protocol for the quantification of TNF-alpha are summarized in Figure 8.1. For each step, a few microliters of solution (5-15 µL) were deposited in the inlets and flowed through the channels by connecting the appropriate outlet to a peristaltic pump in withdrawal mode. After each run, the residual solution trapped at the bottom of the inlets was aspirated to avoid cross-contamination of the sequentially injected solutions.

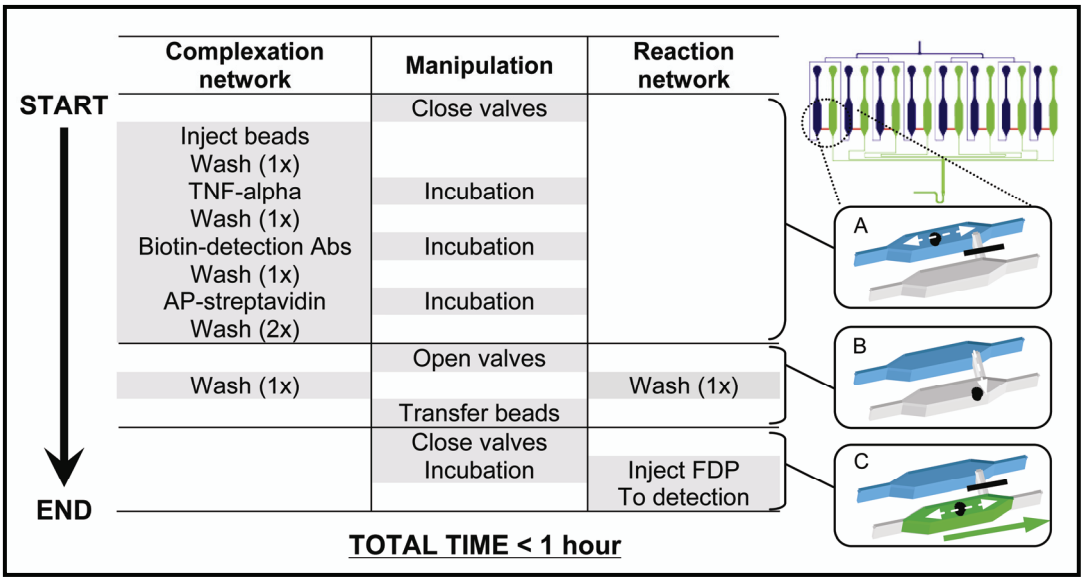

Figure 8.1: Protocol for Dual Network microfluidic ELISA with TNF-alpha. The table indicates the successive steps from top to bottom. The layout of the PDMS chip for 8 parallel reactions is drawn in the top-right corner; the complexation network is colored in blue, the reaction network in green. The windows A, B and C represent close-ups on one pair of dual chambers at different steps of the assay. (A) Complexation phase; the closed valve is represented by the solid black line separating the chambers; the white arrow shows the bead displacement pattern. (B) Magnetic transfer phase. (C) Reaction and detection phases.

8.3.4 Detection and data analysis

An inverted microscope (TE2000-U, Nikon), a stereoscopic zoom microscope (SMZ1500, Nikon) and a digital camera (DXM1200F, Nikon) operated with the ACT-1 software were used to acquire images of the channels along the detection area. For fluorescence imaging, the microscope is equipped with a high pressure mercury lamp (C-SHG1, Nikon) and with the appropriate set of filters for fluorescein (FITC) excitation and emission wavelengths. The intensity of fluorescence in each channel was determined with ImageJ, a Java-based software for image processing and analysis. All data were normalized by subtracting the intensity obtained in the negative control of the same experiment. In order to calculate the sensitivity of the assay for the quantification of TNF-alpha, 3 independent experiments were carried out, each featuring 5 repetitions of the negative control. The standard deviations were then averaged for the 3 experiments.

The sensitivity was calculated by adding 3 times the average standard deviation applied to the equation of the final standard curve.

8.3.5 Fabrication of the Dual Network microfluidic chip

The Dual Network microfluidic chip is composed of two overlaid layers of PDMS (Sylgard184, Dow Corning), both fabricated by casting the pre-cured elastomer on a SU-8 resist (SU-8 1070, Microchem) previously structured by standard photo-lithography. The fluidic bridges, linking the two networks, were fabricated using a positive resist (AZ 50xt, AZ Electronic Materials) and aligned on an aligner EVG 6200 (EV Group, Austria). After development, the master was treated with Trichloro(1H,1H,2H,2H-perfluorooctyl)-silane (Sigma-Aldrich) to obtain a hydrophobic surface and facilitate the release of the cured PDMS. The surface treatment was followed by reflow of the positive resist for 10 minutes at 120°C resulting in fluidic bridges with rounded sections. The two layers of PDMS were cured separately on their respective masters as established by Quake's group.[59] After a pre-curing step of 30 minutes at 80°C, the 4 mm thick top layer was released from its master and aligned on the top of the thin fluidic layer. The bi-layer assembly was further cured at 80°C for at least 2 hours to achieve permanent thermal bonding. Finally, the bi-layer PDMS device was pealed off the fluidic master and the inlets and outlets were punched out. The system was then reversibly sealed on a glass slide and ready for use.

8.4 Results and discussion

8.4.1 Influence of the detection antibody concentration

In immunoassays, an elevated background noise seriously impairs both sensitivity and linear range, and increases variation between tested samples. In our device, the noise generated by non-specific adsorption (NSA) of proteins on the channel walls is eliminated by magnetically transferring the reactive beads into a clean unused reaction chamber. However, some residual background can result from NSA of proteins on the beads themselves. To limit this effect, the functionalized tosylactivated beads are kept for long-term storage in a PBS buffer containing 0.1% BSA as a blocking agent.

Nevertheless, an important parameter to be optimized in this regard is the concentration of detection antibody used for the assay. Ideally, it is necessary to provide enough molecules to bind all previously captured antigens, without adding an excess as to cause an increase in non-specific adsorption and ultimately generate background noise.

Figure 8.2 displays the standard curves obtained for concentrations of TNF-alpha ranging from 10 pg/mL to 1 ng/mL, with respect to increased concentrations of the detection antibody. The incubation and detection times were arbitrary set at 10 minutes, alkaline phosphatase coupled streptavidin was diluted 1:10000 and the bead displacement velocity was adjusted at 400 μm/s. Each curve represents the average of 3 independent experiments realized on separate chips, thus error bars represents the *inter*-assay variations rather than internal variations of the system. The fluorescent signals for each experiment were normalized to the signal obtained in the negative control of the same experiment (all identical steps with no TNF-alpha). In immunoassays, two of the most important parameters are the slope of the curve which reflects the sensitivity of the assay, and the correlation coefficient R^2 which describes its linearity. Accordingly, the optimal concentration for the detection antibody was found to be 0.5 μg/mL. Data obtained with 1.0 μg/mL displayed similar sensitivity values but exhibited lower linearity. With a concentration of 0.25 μg/mL however, the slope was significantly lowered with little improvement in linearity, indicating that not all the captured analytes had been bound by detection antibodies in the allotted time. Conversely, increasing the detection antibody concentration to 2 μg/mL generated considerable background signal, thus impairing both *inter*-assay reproducibility and linearity due to the rapid saturation of the fluorescent signal. Based on this series of experiments, following assays were realized with the optimal detection antibody concentration of 0.5 μg/mL. The standard curve obtained with this specific set of parameters is referred to as the *default* experiment to which later experiments are compared.

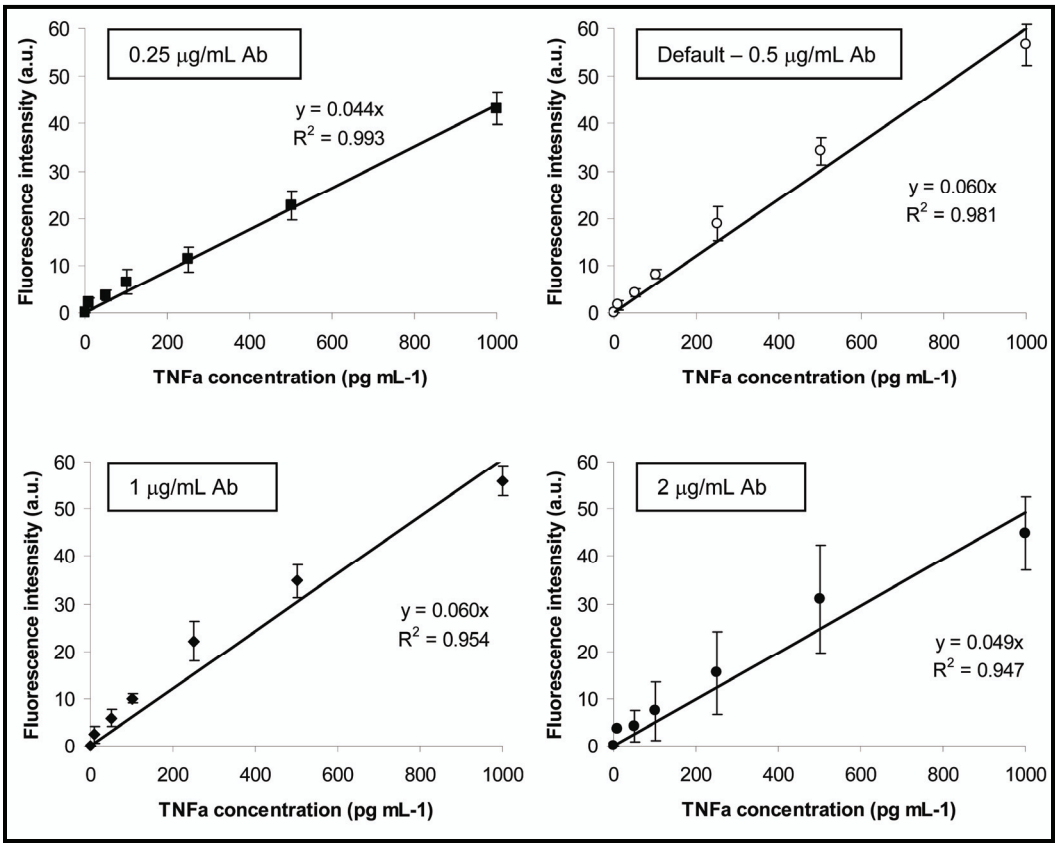

Figure 8.2: Influence of the concentration of detection antibody on the quantification of TNF-alpha by Dual Network microfluidic ELISA. Other parameters were set at their default conditions. All fluorescence intensity data were normalized by subtracting the value of the negative control of the same experiment. Each data point is the average of three independent experiments. Error bars represent the inter-assay variation for each condition.

8.4.2 Influence of bead displacement velocity

Unlike the majority of microfluidic devices, which operate in a continuous flow mode, this immunoassay was designed to work in stop-flow conditions.[133] In this setup, the fluidic channels are filled with the appropriate solution before the flow is stopped for incubation and the next solution is flowed to replace it. This method reduces and improves the control of reagent volumes used, which are defined by the geometry of the channel rather than by the flow rate and manual pipetting. Also it avoids the dependency of the assay performance on the flow rate. In order to prevent local depletion of the analyte molecule at the vicinity of the capture zone,[109] the functionalized beads were

magnetically moved from one end to the other end of the fluidic chamber during incubation periods. This manipulation allowed for the reaching of the analyte molecules in the entire volume of the chamber while creating disturbances in the surrounding solution, thus enhancing the analyte exploitation rate.

Figure 8.3 illustrates the effect of the bead displacement velocity on the outcome of the assay for TNF-alpha. In the *default* experiment, the beads were displaced at the maximum velocity of 400 μm/sec during the three incubation periods, as well as during the enzymatic reaction phase (maximum velocity due to current hardware limitations). When the same experiment was conducted without displacing the beads during the incubation periods (the beads were moved only during the reaction phase), the fluorescent signal was drastically weakened, suggesting rapid local depletion and limited diffusion of the analyte molecules during the 10 minutes of flow stop. When the beads were moved at 200 μm/sec, the overall signal became stronger, coming close to the signal obtained in the *default* experiment. Surprisingly, the curve also displayed a marked saturation profile at higher concentrations of TNF-alpha. This difference in linearity can be explained by the behavior of the beads while being moved inside the fluidic chamber. During flow phase, the beads are held by a strong permanent magnet placed directly under the glass slide that forms the bottom of the chip (approximately 1 mm from the beads). At that distance, the magnetic field is still very strong, thus the beads aggregate in a tight bed with little space between them for the solution to circulate. During incubation phases however, the magnet is moved, followed by a smear of beads, which widens when the movement is faster. The formation of the smear increases bead dispersion which in turn increases the effective surface of capture sites at the functionalized surfaces. According to these results, the bead displacement velocity for further experiments was set at 400 μm/sec.

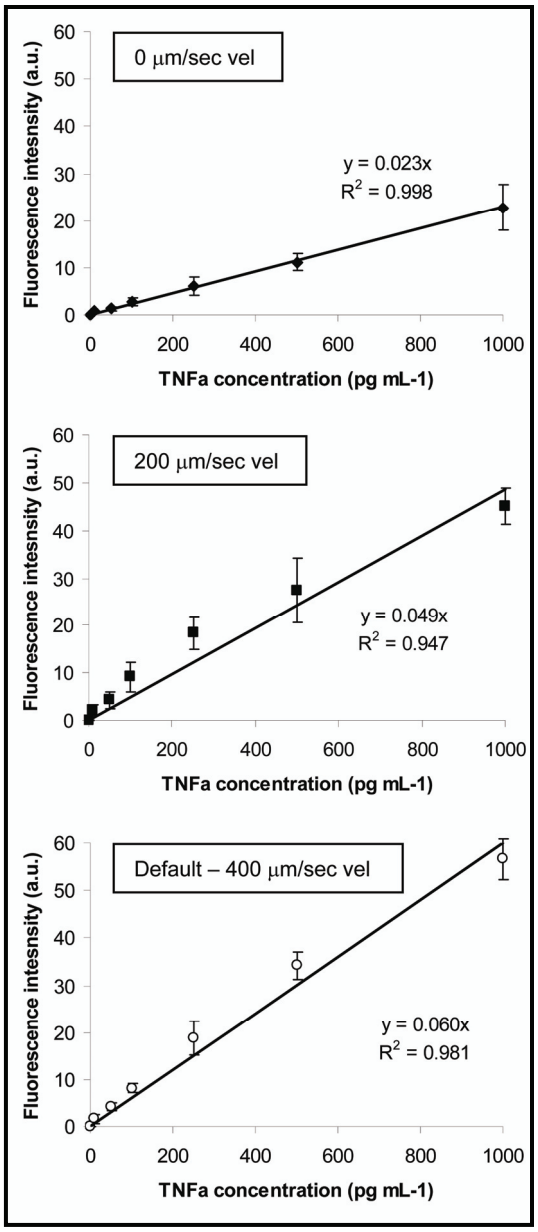

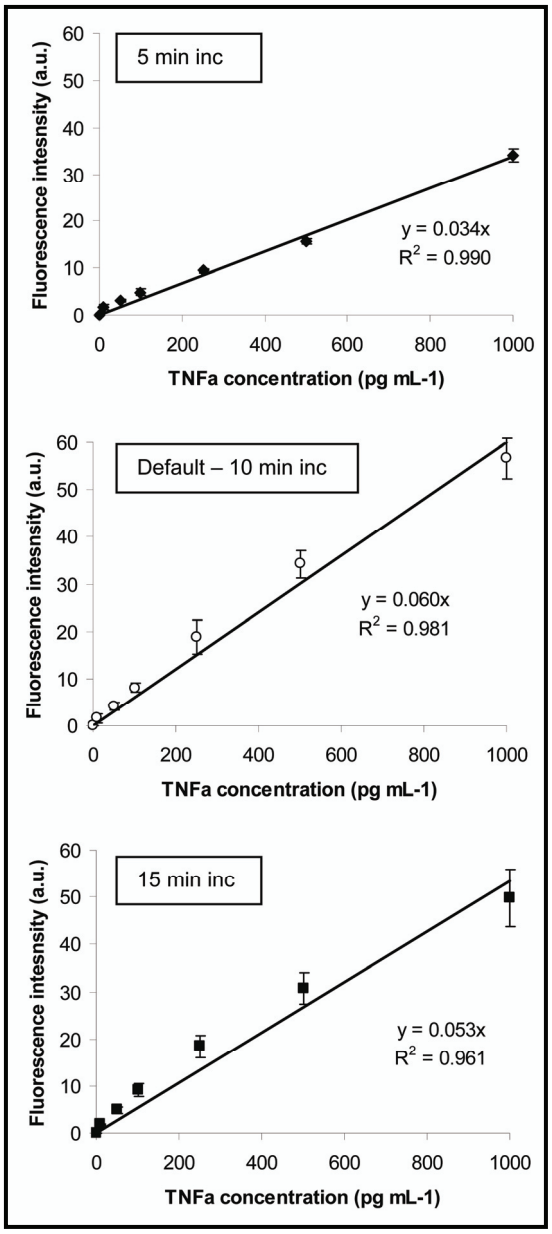

Figure 8.3 (left): Influence of the bead displacement velocity on the quantification of TNF-alpha by Dual Network microfluidic ELISA. Other parameters were set at their default conditions. All fluorescence intensity data were normalized by subtracting the value of the negative control of the same experiment. Each data point is the average of three independent experiments. Error bars represent the inter-assay variation for each condition.

Figure 8.4 (right): Influence of the incubation times on the quantification of TNF-alpha by Dual Network microfluidic ELISA. Other parameters were set at their default conditions. All fluorescence intensity data were normalized by subtracting the value of the negative control of the same experiment. Each data point is the average of three independent experiments. Error bars represent the inter-assay variation for each condition.

8.4.3 Influence of incubation times

Another important parameter affecting the outcome of an immunoassay is the time given for the molecules to interact with each other and form a stable immuno-complex. The present protocol features three sequential incubation periods with respectively, TNF-alpha, the biotinylated detection antibody and the alkaline-phosphatase coupled streptavidin. Variations of the incubation time affected both the slope and the linearity of the standard curve (Figure 8.4). In comparison to the *default* experiment, when the incubation time was reduced by half from 10 to 5 minutes, the slope decreased by about the same factor with only a slight increase in linearity. These data suggest that the saturation of the beads with the maximum loading of TNF-alpha occurs shortly before 10 minutes of incubation, which also explains the slightly saturated profile of the *default* curve. Extending the incubation times to 15 minutes confirmed the bead saturation at higher concentrations, leading to an even less linear and slightly less sensitive curve than the one of the *default* experiment.

8.4.4 Influence of detection time

Following the three incubation periods and the magnetic transfer of the beads carrying the immune complex to the reaction chamber, the reaction network is filled with a solution of the enzymatic substrate for alkaline-phosphatase fluorescein di-phosphate (FDP). The enzymatic reaction converting FDP into green-fluorescent fluorescein then occurs in conditions similar to the previous incubation phase. The extent of the enzymatic amplification period is expected to display a drastic effect on the outcome of the immunoassay and the profile of the standard curve (Figure 8.5). In comparison to the *default* experiment, when the detection time was increased from 10 to 15 minutes, the independent signals obtained for the different concentrations of TNF-alpha were significantly increased. However, the curve can no longer be considered linear on the tested range with a correlation coefficient of only 0.92. The excessively saturated profile in this case stems from at least two major effects. First, the already slightly saturated profile observed in the *default* experiment is further amplified as the enzymatic reaction is extended. Second, the rate of conversion of FDP is likely to decelerate as the concentration of substrate decreases in the substrate solution. Saturation of the detection

device at high fluorescent intensities also enhances the latter effect. Although increasing detection time can significantly improve the overall sensitivity of the assay, it can also be detrimental on both the linearity and the dynamic range as it amplifies minor variations in the signal. For the following experiment, the detection time was maintained at 15 minutes, but incubation periods were shortened from 10 to 5 minutes. Interestingly, the profile obtained was very similar to the one observed in the *default* experiment in terms of both the slope and linearity, with an overall assay time reduced from 40 to 30 minutes. Only a minor increase in the *inter*-assay variability was caused by the extension of the detection time, as the efficiency of the enzymatic reaction differs between each assay due to external conditions, such as temperature or ambient light, and contributes for the largest part to this type of variability.

When setting up an immunoassay, it is important to consider the relevant range of concentrations in which a particular analyte has to be detected and quantified. For a biomarker such as TNF-alpha, although concentrations of several 100 pg/mL can be found in experimental samples, clinical values, for the diagnosis of septic patient for instance, stands typically around 100 pg/mL and below. Therefore, narrowing down the dynamic range to 500 pg/mL, in order to cancel the light saturation effect, might give a more accurate quantification of TNF-alpha around biomedically relevant levels. The doted lines in Figure 8.5 show the corrections made to the standard curves when removing the last data point at 1 ng/mL of TNF-alpha. In all three cases, both the linearity and slope of the curves were improved though to different extents. For the *default* experiment and the experiment with 5 minutes incubation periods, improvements of the slope is moderate (117% and 114% of the respective slopes taken on the full range) while both correlation coefficients approximated 0.99, indicating excellent linearity. The experiment with 10 minutes incubation periods and 15 minutes detection time undergo a more drastic change, with a slope increased by 132% and a linearity approaching 0.97. Nevertheless, because saturation of the signal is still observed in these conditions, this last standard curve can not be used accurately on the designated range of concentrations despite its stronger slope.

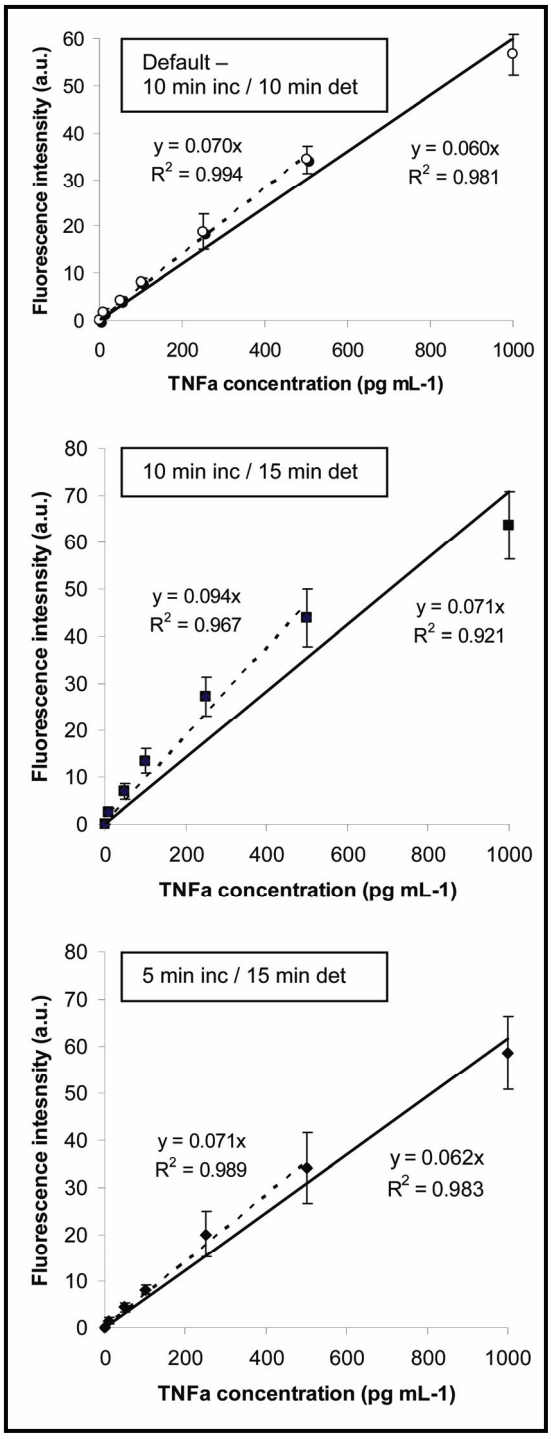

Figure 8.5: Influence of the detection time on the quantification of TNF-alpha by Dual Network microfluidic ELISA. Other parameters were set at their default conditions except for the bottom graph where incubation times were set to 5 minutes each. The solid curve represents the trendline for data points taken between 10 pg/mL and 1 ng/mL; the dashed curve is the trendline for the same data points taken only up to 500 pg/mL. All fluorescence intensity data were normalized by subtracting the value of the negative control of the same experiment. Each data point is the average of three independent experiments. Error bars represent the inter-assay variation for each condition.

8.4.5 Quantification of TNF-alpha in serum

For the adjustment of experimental parameters, all previous experiments were run with TNF-alpha diluted in a TBS buffer supplemented with 0.1% BSA as a protein carrier. In order to show the ability of the Dual Network microfluidic system to perform in conditions close to its final intended use, the previous measurements were repeated with TNF-alpha diluted in a more complex solution (Figure 8.6). First, the experiment was conducted with TNF-alpha diluted in a DMEM cell culture medium supplemented with 10% FBS. The addition of interfering proteins decreased the slope of the standard curve when *default* parameters are used. Nevertheless, by extending the detection incubation period from 10 to 15 minute, the slope was increased to its original value with excellent linearity. Quasi-identical data were obtained with TNF-alpha diluted into pure serum (FBS). The excellent linearity, even with the addition of an extra data point at high concentration of TNF-alpha, demonstrated again the reliability of the standard curve within the tested range of concentrations, from 25 pg/mL to 500 pg/mL. Typically, similar results in cell culture medium and pure FBS are not expected because of the more complex composition of serum containing many uncharacterized proteins that interfere with the reaction. It is very interesting to observe that the Dual Network assay, by getting rid of the larger part of the background noise, manages to maintain the same efficacy in both medium. For clarity, a summary of slope and linearity data for all tested conditions is provided in Table 8.1.

The assay sensitivity was calculated based on 3 independent experiments, each featuring 5 repetitions of the negative control. The value obtained for the quantification of TNF-alpha in a cell culture medium or pure serum was 45 pg/mL (2.56 pM). This sensitivity is considered adequate as it falls within range of concentrations relevant for research and diagnostic purposes. Moreover, concentrations of TNF-alpha as low as 25 pg/mL were consistently detected and fitted very well on the linear standard curve. Error bars represent the variations in the signal obtained from 3 independent experiments performed in identical conditions. The inter-assay coefficient of variation was found to be in the order of 15% or less for concentrations of 50 pg/mL and above. Intra-assay variations were also calculated by running 5 repetitions of a given concentration of TNF-alpha on a single chip along with the appropriate controls. At the exception of the

concentration of 50 pg/mL, for which the intra-assay variation coefficient was calculated at 24%, internal variations were all below 15% for concentrations of 100 pg/mL and above. The specificity of the reaction for TNF-alpha in serum was confirmed by substituting the specific mouse monoclonal capture antibody anti-TNF-alpha with a non-specific mouse IgG control purified from a non-immunized animal (Figure S-8.2). Given inherent variations such as small differences in the number of beads, magnets alignment and fluorescence inhomogeneity, which could be overcome in a more automated and integrated platform, these values are considered very promising at this stage of development.[30]

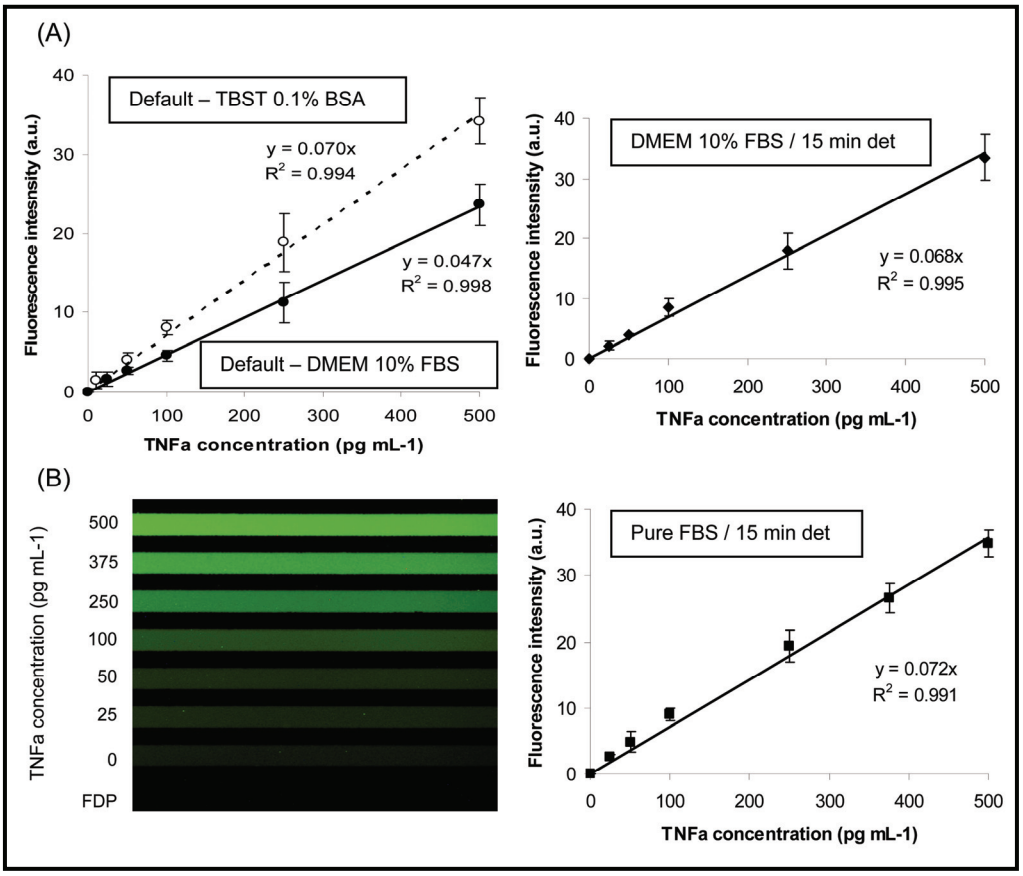

Figure 8.6: Influence of the dilution medium on the quantification of TNF-alpha by Dual Network microfluidic ELISA. (A) The discontinuous curve on the left panel was obtained with default parameters and TNF-alpha diluted in TBST; the continuous curve was obtained in identical conditions with TNF-alpha diluted in a DMEM cell culture medium with 10% FBS. On the right panel, the detection time was extended from 10 to 15 minutes. (B) On the right panel, the standard curve for the quantification of TNF-alpha in pure serum is displayed; all parameters were set to default expect for the 15 minute detection time. The left picture shows a typical fluorescent photograph of the detection area in these conditions.

Table 8.1: Summary of slope and linearity data for all tested conditions. The second set of parameters was arbitrarily chosen as the default conditions and referred to as default experiment throughout the text. For clarity, the most favorable conditions for the quantification of TNF-alpha using the Dual Network microfluidic ELISA platform are shaded in grey.

Nb	Detection Ab concentration (μg/mL)	Bead displacement velocity (μm/sec)	Incubation periods (min)	Detection period (min)	Medium for TNF-alpha dilution	Linear slope up to 1 ng/mL - up to 0.5 ng/mL	Linearity R^2 up to 1 ng/mL - up to 0.5 ng/mL
1	0.25	400	10	10	TBS-T 0.1% BSA	0.044	0.993
2	0.5	400	10	10	TBS-T 0.1% BSA	0.060 - 0.070	0.981 - 0.994
3	1.0	400	10	10	TBS-T 0.1% BSA	0.060	0.954
4	2.0	400	10	10	TBS-T 0.1% BSA	0.049	0.947
5	0.5	0	10	10	TBS-T 0.1% BSA	0.023	0.998
6	0.5	200	10	10	TBS-T 0.1% BSA	0.049	0.947
7	0.5	400	5	10	TBS-T 0.1% BSA	0.034	0.990
8	0.5	400	15	10	TBS-T 0.1% BSA	0.053	0.961
9	0.5	400	10	15	TBS-T 0.1% BSA	0.071 - 0.094	0.921 - 0.967
10	0.5	400	5	15	TBS-T 0.1% BSA	0.062 - 0.071	0.983 - 0.989
11	0.5	400	10	10	DMEM 10% FBS	X - 0.047	X - 0.998
12	0.5	400	10	15	DMEM 10% FBS	X - 0.068	X - 0.995
13	0.5	400	10	15	Pure FBS	X - 0.072	X - 0.991

With low-picomolar sensitivity in both cell culture medium and serum, good reproducibility and a total assay time of less than one hour, the Dual Network microfluidic system places itself among the most achieved microfluidic immunoassays described to date. For the quantification of TNF-alpha specifically, the sensitivity is very near the values obtained with traditional microwell ELISA as well as with the highly sensitive micromosaic assay developed by Cesaro-Tadic *et al.* at IBM Research.[72] Compared to the latter, the overall assay time is significantly reduced, as the combined use of magnetic microbeads and pressure valves removes the need for pre-coating the chip with the capture antibody or blocking the uncoated sites. Reaction volumes of 600 nL, identical to those used in the micromosaic assay, are delimited by the fluidic chambers in which the beads are displaced. No complex design for solution transportation is required since working in stop-flow mode insures minimal influence of the flow rate. Besides, the Dual Network chip is entirely fabricated in PDMS, using only soft-lithography techniques, which makes it simple and inexpensive to produce.

The Dual Network system also compares very well to the most recent commercial products in the field of miniaturized immunoassay, such as the fully automated GyroLab Bioaffy CD platform[76] or the electrochemical-based Gravi-Chip.[99,100] Similar to these systems, the time needed for completion of parallel assays and the throughput of the Dual Network device could benefit greatly from a fully automated platform and a better controlled environment for the enzymatic reaction. Moreover, the sensitivity of the Dual Network assay could be further improved including by integrating the detection device on the platform and by enhancing bead dispersion inside the microfluidic chambers, for example by the use of ultrasonic vibrations or the addition of nanopillars inside the chambers. A better bead dispersion is expected to improve the assay sensitivity in both a direct an a indirect manner: directly by increasing the active capture area, which would also broaden the dynamic range and potentially decrease incubation times for complete analyte exploitation; indirectly by decreasing variability, especially at low concentrations of analyte and for the negative control and by increasing washing efficiency.

8.5 Conclusion

In this paper, we demonstrated the possibility for the rapid quantification of low concentrations of protein biomarkers in serum using the Dual Network microfluidic ELISA platform. By carefully assessing the assay performance as a function of the concentration of the detection antibody, the bead displacement velocity, the incubation and detection time, we have attained a good compromise in terms of sensitivity (2.56 pM), dynamic range of detection (25 – 500 pg/mL), reproducibility (<15% variability) time-efficiency (< 1 hour) and user friendliness. These results suggest that the platform is suitable for fundamental and applied research studies, as well as demonstrates its potential for use in medical applications for the early diagnostic of diseases and infections. These performances, combined to the inexpensive fabrication process and the concept of Dual Network, which removes the need for pretreatment of the chip, contribute to make of this system an extremely sharp, cost-effective and versatile device. The automation of flow injection, the integration of the detection device and the achievement of an enhanced bead dispersion during incubation times are the next

developments to be addressed. These investigations will help to further increase the sensitivity, reproducibility, detection range and throughput of the assay, thereby creating a very competitive platform for performing immunoassays in point-of-care or *on-field* analysis settings.

8.6 Supporting information

The supporting information contains 2 additional figures. The first demonstrates the successful functionalization of the tosyl-activated microbeads (Dynabeads® M-280 Tosylactivated) with monoclonal mouse antibodies directed against human TNF-alpha (Invitrogen, AHC3712) according to the supplier's instructions. The second confirms the specificity of the reaction for TNF-alpha.

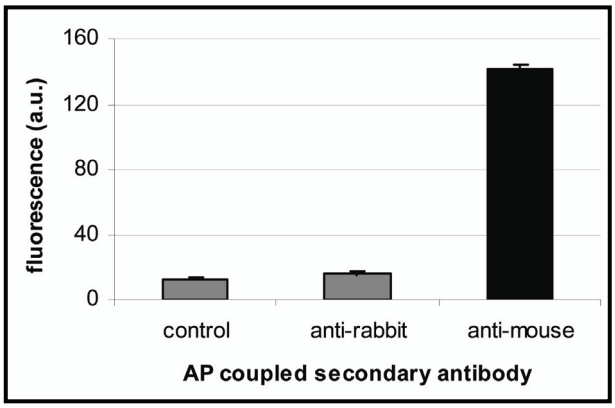

Figure S-8.1: Functionalization test after the coating procedure of the tosylactivated beads with the capture antibody. On a Dual Network microfluidic ELISA chip featuring eight independent pairs of channels, two were used as negative controls in the presence of non-functionalized beads, three for incubating the functionalized beads with an alkaline phosphatase coupled anti-rabbit antibody, and the remaining three for incubating the same beads with an alkaline phosphatase coupled anti-mouse antibody. The controls show very little fluorescence mainly caused by the PDMS bulk and the non-reacted enzymatic substrate FDP. With the anti-rabbit antibody, the registered fluorescent signal is slightly higher, because of minor cross-reactivity of the anti-rabbit antibody with mouse IgG. After 5 minutes incubation of the functionalized beads with the anti-mouse

secondary antibody, a saturating fluorescent signal is observed, which indicates the presence of a high density of capture mouse antibodies at the surface of the functionalized beads.

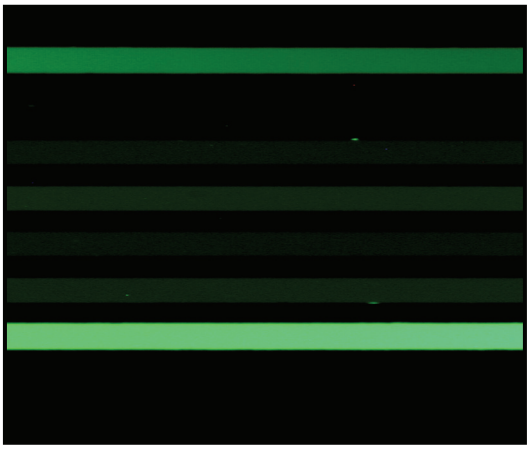

Channel 8: positive control for TNF-alpha (500 pg/mL)
Channel 7: negative control for TNF-alpha (0 pg/mL)
Channel 6: Ms IgG with 500 pg/mL in pure serum
Channel 5: Ms IgG with 500 pg/mL in pure serum
Channel 4: Ms IgG with 250 pg/mL in pure serum
Channel 3: Ms IgG with 250 pg/mL in pure serum
Channel 2: positive control for Ms IgG
Channel 1: FDP control

Figure S-8.2: Confirmation of the specificity of the reaction for TNF-alpha by the substitution of the capture mouse monoclonal antibody anti-TNF-alpha with a non-specific mouse IgG control purified from a non-immunized animal. The eight parallel reaction of the Dual Network microfluidic ELISA chip were set up as follow: 1. FDP control: no beads or proteins were added in this channel. 2. Positive control for functionalization of the tosylactivated beads with the mouse IgG: no TNF-alpha or detection antibodies were added; the AP-coupled streptavidin was replaced by an AP-coupled goat anti-mouse IgG. 3/4. Beads functionalized with mouse IgG were immobilized in these channels. The rest of the reaction was performed with 250 pg/mL of TNF-alpha in serum. 5/6. Beads functionalized with mouse IgG were immobilized in these channels. The rest of the reaction was performed with 500 pg/mL of TNF-alpha in serum. 7. Negative control for the TNF-alpha reaction: beads functionalized with mouse monoclonal anti-TNF-alpha antibodies were immobilized in this channel. The rest of the reaction was performed with no TNF-alpha in serum. 8. Positive control for the TNF-alpha reaction: beads functionalized with mouse monoclonal anti-TNF-alpha antibodies were immobilized in this channel. The rest of the reaction was performed with 500 pg/mL of TNF-alpha in serum.

Despite a slightly more elevated noise in channels 3-6 due to the non-specificity of Ms IgG, no positive reaction was observed with elevated concentrations of TNF-alpha

when using the Ms IgG beads; no concentration-dependent variations were detected. The positive control with Ms IgG (channel 2) confirms the successful functionalization of the beads. Both the negative (channel 7) and positive (channel 8) controls for TNF-alpha in serum were as expected.

Chapter 9
Conclusion and Perspectives

In the first section of this chapter, the objectives established at the beginning of the thesis are reviewed, and a summary of the achievements relative to each of them is given. The second section presents some perspectives on possible future developments, in particular for improvements related to the automation and integration of the current platform. The last section provides a final conclusion to this thesis.

9.1 Summary of achievements and meeting the objectives

1.a. Design a microfluidic chip that is simple and economical to fabricate.

Unlike the majority of devices displaying similar high sensitivities, the Dual Network chip is exclusively fabricated in PDMS. The current method is well adapted for the simple and economical fabrication of prototypes and the production of a reasonably high number of units. Additionally, the Dual Network system eliminates the need for physical or chemical pre-treatments, which further decreases the cost and complexity of fabrication. Other materials, in particular thermoplastic elastomers, could provide an excellent alternative for the inexpensive and rapid production of a large number of these chips, with fabrication procedures more adapted to industrial settings.

1.b. Maintain the versatility and ease of use, and the potential for automation and integration.

With the Dual Network system, no pre-treatment or surface functionalization steps are required prior to the start of the assay. The eight parallel assays on the chip are entirely independent such that the tested protein depends exclusively on the target of the capture entity on the magnetic bead surface. The independent channels can be utilized to test one sample for different biomarkers, or inversely several samples for a unique biomarker. As a result, the Dual Network chip remains extremely versatile. The magnetic microbeads can be functionalized in advance and stored for a long period without a significant loss of activity. The untreated PDMS chips can be kept at room temperature until they are used.

To date, the Dual Network platform is still operated manually. An ordinary peristaltic pump directly connected to one of the chip outlets generates the flow necessary to flush the channels with a new solution. This simple approach is made possible only because of the low influence of the flow rate when working in stop-flow mode. Similarly, simple external devices control the other elementary functions of the platform: a syringe to close the valves, permanent magnets mounted on a 3-axis micromotor to magnetically displace the beads and a standard inverted microscope to capture the parallel fluorescent signals. Despite the multiple steps of the assay protocol, no intervention on the chip itself is required. The PDMS chip is firmly secured onto the platform's holder after the priming step until the final detection step. For these reasons, the implementation of an automated and integrated platform is realistically conceivable. This possibility will be discussed in more detail in the next section.

1.c. Achieve low density parallelization adapted for point-of-care diagnosis while maintaining the possibility for further increasing the throughput.

In the current iteration of the Dual Network chip, up to eight independent reactions can be performed simultaneously. This number has been sufficient to realize a standard curve for the quantification of a single biomarker and for characterization purposes. It could also be adequate for diagnostic applications based on qualitative results. However, this number is still limited when compared to the standard 96-well plate used for bench-top ELISA. In particular, it would be necessary to increase the number of parallel channels on the chip before a precise diagnosis based on quantitative results could be performed. For this type of applications, duplicates or triplicates of samples, standards and controls must be run simultaneously, requiring a larger number of independent reactions. While the current fluidic design does not present any theoretical barrier to increasing the final channel count, the main obstacle preventing the further miniaturization of the system remains the size of the permanent magnets. In a future iteration of the platform, the magnetic bead control device would have to be integrated through the fabrication of electromagnets.

1.d. Equal or surpass the performance of standard bench-top immunoassays while decreasing the time and cost of analysis.

With a quantification range for TNF-alpha between 45 pg/mL and at least 500 pg/mL, the Dual Network platform operates at concentrations comparable to those of standard commercial ELISA kits for the same analyte (10 - 1000 pg/mL). The sensitivity value is also close to the data reported for the optimized micromosaic assay described in section 4.3 (20 pg/mL). Both the inter- and intra-assay variations were below 15 %. The current reproducibility is considered satisfactory, given the lack of control of external conditions (in particular the temperature) and the manual operation of the platform. An automated and integrated platform could further improve the sensitivity, range and reproducibility of the assay, in particular by enhancing the bead dispersion during incubation phases and by better controlling external conditions.

The assay time was decreased from the typically day-long laboratory protocol to about an hour. The volumes of costly reagent and samples were reduced from a minimum of 50 µL in a standard microwell ELISA to 10 µL in the microfluidic assay. This volume was utilized to facilitate manual pipetting, although in actuality, less than 1 µL of solution is required to entirely fill a channel and complete an assay in stop-flow mode. The absence of a blocking step in the Dual Network protocol also contributes to lower the time and cost of analysis. An automated and integrated platform would be expected to increase even further the time- and cost-efficiency of the assay.

2. Demonstrate the potential of the developed platform to perform a rapid and sensitive test for a relevant biomedical application such as the quantification of the cytokine TNF-alpha in the context of sepsis diagnosis.

Following the proof-of-concept established with anti-streptavidin antibodies, the cytokine TNF-alpha was chosen as an example of a biomarker related to various applications. For instance, TNF-alpha is often tested to monitor the reaction of immune cells to stimuli such as chemicals or implantable materials. Also, the upregulation of this protein can reflect pathological conditions, such as the early progress of sepsis following a surgical intervention. After achieving the optimization of the critical assay parameters in a buffer solution, TNF-alpha was diluted in pure serum (or alternatively in a standard cell culture

medium) in order to assess the performance of the assay in more realistic conditions. The sensitivity and quantification range obtained (45 - 500 pg/mL) were within relevant concentration levels for *in-vitro* studies, generally found around several 100 pg/mL. In the context of the sepsis diagnosis, however, pathological values are more commonly situated below 100 pg/mL. Although the potential of the assay was confirmed for the latter application, the sensitivity for the quantification of TNF-alpha would have to be slightly improved to match concentration thresholds as low as 10 pg/mL. Moreover, multiplexed assays with several other biomarkers would have to be implemented and tested on real samples before the platform can be considered a suitable tool for the diagnosis of sepsis.

9.2 Towards an automated and integrated platform

In the previous section, the implementation of an automated and integrated platform was mentioned often as the next important developmental stage to be addressed. While the benefits in terms of costs, assay time and general user friendliness are straightforward, it is also expected to improve the performance of the assay. This section discusses the possibilities of integration for the three main elementary functions of the platform: the fluidic controls, the detection device, and the magnetic bead manipulation device.

9.2.1 Automation and integration of the fluidic controls

In stop-flow mode, the precision of the injected volumes is not critical as the volume used for the assay is defined by the size of the fluidic chamber rather than by the volume delivered in the inlet. As a result, the manual injection of the successive solutions does not contribute to the variability of the assay. Yet, the manual injection requires relatively large inlets to enable convenient loading. The implementation of a series of fluidic pins, which can deliver minute amounts of solution, would permit one to decrease the size of the inlets and increase parallelization. Similar to the injected volume, the precise control of the flow rate is a non-critical issue in stop-flow mode. With the appropriate connections at the two outlets, the generation of the fluidic flow could be controlled by a simple integrated pump delivering sufficient negative pressure to move the solution. The

same pump could be conveniently used to apply and release pressure inside the valves. Finally, the addition of a thermal element enabling work at constant temperature could reduce the incubation times, increase the binding specificity, and improve the reproducibility of the enzymatic reaction.

9.2.2 Automation and integration of the detection device

The miniaturization of several types of detection devices constitutes an important field of interest related to microfluidics. Numerous studies have described the integration of simple optical elements in microfluidic systems for fluorescent measurements.[32,134-139] The standard inverted microscope used in this work could be replaced by a system of diodes (LED) and optical fibers. Ideally, the individual fluorescent measurements should be performed in real-time and converted instantaneously into interpretable values. Moreover, while the current design of the chip was adapted for the enzymatic generation of the fluorescent signal, other detection methods could also benefit from the advantages of the Dual Network system.

9.2.3 Automation and integration of the magnetic bead manipulation device

The miniaturization of the magnetic bead manipulation device would be the most challenging, yet the most essential, aspect of the integrated platform. In the current system, permanent magnets of 3mm in diameter are utilized. Their rather large size constitutes the main obstacle impeding the further miniaturization of the platform. In the future, they could be replaced by a series of electromagnets generating a sufficient force and gradient to capture and move the beads inside the fluidic channels.[40,154,186] The resulting size reduction would lead to the further parallelization of the assays.

Furthermore, when designing the future manipulation device, special care should be given to improving the bead dispersion during the incubation phases, thus increasing the accessibility to binding sites. This feature is expected to enhance the sensitivity, reproducibility, detection range and speed of the assay in a significant manner. The incorporation of microposts inside the fluidic chambers and the use of sophisticated techniques such as diaelectrophoresis (DEP) or ultra-sound waves (USW) are possible approaches to be explored.

9.3 Final Conclusion

The main objective of this thesis was to develop and characterize a microfluidic immunoassay platform adapted for point-of-care diagnosis applications. The assay was conceived to provide high scientific performance comparable to the standard bench-top ELISA, while remaining cost- and time-effective in its fabrication and utilization.

An original design with an adapted detection method was developed to realize rapid parallel microfluidic immunoassays in stop-flow mode. The new concept of Dual Network was also introduced to considerably reduce the background noise due to NSA without costly and complex surface modifications. The last iteration of the Dual Network system combines the multi-purpose use of magnetic beads (as functionalized substrates, mixing elements and carriers for the transfer of the immune-complexes) with the precise control of embedded pressure valves. With these features, a versatile, user friendly and economical microfluidic immunoassay platform was developed.

The characterization of the Dual Network assay was performed using the cytokine TNF-alpha as a model protein biomarker. Through the optimization of the critical assay parameters, a standard curve was established for the rapid quantification of TNF-alpha in serum within the low-picomolar concentration range. The assay performance, comparable to those of commercial ELISA, demonstrated the potential use of this platform for challenging applications such as the cytokine-based diagnosis of sepsis.

The next stage of development should focus on the automation and integration of the platform, with special attention to increasing the number of parallel reactions and the dispersion of beads during the incubation phases. With these future improvements, the Dual Network microfluidic immunoassay platform can become a viable and successful tool for point-of-care diagnosis and other biomolecular analysis applications.

Chapter 10
Cumulative Reference Listing

1 C. Haber, *Lab Chip.*, 2006, **6**, 1118.

2 P. Yager, T. Edwards, E. Fu, K. Helton, K. Nelson, M. R. Tam and B. H. Weigl, *Nature*, 2006, **442**, 412.

3 S. D. Carrigan, G. Scott and M. Tabrizian, *Clin.Chem.*, 2004, **50**, 1301.

4 B. Lu, M. R. Smyth and R. O'Kennedy, *Analyst*, 1996, **121**, 29R.

5 K. Nielsen, M. Lin, D. Gall and M. Jolley, *Methods*, 2000, **22**, 71.

6 T. Pulli, M. Hoyhtya, H. Soderlund and K. Takkinen, *Anal.Chem.*, 2005, **77**, 2637.

7 D. Schmalzing, S. Buonocore and C. Piggee, *Electrophoresis*, 2000, **21**, 3919.

8 P. Englebienne, A. Van Hoonacker and J. Valsamis, *Clin.Chem.*, 2000, **46**, 2000.

9 P. Peluso, D. S. Wilson, D. Do, H. Tran, M. Venkatasubbaiah, D. Quincy, B. Heidecker, K. Poindexter, N. Tolani, M. Phelan, K. Witte, L. S. Jung, P. Wagner and S. Nock, *Anal.Biochem.*, 2003, **312**, 113.

10 S. L. Seurynck-Servoss, C. L. Baird, K. D. Rodland and R. C. Zangar, *Front Biosci.*, 2007, **12**, 3956.

11 R. Ekins, *Nucl.Med.Biol.*, 1994, **21**, 495.

12 C. Hempen, U. Karst, *Anal.Bioanal.Chem.*, 2006, **384**, 572.

13 M. Zayats, I. Willner, *Adv.Biochem.Eng Biotechnol.*, 2008, **109**, 255.

14 F. Ricci, G. Volpe, L. Micheli and G. Palleschi, *Anal.Chim.Acta*, 2007, **605**, 111.

15 B. W. Blais, J. Leggate, J. Bosley and A. Martinez-Perez, *Lett.Appl.Microbiol.*, 2004, **39**, 516.

16 H. Zhang, Q. Zhao, X. F. Li and X. C. Le, *Analyst*, 2007, **132**, 724.

17 M. Schaferling, S. Nagl, *Anal.Bioanal.Chem.*, 2006, **385**, 500.

18 D. A. Vignali, *J.Immunol.Methods*, 2000, **243**, 243.

19 E. Morgan, R. Varro, H. Sepulveda, J. A. Ember, J. Apgar, J. Wilson, L. Lowe, R. Chen, L. Shivraj, A. Agadir, R. Campos, D. Ernst and A. Gaur, *Clin.Immunol.*, 2004, **110**, 252.

20 M. M. Ling, C. Ricks and P. Lea, *Expert.Rev.Mol.Diagn.*, 2007, **7**, 87.

21 D. J. Beebe, G. A. Mensing and G. M. Walker, *Annu.Rev.Biomed.Eng*, 2002, **4**, 261.

22 G. S. Fiorini, D. T. Chiu, *Biotechniques*, 2005, **38**, 429.

23 D. C. Duffy, J. C. McDonald, O. J. A. Schueller and G. M. Whitesides, *Anal.Chem.*, 1998, **70**, 4974.

24 J. M. Ng, I. Gitlin, A. D. Stroock and G. M. Whitesides, *Electrophoresis*, 2002, **23**, 3461.

25 J. C. McDonald, G. M. Whitesides, *Acc.Chem.Res.*, 2002, **35**, 491.

26 K. Hosokawa, T. Fujii and I. Endo, *Anal.Chem.*, 1999, **71**, 4781.

27 R. F. Ismagilov, T. D. Rosmarin, J. A. Kenis, D. T. Chiu, W. Zhang, H. A. Stone and G. M. Whitesides, *Anal.Chem.*, 2001, **73**, 4682.

28 Y. Gao, G. Hu, F. Y. Lin, P. M. Sherman and D. Li, *Biomed.Microdevices.*, 2005, **7**, 301.

29 S. Haeberle, R. Zengerle, *Lab Chip.*, 2007, **7**, 1094.

30 Y. Gao, P. M. Sherman, Y. Sun and D. Li, *Anal.Chim.Acta*, 2008, **606**, 98.

31 P. Morier, C. Vollet, P. E. Michel, F. Reymond and J. S. Rossier, *Electrophoresis*, 2004, **25**, 3761.

32 J. Steigert, M. Grumann, T. Brenner, K. Mittenbuhler, T. Nann, J. Ruhe, I. Moser, S. Haeberle, L. Riegger, J. Riegler, W. Bessler, R. Zengerle and J. Ducree, *JALA*, 2005, **10**, 331.

33 M. Madou, J. Zoval, G. Jia, H. Kido, J. Kim and N. Kim, *Annu.Rev.Biomed.Eng*, 2006,

34 T. H. Schulte, R. L. Bardell and B. H. Weigl, *Clin.Chim.Acta*, 2002, **321**, 1.

35 C. J. Campbell, B. A. Grzybowski, *Philos.Transact.A Math.Phys.Eng Sci.*, 2004, **362**, 1069.

36 B. He, B. J. Burke, X. Zhang, R. Zhang and F. E. Regnier, *Anal.Chem.*, 2001, **73**, 1942.

37 A. D. Stroock, S. K. Dertinger, A. Ajdari, I. Mezic, H. A. Stone and G. M. Whitesides, *Science*, 2002, **295**, 647.

38 N. S. Lynn, D. S. Dandy, *Lab Chip.*, 2007, **7**, 580.

39 T. Park, M. Lee, J. Choo, Y. S. Kim, E. K. Lee, D. J. Kim and S. H. Lee, *Appl.Spectrosc.*, 2004, **58**, 1172.

40 A. Rida, M. A. Gijs, *Anal.Chem.*, 2004, **76**, 6239.

41 N. Pamme, *Lab Chip.*, 2006, **6**, 24.

42 M. Grumann, A. Geipel, L. Riegger, R. Zengerle and J. Ducree, *Lab Chip.*, 2005, **5**, 560.

43 K. S. Ryu, K. Shaikh, E. Goluch, Z. Fan and C. Liu, *Lab Chip.*, 2004, **4**, 608.

44 N. Sasaki, T. Kitamori and H. B. Kim, *Lab Chip.*, 2006, **6**, 550.

45 S. T. Chang, E. Beaumont, D. N. Petsev and O. D. Velev, *Lab Chip.*, 2008, **8**, 117.

46 A. Gunther, M. Jhunjhunwala, M. Thalmann, M. A. Schmidt and K. F. Jensen, *Langmuir*, 2005, **21**, 1547.

47 P. Garstecki, J. Fuerstman, M. A. Fischbach, S. K. Sia and G. M. Whitesides, *Lab Chip.*, 2006, **6**, 207.

48 G. Takei, M. Nonogi, A. Hibara, T. Kitamori and H. B. Kim, *Lab Chip.*, 2007, **7**, 596.

49 C. H. Ahn, J. W. Choi, G. Beaucage, J. H. Nevin, J. B. Lee, A. Puntambekar and J. Y. Lee, *Proceedings of the IEEE*, 2004, **92**, 154.

50 N. Nashida, W. Satoh, J. Fukuda and H. Suzuki, *Biosens.Bioelectron.*, 2007, **22**, 3167.

51 J. M. Park, Y. K. Cho, B. S. Lee, J. G. Lee and C. Ko, *Lab Chip.*, 2007, **7**, 557.

52 Y. K. Cho, J. G. Lee, J. M. Park, B. S. Lee, Y. Lee and C. Ko, *Lab Chip.*, 2007, **7**, 565.

53 J. Y. Cheng, L. C. Hsiung, *Biomed.Microdevices.*, 2004, **6**, 341.

54 J. Wang, Z. Chen, M. Mauk, K. S. Hong, M. Li, S. Yang and H. H. Bau, *Biomed.Microdevices.*, 2005, **7**, 313.

55 D. Kim, D. J. Beebe, *Lab Chip.*, 2007, **7**, 193.

56 P. M. Pilarski, S. Adamia and C. J. Backhouse, *J.Immunol.Methods*, 2005, **305**, 48.

57 W. H. Grover, R. H. Ivester, E. C. Jensen and R. A. Mathies, *Lab Chip.*, 2006, **6**, 623.

58 D. B. Weibel, M. Kruithof, S. Potenta, S. K. Sia, A. Lee and G. M. Whitesides, *Anal.Chem.*, 2005, **77**, 4726.

59 M. A. Unger, H. P. Chou, T. Thorsen, A. Scherer and S. R. Quake, *Science*, 2000, **288**, 113.

60 V. Studer, A. Pandolfi, M. Ortiz, W. F. Anderson and S. R. Quake, *Journal of Applied Physics*, 2004, **95**, 393.

61 T. Thorsen, S. J. Maerkl and S. R. Quake, *Science*, 2002, **298**, 580.

62 C. L. Hansen, M. O. Sommer and S. R. Quake, *Proc.Natl.Acad.Sci.U.S.A*, 2004, **101**, 14431.

63 J. W. Hong, V. Studer, G. Hang, W. F. Anderson and S. R. Quake, *Nat.Biotechnol.*, 2004, **22**, 435.

64 J. S. Marcus, W. F. Anderson and S. R. Quake, *Anal.Chem.*, 2006, **78**, 956.

65 J. S. Marcus, W. F. Anderson and S. R. Quake, *Anal.Chem.*, 2006, **78**, 3084.

66 E. P. Kartalov, J. F. Zhong, A. Scherer, S. R. Quake, C. R. Taylor and W. F. Anderson, *Biotechniques*, 2006, **40**, 85.

67 S. W. Nam, D. V. Noort, Y. Yang and S. Park, *Lab Chip.*, 2007, **7**, 638.

68 L. J. Lee, S. T. Yang, S. Lai, Y. Bai, W. C. Huang and Y. J. Juang, *Adv.Clin.Chem.*, 2006, **42**, 255.

69 C. T. Lim, Y. Zhang, *Biosens.Bioelectron.*, 2007, **22**, 1197.

70 T. G. Henares, F. Mizutani and H. Hisamoto, *Anal.Chim.Acta*, 2008, **611**, 17.

71 A. Hatch, A. E. Kamholz, K. R. Hawkins, M. S. Munson, E. A. Schilling, B. H. Weigl and P. Yager, *Nat.Biotechnol.*, 2001, **19**, 461.

72 S. Cesaro-Tadic, G. Dernick, D. Juncker, G. Buurman, H. Kropshofer, B. Michel, C. Fattinger and E. Delamarche, *Lab Chip.*, 2004, **4**, 563.

73 M. Wolf, D. Juncker, B. Michel, P. Hunziker and E. Delamarche, *Biosens.Bioelectron.*, 2004, **19**, 1193.

74 S. K. Sia, V. Linder, B. A. Parviz, A. Siegel and G. M. Whitesides, *Angew.Chem.Int.Ed Engl.*, 2004, **43**, 498.

75 Q. Xiang, G. Hu, Y. Gao and D. Li, *Biosens.Bioelectron.*, 2005,

76 N. Honda, U. Lindberg, P. Andersson, S. Hoffmann and H. Takei, *Clin.Chem.*, 2005, **51**, 1955.

77 V. Linder, S. K. Sia and G. M. Whitesides, *Anal.Chem.*, 2005, **77**, 64.

78 C. Luo, Q. Fu, H. Li, L. Xu, M. Sun, Q. Ouyang, Y. Chen and H. Ji, *Lab Chip.*, 2005, **5**, 726.

79 Y. Dong, K. S. Phillips and Q. Cheng, *Lab Chip.*, 2006, **6**, 675.

80 J. F. Dishinger, R. T. Kennedy, *Anal.Chem.*, 2007, **79**, 947.

81 E. Fu, T. Chinowsky, K. Nelson, K. Johnston, T. Edwards, K. Helton, M. Grow, J. W. Miller and P. Yager, *Ann.N.Y.Acad.Sci.*, 2007, **1098**, 335.

82 A. E. Herr, A. V. Hatch, D. J. Throckmorton, H. M. Tran, J. S. Brennan, W. V. Giannobile and A. K. Singh, *Proc.Natl.Acad.Sci.U.S.A*, 2007, **104**, 5268.

83 A. E. Herr, A. V. Hatch, W. V. Giannobile, D. J. Throckmorton, H. M. Tran, J. S. Brennan and A. K. Singh, *Ann.N.Y.Acad.Sci.*, 2007, **1098**, 362.

84 K. E. Nelson, J. O. Foley and P. Yager, *Anal.Chem.*, 2007, **79**, 3542.

85 V. N. Morozov, S. Groves, M. J. Turell and C. Bailey, *J.Am.Chem.Soc.*, 2007, **129**, 12628.

86 B. M. Murphy, X. He, D. Dandy and C. S. Henry, *Anal.Chem.*, 2008, **80**, 444.

87 M. A. Hayes, T. N. Polson, A. N. Phayre and A. A. Garcia, *Anal.Chem.*, 2001, **73**, 5896.

88 K. Sato, M. Tokeshi, T. Odake, H. Kimura, T. Ooi, M. Nakao and T. Kitamori, *Anal.Chem.*, 2000, **72**, 1144.

89 E. D. Goluch, J. M. Nam, D. G. Georganopoulou, T. N. Chiesl, K. A. Shaikh, K. S. Ryu, A. E. Barron, C. A. Mirkin and C. Liu, *Lab Chip.*, 2006, **6**, 1293.

90 T. Yasukawa, M. Suzuki, T. Sekiya, H. Shiku and T. Matsue, *Biosens.Bioelectron.*, 2007, **22**, 2730.

91 M. M. Caulum, B. M. Murphy, L. M. Ramsay and C. S. Henry, *Anal.Chem.*, 2007, **79**, 5249.

92 Y. K. Hahn, Z. Jin, J. H. Kang, E. Oh, M. K. Han, H. S. Kim, J. T. Jang, J. H. Lee, J. Cheon, S. H. Kim, H. S. Park and J. K. Park, *Anal.Chem.*, 2007, **79**, 2214.

93 L. J. Lucas, J. N. Chesler and J. Y. Yoon, *Biosens.Bioelectron.*, 2007, **23**, 675.

94 F. Lacharme, C. Vandevyver and M. A. Gijs, *Anal.Chem.*, 2008,

95 E. Eteshola, M. Balberg, *Biomed.Microdevices.*, 2004, **6**, 7.

96 S. Lai, S. Wang, J. Luo, L. J. Lee, S. T. Yang and M. J. Madou, *Anal.Chem.*, 2004, **76**, 1832.

97 R. Kurita, Y. Yokota, Y. Sato, F. Mizutani and O. Niwa, *Anal.Chem.*, 2006, **78**, 5525.

98 A. Bhattacharyya, C. M. Klapperich, *Biomed.Microdevices.*, 2007, **9**, 245.

99 D. Hoegger, P. Morier, C. Vollet, D. Heini, F. Reymond and J. S. Rossier, *Anal.Bioanal.Chem.*, 2007, **387**, 267.

100 J. S. Rossier, H. H. Girault, *Lab Chip.*, 2001, **1**, 153.

101 H. Dong, C. M. Li, Y. F. Zhang, X. D. Cao and Y. Gan, *Lab Chip.*, 2007, **7**, 1752.

102 J. W. Choi, K. W. Oh, J. H. Thomas, W. R. Heineman, H. B. Halsall, J. H. Nevin, A. J. Helmicki, H. T. Henderson and C. H. Ahn, *Lab Chip.*, 2002, **2**, 27.

103 J. Moorthy, G. A. Mensing, D. Kim, S. Mohanty, D. T. Eddington, W. H. Tepp, E. A. Johnson and D. J. Beebe, *Electrophoresis*, 2004, **25**, 1705.

104 Y. Murakami, T. Endo, S. Yamamura, N. Nagatani, Y. Takamura and E. Tamiya, *Anal.Biochem.*, 2004, **334**, 111.

105 K. Sato, M. Yamanaka, T. Hagino, M. Tokeshi, H. Kimura and T. Kitamori, *Lab Chip.*, 2004, **4**, 570.

106 J. Do, C. H. Ahn, *Lab Chip.*, 2008, **8**, 542.

107 J. H. Maeng, B. C. Lee, Y. J. Ko, W. Cho, Y. Ahn, N. G. Cho, S. H. Lee and S. Y. Hwang, *Biosens.Bioelectron.*, 2008, **23**, 1319.

108 H. Makamba, J. H. Kim, K. Lim, N. Park and J. H. Hahn, *Electrophoresis*, 2003, **24**, 3607.

109 M. Zimmermann, E. Delamarche, M. Wolf and P. Hunziker, *Biomed.Microdevices.*, 2005, **7**, 99.

110 B. Huang, H. Wu, S. Kim and R. N. Zare, *Lab Chip.*, 2005, **5**, 1005.

111 L. S. Roach, H. Song and R. F. Ismagilov, *Anal.Chem.*, 2005, **77**, 785.

112 E. Delamarche, C. Donzel, M. Geissler, A. Bernard, H. Wolf, B. Michel, J. Hilborn and E. Delamarche, *Advanced materials*, 2001, **13**, 1164.

113 E. Delamarche, C. Donzel, F. S. Kamounah, H. Wolf, M. Geissler, R. Stutz, P. Schmidt-Winkel, B. Michel, H. J. Mathieu and K. Schaumberg, *Langmuir*, 2003, **19**, 8749.

114 A. Papra, A. Bernard, D. Junker, N. B. Larsen, B. Michel and E. Delamarche, *Langmuir*, 2001, **17**, 4090.

115 H. Mao, T. Yang and P. S. Cremer, *Anal.Chem.*, 2002, **74**, 379.

116 T. Yang, O. K. Baryshnikova, H. Mao, M. A. Holden and P. S. Cremer, *J.Am.Chem.Soc.*, 2003, **125**, 4779.

117 K. S. Phillips, Q. Cheng, *Anal.Chem.*, 2005, **77**, 327.

118 Y. Liu, J. C. Fanguy, J. M. Bledsoe and C. S. Henry, *Anal.Chem.*, 2000, **72**, 5939.

119 H. Makamba, Y. Y. Hsieh, W. C. Sung and S. H. Chen, *Anal.Chem.*, 2005, **77**, 3971.

120 W. C. Sung, C. C. Chang, H. Makamba and S. H. Chen, *Anal.Chem.*, 2008,

121 W. Hellmich, J. Regtmeier, T. T. Duong, R. Ros, D. Anselmetti and A. Ros, *Langmuir*, 2005, **21**, 7551.

122 M. R. Dusseiller, B. Niederberger, B. Stadler, D. Falconnet, M. Textor and J. Voros, *Lab Chip.*, 2005, **5**, 1387.

123 J. Lahann, M. Balcells, H. Lu, T. Rodon, K. F. Jensen and R. Langer, *Anal.Chem.*, 2003, **75**, 2117.

124 H. Y. Chen, Y. Elkasabi and J. Lahann, *J.Am.Chem.Soc.*, 2006, **128**, 374.

125 K. C. Popat, T. A. Desai, *Biosens.Bioelectron.*, 2004, **19**, 1037.

126 D. Xiao, T. V. Le and M. J. Wirth, *Anal.Chem.*, 2004, **76**, 2055.

127 S. Hu, X. Ren, M. Bachman, C. E. Sims, G. P. Li and N. Allbritton, *Anal.Chem.*, 2002, **74**, 4117.

128 S. Hu, X. Ren, M. Bachman, C. E. Sims, G. P. Li and N. L. Allbritton, *Anal.Chem.*, 2004, **76**, 1865.

129 H. Wu, J. Zhai, Y. Tian, H. Lu, X. Wang, W. Jia, B. Liu, P. Yang, Y. Xu and H. Wang, *Lab Chip.*, 2004, **4**, 588.

130 G. T. Roman, T. Hlaus, K. J. Bass, T. G. Seelhammer and C. T. Culbertson, *Anal.Chem.*, 2005, **77**, 1414.

131 K. B. Mogensen, H. Klank and J. P. Kutter, *Electrophoresis*, 2004, **25**, 3498.

132 E. Eteshola, D. Leckband, *Sensors and Actuators B: Chemical*, 2001, **72**, 129.

133 M. Herrmann, T. Veres and M. Tabrizian, *Lab Chip.*, 2006, **6**, 555.

134 L. Novak, P. Neuzil, J. Pipper, Y. Zhang and S. Lee, *Lab Chip.*, 2007, **7**, 27.

135 O. Schmidt, M. Bassler, P. Kiesel, C. Knollenberg and N. Johnson, *Lab Chip.*, 2007, **7**, 626.

136 K. Miyaki, Y. Guo, T. Shimosaka, T. Nakagama, H. Nakajima and K. Uchiyama, *Anal.Bioanal.Chem.*, 2005, **382**, 810.

137 M. L. Chabinyc, D. T. Chiu, J. C. McDonald, A. D. Stroock, J. F. Christian, A. M. Karger and G. M. Whitesides, *Anal.Chem.*, 2001, **73**, 4491.

138 O. Hofmann, X. Wang, A. Cornwell, S. Beecher, A. Raja, D. D. Bradley, A. J. deMello and J. C. deMello, *Lab Chip.*, 2006, **6**, 981.

139 J. E. Knittle, D. Roach, P. B. Horn and K. O. Voss, *Anal.Chem.*, 2007, **79**, 9478.

140 E. Yacoub-George, L. Meixner, W. Scheithauer, A. Koppi, S. Drost, H. Wolf, C. Danapel and K. A. Feller, *Analytica.Chemica.Acta.*, 2002, **457**, 3.

141 S. P. Mulvaney, C. L. Cole, M. D. Kniller, M. Malito, C. R. Tamanaha, J. C. Rife, M. W. Stanton and L. J. Whitman, *Biosens.Bioelectron.*, 2007,

142 N. J. Ronkainen-Matsuno, J. H. Thomas, H. B. Halsall and W. R. Heineman, *TrAC Trends in Analytical Chemistry*, 2002, **21**, 213.

143 M. S. Wilson, *Anal.Chem.*, 2005, **77**, 1496.

144 K. J. Soo, H. C. Yoon, H. Yang, H. B. Pyo, C. K. Hyo, K. S. Jin and K. Y. Tae, *Lab Chip.*, 2003, **3**, 106.

145 A. Bange, H. B. Halsall and W. R. Heineman, *Biosens.Bioelectron.*, 2005, **20**, 2488.

146 J. Steigert, M. Grumann, T. Brenner, K. Mittenbuhler, T. Nann, J. Ruhe, I. Moser, S. Haeberle, L. Riegger, J. Riegler, W. Bessler, R. Zengerle and J. Ducree, *JALA*, 2005, **10**, 331.

147 A. Bernard, B. Michel and E. Delamarche, *Anal.Chem.*, 2001, **73**, 8.

148 J. P. Golden, C. R. Taitt, L. C. Shriver-Lake, Y. S. Shubin and F. S. Ligler, *Talenta*, 2005, **65**, 1078.

149 J. C. McDonald, S. J. Metallo and G. M. Whitesides, *Anal.Chem.*, 2001, **73**, 5645.

150 A. Gulliksen, L. A. Solli, K. S. Drese, O. Sorensen, F. Karlsen, H. Rogne, E. Hovig and R. Sirevag, *Lab Chip.*, 2005, **5**, 416.

151 S. Cesaro-Tadic, G. Dernick, D. Juncker, G. Buurman, H. Kropshofer, B. Michel, C. Fattinger and E. Delamarche, *Lab Chip.*, 2004, **4**, 563.

152 N. B. Liabakk, K. Nustad and T. Espevik, *J.Immunol.Methods*, 1990, **134**, 253.

153 J. C. Forest, J. Masse and A. Lane, *Clin.Biochem.*, 1998, **31**, 81.

154 M. A. M. Gijs, *Microfluidic Nanofluidic*, 2004, 22.

155 M. A. Hayes, T. N. Polson and A. A. Garcia, *Langmuir*, 2001, **17**, 2866.

156 M. A. Hayes, T. N. Polson and A. A. Garcia, *Langmuir*, 2001, **17**, 2866.

157 Tao Deng, Mara Prentiss and Georges M.Whitesides, *Applied Physics Letters*, 2002, **80**, 461.

158 H. Hartshorne, C. J. Backhouse and W. E. Lee, *Sensors and Actuators B*, 2004, **99**, 592.

159 K. S. Kim, J. K. Park, *Lab Chip.*, 2005, **5**, 657.

160 G. Degre, E. Brunet, A. Dodge and P. Tabeling, *Lab Chip.*, 2005, **5**, 691.

161 J. Montalibet, K. I. Skorey and B. P. Kennedy, *Methods*, 2005, **35**, 2.

162 S. Farrell, H. B. Halsall and W. R. Heineman, *Analyst*, 2005, **130**, 489.

163 E. Eteshola, M. Balberg, *Biomed.Microdevices.*, 2004, **6**, 7.

164 H. Makamba, J. H. Kim, K. Lim, N. Park and J. H. Hahn, *Electrophoresis*, 2003, **24**, 3607.

165 P. Yager, T. Edwards, E. Fu, K. Helton, K. Nelson, M. R. Tam and B. H. Weigl, *Nature*, 2006, **442**, 412.

166 D. A. Barrett, M. S. Hartshome, M. A. Hussain, P. N. Shaw and M. C. Davies, *Anal.Chem.*, 2001, **73**, 5232.

167 T. Rohr, D. F. Ogletree, F. Svec and J. M. J. Frechet, *Adv.Funct.Mater.*, 2003, **13**, 264.

168 J. Liu, T. Pan, A. T. Woolley and M. L. Lee, *Anal.Chem.*, 2004, **76**, 6948.

169 C. Li, Y. Yang, H. G. Craighead and K. H. Lee, *Electrophoresis*, 2005, **26**, 1800.

170 R. Lin, M. A. Burns, *Journal of Micromechanics and Microengineering*, 2005, **15**, 2156.

171 M. Salim, G. Mishra, G. J. Fowler, B. O'sullivan, P. C. Wright and S. L. McArthur, *Lab Chip.*, 2007, **7**, 523.

172 M. Herrmann, T. Veres and M. Tabrizian, *Technical Proceedings of the 2006 NSTI Nanotechnology Conference*, 2006, **2**, 244.

173 E. Delamarche, D. Juncker and H. Schmid, *Adv.mater.*, 2005,

174 H. Chen, Z. Zhang, Y. Chen, M. A. Brook and H. Sheardown, *Biomaterials*, 2005, **26**, 2391.

175 G. Sui, J. Wang, C. C. Lee, W. Lu, S. P. Lee, J. V. Leyton, A. M. Wu and H. R. Tseng, *Anal.Chem.*, 2006, **78**, 5543.

176 D. Wu, B. Zhao, Z. Dai, J. Qin and B. Lin, *Lab Chip.*, 2006, **6**, 942.

177 M. W. Toepke, D. J. Beebe, *Lab Chip.*, 2006, **6**, 1484.

178 J. Monahan, A. A. Gewirth and R. G. Nuzzo, *Anal.Chem.*, 2001, **73**, 3193.

179 R. C. Bailey, G. A. Kwong, C. G. Radu, O. N. Witte and J. R. Heath, *J.Am.Chem.Soc.*, 2007, **129**, 1959.

180 J. H. Curfs, J. F. Meis and J. A. Hoogkamp-Korstanje, *Clin.Microbiol.Rev.*, 1997, **10**, 742.

181 M. Segura, Z. Su, C. Piccirillo and M. M. Stevenson, *Eur.J.Immunol.*, 2007, **37**, 1887.

182 E. Leguen, A. Chassepot, G. Decher, P. Schaaf, J. C. Voegel and N. Jessel, *Biomol.Eng*, 2007, **24**, 33.

183 M. A. Palladino, F. R. Bahjat, E. A. Theodorakis and L. L. Moldawer, *Nat.Rev.Drug Discov.*, 2003, **2**, 736.

184 J. W. Choi, T. M. Liakopoulos and C. H. Ahn, *Biosens.Bioelectron.*, 2001, **16**, 409.

185 M. Herrmann, E. Roy, T. Veres and M. Tabrizian, *Lab Chip.*, 2007, **7**, 1546.

186 A. Rida, V. Fernandez and M. A. Gijs, *Applied Physics Letters*, 2003, **83**, 2396.

Appendix A
Article Reprints and Copyright Waivers

Lab-on-a-Chip: permission to include manuscripts and selected figures (1.1, 4.4) in thesis

Dear Mr Herrmann

For the whole papers you wish to reproduce in your thesis, The Royal Society of Chemistry (RSC) hereby grants permission for the use of your whole papers specified below in the printed and microfilm version of your thesis. You may also make available the PDF version of your papers that the RSC sent to the corresponding author(s) of your papers upon publication of the papers in the following ways: in your thesis via any website that your university may have for the deposition of theses, via your university's Intranet or via your own personal website. We are however unable to grant you permission to include the PDF version of the papers on its own in your institutional repository. The Royal Society of Chemistry is a signatory to the STM Guidelines on Permissions (available on request).

Please note that if the material specified below or any part of it appears with credit or acknowledgement to a third party then you must also secure permission from that third party before reproducing that material. Please ensure that the published article states the following:

Reproduced by permission of The Royal Society of Chemistry

For the figures you wish to reproduce in your thesis, The Royal Society of Chemistry hereby grants permission for the use of the material specified below in the work described and in all subsequent editions of the work for distribution throughout the world, in all media including electronic and microfilm. You may use the material in conjunction with computer-based electronic and information retrieval systems, grant permissions for photocopying, reproductions and reprints, translate the material and to publish the translation, and authorize document delivery and abstracting and indexing services. The Royal Society of Chemistry is a signatory to the STM Guidelines on Permissions (available on request).

Please note that if the material specified below or any part of it appears with credit or acknowledgement to a third party then you must also secure permission from that third party before reproducing that material. Please ensure that the published article carries a credit to The Royal Society of Chemistry in the following format:

[Original citation] – Reproduced by permission of The Royal Society of Chemistry

and that any electronic version of the work includes a hyperlink to the article on the Royal Society of Chemistry website. The recommended form for the hyperlink is http://dx.doi.org/10.1039/*DOI suffix*, for example in the link http://dx.doi.org/10.1039/b110420a the DOI suffix is 'b110420a'. To find the relevant DOI suffix for the RSC paper in question, go to the Journals section of the website and locate your paper in the list of papers for the volume and issue of your specific journal. You will find the DOI suffix quoted there.

Regards

Gill Cockhead
Contracts & Copyright Executive

Gill Cockhead (Mrs), Contracts & Copyright Executive
Royal Society of Chemistry, Thomas Graham House
Science Park, Milton Road, Cambridge CB4 0WF, UK
Tel +44 (0) 1223 432134, Fax +44 (0) 1223 423623
http://www.rsc.org

Enzymatically-generated fluorescent detection in micro-channels with internal magnetic mixing for the development of parallel microfluidic ELISA

M. Herrmann,[a] T. Veres[b] and M. Tabrizian*[a]

Received 11th November 2005, Accepted 3rd February 2006
First published as an Advance Article on the web 3rd March 2006
DOI: 10.1039/b516031f

The Enzyme-Linked Immuno-Sorbent Assay, or ELISA, is commonly utilized to quantify small concentrations of specific proteins for a large variety of purposes, ranging from medical diagnosis to environmental analysis and food safety. However, this technique requires large volumes of costly reagents and long incubation periods. The use of microfluidics permits one to specifically address these drawbacks by decreasing both the volume and the distance of diffusion inside the micro-channels. Existing microfluidic systems are limited by the necessary control of extremely low flow rates to provide sufficient time for the molecules to interact with each other by diffusion only. In this paper, we describe a new microfluidic design for the realization of parallel ELISA in stop-flow conditions. Magnetic beads were used both as a solid phase to support the formation of the reactive immune complex and to achieve a magnetic mixing inside the channels. In order to test the detection procedure, the formation of the immune complex was performed off-chip before the reactive beads were injected into the reaction chamber. Anti-streptavidin antibodies were quantified with low picomolar sensitivity (0.1–6.7 pM), a linear range of 2 orders of magnitude and good reproducibility. This work represents the first step toward a new platform for simple, highly effective and parallel microfluidic ELISA.

1.0 Introduction

The sensitive detection of specific proteins is an important analysis for applications in biotechnology, biomedical diagnosis, food and environmental safety. Label-free methods, such as Surface Plasmon Resonance (SPR) or Quartz Crystal Microbalance (QCM), provide simple and real-time measurements, but they are limited by a lack of sensitivity.[1] Alternatively, sandwich immunoassays allow the detection of a specific protein with greater sensitivity at the cost of a more complex procedure. In particular, the Enzyme-Linked Immuno-Sorbent Assay (ELISA), in which the enzymatic amplification of the signal greatly lowers the limit of detection, is the current standard for protein quantification. However, this method requires large volumes of reagents as well as long incubation times due to the high volume-to-surface ratio. The use of microfluidics to perform sandwich immunoassays permits one to specifically address these drawbacks. The low scale of these devices reduces the volumes and diffusion distances inside the micro-channels, therefore decreasing the duration of the successive incubation periods.

Many microfluidic platforms have been described using various methods of detection such as indirect fluorescence,[2–5] electro-chemistry[6–8] or fluorescence generated through an enzymatic reaction.[9–12] Fluorescence is a popular technique as it provides powerful detection tools, increasing sensitivity and gives the possibility of imaging numerous sites on a restricted area.[13,14] Interestingly, optical fibers and diodes (LED) have been successfully incorporated in some microfluidic platforms in order to miniaturize and integrate the fluorescent detection device.[15,16] To date, the highest sensitivity achieved in a microfluidic immunoassay has been reported for the quantification of the cytokine TNFα with a detection limit of 20 pg mL^{-1} (1.14 pM).[17] This system is however restricted by the number of necessary manipulations and the requirement for sophisticated equipment, which increase the complexity and the cost of the assay. Moreover, it has been demonstrated that one of the main challenges to performing highly sensitive microfluidic immunoassays is related to the fine tuning of the flow velocity.[18] When the flow velocity is high, the kinetics of the analyte capture is reaction-limited. In this regime, the exploitation of the analyte present in the solution is only about 5%. Conversely, when the flow velocity is extremely slow, or even stopped, the analyte exploitation reaches values up to 90%. The regime is then transport-limited as the incubation time required to attain such high exploitation rates is extended due to the absence of mixing.

Micro-beads have been used for more than a decade in immunoassays as a means of concentrating specific molecules and of increasing the available surface area supporting the formation of the immune complex.[19–21] In particular, paramagnetic micro-beads can be easily manipulated by applying variable magnetic fields with permanent magnets or electromagnets. Magnetic beads are for instance commonly utilized in macroscopic automated systems such as the immunoassay

[a] *Biomedical Engineering Department, McGill University, Montreal, QC, H3A 2B4, Canada. E-mail: maryam.tabrizian@mcgill.ca; Fax: +1-514-398-7461; Tel: +1-514-398-8129*
[b] *Industrial Materials Institute, National Research Council, Boucherville, QC, J4B 6Y4, Canada*

analyzer Elecsys.[22] In microfluidic systems, they have been employed to capture specific molecules[23–29] as well as to produce mixing inside micro-channels or microfluidic chambers.[30,31]

Based on these observations, we designed a system to perform microfluidic ELISA in stop-flow rather than in continuous-flow conditions. In stop-flow conditions, the channel is first rapidly filled with the desired solution. The flow is then stopped for a defined incubation period. This approach has two major advantages, (i) the volume of solution in the system is precisely defined by the volume of the channel, thus avoiding imprecision due to pipetting and (ii) the assay is not limited by the complex control of extremely low flow rates. The outcome of the assay is hence not dependent on the flow rate but only on the incubation time corresponding to the stop period. The issue of transport limitation is circumvented by using magnetic micro-beads both as a solid phase to support the formation of the immune complex and as a means to create an internal mixing.

An original microfluidic design to perform parallel ELISA in stop-flow conditions is described. The enzymatic amplification and detection of the fluorescent signal was tested on-chip following the off-chip formation of the immune complex. Rapid prototyping in PDMS, manipulation of magnetic beads and epifluorescence microscopy have been combined in order to achieve the detection and quantification of anti-streptavidin antibodies.

2.0 Materials and methods

2.1 Fabrication method

Micro-channels were molded in Poly(dimethylsiloxane) (PDMS) (Dow Corning, MI) by the technique of replica molding. A negative photo-resist (SU-8 2035, MicroChem, MA) was spin-coated on to a silicon wafer to achieve a homogenous layer of 50 μm. The patterns were exposed with UV-light (I-liner, 365 nm) through a high-definition transparent mask and then developed to obtain a negative master of the channel network. PDMS was prepared by mixing the elastomer and the curing solutions in a 10 : 1 ratio and baked in an oven at 80 °C for 2 hours or more. The PDMS was then peeled off the wafer and the connection holes were pierced before assembling.

Both the PDMS block and a 5 cm × 7.5 cm glass slide were cleaned and carefully dried under a nitrogen flow before they were brought into contact to form a tight waterproof reversible bond. The platform was then placed onto the homemade trapping/mixing device. The channels were primed with ethanol to prevent the formation of air bubbles and then connected to a syringe pump (Model 210, Lomir biomedical, NY) *via* a single outlet. The fluidic tests were carried out with a buffer solution mixed with a red food dye for visualization.

2.2 Bead preparation and formation of the immune-complex

Phosphate Buffer Saline (PBS), Trizma Base (TRIS), Tween-20, glycine and Bovine Serum Albumin (BSA) were obtained from Sigma-Aldrich (Oakville, ON). Magnesium chloride was purchased from ACP Chemicals (Montreal, QC).

The desired amount of streptavidin-coated beads (Dynabeads® MyOne™ Streptavidin, Dynal Biotech, NY) was diluted 10 times in PBS 0.05% Tween-20 (PBS-T). The beads were washed 3 times in PBS-T and separated into different Eppendorf tubes. They were then incubated for 30 min with the anti-streptavidin IgG (Rockland Immunochemicals, PA) diluted at the appropriate concentration in a solution of PBS 1% BSA, under constant mixing. A volume of 10 μL of the protein solution per microlitre of beads was used (equivalent to 1 assay). Following incubation, the beads were washed 3 times in PBS-T. They were then incubated another 30 minutes in a 1 μg mL^{-1} solution of anti-rabbit IgG coupled with Alkaline Phosphatase (AP) (Rockland Immunochemicals, PA) diluted in PBS 1% BSA. Finally, the beads were washed 3 times and kept in PBS-T at 4 °C until used.

2.3 Procedure for on-chip signal generation and enzymatic amplification

The channels were rinsed twice with 10 μL of PBS-T. The remaining solutions trapped at the bottom of each inlet were rapidly withdrawn with a pipette between each run to avoid cross-contamination of the sequentially injected solutions inside the inlets. The beads were then injected into the channel and trapped by an external rare earth magnet in the reaction chamber, forming a loose bed that can be moved by displacing the magnet back and forth along the direction of the channel. The beads were washed twice with 10 μL of TRIS buffer pH = 9, 10 mM $MgCl_2$, 10 mM Glycine (TRIS). The solution containing the enzymatic substrate, namely 20 μM Fluorescein Diphosphate (FDP) (Biotum, CA) in TRIS, was subsequently flown into the channels and incubated for 5 min with 30 s mixing every minute.

2.4 Detection method and data processing

An inverted microscope (TE2000-U, Nikon), a stereoscopic zoom microscope (SMZ1500, Nikon) and a digital camera (DXM1200F, Nikon) operated with ACT-1 software were used to acquire pictures of the channels. For fluorescence imaging, the microscope is equipped with a high pressure mercury lamp (C-SHG1, Nikon) and with the appropriate set of filters for fluorescein (FITC) excitation and emission wavelengths. The intensity of fluorescence in each channel was measured with ImageJ (software for image processing and analysis in Java) over the total section of the captured channel (100 × magnifications). All data were normalized by subtracting the intensity obtained in the negative control.

3.0 Results and discussion

3.1 Microfluidic design

Employing the technique of replica molding,[32] the network of 3 walled micro-channels was fabricated in PDMS. After cleaning and drying, the PDMS block was placed on the surface of a microscope glass slide, closing the channels and creating a reversible watertight seal. The original design of the system enables the simple parallelization of individual ELISA on a single chip. Fig. 1 presents a photograph of the entire

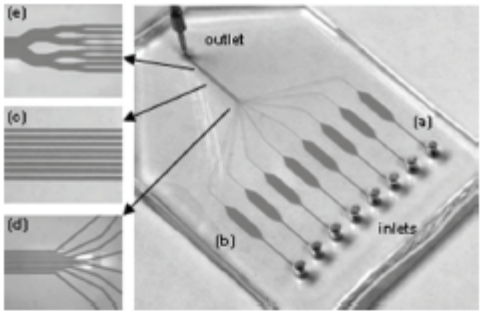

Fig. 1 PDMS chip for the realization of simultaneous microfluidic ELISA: (a) individual channel with a cross-section of 200 × 50 μm acting as a diffusion barrier; (b) reaction chamber with dimensions of 6 mm × 2 mm × 50 μm (L × W × H); (c) network of channels with a cross-section of 50 × 50 μm referred as the detection area; (d) gathering of the independent channels; (e) merging of the channels into a unique outlet channel connected to a syringe pump in withdrawal mode.

platform, along with close-ups at various strategic locations. The system comprises eight independent micro-channels for the realization of parallel simultaneous measurements with identical experimental conditions. Each channel is composed of three different sections: (a) an independent inlet linked to a wide channel acting as a diffusion barrier, (b) a reaction chamber where the generation of the signal and the magnetic mixing are realized, and (c) a smaller channel where the intensity of the fluorescent signal is measured before the solution is discarded *via* the single outlet of the system.

Section (a), linking the inlet to the reaction chamber, is formed by a rectangular segment of 200 μm in width and 50 μm in height (Fig. 1a). Its relatively large dimension slows down the diffusion of liquid from the inlet into the rest of the system when the flow is stopped, thus acting as a diffusion barrier between the sequentially injected solutions. In addition, it allows for a better lateral distribution of the beads and the various solutions, which flow through the gradual opening into the wider reaction chamber.

Section (b), or reaction chamber, is 2 mm wide, 6 mm long and 50 μm high (Fig. 1b). These dimensions keep the fluid regime in the laminar domain, where solutions injected sequentially follow each other with only minimal mixing at the interface. The reaction chamber is terminated with two symmetrical cone-shaped ends, opening and closing over a 2 mm long path. The gradual change of width leads the solutions from and to the narrower channels with no apparent dead-volumes or liquid retention in the corners. The reaction chamber defines a volume of 600 nL, which has been demonstrated to be suitable in achieving the highly sensitive detection of TNFα in a dendritic cell culture medium.[17] The larger dimension of the chamber also contributes to decrease the linear flow velocity, thus reducing the hydrodynamic forces applied on the beads. As a result, the magnetic force necessary to capture and hold the beads at the desired location is also diminished.

However, as the flow is laminar within the entire system, turbulent mixing does not spontaneously occur inside the micro-channels. Additionally, when working in stop-flow conditions, fresh solution is not continuously transported toward the capture area. As a result, it is necessary to actively produce an internal mixing in order to promote binding events of complementary proteins, increase enzymatic substrate availability and homogenize the generated fluorescent signal. For our microfluidic platform, a prototype device was fabricated in order to efficiently trap and manipulate the magnetic beads inside the micro-channels. The microfluidic chip is placed on the top of the device, bringing the external rare earth magnet in close contact with the bottom of the glass slide used to seal the channels. The magnet can be manually displaced from one end of the reaction chamber to the other entraining the beads along in its course. The displacement of the external magnet moves the beads in a synchronized way, causing the fluid to circulate around them and mixing the surrounding solution. With about 10^6 beads of 1 μm in diameter trapped in the chamber (equivalent of 1 μL of Dynabeads concentrated solution), only a few seconds were necessary to initiate the mixing, and moving the magnet for less than 2 minutes was enough time to ensure the good homogeneity of the solution in the entire reaction chamber (Fig. 2).

Section (c), or detection area, corresponds to the portion of the system where the eight independent 50 μm wide channels gather to form a network with a 100 μm pitch (Fig. 1c and d). The total width of the detection area is about 750 μm, which allows the simultaneous observation and acquisition of the signal from all channels in one single shot. At the end of the detection area, the channels merged into one larger channel

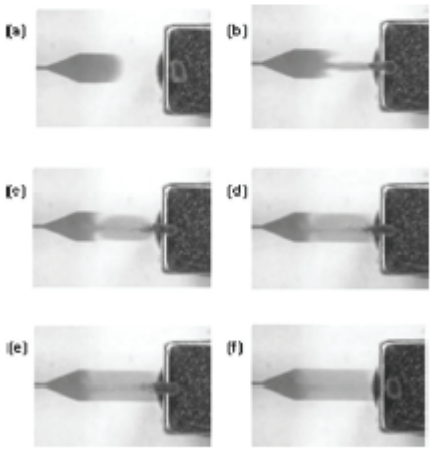

Fig. 2 Magnetic mixing inside the reaction chamber: (a) about 10^6 beads of 1 μm in diameter are injected and trapped by an external permanent magnet. The reaction chamber is half-filled with a solution of red-food dye and left aside for 1 minute to ensure that the solution is not advancing anymore; mixing of the solution after (b) 5 s, (c) 30 s, (d) 60 s, (e) 90 s, (f) 120 s.

leading to the single outlet connected to a syringe pump in withdrawal mode (Fig. 1e). This particular design necessitates the utilization of only one source of vacuum, simultaneously driving the solution into multiple channels, thereby facilitating the parallelization and the synchronization of individual reactions.

3.2 Fluorescent signal generation and detection

In order to demonstrate the efficiency of the microfluidic platform for protein quantification, a generic detection scheme has been utilized that can be adapted for potentially any desired application. In addition, the chip does not require that it be pre-coated with either capture proteins or antibodies, thus it can be used for a specific application without the need for any further modifications. The analytical concept of the system is described in Fig. 3. Paramagnetic beads of 1 μm in diameter, coated with a layer of streptavidin, were used as a support for the formation of the immune complex. In that experiment, streptavidin was not used for its affinity for biotynilated molecules, but rather as a target protein to be recognized by anti-streptavidin polyclonal antibodies. The streptavidin-coated beads were first incubated with various concentrations of anti-streptavidin antibody, followed by a solution of secondary antibody coupled with alkaline phosphatase (AP). The enzymatic substrate fluorescein diphosphate (FDP) was subsequently used to generate the fluorescent signal. FDP is a very efficient fluorogenic enzymatic substrate for alkaline phosphatase, which has been previously utilized both for enzymatic assays and ELISA.[33,34] The enzymatic reaction generates fluorescein, a strongly green fluorescent molecule, through the hydrolysis of the two phosphate groups of the colorless and non-fluorescent fluorescein diphosphate.

As the beads aggregate to form a loose bed, the reactive surface with the AP-coupled-antibodies becomes extremely concentrated and localized into the reaction chamber (Fig. 4). The reaction then occurs very rapidly around the bead bed but the rest of the enzymatic substrate solution is left unreacted. Moving the beads and mixing the solution thus improve the substrate availability and the resulting signal homogeneity. The transformation of FDP into fluorescein is processed at a steady rate into the reaction chamber, yielding to a final

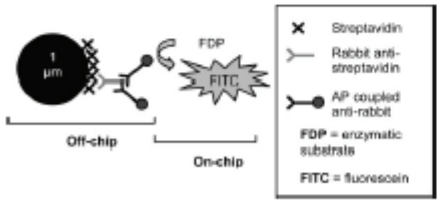

Fig. 3 Analytical concept for the quantification of anti-streptavidin antibodies: the formation of the immune complex is performed off-chip by incubating the streptavidin-coated micro-beads first with rabbit anti-streptavidin antibodies and then with 1 μg mL^{-1} of secondary anti-rabbit antibodies coupled with Alkaline Phosphatase. The beads are then injected into the micro-channels and both signal generation and detection are performed on-chip.

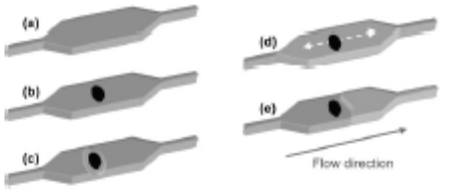

Fig. 4 Schematic presentation of the procedure for the on-chip generation of fluorescein and signal detection in the downstream channels: (a) filling and washing with PBS-T; (b) injection of about 10^6 beads, trapping in the reaction-chamber and washing with PBS-T and TRIS buffer; (c) introduction of the substrate solution (20 μM FDP in TRIS buffer), 5 minutes incubation with (d) alternate magnetic mixing and (e) detection. The total procedure takes about 10 minutes to complete.

fluorescent intensity which depends both on the duration of the incubation period and the number of immobilized enzymes. As a result, when the incubation period is fixed, the intensity of the fluorescent signal is only dependent on the number of immobilized enzymes, which itself is directly proportional to the quantity of anti-streptavidin antibodies bound on the surface of the streptavidin-coated beads. After 5 minutes of incubation and alternate mixing, the reacted solution is simply driven away from the magnetic beads, physically stopping all reactions at the same time, and giving a precise control over the duration of the multiple individual enzymatic reactions. The relatively large volume of the reaction chamber permits the downstream detection channel to be entirely filled up without the need for an extremely precise control of the flow.

Fig. 5a shows the fluorescent image obtained for multiple reactions performed in parallel on a single chip. No beads were introduced in the first and last channels. They served as controls to ensure that the solution of FDP did not exhibit auto-fluorescence due to deterioration of the substrate molecule during the storage period. From the top to the bottom, the second channel corresponds to the negative control where beads have been incubated with the secondary AP-antibody only. The weak signal obtained in this channel represents the background signal due to the unspecific binding of AP-coupled antibodies to the streptavidin-coated beads. Channels 3 to 7 correspond to increasing concentrations of anti-streptavidin antibodies, ranging from 12.5 pg mL^{-1} (0.1 pM) to 1 ng mL^{-1} (6.7 pM). The same experiment was repeated 3 times and a standard curve for the quantification of anti-streptavidin antibodies was plotted in Fig. 5b. The linear range of quantification for this model was approximately 2 orders of magnitude (R^2 = 0.987). The low picomolar sensitivity showed promising potential with regards to the performance of the optimized immunoassay for TNFα (1.14 pM).[17] A 3 to 4 fold increase in sensitivity was observed with systems using indirect fluorescence (1 nM).[4] The sensitivity was also enhanced by at least a factor of 10 when compared to previously described microfluidic ELISA (17 pM to 31 nM).[9–11] The standard deviations varied from 3% to 15% of the highest fluorescent intensity. The inter-assay coefficient

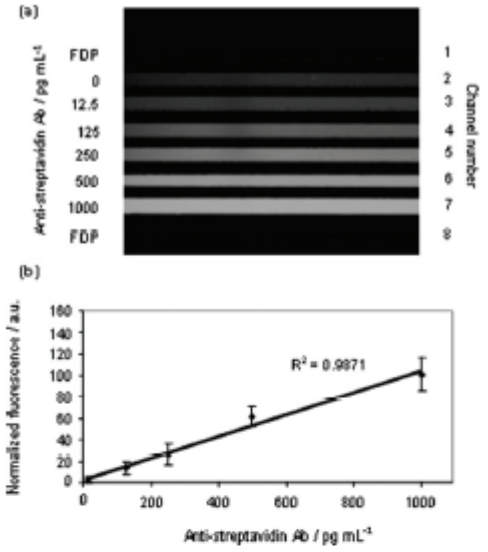

Fig. 5 Standard curve for the quantification of anti-streptavidin antibodies: (a) fluorescent imaging of the downstream channels after 5 minutes incubation with concentrations of anti-streptavidin antibodies varying from 12.5 pg mL^{-1} to 1000 pg mL^{-1} (100×); (b) linear range of quantification for anti-streptavidin antibodies. The averages and error bars were calculated from 3 independent assays.

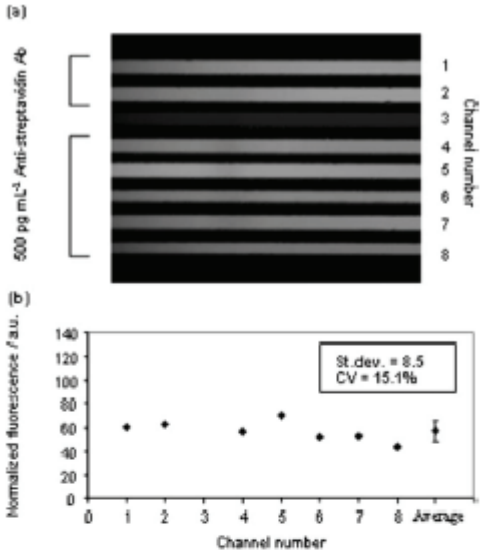

Fig. 6 Determination of the intra-assay coefficient of variation: all channels were filled with beads previously incubated with a solution of 500 pg mL^{-1} anti-streptavidin antibodies and secondary AP-coupled antibodies, except for channel 3 where the beads were incubated with the secondary antibody only. The average fluorescent intensity after normalization was 56.3 a.u., the associated standard deviation was 8.5 a.u., which represented a coefficient of variation of 15.1%.

of variation, which is defined by the ratio between the standard deviation and the mean fluorescence intensity, was about 15% for concentrations above 500 pg mL^{-1} (3.3 pM). Similarly, Fig. 6a displays a fluorescent picture where all channels, except for the negative control in channel 3, were filled with beads incubated with a solution of 500 pg mL^{-1} of anti-streptavidin antibodies. The measured intra-assay coefficient of variation was 15.1% (Fig. 6b). Both inter- and intra-assay variability were comparable to those recently obtained by Honda *et al.* using indirect fluorescence on a compact disk-shaped microfluidic device.[35] Additionally, the automation of the assay procedure is currently under development, which is expected to further reduce the variability of the system.

Employing streptavidin-coated micro-beads as the solid phase, the formation of the immune complex was realized off-chip. With this method, the issue of non-specific adsorption of proteins on the channel walls has been circumvented, thus largely eliminating the potential background noise for the enzymatic reaction that can cause a damageable loss in sensitivity. However, this approach slightly increases the quantity of reagents used, as sub-microliter volumes are not conveniently manipulated outside the chip. The overall duration of the assay is also augmented. Therefore, current efforts are focused on the realization of the entire assay on-chip, including the formation of the immune complex. This next stage of development has so far been limited by the difficulty of obtaining effectively passivated surfaces to avoid random adsorption of proteins on the channel walls.[36,37]

4.0 Conclusion

As a first step toward a microfluidic platform for parallel ELISA in stop-flow conditions, we have developed a system featuring micro-channels molded in PDMS, manipulation of paramagnetic micro-beads and fluorescence detection. The original microfluidic design enables one to conveniently work in stop-flow conditions. The magnetic beads are used both as a solid phase to support the formation of the reactive immune complex and as a means to produce an internal mixing of the solution. In order to test the amplification and detection of the signal inside the microfluidic system, the formation of the immune complex was performed off-chip before the reactive beads were injected into the reaction chamber. A standard curve for the quantification of anti-streptavidin antibodies was realized, exhibiting low picomolar sensitivity, a dynamic range of quantification of 2 orders of magnitude, and inter- and intra- coefficients of variation of about 15%. Current developments include the optimization of the fluidic network, the automation of the magnetic mixing and the treatment of internal surfaces to proceed to the on-chip formation of the immune complex, as well as the quantification of biomedically relevant proteins.[38] Finally, we believe that the design of the system could allow further integration into a portable biosensor using a miniaturized pump and electromagnets.

Acknowledgements

This work is supported by a joint grant from the Canadian Institute for Health Research and the National Research Council, as well as by the Fonds québecois de la recherche de la nature et des technologies through the Centre for Biorecognition and Biosensors. The authors wish to thank Francois Normandin for technical help in building the mixing device.

References

1 S. D. Carrigan, G. Scott and M. Tabrizian, *Langmuir*, 2005, **21**, 5966–5973.
2 A. Bernard, B. Michel and E. Delamarche, *Anal. Chem.*, 2001, **73**, 8–12.
3 M. A. Hayes, T. N. Polson, A. N. Phayre and A. A. Garcia, *Anal. Chem.*, 2001, **73**, 5896–5902.
4 V. Linder, S. K. Sia and G. M. Whitesides, *Anal. Chem.*, 2005, **77**, 64–71.
5 J. P. Golden, C. R. Taitt, L. C. Shriver-Lake, Y. S. Shubin and F. S. Ligler, *Talanta*, 2005, **65**, 1078–1085.
6 J. W. Choi, K. W. Oh, J. H. Thomas, W. R. Heineman, H. B. Halsall, J. H. Nevin, A. J. Helmicki, H. T. Henderson and C. H. Ahn, *Lab Chip*, 2002, **2**, 27–30.
7 J. S. Rossier and H. H. Girault, *Lab Chip*, 2001, **1**, 153–157.
8 M. S. Wilson, *Anal. Chem.*, 2005, **77**, 1496–1502.
9 E. Eteshola and D. Leckband, *Sens. Actuators, B*, 2001, **72**, 129–133.
10 E. Eteshola and M. Balberg, *Biomed. Microdevices*, 2004, **6**, 7–9.
11 S. Lai, S. Wang, J. Luo, L. J. Lee, S. T. Yang and M. J. Madou, *Anal. Chem.*, 2004, **76**, 1832–1837.
12 J. C. McDonald, S. J. Metallo and G. M. Whitesides, *Anal. Chem.*, 2001, **73**, 5645–5650.
13 M. Wolf, D. Juncker, B. Michel, P. Hunziker and E. Delamarche, *Biosens. Bioelectron.*, 2004, **19**, 1193–1202.
14 A. Gulliksen, L. A. Solli, K. S. Drese, O. Sorensen, F. Karlsen, H. Rogne, E. Hovig and R. Sirevag, *Lab Chip*, 2005, **5**, 416–420.
15 M. L. Chabinyc, D. T. Chiu, J. C. McDonald, A. D. Stroock, J. F. Christian, A. M. Karger and G. M. Whitesides, *Anal. Chem.*, 2001, **73**, 4491–4498.
16 K. Miyaki, Y. Guo, T. Shimosaka, T. Nakagama, H. Nakajima and K. Uchiyama, *Anal. Bioanal. Chem.*, 2005, **382**, 810–816.
17 S. Cesaro-Tadic, G. Dernick, D. Juncker, G. Buurman, H. Kropshofer, B. Michel, C. Fattinger and E. Delamarche, *Lab Chip*, 2004, **4**, 563–569.
18 M. Zimmermann, E. Delamarche, M. Wolf and P. Hunziker, *Biomed. Microdevices*, 2005, **7**, 99–110.
19 N. B. Liabakk, K. Nustad and T. Espevik, *J. Immunol. Methods*, 1990, **134**, 253–259.
20 K. Sato, M. Tokeshi, T. Odake, H. Kimura, T. Ooi, M. Nakao and T. Kitamori, *Anal. Chem.*, 2000, **72**, 1144–1147.
21 Y. Murakami, T. Endo, S. Yamamura, N. Nagatani, Y. Takamura and E. Tamiya, *Anal. Biochem.*, 2004, **334**, 111–116.
22 J. C. Forest, J. Masse and A. Lane, *Clin. Biochem.*, 1998, **31**, 81–88.
23 M. A. M. Gijs, *Microfluidic Nanofluidic*, 2004, 22–40.
24 M. A. Hayes, T. N. Polson and A. A. Garcia, *Langmuir*, 2001, **17**, 2866–2871.
25 Tao Deng, Mara Prentiss and Georges M. Whitesides, *Appl. Phys. Lett.*, 2002, **80**, 461–463.
26 Tao Deng, Georges M. Whitesides, Mala Radhakrishnan, Gary Zabow and Mara Prentiss, *Appl. Phys. Lett.*, 2001, **78**, 1775–1777.
27 H. Hartshorne, C. J. Backhouse and W. E. Lee, *Sens. Actuators, B*, 2004, **99**, 592–600.
28 K. S. Kim and J. K. Park, *Lab Chip*, 2005, **5**, 657–664.
29 G. Degre, E. Brunet, A. Dodge and P. Tabeling, *Lab Chip*, 2005, **5**, 691–694.
30 A. Rida and M. A. Gijs, *Anal. Chem.*, 2004, **76**, 6239–6246.
31 M. Grumann, A. Geipel, L. Riegger, R. Zengerle and J. Ducree, *Lab Chip*, 2005, **5**, 560–565.
32 D. C. Duffy, J. C. McDonald, O. J. A. Schueller and G. M. Whitesides, *Anal. Chem.*, 1998, **70**, 4974–4984.
33 J. Montalibet, K. I. Skorey and B. P. Kennedy, *Methods*, 2005, **35**, 2–8.
34 S. Farrell, H. B. Halsall and W. R. Heineman, *Analyst*, 2005, **130**, 489–497.
35 N. Honda, U. Lindberg, P. Andersson, S. Hoffmann and H. Takei, *Clin. Chem.*, 2005.
36 A. Papra, A. Bernard, D. Juncker, N. B. Larsen, B. Michel and E. Delamarche, *Langmuir*, 2001, **17**, 4090–4095.
37 H. Makamba, J. H. Kim, K. Lim, N. Park and J. H. Hahn, *Electrophoresis*, 2003, **24**, 3607–3619.
38 S. D. Carrigan, G. Scott and M. Tabrizian, *Clin. Chem.*, 2004, **50**, 1301–1314.

PAPER www.rsc.org/loc | Lab on a Chip

Microfluidic ELISA on non-passivated PDMS chip using magnetic bead transfer inside dual networks of channels

Marc Herrmann,[a,b] Emmanuel Roy,[b] Teodor Veres†*[b] and Maryam Tabrizian†*[a]

Received 24th May 2007, Accepted 17th July 2007
First published as an Advance Article on the web 9th August 2007
DOI: 10.1039/b707883h

Achieving efficient passivation of micro-channels against non-specific adsorption of biomolecules is a critical aspect in the development of microfluidic ELISA systems. Usual surface treatments such as pre-coating of the channels with serum albumin, exposure to oxygen plasma, polyethylene glycol grafting however exhibit a lack of long-term stability, with procedures that can be time-consuming, complex or associated with costly materials and instruments. In this paper, we present a new fluidic design combined with an original strategy of manipulating magnetic beads in order to reduce assay noise in bead-based microfluidic ELISA without the need for prior channel pre-treatment. The novelty of the system relies on the physical separation of the immune complex formation phase and the enzymatic reaction phase into two independent networks of channels. These networks are linked by fluidic bridges, whose openings are controlled by pressure valves, and through which the beads are magnetically transferred. A standard curve for the quantification of a model antibody was obtained within 30 minutes. A detection limit of 100 pg mL^{-1} (660 fM) and good linearity of the signal up to 4 ng mL^{-1} were observed.

1.0 Introduction

For more than a decade, microfluidics has been employed to adapt standard bench-work bioassays into time- and cost-effective devices. As a result, techniques such as immunoassays are being increasingly used in clinical diagnostics, food safety and environmental applications.[1–4] In particular, various platforms for the realization of microfluidic Enzyme-Linked Immuno-Sorbent Assay (ELISA) have been proposed in an effort to reduce the use of large volumes of expensive reagents and hour-long incubation periods, whilst preserving the specificity and the sensitivity of the original assay.[5]

In conjunction with improvement in design and functionality, an important part of the development of microfluidic-based systems has focused on creating bio-functional surfaces and, alternatively, on finding means to efficiently passivate microchannels against non-specific adsorption (NSA) of biomolecules. The latter is especially critical in microfluidic ELISA systems, as the large surface-to-volume ratio greatly amplifies the undesired surface effects that generate noise and lower sensitivity. Many research groups have investigated chemical surface modifications of various polymeric materials to limit the effects of NSA.[6–12] In particular, surface modifications of poly(dimethylsiloxane) (PDMS) have been extensively explored as it is currently the preferred polymer for biochip fabrication.[13–21] Despite many advantages, PDMS is notorious for its high native hydrophobicity and its tendency to rapidly adsorb biological materials.[22] Usual surface treatments such as pre-coating of the channels with serum albumin, exposure to oxygen plasma and polyethylene glycol grafting lack long-term stability, and require procedures that are often time-consuming, complex or associated with costly materials and instruments.

In a previous publication, we proposed an innovative concept of stop-flow microfluidic ELISA in which functionalized magnetic beads were used both as a solid-support to sustain the reactive immune complex formation and as a means to increase mixing of the surrounding solution during incubation steps.[23] In order to establish the fluidic design and protocol for the enzymatic amplification and fluorescent detection, the reactive immune complex was formed *off-chip* at the surface of the beads, before the reactive beads were injected inside the microfluidic system. With this method, the enzymatic reaction occurred in unused protein-free channels thus considerably limiting the assay noise. The necessity to passivate the PDMS chip was then avoided, which represented a substantial reduction in both the time and the complexity of the assay.

In this paper, we describe the next generation of the system, which combines an original fluidic design and the manipulation of magnetic beads to reduce the noise in bead-based microfluidic immunoassays and realize microfluidic ELISA entirely *on-chip*, without prior channel passivation. This new approach relies on the physical separation of the immune complex formation phase and the enzymatic reaction phase. Two independent networks of channels are used (dual networks), linked by fluidic bridges through which the beads are magnetically transferred. Pressure valves embedded in bi-layered PDMS[24] have been engineered which seal the fluidic bridges when pressure is applied, thus ensuring the complete isolation of the networks and avoiding contamination. Using this new fluidic design and an adapted protocol, a standard curve for the quantification of a model

[a]*Department of Biomedical Engineering, McGill University, Montreal, QC, H3A 2B4, Canada. E-mail: maryam.tabrizian@mcgill.ca; Fax: (514) 398 7461; Tel: (514) 398 8129*
[b]*Industrial Materials Institute, National Research Council of Canada, Boucherville, QC, J4B 6Y4, Canada. E-mail: teodor.veres@imi.cnrc-nrc.gc.ca; Fax: (450) 641 5105; Tel: (450) 641 5232*
† Co-corresponding authors contributed equally to this work.

antibody was obtained within 30 minutes. A detection limit of 100 pg mL^{-1} (660 fM) and good linearity up to a concentration of 4 ng mL^{-1} were observed.

2.0 Material and methods

2.1 Fabrication of the bi-layer PDMS microfluidic ELISA chip

The master for the control layer was fabricated by standard SU-8 photo-lithography. SU-8 1070 photo-resist (Microchem, Newton, MA) was spin-coated on a silicon wafer to achieve a homogenous layer of 40 μm. The patterns were exposed through a high-definition transparent mask (Fineline Imaging, Colorado Springs, CO) with UV-light and developed, resulting in channels with rectangular cross-sections. The features on the control mask were designed at a 101.6% ratio of the desired dimensions to compensate for the shrinkage of PDMS before alignment. For the fabrication of the master corresponding to the fluidic level, a similar method was applied to construct the two networks of channels. The fluidic bridges were fabricated using AZ 50xt positive resist (AZ Electronic Materials, Branchburg, NJ) and aligned on an aligner EVG 6200 (EV Group, Schaerding, Austria). After development, the master was treated with Trichloro(1*H*,1*H*,2*H*,2*H*-perfluorooctyl)silane (Sigma-Aldrich, St. Louis, MO) to obtain a hydrophobic surface and facilitate the release of cured PDMS. The surface treatment was followed by reflow of the positive resist for 10 minutes at 120 °C resulting in fluidic bridges with semi-circular cross-sections.

The two layers of PDMS Sylgard184 (Dow Corning, Midland, MI) were cured separately on their respective masters as established by Quake *et al.*[24] For the control layer, PDMS 5 : 1 (elastomer base : curing agent) was mixed, degassed at room temperature and poured to obtain a thickness of about 4 mm. For the fluidic layer, PDMS 20 : 1 was prepared and spin-coated on the fluidic master at a thickness of about 70 μm, forming a 10 μm thick membrane above the 60 μm high fluidic bridges. After a 30 minutes pre-curing step in an oven at 80 °C aimed at minimally hardening both layers of PDMS, the control layer was released from its master and the control inlet punched out. It was then aligned on top of the fluidic layer. The bi-layer assembly was further cured at 80 °C for at least 2 hours to achieve permanent thermal bonding. Finally, the bi-layer PDMS device was peaked off the fluidic master and the inlets and outlets were punched out. The system was then reversibly sealed on a glass slide and ready for use.

2.2 Microfluidic ELISA with dual networks of channels

Trizma Base, Tween-20 and glycine were obtained from Sigma-Aldrich (St. Louis, MO) and magnesium chloride from ACP Chemicals (Slough, UK). The streptavidin-coated magnetic beads (Dynabeads® M-280 Streptavidin) were purchased from Invitrogen (Burlington, ON) and the rabbit anti-streptavidin IgG from Rockland Immunochemicals (Gilbertsville, PA). The secondary alkaline phosphatase (AP) anti-rabbit antibodies and the enzymatic substrate fluorescein diphosphate (FDP) were purchased from Anaspec (San Jose, CA). All protein dilutions and washing steps were performed in 0.1 M Tris, 150 mM NaCl, 0.02% Tween-20, pH = 7.4 (TBS-T). FDP was diluted to a final concentration of 4 μM in the reaction buffer consisting of 0.1 M Tris, 10 mM $MgCl_2$, 10 mM Glycine, pH = 9.0.

Before mounting the PDMS chip on the mixing platform and securing the valve connection, both the fluidic and the control channels were filled with TBS-T using the Channel Outgas Technique (COT).[25] Unless specified otherwise, the protocol for completion of the microfluidic ELISA was performed as reported in Table 1. For each step, a few microlitres of solution (5–15 μL) were deposited in the inlets and flown through the channels by connecting the appropriate outlet to a peristaltic pump in withdrawal mode. After each run, the residual solution trapped at the bottom of the inlets was aspirated to avoid cross-contamination of the sequentially injected solutions.

2.3 Fluorescent signal detection

An inverted microscope (TE2000-U, Nikon), a stereoscopic zoom microscope (SMZ1500, Nikon) and a digital camera (DXM1200F, Nikon) operated with the ACT-1 software were used to acquire pictures of the channels. For fluorescence imaging, the microscope is equipped with a high-pressure mercury lamp (C-SHG1, Nikon) and with the appropriate set of filters for fluorescein (FITC) excitation and emission wavelengths. The intensity of fluorescence in each channel was measured with ImageJ (software for image processing and analysis in Java, http://rsb.info.nih.gov/ij/). All data were normalized by subtracting the fluorescence intensity obtained in the negative control.

3.0 Results and discussion

3.1 Design of microfluidic ELISA with dual networks of channels

The concept of microfluidic ELISA with dual networks of channels relies on the physical separation of the immune complex formation phase and the enzymatic reaction phase

Table 1 Protocol for the realization of the microfluidic ELISA with dual networks

Step number	Complexation network	Manipulation	Reaction network
1		Close valves	
2	Inject beads		
3	Wash (1 ×)		
4	Inject primary antibody (antigen)	5 min incubation with mixing	
5	Wash (1 ×)		
6	Inject AP-coupled secondary antibody	5 min incubation with mixing	
7	Wash (2 ×)		
8		Open valves	
9	Wash (1 ×)		
10		Transfer beads	
11		Close valves	
12		5 min incubation with mixing	Inject FDP solution
13			Move reacted solution to the detection area

(Fig. 1(a)). A first network of channels (complexation network) is used to achieve the formation of the immune complex, consisting of binding consecutive antibodies and antigens to the surface of the magnetic beads. During this phase, several complex solutions are successively pumped through the network, resulting in the non-specific adsorption of proteins on the channel walls, especially secondary antibodies that would normally cause an elevation in the assay noise. Instead, a second network of channels (reaction network), so far unused and thus free of non-specifically adsorbed proteins, is employed to carry on the enzymatic reaction at the surface of the beads that generates the fluorescent signal. Both networks are independent, linked only by fluidic bridges through which the reactive beads are magnetically transferred.

The complexation network is composed of eight inlets connected by 500 μm wide channels, acting as a diffusion barrier, to the same number of complexation chambers. Each chamber forms a 480 nL volume in which the beads are magnetically trapped and displaced to prevent local depletion of proteins and homogenize the surrounding solution during incubation periods. Outlet channels connect the eight complexation chambers to a single outlet from which the successive solutions can be flown using a peristaltic pump in withdrawal mode.

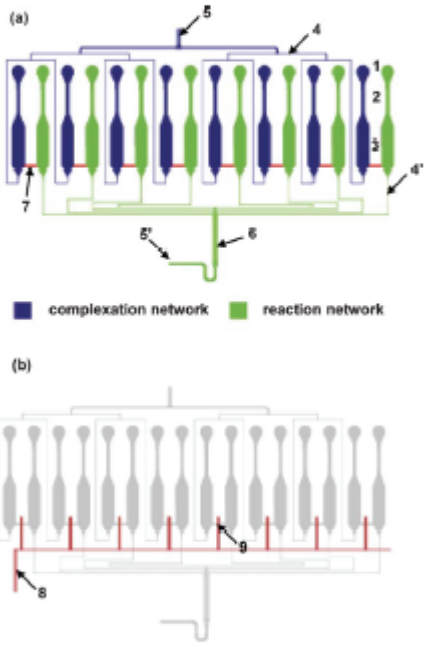

Fig. 1 Layout of the bi-layer PDMS microfluidic ELISA chip (a) Fluidic level: the solutions are injected into the inlets (1), which are connected to the complexation/reaction chambers (3) *via* large channels acting as diffusion barriers (2). In the complexation network, outlet channels (4) of equal length link the complexation chambers to the upper outlet (5). In the reaction network, outlet channels (4') adjusted to the same length come closer to form the detection area (6) and then gather into a larger channel connected to the lower outlet (5'). The two networks are linked by the fluidic bridges (7). (b) Control level: the control level is composed of a single closed channel (8) fanning into eight branches to form the pressure valves (9) on the top of the fluidic bridges. The fluidic level is represented in light grey to display the overlap of the control channel on the top of the fluidic channels.

The reaction network is very similar to the complexation one. Inlets, diffusion barriers and chambers, referred to as reaction chambers, are laid out in an identical manner, parallel to those of the complexation network. The outlet section is however different as the eight independent channels converge to form the detection area. Upstream of the detection area, the outlet channels are adjusted to the same length in order to ensure identical flowing conditions. Downstream from the detection area, the outlet channels merged into a second outlet.

3.2 Engineering of pressure valves

In order to avoid contamination of the reaction chambers, pressure valves were engineered to close the fluidic bridges and completely isolate the two networks from one another. The valves are opened to allow the passage of the beads into the reaction network and then closed again to perform the final steps of the assay.

Due to the design of the fluidic network, the control line for the valves necessarily overlaps fluidic channels in order to reach the bridges (Fig. 1(b)). As the fluidic bridges should be able to close when pressure is applied without disrupting the flow inside the outlet channels, the widths of both the fluidic and control channels were tuned as established by Studer *et al*.[26] They have demonstrated that as the widths of the overlapping channels increased, less pressure was required to close the valves. In our design, the overlap for operational valves features a 300 × 300 μm area. Non-functional crossings display a limited area of only 50 × 50 μm, thus enabling the selective closing of the bridges.

For the same reason, the fluidic bridges were given a semi-circular cross-section, as opposed to the outlet channels which display a rectangular cross-section.[24] Yet, semi-circular channels are difficult to obtain using a negative resist such as SU-8. They are preferably produced by reflow of a positive resist. Consequently, the fluidic master was fabricated in three consecutive steps (Fig. 2). First, all the fluidic features but the bridges were realized in SU-8 at a 40 μm thickness. Next, the fluidic bridges, realized in positive resist at a thickness of 50 μm, were aligned so to connect the pairs of chambers. A final baking step at elevated temperature allowed for the positive resist to reflow giving the bridges their final semi-circular shapes.

Using the fabricated fluidic master, bi-layer PDMS microfluidic ELISA chips were produced in large quantities with high reproducibility of the valve functionality. The pressure necessary to close the valves is supplied by connecting the control channel to a screw syringe with a blunt-ended needle. To prevent leakage at the connection site, the modified needle is passed through a tight piece of rubber and strongly held down together with the PDMS device. A pressure of about

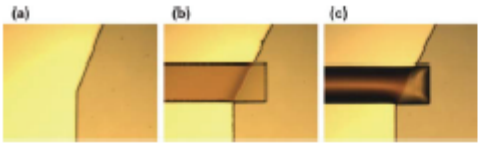

Fig. 2 Fabrication steps for the fluidic master. (a) The two independent networks of channels are fabricated in the negative resist SU-8. (b) The fluidic bridges are made using the positive resist AZ 50xt. (c) The master is post-baked, hardening the SU-8 and inducing the reflow of fluidic bridges.

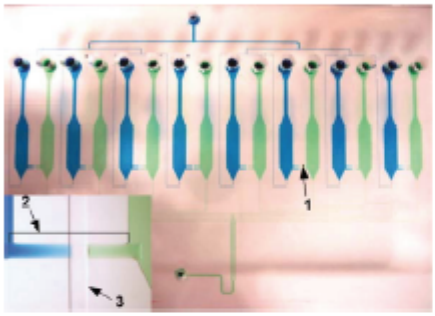

Fig. 3 Photograph of the PDMS microfluidic ELISA device showing the two independent networks of channels. The complexation network is filled with a blue dye solution; the detection network is filled with green. All eight pressure valves (1) are closed resulting in the complete isolation of the two networks. The insert provides a close-up view of an interrupted fluidic bridge (2) crossed by the control channel (3).

20 PSI in the control line was found to be appropriate to completely and reversibly close the eight valves without disrupting the flow in the outlet channels (Fig. 3). The pressure valves proved to be operational for at least several hours, without observable leakage, pressure drop or contamination between the pairs of chambers.

3.3 Proof-of-concept: quantification of a model antibody

The operational setup for the realization of the microfluidic ELISA is described in Fig. 4. After priming the channels, the PDMS chip is inserted into its support and the connection for the control channel is secured. A blunt-ended needle, which tightly fits the outlets of the system, is adapted at the end of a tube linked to a peristaltic pump. The pump is then used to flow the diverse solutions through the channels at the required flow rate. The needle can be reversibly and easily switched from one outlet to the other depending on which network is to be operated. Round permanent magnets of 3 mm in diameter are placed directly under the PDMS-glass chip. Eight magnets, one for each of the complexation chamber, are precisely aligned and held together by a plastic piece in which holes the size of the magnets have been drilled. The plastic piece is attached to a mixing platform, which can be moved in all directions with micrometre precision in a pre-determined sequence *via* a Labview software developed in-house.

In order to demonstrate the concept of dual networks to reduce the noise in bead-based microfluidic ELISA, a standard curve for the quantification of a model antibody was realized without prior channel passivation. For this purpose, commercially available magnetic beads coated with a layer of streptavidin, the model antigen, were used to detect anti-streptavidin antibodies, the model analyte (Fig. 5). The protocol for the realization of the microfluidic ELISA is

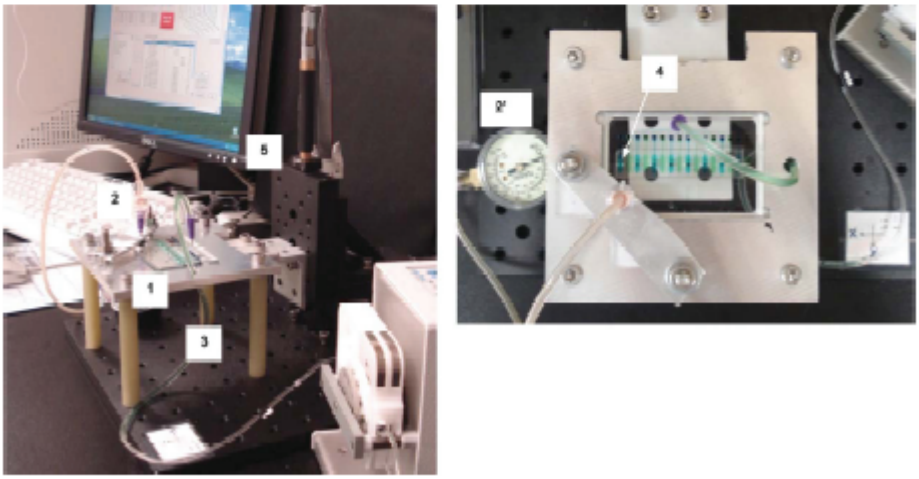

Fig. 4 Operational platform for microfluidic ELISA: the microfluidic chip is inserted into its support (1). The control channel (2) is connected to a manometer syringe (2') and secured to avoid leakage. One of the fluidic outlets is connected to a peristaltic pump in withdrawal mode (3). Below the chip, the eight permanent magnets (4), mounted on the mixing device (5), are aligned with the complexation chambers.

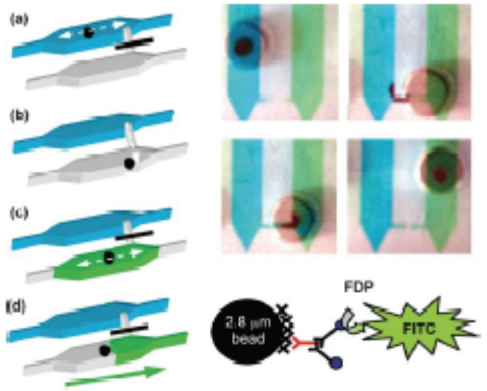

Fig. 5 Schematic of the immune complex formation and detection procedure: (a) About 10^6 streptavidin-coated magnetic beads are trapped inside the complexation chamber. The anti-streptavidin antibody (analyte) binds specifically to the streptavidin (antigen)-coated beads during a five minute incubation period with mixing. Similarly, the AP-coupled secondary antibody is added to form the reactive immune complex. (b) The valve is transiently opened and the reactive beads are magnetically transferred into the reaction chamber. (c) The enzyme processes the FDP substrate into the fluorescent molecule FITC. While the reaction takes place, the solution is homogenized by displacing the beads. (d) The reacted solution is then pushed into the detection area.

presented in Table 1. The total assay time was about 30 minutes, mostly due to many pipetting steps, and could be further reduced in a fully automated system. About 10^6 beads were injected and trapped in each of the eight complexation chambers. During the several incubation periods, the beads were continuously displaced from end to end of the chambers at a velocity of 400 μm s^{-1}. The velocity and distance of the magnet to the beads were adjusted so they form a loose bed that is dragged behind the magnet, thus facilitating the penetration and diffusion of solutions between the beads. After both incubation steps with the analyte antibody and the AP-coupled secondary antibody, the beads were washed twice with TBS-T and transferred to the reaction chambers *via* the fluidic bridges with transiently opened valves. No pre-treatment of the PDMS chip or glass was performed. As a control experiment, the whole assay was also performed in a single network with identical experimental conditions.

From the fluorescent microscopy images (Fig. 6(a)), it is striking that the level of noise caused by NSA on the channel walls is greatly reduced in the dual network system. Some residual noise is noticeable when comparing channels 1 and 2 in the dual network system (respectively corresponding to unreacted FDP solution and the negative control, where only the analyte was omitted from the reaction), which might be due to very low NSA at the surface of the beads, however much less than for the same reactions in the single network system.

The reported data are the average of four independent experiments for each of the curves (Fig. 6(b)). To facilitate inter-assay comparison, all values have been normalized by subtracting the signal obtained for the negative control on the same chip. With the dual network protocol, a limit of detection (LOD) of 100 pg mL^{-1}, corresponding to a molarity of about 660 fM (MW = 150 kDa) and good linearity up to 4 ng mL^{-1} were observed for the tested anti-streptavidin antibody. The LOD was taken as 3-times the standard deviation of 5 negative control replicas. For the two highest concentrations, the standard deviations are quite elevated due to the variation in the reaction kinetic from assay to assay performed on separate chips. This variation could surely be minimized in a platform with automated injection and a better control of external conditions such as temperature and ambient light.

When comparing the assays of the single network to the dual networks, both the sensitivity and linearity are significantly improved for the dual network system. While the absolute values are generally higher in the single network experiment, the normalization to the negative control highlights the weaker contrast in this setup between the lowest and the highest concentrations due to the elevated noise that quickly saturates the signal. The sudden increase between the negative control and the lowest concentration of 50 pg mL^{-1} can be explained by the fact that several secondary antibodies can bind a non-specifically adsorbed analyte thereby amplifying the noise as compared to directly non-specifically adsorbed secondary antibodies.

The results achieved with the dual network system are close to those obtained in the first iteration of our system where the immune complex was formed *off-chip*. The decrease in sensitivity, from about 70 fM previously to 660 fM, can be explained by the lesser dispersion of the beads and shorter incubation periods of the *on-chip* procedure. However, the reduction of the sample size (by a factor of 5) and the shorter total assay time (from several hours to 30 minutes) represent a strong improvement to the global performance of the assay. Moreover, improving bead dispersion and compromising on the incubation times would increase the sensitivity of the assay significantly. Nevertheless, even with the current protocol, the dual network system is among the most sensitive microfluidic immunoassays reported to date,[3,4,27–38] without the use of costly, complex and time-consuming pre-treatments.

4.0 Conclusion

In this paper, the novel concept of dual networks of channels was presented. This approach permits noise reduction in bead-based microfluidic ELISA without the need for prior channel passivation. The original design features two independent networks linked by fluidic bridges, whose openings are controlled by pressure valves. Following the formation of the immune complex, the reactive beads are magnetically transferred through the bridges before performing the final steps of the assay in unused protein-free channels. A three-step lithography process was developed for the fabrication of the fluidic master, on which the bi-layer PDMS device was produced in large quantities with constant functionality. The pressure valves were tested and proved to be operational for at least several hours, without observable leakage, pressure drop or contamination between the dual chambers. A protocol was established, which has enabled standard curves to be obtained

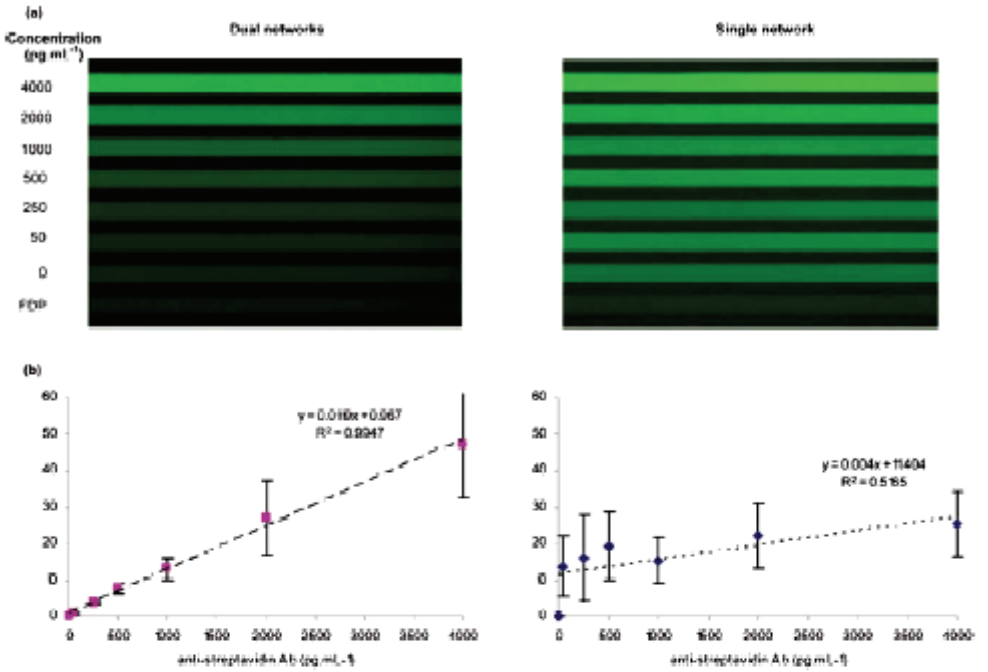

Fig. 6 Comparative results for microfluidic ELISA without pre-treatment against NSA using a single network and dual networks of channels. (a) Simultaneous fluorescent detection in all eight channels of the device. (b) Standard curves for the quantification of anti-streptavidin antibodies. Each point represents the average obtained in 4 separate experiments.

for the quantification of a model antibody in about 30 minutes. A detection limit of 100 pg mL^{-1} (660 fM) and good linearity up to 4 ng mL^{-1} were observed. These data are comparable to the performance of the most sensitive microfluidic immunoassays reported to date without the need for channel pre-treatment.

Acknowledgements

This work is supported by a joint grant from the Canadian Institute for Health Research and the National Research Council of Canada, as well as by the Fonds quebecois de la recherche de la nature et des technologies through the Centre for Biorecognition and Biosensors. The authors wish to thank Francois Normandin for technical help in building the mixing platform.

References

1 P. Yager, T. Edwards, E. Fu, K. Helton, K. Nelson, M. R. Tam and B. H. Weigl, *Nature*, 2006, **442**, 412–418.
2 S. K. Sia, V. Linder, B. A. Parviz, A. Siegel and G. M. Whitesides, *Angew. Chem., Int. Ed.*, 2004, **43**, 498–502.
3 D. Hoegger, P. Morier, C. Vollet, D. Heini, F. Reymond and J. S. Rossier, *Anal. Bioanal. Chem.*, 2007, **387**, 267–275.
4 Y. K. Hahn, Z. Jin, J. H. Kang, E. Oh, M. K. Han, H. S. Kim, J. T. Jang, J. H. Lee, J. Cheon, S. H. Kim, H. S. Park and J. K. Park, *Anal. Chem.*, 2007, **79**, 2214–2220.
5 L. J. Lee, S. T. Yang, S. Lai, Y. Bai, W. C. Huang and Y. J. Juang, *Adv. Clin. Chem.*, 2006, **42**, 255–295.
6 D. A. Barrett, M. S. Hartshorne, M. A. Hussain, P. N. Shaw and M. C. Davies, *Anal. Chem.*, 2001, **73**, 5232–5239.
7 T. Rohr, D. F. Ogletree, F. Svec and J. M. J. Frechet, *Adv. Funct. Mater.*, 2003, **13**, 264–270.
8 J. Liu, T. Pan, A. T. Woolley and M. L. Lee, *Anal. Chem.*, 2004, **76**, 6948–6955.
9 C. Li, Y. Yang, H. G. Craighead and K. H. Lee, *Electrophoresis*, 2005, **26**, 1800–1806.
10 R. Lin and M. A. Burns, *J. Micromech. Microeng.*, 2005, **15**, 2156–2162.
11 M. Salim, G. Mishra, G. J. Fowler, B. O'sullivan, P. C. Wright and S. L. McArthur, *Lab Chip*, 2007, **7**, 523–525.
12 M. Herrmann, T. Veres and M. Tabrizian, *Technical Proceedings of the 2006 NSTI Nanotechnology Conference*, 2006, **vol. 2**, pp. 244–247.
13 H. Makamba, J. H. Kim, K. Lim, N. Park and J. H. Hahn, *Electrophoresis*, 2003, **24**, 3607–3619.
14 E. Delamarche, D. Juncker and H. Schmid, *Adv. Mater.*, 2005.
15 H. Chen, Z. Zhang, Y. Chen, M. A. Brook and H. Sheardown, *Biomaterials*, 2005, **26**, 2391–2399.
16 H. Makamba, Y. Y. Hsieh, W. C. Sung and S. H. Chen, *Anal. Chem.*, 2005, **77**, 3971–3978.
17 W. Hellmich, J. Regtmeier, T. T. Duong, R. Ros, D. Anselmetti and A. Ros, *Langmuir*, 2005, **21**, 7551–7557.
18 H. Y. Chen, Y. Elkasabi and J. Lahann, *J. Am. Chem. Soc.*, 2006, **128**, 374–380.
19 Y. Dong, K. S. Phillips and Q. Cheng, *Lab Chip*, 2006, **6**, 675–681.
20 G. Sui, J. Wang, C. C. Lee, W. Lu, S. P. Lee, J. V. Leyton, A. M. Wu and H. R. Tseng, *Anal. Chem.*, 2006, **78**, 5543–5551.

21 D. Wu, B. Zhao, Z. Dai, J. Qin and B. Lin, *Lab Chip*, 2006, **6**, 942–947.
22 M. W. Toepke and D. J. Beebe, *Lab Chip*, 2006, **6**, 1484–1486.
23 M. Herrmann, T. Veres and M. Tabrizian, *Lab Chip*, 2006, **6**, 555–560.
24 M. A. Unger, H. P. Chou, T. Thorsen, A. Scherer and S. R. Quake, *Science*, 2000, **288**, 113–116.
25 J. Monahan, A. A. Gewirth and R. G. Nuzzo, *Anal. Chem.*, 2001, **73**, 3193–3197.
26 V. Studer, A. Pandolfi, M. Ortiz, W. F. Anderson and S. R. Quake, *J. Appl. Phys.*, 2004, **95**, 393–398.
27 E. Eteshola and D. Leckband, *Sens. Actuators, B*, 2001, **72**, 129–133.
28 E. Eteshola and M. Balberg, *Biomed. Microdev.*, 2004, **6**, 7–9.
29 J. S. Rossier and H. H. Girault, *Lab Chip*, 2001, **1**, 153–157.
30 S. Cesaro-Tadic, G. Dernick, D. Juncker, G. Buurman, H. Kropshofer, B. Michel, C. Fattinger and E. Delamarche, *Lab Chip*, 2004, **4**, 563–569.
31 N. Honda, U. Lindberg, P. Andersson, S. Hoffmann and H. Takei, *Clin. Chem.*, 2005, **51**, 1955–1961.
32 V. Linder, S. K. Sia and G. M. Whitesides, *Anal. Chem.*, 2005, **77**, 64–71.
33 E. P. Kartalov, J. F. Zhong, A. Scherer, S. R. Quake, C. R. Taylor and W. F. Anderson, *Biotechniques*, 2006, **40**, 85–90.
34 T. Yasukawa, M. Suzuki, T. Sekiya, H. Shiku and T. Matsue, *Biosens. Bioelectron.*, 2007, **22**, 2730–2736.
35 J. F. Dishinger and R. T. Kennedy, *Anal. Chem.*, 2007, **79**, 947–954.
36 R. C. Bailey, G. A. Kwong, C. G. Radu, O. N. Witte and J. R. Heath, *J. Am. Chem. Soc.*, 2007, **129**, 1959–1967.
37 E. D. Goluch, J. M. Nam, D. G. Georganopoulou, T. N. Chiesl, K. A. Shaikh, K. S. Ryu, A. E. Barron, C. A. Mirkin and C. Liu, *Lab Chip*, 2006, **6**, 1293–1299.
38 K. Sato, M. Yamanaka, T. Hagino, M. Tokeshi, H. Kimura and T. Kitamori, *Lab Chip*, 2004, **4**, 570–575.

Analytical Chemistry: permission to include the manuscript and figure (4.6) in thesis

Anal. Chem. **XXXX**, *xxx*, 000–000

Quantification of Low-Picomolar Concentrations of TNF-α in Serum Using the Dual-Network Microfluidic ELISA Platform

Marc Herrmann,[†,‡] Teodor Veres,[*,‡] and Maryam Tabrizian[*,†]

Biomedical Engineering Department and Faculty of Dentistry, McGill University, Montreal, QC, H3A 2B4, Canada, and Industrial Materials Institute, National Research Council, Boucherville, QC, J4B 6Y4, Canada

For both research and diagnostic purposes, the ability to detect low levels of proteins in a cost- and time-effective manner is essential. In this study, the cytokine TNF-α (tumor necrosis factor-α), a widely used protein indicator of inflammatory response, was chosen to demonstrate the ability of the dual-network microfluidic ELISA (enzyme-linked immunosorbent assay) platform developed by the authors to rapidly quantify low concentrations of this biomarker in serum. Through the optimization of several experimental parameters, the system was shown to meet the requirements for fundamental and applied studies, while also being relevant for challenging clinical applications such as the diagnosis of septic patients. A sensitivity of 45 pg/mL (2.6 pM) in both culture medium and serum, with inter- and intravariations of less than 15%, was attained for the quantification of human TNF-α to a concentration of up to 500 pg/mL. The overall time for completion of the assay in eight parallel reactions was less than 1 h.

Tumor necrosis factor-α (TNF-α) is a biomarker frequently assayed for diverse research and diagnostic purposes. It is a small circulating protein of the cytokine family (17.4 kDa), secreted primarily by monocytes and macrophages as a mediator in the early stage of the inflammatory and immune functions.[1] Alone or in combination with other proteins, TNF-α is used as an indicator to follow cellular reactions to external stimuli or to detect certain pathological conditions. Among other applications, TNF-α secretion is commonly assessed in immunological studies,[2] and its levels are measured to determine the biocompatibility of various types of materials and implants.[3] In these studies, the accepted relevant concentrations of TNF-α range in the 100 pg/mL bracket. For diagnostic purposes, TNF-α is used as an early indicator of inflammatory reactions. When such a reaction occurs, the fine balance between pro- and anti-inflammatory cytokines has to be monitored and maintained in the patient's blood.[4] The up-regulation of proinflammatory cytokines, in particular TNF-α, can lead to acute inflammatory reactions, tissue injuries, or in the instance of a severe infection, to a dangerous state of septic shock. The concentration of TNF-α in septic patients typically ranges from 20 to 100 pg/mL, rendering the diagnosis of sepsis particularly challenging even for the most sensitive immunoassays currently in use. Elevated levels of TNF-α have also been associated with chronic inflammatory syndromes such as rheumatic arthritis or Crohn's disease.[5]

Conventional immunoassays are time- and resource-consuming, particularly when extensive automation is not economically beneficial or when portability becomes a predominant requirement. Consequently, there has been a sustained effort in the past decade to develop reliable diagnostic tools while reducing the complexity and associated costs of such assays. The miniaturization of immunoassays using microfluidics has been with no contest one of the most popular techniques, as it permits one to significantly reduce reagent volumes and incubation times.[6–13] However, to date, a very few number of microfluidic systems have achieved fast, parallel, and highly sensitive detection of biomedically relevant proteins using a single fully functional microfluidic chip.[14–16] The dual-network microfluidic ELISA (enzyme-linked immunosorbent assay) platform developed in our laboratory has

* Corresponding authors. Phone: 514-398-8129 (M.T.), 450-641-5232 (T.V.). Fax: 514-398-7461 (M.T.), 450-641-5105 (T.V.). E-mail: maryam.tabrizian@mcgill.ca (M.T.), teodor.veres@imi.cnrc-nrc.gc.ca (T.V.).

† McGill University.

‡ National Research Council.

(1) Curfs, J. H.; Meis, J. F.; Hoogkamp-Korstanje, J. A. *Clin. Microbiol. Rev.* **1997**, *10*, 742–780.

(2) Segura, M.; Su, Z.; Piccirillo, C.; Stevenson, M. M. *Eur. J. Immunol.* **2007**, *37*, 1887–1904.

(3) Leguen, E.; Chassepot, A.; Decher, G.; Schaaf, P.; Voegel, J. C.; Jessel, N. *Biomol. Eng.* **2007**, *24*, 33–41.

(4) Carrigan, S. D.; Scott, G.; Tabrizian, M. *Clin. Chem.* **2004**, *50*, 1301–1314.

(5) Palladino, M. A.; Bahjat, F. R.; Theodorakis, E. A.; Moldawer, L. L. *Nat. Rev. Drug Discovery* **2003**, *2*, 736–746.

(6) Lee, L. J.; Yang, S. T.; Lai, S.; Bai, Y.; Huang, W. C.; Juang, Y. J. *Adv. Clin. Chem.* **2006**, *42*, 255–295.

(7) Eteshola, E.; Leckband, D. *Sens. Actuators, B* **2001**, *72*, 129–133.

(8) Choi, J. W.; Liakopoulos, T. M.; Ahn, C. H. *Biosens. Bioelectron.* **2001**, *16*, 409–416.

(9) Lai, S.; Wang, S.; Luo, J.; Lee, L. J.; Yang, S. T.; Madou, M. J. *Anal. Chem.* **2004**, *76*, 1832–1837.

(10) Sato, K.; Tokeshi, M.; Odake, T.; Kimura, H.; Ooi, T.; Nakao, M.; Kitamori, T. *Anal. Chem.* **2000**, *72*, 1144–1147.

(11) Gao, Y.; Hu, G.; Lin, F. Y.; Sherman, P. M.; Li, D. *Biomed. Microdevices* **2005**, *7*, 301–312.

(12) Herr, A. E.; Hatch, A. V.; Throckmorton, D. J.; Tran, H. M.; Brennan, J. S.; Giannobile, W. V.; Singh, A. K. *Proc. Natl. Acad. Sci. U.S.A* **2007**, *104*, 5268–5273.

(13) Sia, S. K.; Linder, V.; Parviz, B. A.; Siegel, A.; Whitesides, G. M. *Angew. Chem., Int. Ed.* **2004**, *43*, 498–502.

(14) Cesaro-Tadic, S.; Dernick, G.; Juncker, D.; Buurman, G.; Kropshofer, H.; Michel, B.; Fattinger, C.; Delamarche, E. *Lab Chip* **2004**, *4*, 563–569.

(15) Honda, N.; Lindberg, U.; Andersson, P.; Hoffmann, S.; Takei, H. *Clin. Chem.* **2005**, *51*, 1955–1961.

(16) Goluch, E. D.; Nam, J. M.; Georganopoulou, D. G.; Chiesl, T. N.; Shaikh, K. A.; Ryu, K. S.; Barron, A. E.; Mirkin, C. A.; Liu, C. *Lab Chip* **2006**, *6*, 1293–1299.

10.1021/ac800427z CCC: $40.75 © XXXX American Chemical Society
Published on Web 05/13/2008

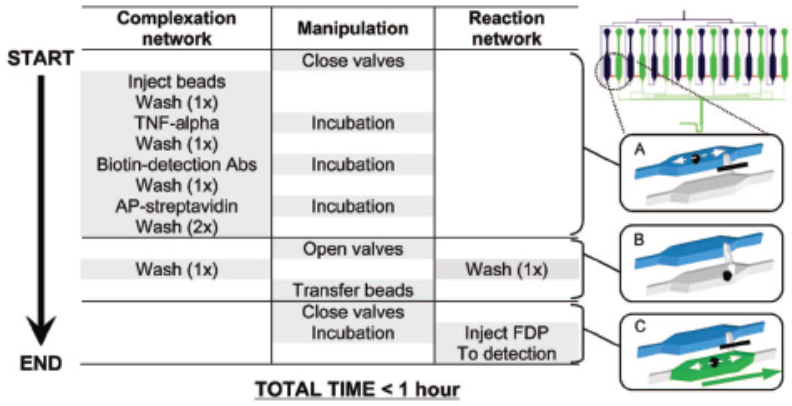

Figure 1. Protocol for dual-network microfluidic ELISA with TNF-α. The table indicates the successive steps from top to bottom. The layout of the poly(dimethylsiloxane) (PDMS) chip for eight parallel reactions is drawn in the top-right corner; the complexation network is colored in blue, the reaction network in green. The windows A, B, and C represent close-ups on one pair of dual chambers at different steps of the assay. (A) Complexation phase; the closed valve is represented by the solid black line separating the chambers; the white arrow shows the bead displacement pattern. (B) Magnetic transfer phase. (C) Reaction and detection phases.

displayed promising characteristics to achieve that goal.[17] Its original concept relies on the physical separation of the immune complex formation phase and the enzymatic reaction phase into two independent networks of channels. These two networks are linked only by fluidic bridges whose openings are controlled by embedded pressure valves through which the reactive beads are magnetically transferred before the final immunodetection step is performed. As a result, the background noise originating from nonspecific adsorption (NSA) of protein on the channel walls was eliminated, thereby removing the need for long, costly, or unstable pretreatments.

In this article, we demonstrate that the dual-network microfluidic ELISA can be successfully tuned in order to quantify low levels of biomarkers in both cell culture medium and serum, through the adjustment of its most critical assay parameters. The variables regulated were the amount of detection antibody, the bead displacement velocity, and the duration of the incubation and detection periods. By doing so, low-picomolar concentrations of TNF-α were detected in eight parallel reactions with good reproducibility in less than 1 h, thus confirming the potential use of this system for biomedical applications in research or for the diagnosis of septic patients in clinical conditions.

MATERIAL AND METHODS

Proteins and Reagents. Trizma base (Tris), Tween-20, and glycine were obtained from Sigma-Aldrich, and magnesium chloride was from ACP Chemicals. Tosylactivated paramagnetic microbeads (Dynabeads M-280 tosylactivated) were purchased from Invitrogen, as well as the pair of capture (AHC 3712) and biotin-labeled detection (AHC 3419) monoclonal antibodies against TNF-α. The human recombinant TNF-α was obtained from Peprotech, and the alkaline phosphatase coupled streptavidin, alkaline phosphatase coupled antirabbit, and antimouse antibodies were from Rockland Immunochemicals. The enzymatic substrate fluorescein diphosphate (FDP) was purchased from Anaspec. The washing buffer, also used for priming of the channels, is a Tris buffer saline (0.1 M Tris, 150 mM NaCl, pH = 7.4) supplemented with 0.02% Tween-20 (TBS-T). All proteins were diluted in TBS-T 0.1% BSA (bovine serum albumin) as carrier protein, unless mentioned otherwise. The enzymatic substrate FDP was diluted to a final concentration of 4 μM in the reaction buffer consisting of 0.1 M Tris, 10 mM $MgCl_2$, 10 mM glycine, pH = 9.0.

Tosylactivated Beads Functionalization. Dynabeads M-280 tosylactivated were functionalized according to the manufacturer's instructions. Briefly, 200 μL of beads (40×10^7 beads) was thoroughly washed in a 0.1 M borate buffer pH 9.5. The beads were then incubated overnight at 37 °C with slow tilt rotation in a solution of the same borate buffer containing the mouse monoclonal capture antibody at a ratio of 3 μg of antibody/10^7 beads. Subsequently, the beads were washed twice in phosphate-buffered saline (PBS) buffer, pH 7.4, 0.1% BSA at 4 °C, once in 0.2 M Tris, pH 8.5, 0.1% BSA for 4 h at 37 °C for blocking the free tosyl groups, and a last time with the PBS buffer at 4 °C. The beads were resuspended and stored in 200 μL of PBS, pH 7.4, 0.1% BSA supplemented with 0.02% sodium azide as preservative. Following the above procedure, the functionalized beads were tested to ensure the successful binding of the capture antibodies. On a dual-network microfluidic ELISA chip featuring eight independent pairs of channels, two were used as negative controls in the presence of nonfunctionalized beads, three for incubation of the functionalized beads with an alkaline phosphatase coupled antirabbit antibody, and the remaining three for incubation of the same beads with an alkaline phosphatase coupled antimouse antibody. The results of such a test are provided as Supporting Information (Figure S-1).

Protocol for Dual-Network Microfluidic ELISA with TNF-α. Before mounting the chip on the mixing platform and securing the valve connection, both the fluidic and the control channels were filled with TBS-T using the channel outgas technique (COT).[18] The concept of dual network and protocol for the quantification of TNF-α are summarized in Figure 1. For each step, a few microliters of solution (5–15 μL) was deposited in the

(17) Herrmann, M.; Roy, E.; Veres, T.; Tabrizian, M. *Lab Chip* **2007**, *7*, 1546–1552.
(18) Monahan, J.; Gewirth, A. A.; Nuzzo, R. G. *Anal. Chem.* **2001**, *73*, 3193–3197.

inlets and flown through the channels by connecting the appropriate outlet to a peristaltic pump in withdrawal mode. After each run, the residual solution trapped at the bottom of the inlets was aspirated to avoid cross-contamination of the sequentially injected solutions.

Detection and Data Analysis. An inverted microscope (TE2000-U, Nikon), a stereoscopic zoom microscope (SMZ1500, Nikon), and a digital camera (DXM1200F, Nikon) operated with the ACT-1 software were used to acquire images of the channels along the detection area. For fluorescence imaging, the microscope is equipped with a high-pressure mercury lamp (C-SHG1, Nikon) and with the appropriate set of filters for fluorescein (FITC) excitation and emission wavelengths. The intensity of fluorescence in each channel was determined with ImageJ, a Java-based software for image processing and analysis. All data were normalized by subtracting the intensity obtained in the negative control of the same experiment. In order to calculate the sensitivity of the assay for the quantification of TNF-α, three independent experiments were carried out, each featuring five repetitions of the negative control. The standard deviations were then averaged for the three experiments. The sensitivity was calculated by adding 3 times the average standard deviation applied to the equation of the final standard curve.

Fabrication of the Dual-Network Microfluidic Chip. The dual-network microfluidic chip is composed of two overlaid layers of poly(dimethylsiloxane) (PDMS) (Sylgard184, Dow Corning), both fabricated by casting the precured elastomer on an SU-8 resist (SU-8 1070, Microchem) previously structured by standard photolithography. The fluidic bridges, linking the two networks, were fabricated using a positive resist (AZ 50xt, AZ Electronic Materials) and aligned on an aligner EVG 6200 (EV Group, Austria). After development, the master was treated with trichloro(1H,1H,2H,2H-perfluorooctyl)-silane (Sigma-Aldrich) to obtain a hydrophobic surface and facilitate the release of the cured PDMS. The surface treatment was followed by reflow of the positive resist for 10 min at 120 °C resulting in fluidic bridges with rounded sections. The two layers of PDMS were cured separately on their respective masters as established by Quake's group.[19] After a precuring step of 30 min at 80 °C, the 4 mm thick top layer was released from its master and aligned on the top of the thin fluidic layer. The bilayer assembly was further cured at 80 °C for at least 2 h to achieve permanent thermal bonding. Finally, the bilayer PDMS device was pealed off the fluidic master and the inlets and outlets were punched out. The system was then reversibly sealed on a glass slide and ready for use.

RESULTS AND DISCUSSION

Influence of the Detection Antibody Concentration. In immunoassays, an elevated background noise seriously impairs both sensitivity and linear range and increases variations between tested samples. In our device, the noise generated by NSA of proteins on the channel walls is eliminated by magnetically transferring the reactive beads into a clean unused reaction chamber. However, some residual background can result from NSA of proteins on the beads themselves. To limit this effect, the functionalized tosylactivated beads are kept for long-term storage in a PBS buffer containing 0.1% BSA as a blocking agent. Nevertheless, an important parameter to be optimized in this regard is the concentration of detection antibody used for the assay. Ideally, it is necessary to provide enough molecules to bind all previously captured antigens, without adding an excess as to cause an increase in NSA and ultimately generate background noise.

Figure 2 displays the standard curves obtained for concentrations of TNF-α ranging from 10 pg/mL to 1 ng/mL, with respect to increased concentrations of the detection antibody. The incubation and detection times were arbitrary set at 10 min, alkaline phosphatase coupled streptavidin was diluted 1:10 000, and the bead displacement velocity was adjusted at 400 μm/s. Each curve represents the average of three independent experiments realized on separate chips; thus, error bars represents the interassay variations rather than internal variations of the system. The fluorescent signals for each experiment were normalized to the signal obtained in the negative control of the same experiment (all identical steps with no TNF-α). In immunoassays, two of the most important parameters are the slope of the curve which reflects the sensitivity of the assay and the correlation coefficient R^2 which describes its linearity. Accordingly, the optimal concentration for the detection antibody was found to be 0.5 μg/mL. Data obtained with 1.0 μg/mL displayed similar sensitivity values but exhibited lower linearity. With a concentration of 0.25 μg/mL, however, the slope was significantly lowered with little improvement in linearity, indicating that not all the captured analytes had been bound by detection antibodies in the allotted time. Conversely, increasing the detection antibody concentration to 2 μg/mL generated considerable background signal, thus impairing both interassay reproducibility and linearity due to the rapid saturation of the fluorescent signal. On the basis of this series of experiments, following assays were realized with the optimal detection antibody concentration of 0.5 μg/mL. The standard curve obtained with this specific set of parameters is referred to as the *default* experiment to which later experiments are compared.

Influence of Bead Displacement Velocity. Unlike the majority of microfluidic devices, which operate in a continuous flow mode, this immunoassay was designed to work in stop-flow conditions.[20] In this setup, the fluidic channels are filled with the appropriate solution before the flow is stopped for incubation and the next solution is flown to replace it. This method reduces and improves the control of reagent volumes used, which are defined by the geometry of the channel rather than by the flow rate and manual pipetting. Also it avoids the dependency of the assay performance on the flow rate. In order to prevent local depletion of the analyte molecule at the vicinity of the capture zone,[21] the functionalized beads were magnetically moved from one end to the other end of the fluidic chamber during incubation periods. This manipulation allowed for the reaching of the analyte molecules in the entire volume of the chamber while creating disturbances in the surrounding solution, thus enhancing the analyte exploitation rate.

Figure 3 illustrates the effect of the bead displacement velocity on the outcome of the assay for TNF-α. In the default experiment, the beads were displaced at the maximum velocity of 400 μm/s

(19) Unger, M. A.; Chou, H. P.; Thorsen, T.; Scherer, A.; Quake, S. R. *Science* 2000, *288*, 113–116.

(20) Herrmann, M.; Veres, T.; Tabrizian, M. *Lab Chip* 2006, *6*, 555–560.

(21) Zimmermann, M.; Delamarche, E.; Wolf, M.; Hunziker, P. *Biomed. Microdevices* 2005, *7*, 99–110.

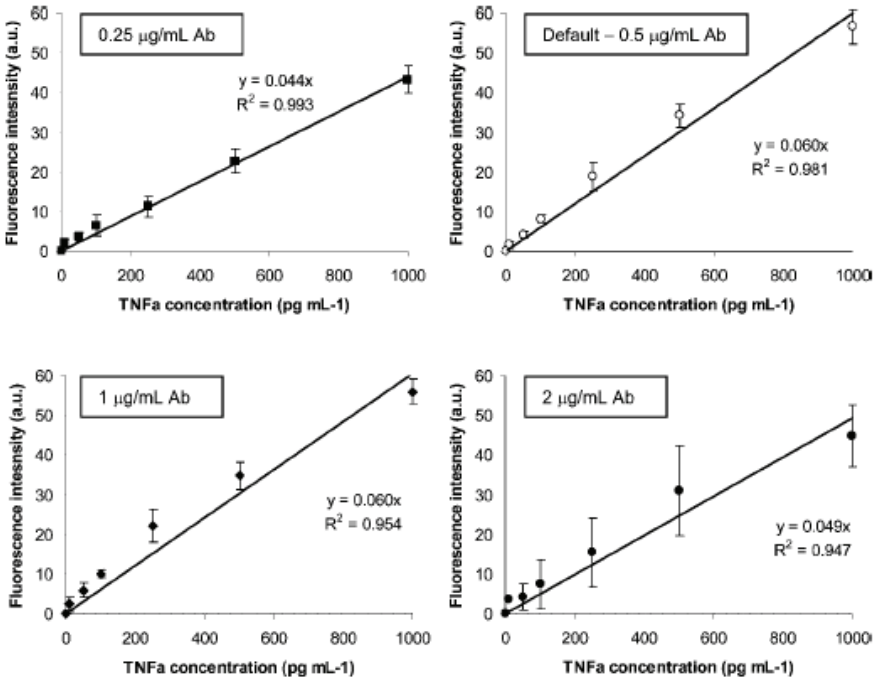

Figure 2. Influence of the concentration of detection antibody on the quantification of TNF-α by dual-network microfluidic ELISA. Other parameters were set at their default conditions. All fluorescence intensity data were normalized by subtracting the value of the negative control of the same experiment. Each data point is the average of three independent experiments. Error bars represent the interassay variation for each condition.

during the three incubation periods, as well as during the enzymatic reaction phase (maximum velocity due to current hardware limitations). When the same experiment was conducted without displacing the beads during the incubation periods (the beads were moved only during the reaction phase), the fluorescent signal was drastically weakened, suggesting rapid local depletion and limited diffusion of the analyte molecules during the 10 min of flow stop. When the beads were moved at 200 μm/s, the overall signal became stronger, coming close to the signal obtained in the default experiment. Surprisingly, the curve also displayed a marked saturation profile at higher concentrations of TNF-α. This difference in linearity can be explained by the behavior of the beads while being moved inside the fluidic chamber. During flow phase, the beads are held by a strong permanent magnet placed directly under the glass slide that forms the bottom of the chip (approximately 1 mm from the beads). At that distance, the magnetic field is still very strong; thus, the beads aggregate in a tight bed with little space between them for the solution to circulate. During incubation phases, however, the magnet is moved, followed by a smear of beads, which widens when the movement is faster. The formation of the smear increases bead dispersion which in turn increases the effective surface of capture sites at the functionalized surfaces. According to these results, the bead displacement velocity for further experiments was set at 400 μm/s.

Influence of Incubation Times. Another important parameter affecting the outcome of an immunoassay is the time given for the molecules to interact with each other and form a stable immunocomplex. The present protocol features three sequential incubation periods with, respectively, TNF-α, the biotinylated detection antibody, and the alkaline phosphatase coupled streptavidin. Variations of the incubation time affected both the slope and the linearity of the standard curve (Figure 4). In comparison to the default experiment, when the incubation time was reduced by half, from 10 to 5 min, the slope decreased by about the same factor with only a slight increase in linearity. These data suggest that the saturation of the beads with the maximum loading of TNF-α occurs shortly before 10 min of incubation, which also explains the slightly saturated profile of the default curve. Extending the incubation times to 15 min confirmed the bead saturation at higher concentrations, leading to an even less linear and slightly less sensitive curve than the one of the default experiment.

Influence of Detection Time. Following the three incubation periods and the magnetic transfer of the beads carrying the immune complex to the reaction chamber, the reaction network is filled with a solution of the enzymatic substrate for alkaline phosphatase FDP. The enzymatic reaction converting FDP into green-fluorescent fluorescein then occurs in conditions similar to the previous incubation phase. The extent of the enzymatic amplification period is expected to display a drastic effect on the outcome of the immunoassay and the profile of the standard curve (Figure 5). In comparison to the default experiment, when the detection time was increased from 10 to 15 min, the independent signals obtained for the different concentrations of TNF-α were significantly increased. However, the curve can no longer be considered linear on the tested range with a correlation coefficient of only 0.92. The excessively saturated profile in this case stems

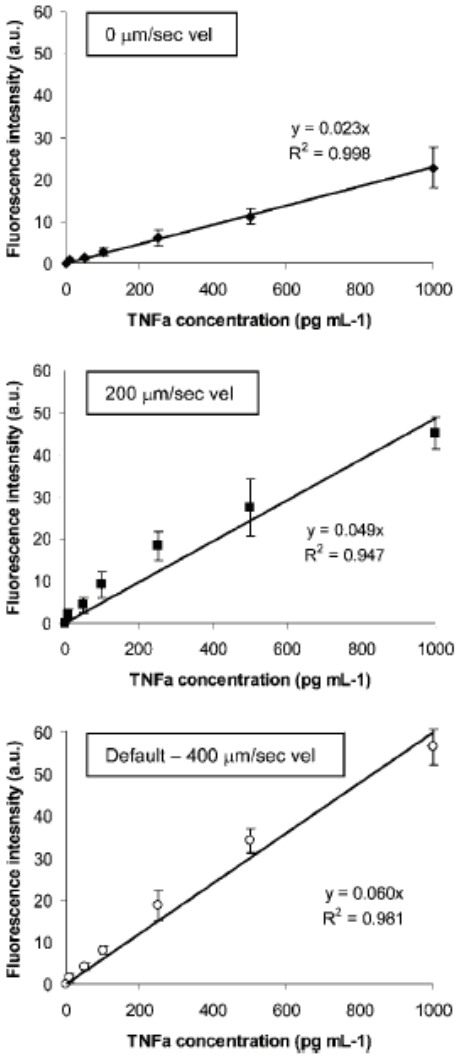

Figure 3. Influence of the bead displacement velocity on the quantification of TNF-α by dual-network microfluidic ELISA. Other parameters were set at their default conditions. All fluorescence intensity data were normalized by subtracting the value of the negative control of the same experiment. Each data point is the average of three independent experiments. Error bars represent the interassay variation for each condition.

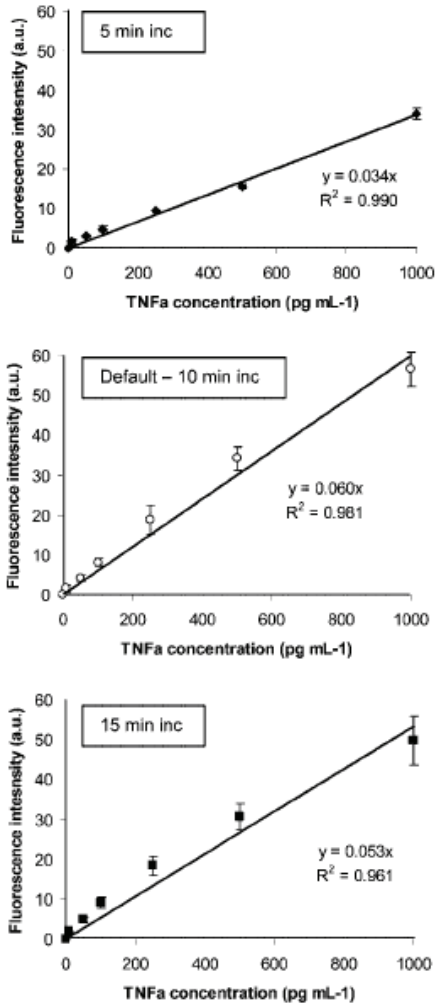

Figure 4. Influence of the incubation times on the quantification of TNF-α by dual-network microfluidic ELISA. Other parameters were set at their default conditions. All fluorescence intensity data were normalized by subtracting the value of the negative control of the same experiment. Each data point is the average of three independent experiments. Error bars represent the interassay variation for each condition.

from at least two major effects. First, the already slightly saturated profile observed in the default experiment is further amplified as the enzymatic reaction is extended. Second, the rate of conversion of FDP is likely to decelerate as the concentration of substrate decreases in the substrate solution. Saturation of the detection device at high fluorescent intensities also enhances the latter effect. Although increasing detection time can significantly improve the overall sensitivity of the assay, it can also be detrimental on both the linearity and the dynamic range as it amplifies minor variations in the signal. For the following experiment, the detection time was maintained at 15 min, but incubation periods were shortened from 10 to 5 min. Interestingly, the profile obtained was quasi-identical to the one observed in the default experiment in terms of both the slope and linearity, with an overall assay time reduced from 40 to 30 min. Only a minor increase in the interassay variability was caused by the extension of the detection time, as the efficiency of the enzymatic reaction differs between each assay due to external conditions, such as temperature or ambient light, and contributes for the largest part to this type of variability.

When setting up an immunoassay, it is important to consider the relevant range of concentrations in which a particular analyte has to be detected and quantified. For a biomarker such as TNF-α, although concentrations of several 100 pg/mL can be found in experimental samples, clinical values, for the diagnosis of septic patient for instance, stand typically around 100 pg/mL and below. Therefore, narrowing down the dynamic range to 500 pg/mL, in

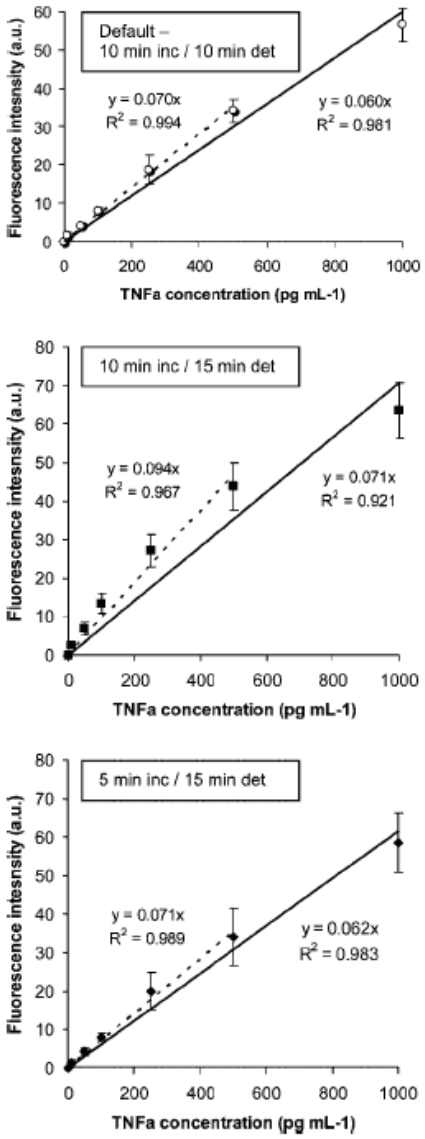

Figure 5. Influence of the detection time on the quantification of TNF-α by dual-network microfluidic ELISA. Other parameters were set at their default conditions except for the bottom graph where incubation times were set to 5 min each. The solid curve represents the trend line for data points taken between 10 pg/mL and 1 ng/mL; the dashed curve is the trend line for the same data points taken only up to 500 pg/mL. All fluorescence intensity data were normalized by subtracting the value of the negative control of the same experiment. Each data point is the average of three independent experiments. Error bars represent the interassay variation for each condition.

order to cancel the light saturation effect, might give a more accurate quantification of TNF-α around biomedically relevant levels. The doted lines in Figure 5 show the corrections made to the standard curves when removing the last data point at 1 ng/mL of TNF-α. In all three cases, both the linearity and slope of the curves were improved though to different extents. For the default experiment and the experiment with 5 min incubation periods, improvements of the slope is moderate (117% and 114% of the respective slopes taken on the full range) while both correlation coefficients approximated 0.99, indicating excellent linearity. The experiment with 10 min incubation periods and 15 min detection time undergoes a more drastic change, with a slope increased by 132% and a linearity approaching 0.97. Nevertheless, because saturation of the signal is still observed in these conditions, this last standard curve cannot be used accurately on the designated range of concentrations despite its stronger slope.

Quantification of TNF-α in Serum. For the adjustment of experimental parameters, all previous experiments were run with TNF-α diluted in a TBS buffer supplemented with 0.1% BSA as a protein carrier. In order to show the ability of the dual-network microfluidic system to perform in conditions close to its final intended use, the previous measurements were repeated with TNF-α diluted in a more complex solution (Figure 6). First, the experiment was conducted with TNF-α diluted in a Dulbecco's modified Eagle's medium (DMEM) cell culture medium supplemented with 10% fetal bovine serum (FBS). The addition of interfering proteins decreased the slope of the standard curve when default parameters are used. Nevertheless, by extending the detection incubation period from 10 to 15 min, the slope was increased to its original value with excellent linearity. Quasi-identical data were obtained with TNF-α diluted into pure serum (FBS). The excellent linearity, even with the addition of an extra data point at high concentration of TNF-α, demonstrated again the reliability of the standard curve within the tested range of concentrations, from 25 to 500 pg/mL. Typically, similar results in cell culture medium and pure FBS are not expected because of the more complex composition of serum containing many uncharacterized proteins that interfere with the reaction. It is very interesting to observe that the dual-network assay, by getting rid of the larger part of the background noise, manages to maintain the same efficacy in both medium. For clarity, a summary of slope and linearity data for all tested conditions is provided in Table 1.

The assay sensitivity was calculated based on three independent experiments, each featuring five repetitions of the negative control. The value obtained for the quantification of TNF-α in a cell culture medium or pure serum was 45 pg/mL (2.56 pM). This sensitivity is considered adequate as it falls within range of concentrations relevant for research and diagnostic purposes. Moreover, concentrations of TNF-α as low as 25 pg/mL were consistently detected and fitted very well on the linear standard curve. Error bars represent the variations in the signal obtained from three independent experiments performed in identical conditions. The interassay coefficient of variation was found to be in the order of 15% or less for concentrations of 50 pg/mL and above. Intra-assay variations were also calculated by running five repetitions of a given concentration of TNF-α on a single chip along with the appropriate controls. At the exception of the concentration of 50 pg/mL, for which the intra-assay variation coefficient was calculated at 24%, internal variations were all below 15% for concentrations of 100 pg/mL and above. The specificity of the reaction for TNF-α in serum was confirmed by substituting the specific mouse monoclonal capture antibody anti-TNF-α with a nonspecific mouse IgG control purified from a nonimmunized

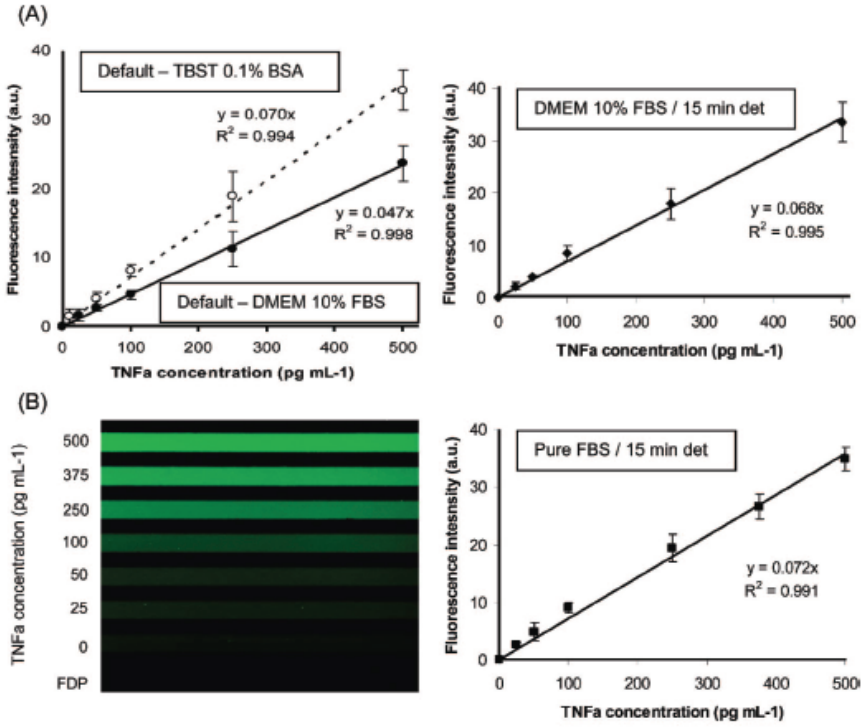

Figure 6. Influence of the dilution medium on the quantification of TNF-α by dual-network microfluidic ELISA. (A) The discontinuous curve on the left panel was obtained with default parameters and TNF-α diluted in TBS-T; the continuous curve was obtained in identical conditions with TNF-α diluted in a DMEM cell culture medium with 10% FBS. On the right panel, the detection time was extended from 10 to 15 min. (B) On the right panel, the standard curve for the quantification of TNF-α in pure serum is displayed; all parameters were set to default expect for the 15 min detection time. The left picture shows a typical fluorescent photograph of the detection area in these conditions.

animal (Supporting Information Figure S-2). Given inherent variations such as small differences in the number of beads, magnets alignment, and fluorescence inhomogeneity, which could be overcome in a more automated and integrated platform, these values are considered very promising at this stage of development.[22]

With a low-picomolar sensitivity in both cell culture medium and serum, good reproducibility, and a total assay time of less than 1 h, the dual-network microfluidic system places itself among the most achieved microfluidic immunoassays described to date. For the quantification of TNF-α specifically, the sensitivity is very near the values obtained with traditional microwell ELISA as well as with the highly sensitive micromosaic assay developed by Cesaro-Tadic et al. at IBM Research.[14] In comparison to the latter, the overall assay time is significantly reduced, as the combined use of magnetic microbeads and pressure valves removes the need for precoating the chip with the capture antibody or blocking the uncoated sites. Reaction volumes of 600 nL, identical to those used in the micromosaic assay, are delimited by the fluidic chambers in which the beads are displaced. No complex design for solution transportation is required since working in stop-flow mode insures minimal influence of the flow rate. Besides, the dual-network chip is entirely fabricated in PDMS, using only soft-lithography techniques, which makes it simple and inexpensive to produce.

The dual-network system also compares very well to the most recent commercial products in the field of miniaturized immunoassay, such as the fully automated GyroLab Bioaffy CD platform[15] or the electrochemical-based Gravi-Chip.[23,24] Similar to these systems, the time needed for completion of parallel assays and the throughput of the dual-network device could benefit greatly from a fully automated platform and a better controlled environment for the enzymatic reaction. Moreover, the sensitivity of the dual-network assay could be further improved including by integrating the detection device on the platform and by enhancing bead dispersion inside the microfluidic chambers, for example, by the use of ultrasonic vibrations or the addition of nanopillars inside the chambers. A better bead dispersion is expected to improve the assay sensitivity in both a direct an a indirect manner: directly by increasing the active capture area, which would also broaden the dynamic range and potentially decrease incubation times for complete analyte exploitation; indirectly by decreasing variability, especially at low concentrations of analyte and for the negative control and by increasing washing efficiency.

CONCLUSION

In this article, we demonstrated the possibility for the rapid quantification of low concentrations of protein biomarkers in

(22) Gao, Y.; Sherman, P. M.; Sun, Y.; Li, D. *Anal. Chim. Acta* 2008, *606*, 98–107.
(23) Rossier, J. S.; Girault, H. H. *Lab Chip* 2001, *1*, 153–157.
(24) Hoegger, D.; Morier, P.; Vollet, C.; Heini, D.; Reymond, F.; Rossier, J. S. *Anal. Bioanal. Chem.* 2007, *387*, 267–275.

Table 1. Summary of Slope and Linearity Data for All Tested Conditions[a]

Nb	Detection Ab concentration (μg/mL)	Bead displacement velocity (μm/sec)	Incubation periods (min)	Detection period (min)	Medium for TNF-alpha dilution	Linear slope up to 1 ng/mL - up to 0.5 ng/mL	Linearity R^2 up to 1 ng/mL - up to 0.5 ng/mL
1	0.25	400	10	10	TBS-T 0.1% BSA	0.044	0.993
2	0.5	400	10	10	TBS-T 0.1% BSA	0.060 - 0.070	0.981 - 0.994
3	1.0	400	10	10	TBS-T 0.1% BSA	0.060	0.954
4	2.0	400	10	10	TBS-T 0.1% BSA	0.049	0.947
5	0.5	0	10	10	TBS-T 0.1% BSA	0.023	0.998
6	0.5	200	10	10	TBS-T 0.1% BSA	0.049	0.947
7	0.5	400	5	10	TBS-T 0.1% BSA	0.034	0.990
8	0.5	400	15	10	TBS-T 0.1% BSA	0.053	0.961
9	0.5	400	10	15	TBS-T 0.1% BSA	0.071 - 0.094	0.921 - 0.967
10	0.5	400	5	15	TBS-T 0.1% BSA	0.062 - 0.071	0.983 - 0.989
11	0.5	400	10	10	DMEM 10% FBS	X - 0.047	X - 0.998
12	0.5	400	10	15	DMEM 10% FBS	X - 0.068	X - 0.995
13	0.5	400	10	15	Pure FBS	X - 0.072	X - 0.991

[a] The second set of parameters was arbitrarily chosen as the default condition and is referred to as the default experiment throughout the text. For clarity, the most favorable conditions for the quantification of TNF-α using the dual-network microfluidic ELISA platform are shaded in gray.

serum using the dual-network microfluidic ELISA platform. By carefully assessing the assay performance as a function of the concentration of the detection antibody, the bead displacement velocity, and the incubation and detection times, we have attained a good compromise in terms of sensitivity (2.56 pM), dynamic range of detection (25−500 pg/mL), reproducibility (<15% variability), time efficiency (<1 h), and user friendliness. These results suggest that the platform is suitable for fundamental and applied research studies, as well as demonstrate its potential for use in medical applications for the early diagnosis of diseases and infections. These performances, combined with the inexpensive fabrication process and the concept of dual network, which removes the need for pretreatment of the chip, contribute to make of this system an extremely sharp, cost-effective, and versatile device. The automation of flow injection, the integration of the detection device, and the achievement of an enhanced bead dispersion during incubation times are the next developments to be addressed. These investigations will help to further increase the sensitivity, reproducibility, detection range, and throughput of the assay, thereby creating a very competitive platform for performing immunoassays in point-of-care or on-field analysis settings.

ACKNOWLEDGMENT

This work is supported by a joint Grant from the Canadian Institute for Health Research and the National Research Council of Canada, as well as by the Fonds Quebecois de la Recherche de la Nature et des Technologies through the Centre for Biorecognition and Biosensors, and NanoQuebec. The authors thank F. Normandin for technical help in building the mixing platform, Dr. C. Piccirillo for his participation in inspiring talks, and Dr. M. Roberts for his assistance in editing the manuscript.

SUPPORTING INFORMATION AVAILABLE

Additional information as noted in text. This material is available free of charge via the Internet at http://pubs.acs.org.

Received for review February 29, 2008. Accepted April 15, 2008.

AC800427Z

SPRINGER LICENSE
TERMS AND CONDITIONS

May 22, 2008

This is a License Agreement between Marc Herrmann ("You") and Springer ("Springer"). Please note that you are liable to account for Value Added Tax (VAT). The license consists of your order details, the terms and conditions provided by Springer, and the payment terms and conditions.

License Number	1954360099953
License date	May 22, 2008
Licensed content publisher	Springer
Licensed content publication	Analytical and Bioanalytical Chemistry
Licensed content title	Disposable microfluidic ELISA for the rapid determination of folic acid content in food products
Licensed content author	Daniela Hoegger
Licensed content date	Nov 30, 2006
Volume number	387
Issue number	1
Pages	267 - 275
Type of Use	Thesis / Dissertation
Details of use	Print
Requestor Type	Individual
Portion of the article	Figures
Title of your thesis / dissertation	Development of a Microfluidic Immunoassay Platform for the Rapid Quantification of Low-Picomolar Concentrations of Protein Biomarkers
Expected completion date	Jun 2008
Total	0.00 USD
Terms and Conditions	

Introduction
The publisher for this copyrighted material is Springer Science + Business Media. By clicking "accept" in connection with completing this licensing transaction, you agree that the following terms and conditions apply to this transaction (along with the Billing and Payment terms and conditions established by Copyright Clearance Center, Inc. ("CCC"), at the time that you opened your Rightslink account and that are available at any time at http://myaccount.copyright.com).

Limited License
With reference to your request to reprint in your thesis material on which Springer Science and Business Media control the copyright, permission is granted, free of charge, for the use indicated in your enquiry. Licenses are for one-time use only with a maximum

distribution equal to the number that you identified in the licensing process.

This License includes use in an electronic form, provided it is password protected or on the university's intranet, destined to microfilming by UMI and University repository. For any other electronic use, please contact Springer at (permissions.dordrecht@springer.com or permissions.heidelberg@springer.com)

The material can only be used for the purpose of defending your thesis, and with a maximum of 100 extra copies in paper.

Although Springer holds copyright to the material and is entitled to negotiate on rights, this license is only valid, provided permission is also obtained from the (co) author (address is given with the article/chapter) and provided it concerns original material which does not carry references to other sources (if material in question appears with credit to another source, authorization from that source is required as well). Permission free of charge on this occasion does not prejudice any rights we might have to charge for reproduction of our copyrighted material in the future.

Altering/Modifying Material: Not Permitted
However figures and illustrations may be altered minimally to serve your work. Any other abbreviations, additions, deletions and/or any other alterations shall be made only with prior written authorization of the author(s) and/or Springer Science + Business Media. (Please contact Springer at permissions.dordrecht@springer.com or permissions.heidelberg@springer.com)

Reservation of Rights
Springer Science + Business Media reserves all rights not specifically granted in the combination of (i) the license details provided by you and accepted in the course of this licensing transaction, (ii) these terms and conditions and (iii) CCC's Billing and Payment terms and conditions.

Copyright Notice:
Please include the following copyright citation referencing the publication in which the material was originally published. Where wording is within brackets, please include verbatim.
"With kind permission from Springer Science+Business Media: <book/journal title, chapter/article title, volume, year of publication, page, name(s) of author(s), figure number(s), and any original (first) copyright notice displayed with material>."

Warranties: Springer Science + Business Media makes no representations or warranties with respect to the licensed material.

Indemnity
You hereby indemnify and agree to hold harmless Springer Science + Business Media and CCC, and their respective officers, directors, employees and agents, from and against any and all claims arising out of your use of the licensed material other than as specifically authorized pursuant to this license.

No Transfer of License
This license is personal to you and may not be sublicensed, assigned, or transferred by you to any other person without Springer Science + Business Media's written permission.

No Amendment Except in Writing
This license may not be amended except in a writing signed by both parties (or, in the case of Springer Science + Business Media, by CCC on Springer Science + Business Media's behalf).

Objection to Contrary Terms
Springer Science + Business Media hereby objects to any terms contained in any purchase order, acknowledgment, check endorsement or other writing prepared by you, which terms are inconsistent with these terms and conditions or CCC's Billing and Payment terms and conditions. These terms and conditions, together with CCC's Billing and Payment terms and conditions (which are incorporated herein), comprise the entire agreement between you and Springer Science + Business Media (and CCC) concerning this licensing transaction. In the event of any conflict between your obligations established by these terms and conditions and those established by CCC's Billing and Payment terms and conditions, these terms and conditions shall control.

Jurisdiction
All disputes that may arise in connection with this present License, or the breach thereof, shall be settled exclusively by the country's law in which the work was originally published.

v1.2

Recent Patents on Engineering: permission to include the manuscript in thesis

June 23, 2008

Dear Mr. Herrmann:

Thank you for your interest in our copyrighted material, and for requesting permission for its use.

Permission is granted for non-exclusive use of the material requested. Also, reference must be given in the text to the original source of the material.

Thank you for your patience while your request was being processed. If you wish to contact us further, please use the address below.

Sincerely yours

AMBREEN IRSHAD

Permissions Billing Officer
Bentham Science Publishers Ltd
Email: permission@bentham.org
URL: www.bentham.org
FAX No.: +92 21 4971796

Current State of Intellectual Property in Microfluidic Nucleic Acid Analysis

Lidija Malic[1,3,#], Marc Herrmann[1,3,#], Xuyen D. Hoa[1,3,#], and Maryam Tabrizian[1,2,3,4+]

[1]*Department of Biomedical Engineering, McGill University,* [2]*Faculty of Dentistry,* [3]*Centre for Biorecognition and Biosensors,* [4]*McGill Institute for Advanced Materials, Montréal, QC, H3A 2A4, Canada*

Received: October 2, 2006; Accepted: November 10, 2006; Revised: November 10, 2006

Abstract: The development of novel fabrication methods, materials and surface chemistries to implement nucleic acid analysis brings reduced cost, reduced reagent consumption, increased analysis efficiency, portability, ease of use and reliability to today's genomic approach. This trend, as evident by the exponential growth in the number of patent applications, granted patents and commercialized systems, is motivated by the promise for significant breakthroughs and benefits of nucleic acid analysis to drug discovery and point-of-care diagnosis. This review paper aims at identifying the enabling technologies and key patents in microfluidics for nucleic acid analysis. In particular, it seeks to identify granted and pending patents for cell sorting and lysis, nucleic acid extraction and purification, followed by nucleic acid amplification, separation and detection. Additionally, it presents an overview of the current intellectual property environment and seeks to identify trends for the future development. Much of this development is geared increasingly toward fully integrated systems. The convergence of technology and interdisciplinary interests is expected to foster further breakthroughs and commercialization.

Keywords: Microfluidic nucleic acid analysis, cell sorting, cell lysis, nucleic acid extraction, nucleic acid separation, polymerase chain reaction, electrophoresis, integrated systems, Lab-on-a-Chip.

INTRODUCTION

In the near future, one can imagine a device no larger than a credit card able to detect infections and diseases directly from a single drop of blood within minutes. Such is the promise of lab-on-a-chip and microfluidic technologies.

With microfluidics, the precise control and manipulation of microliter or nanoliter volumes of fluids poses significant technological challenges, and yet offers considerable benefits: rapid analysis, minimal reagent and sample consumption. The integration of functional components for sample processing and detection onto a single platform as to create a *lab on a chip*, provides additional advantages: portability, reliability and reduced cost. For point-of-care diagnosis, these advantages must be leveraged to provide a viable and effective tool [1,2]. Generally, in molecular biology or nucleic acid (NA) analysis, these advantages are sought for new applications in drug discovery, cancer research, food and environmental safety.

Over the past decade, much progress has been achieved in the development of novel materials and fabrication processes to overcome the limitations of early microfluidic systems. These devices were the initial attempts to adapt materials, silicon and glass, and microfabrication processes from the semiconductor industry to a novel application. However, the high cost associated with the clean-room processes (photolithography, etching, and bonding) limited the development of disposable devices. Polymer-based chips with alternative low cost manufacturing processes were introduced to address these issues [3,4]. Increasingly, microfluidic devices are fabricated from rigid transparent polymers such as acrylics or flexible polymers like silicone rubber using the cost-effective techniques of injection molding, embossing and replica molding [5]. Additionally, the development of novel chemistries were introduced to enhance the surface properties of these materials [6-8]. Growing access of these technologies to both research groups and companies has led to a commensurate increase of innovations in the development of NA on-chip analysis [9,10].

In this paper, inventions describing microfluidic technologies for the implementation of on-chip NA analysis systems are presented. In contrast to existent literature reviews, which provide excellent overview of most recent developments, this review focuses on the state of intellectual property as to identify the trends and contributors from which future commercial development must build upon. Given the protracted process of a successful patent prosecution reaching sometimes over 3 years, this review also covers patent pending inventions (published patent applications) as to provide a timely overview of recent trends. The approach is three-fold. In the first tier, key inventions and methods that implement the individual functional components of NA analysis are catalogued. For clarity, a short description of the manipulation steps of NA analysis is provided. A wide variety of materials and physical and chemical approaches are described for the handling of fluids and processing of the genomic samples. The second tier addresses strategies and challenges of the integration of these components into a functional, application-oriented microfluidic NA analysis platform. Examples of patents, granted and pending, of integrated systems are identified. In the final tier of this review, the

*Address correspondence to this author at the Department of Biomedical Engineering, McGill University, 3775 University Street, Montréal, QC, H3A 2A4, Canada; Tel: (514)398-8129; Fax: (514)398-7461; E-mail: maryam.tabrizian@mcgill.ca

#*First author - equal contribution.*

1872-2121/07 $100.00+.00

current outlook and trends in the development and commercialization of microfluidic NA analysis platforms are discussed. Much of the focus of current work is on the integration issues, which includes the introduction of novel NA analysis techniques. Finally, the major inventors and companies are identified, as to provide a glance of the microfluidic NA analysis market.

1. INTELLECTUAL PROPERTY FOR NUCLEIC ACID ANALYSIS

1.1. Principles of Nucleic Acid Analysis

The analysis of the NA content of a given sample requires a succession of manipulation steps, as illustrated by Fig. (**1**). The sequence of individual steps varies according to the chosen method of analysis and the required information. The procedure starts with the collection of a sample, which contains the genetic material to be analyzed. This sample can be a body fluid, such as blood, urine, saliva; cultured cells in their medium; solubilized grinded tissue or an environmental water sample. For more complex samples that contain higher quantities of potential contaminants, it is critical to prepare the sample prior to analysis.

The first step for sample preparation is the sorting and enriching of the cells and organisms of interest. In this review, cell sorting will be discussed. Generally, these techniques can be applied to eukaryotic cells, bacteria, viruses as well as other NA containing organisms. Although not always necessary, cell sorting and enrichment is often desired. For instance, to isolate white blood cells from the more abundant red blood cells and platelets, or to concentrate bacterial cells from a diluted water sample, to collect rare stem cells, or to study the genetic expression profiles of healthy cells versus cancer cells, this initial step must be performed. After the cells of interest have been isolated in sufficient number, the genetic material is extracted by disrupting the cellular membranes or other protective layers. This particular step is called *cell lysis*. Although it is an essential step in sample preparation, during cell lysis, cellular debris is generated and harmful substances are released along with the NA material, which can hinder

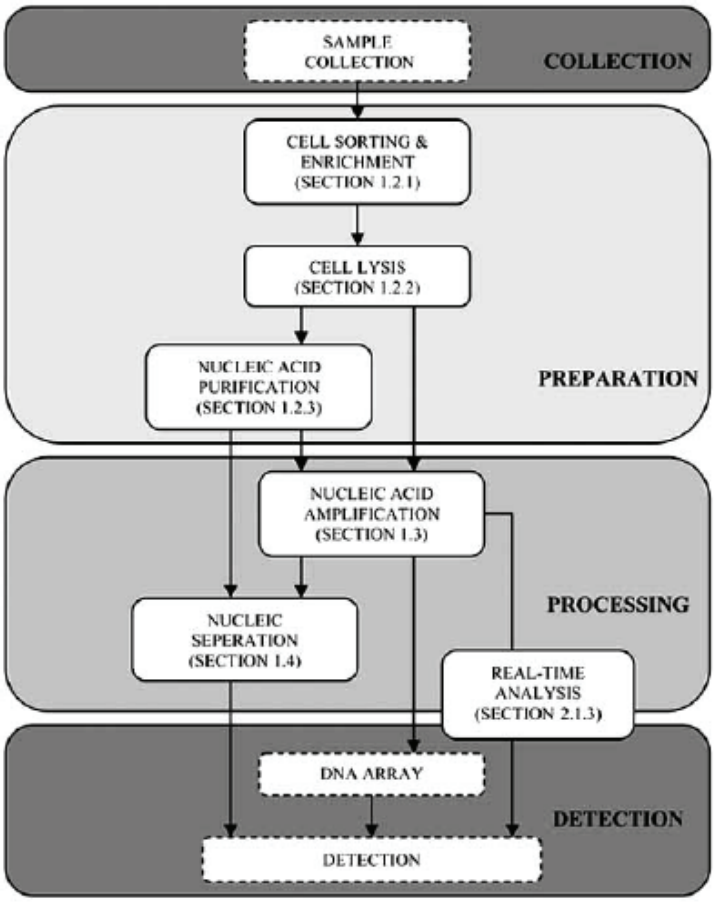

Fig. (1). Manipulation steps for nucleic acid analysis. The steps depicted in boxes with solid lines are covered in this review. The numbers provided in each box refer to the section in which the particular topic is presented. The boxes with dotted lines are beyond the focus of the review.

subsequent manipulations. Consequently, the released NAs are often purified before they can be further processed.

After the genetic material has been extracted and purified, it can be processed by a variety of techniques. The processing greatly depends on a given application. For instance, the NAs can be readily separated by electrophoresis for sequencing purposes or single nucleotide polymorphism identification. Due to the limited amount of sample available, sensitive instruments such as laser induced fluorescence or mass spectrometry are often required for detection. Alternatively, a specific NA sequence can be amplified by polymerase chain reaction (PCR) prior to the separation to facilitate the detection. NA amplification of a particular nucleic acid sequence can also be monitored in real-time (RT-PCR) to study for example the level of expression of a disease-associated gene or to identify the presence of a particular microorganism. Additionally, for more exhaustive studies such as the comparison of the expression profiles of healthy versus cancer cells, or cells following a particular treatment, the whole NA extract can be amplified and subsequently hybridized on a microarray chip.

The following sections examine the different microfluidic approaches to NA analysis, as described in patents or patent applications, focusing on sample preparation and processing. Although the detection methods are necessarily associated to the analysis [11], they are issued from different technologies and thus are discussed only as a part of a system where they are integrated with one or several of the previous steps of the NA analysis.

1.2. Microfluidics for Sample Preparation

1.2.1. Cell Sorting and Enrichment

For cell sorting and enrichment, the conversion of laboratory instruments into a microfluidic format, as well as specifically adapted microfluidic solutions have been described. These inventions are presented in the following section.

1.2.1.1. Fluorescence Activated Cell Sorting

Fluorescence Activated Cell Sorting (FACS) is frequently used in biological and medical laboratories for its high efficiency and specificity. However, the associated costs, the requirement for a highly qualified operator, and the risk of cross-contamination between samples are important limitations, which impair the routine use of this technique. Therefore, researchers have naturally concentrated their efforts on developing an inexpensive, easy-to-use and disposable device based on the same principles as FACS.

FACS involves a sequence of three independent events to sort cells as depicted in Fig. (**2**). Individual events or their integration into a functional device have all been the subject of recent patents and patent applications. First, the cells are separated and aligned into a ribbon of cells, a process called *cell focusing*. In microfluidic systems, this initial step is achieved by generating three parallel laminar streams with a central stream large enough to allow the passage of only one cell at a time. In 2000, Wada *et al.* from Caliper

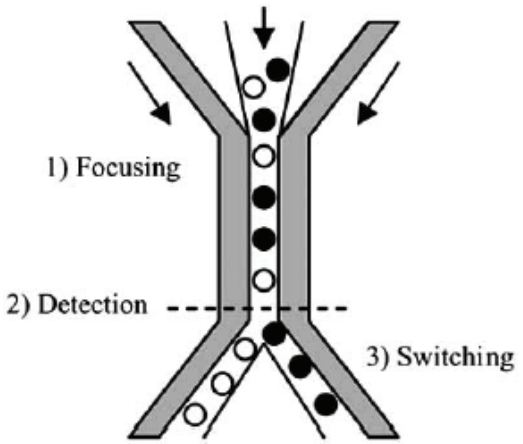

Fig. (2). Microfluidic Fluorescent Activated Cell Sorting (FACS). Sequence of the three independent events for cell sorting with microfluidic FACS. The grey streams represent the focusing buffer, while the middle white stream represents the cell containing sample. Two types of cells are depicted by white and black circles

Technologies proposed several methods for cell focusing in microfluidic systems [12]. In 2003, Micronics filed a patent application for an injection device, a so-called sheath injector, for hydrodynamic focusing and sorting of cells [13]. A year later, they patented a device for the separation of white blood cells from a whole blood sample [14].

Following the focusing step, positive cells, namely the cells that are separated from the other components of the flowing solution, are detected. Several methods for positive *cell detection* have been elaborated. The large majority of systems however use fluorescent detection, whether the cells are tagged with specific fluorescently-labeled antibodies or they express a modified fluorescent protein. The detection event actuates a switch, whose activation directs the positive cells into a separate collection channel. *Flow switching* can be implemented in several manners such as electromechanical valves [15,16], pressure-driven [17] or electroosmotic switches [18-20]. In particular, electroosmotic force (EOF) has been frequently employed as it is a robust, rapid and easily miniaturized means of directing flows in microfluidic channels. In 1999, Quake *et al.* patented a microfabricated FACS device based on fluorescent detection and electroosmotic flow switching to separate, as a proof-of-principle, GFP expressing *E. coli* [18,19]. More recently, Liu *et al.* elaborated a very similar device with integrated optics for cell detection, seeking further miniaturization and portability [20]. In 2005, Evotec also released two patent applications describing the operation of similar FACS devices [21,22].

Nevertheless, the biggest challenge yet to be overcome in microfluidic FACS design lies in the optimization of the

separation rate while minimizing the occurrence of false positive events. Essentially, the faster the flow of cells, the lesser time is available for accurate detection and sorting. In this regard, the use of microfluidics permits to increase the separation rate by parallelizing multiple microsystems rather than by accelerating the flow. Moreover, multiple embranchments can be laid in a sequence to perform multi-step sorting with re-sorting decisions, thereby decreasing the number of false-positive events [16].

Although the majority of reported devices use planar channels, mostly due to fabrication constraints, other schemes have been proposed. Foster J.S., for instance, patented a device in which the cells are isolated and detected in parallel vertical channels and then oriented toward the appropriate outlet by electromechanical valves [15]. The smaller planar area occupied by vertical channels, as compared to an array of horizontal channels, allows for massive multiplexing, which in turn greatly increases the overall separation rate. The patented micromechanical actuator is capable of sorting hematopoietic stem cells individually at an operation rate of 3.3 kHz. With the massively parallel 1024-fold device, a throughput of 3.3 million events per second was demonstrated.

1.2.1.2. Magnetic Activated Cell Sorting

Besides fluorescence, other types of labeling are also available. In particular, magnetic labeling is often used as it represents a more affordable alternative method for cell separation. By analogy, cell sorting using magnetic labeling is referred to as MACS. In one embodiment of the aforementioned patent application from Micronics [13], the flowing cells are attached to magnetically-labeled antibodies. After focusing, the positive cells are attracted into a secondary channel by a magnet positioned on one side of the *T-junction*. This approach could be described as *dynamic*, as opposed to a *static* approach, where the positive cells are not only rerouted into a secondary channel but are rather magnetically trapped inside a unique linear channel. For instance, Cosman *et al*. described a device, in which magnetic beads with capture moieties are immobilized inside the channel prior to the injection of the cell containing solution [23]. The cells are selectively trapped and can later be collected by demagnetizing the trapping device and releasing the beads. Such trapping device can consist of external permanent magnets or more conveniently of microfabricated electromagnets, such as described by Whitesides G.M. [24] or Ahn *et al*. [25].

1.2.1.3. Filter-based Cell Sorting

Various strategies, which do not require prior labeling of cells, have also been adapted to microfluidic systems. Despite a lower specificity, they offer the possibility of readily sorting cells from a complex sample without further manipulations or introduction of foreign labeling species. Among these techniques, microfabricated filters (or sieves), which separate cells based on their size, shape and deformability, are very popular [26-30]. The company AVIVA Biosciences, for instance, disclosed a patent application on several methods, compositions, and automated systems for separating rare cells from fluid samples [28]. Although microfabricated filters are easily implemented in microfluidic systems, their inherent small area increases the susceptibility to clogging. In this regard, Sethu and Toner developed a device for the removal of red blood cells and platelets from blood, featuring a junction with a lateral sieve rather than a frontal filter [27]. In this device, a force generator perpendicular to the main stream leads the red blood cells and platelets through the lateral sieve into a secondary channel, while the larger white blood cells continue their course into the main stream, thus avoiding clogging the filter. Alternatively, Wilding and Kricka included a secondary flow channel connected with the separation zone, which allows the discharge of collected cells [29]. Less conventional methods, such as differential cell disruption in a serpentine channel [26], separation based on gravitational acceleration [31], or the separation of white blood cells based on lateral migration due to frequent collisions with red blood cells, have also been proposed [32].

1.2.1.4. Dielectrophoresis

Another common approach for cell separation is based on dielectrophoresis (DEP). DEP is the translational motion of charge-neutral matter caused by polarization effects in non-uniform electric fields. Positive DEP occurs when a cell is more polarizable than the surrounding medium, and results in the cell being drawn toward a region of higher field gradient. Conversely, negative DEP occurs when a cell is less polarizable than the medium, and results in the cell being drawn toward a region of lesser field gradient. Due to the ease of integration of microelectrodes, DEP provides an especially attractive method for on-chip cell manipulation. Moreover, the limited height of microfluidic channels constrains the flow of cells to few tens of microns above the electrodes, where the electric field is the strongest. The electrodes can be arranged in a perpendicular array to the main stream, thereby differentially changing the linear velocity of various types of cells, either separating or trapping a specific cell population [33]. They can also be disposed in a parallel array, displacing the cells laterally toward distinct outlet channels [34,35]. Yet another advantage of this technique relies on the possible utilization of the same electrodes for subsequent steps such as the extraction of the genetic material and further amplification as described by Nanogen [36] and Iliescu *et al* [37].

Interestingly, the dielectric properties of cells have also been employed to separate various populations by optical trapping or guiding. In two patent applications, Arryx described the use of holographic laser steering for this purpose [38,39]. Essentially, this technique uses the gradient forces of a beam of light to trap a particle based on its dielectric constant. Particles with a slight dielectric constant differential with their surroundings are sensitive to this gradient and are either attracted to or repelled from the point of highest light intensity. When the beam is shined perpendicular to a microfluidic channel, the flowing cells are separated and collected at various lateral positions.

1.2.2. Cell Lysis

Standard laboratory methods for cell lysis employ chemical, mechanical, thermal and electrical means to disrupt cellular membranes. Although similar approaches have been used to lyse the cells in microfluidic systems, the

miniaturization of these techniques is not always straightforward and fluidic designs often have to be adapted.

1.2.2.1. Chemical Cell Lysis

Chemical lysis methods are often used in microfluidic systems, as many well defined protocols, which are adapted to break down specific types of eukaryotic cells, bacteria, viruses, etc., have been developed over the years. Furthermore, no large external device that requires independent controls, space and power supply is needed. For instance, Kayyem J.F. proposed to use lysing agents such as guanidium chloride, chaotropic salts and lysozymes [40]. Parthasarathy *et al*. from 3M Innovative Properties Company have likewise suggested freeze/thawing, hypotonic shock an alkaline treatment with sodium hydroxide to lyse cells from a blood sample [41]. However, stringent buffers containing the lytic agent might interfere with the subsequent NA analysis by inhibiting the enzymes necessary to perform, for example, a PCR amplification. Thus the lytic agent needs to be neutralized or replaced without loosing the genetic material that was previously released. This manipulation often leads to the undesirable dilution of the sample, and frequently demands a more complex fluidic design with integrated valves [42]. Hong *et al.* from the California Institute of Technology, for instance, described a microfluidic system that uses the two-layer PDMS valves developed by Quake's group [43]. In particular, they realized a parallelized isolation and lysis of cells, DNA affinity purification on beads and recovery of the purified DNA on a single chip.

More recently, Irimia D. and Toner M. developed an ingenious device capable of trapping and chemically lysing a single cell within an extremely limited volume of 50-pL, thus greatly reducing the dilution factor of the released molecules [44]. In this device, a cell is first trapped between two air-bubbles delimiting a 25-pL chamber. This chamber is connected via a thin channel to a second 25-pL compartment containing the lysis buffer. The two solutions are then mixed together and the cellular membrane is disrupted. The released molecules are free to diffuse inside the second compartment while cell debris remains in the cell-trapping chamber.

1.2.2.2. Mechanical Cell Lysis

Mechanical cell lysis methods comprise a large variety of means to break down cellular membranes and organisms. One of the most popular methods in conventional laboratories uses ultrasonication. The generation of ultrasonic waves creates microscopic bubbles in the medium, which burst out violently thus creating holes in membranes and lysing the cells [45]. Although certain limitations are associated with the utilization of sonication in microfluidic systems, such as the resulting presence of foam and bubbles, as well as high power consumption and lack of portability, Cepheid currently commercializes a microfluidic cartridge, which coupled to an ultrasonic horn, delivers ultrasonic energy to the sample in the lysing region [46,47]. In addition to ultrasonic agitation, solid particles, such as glass beads, can be injected in the system thereby adding mechanical stress and increasing the lysing efficiency [47]. Very recently, Yuan *et al.* from Microfluidic Systems described a similar device [48].

Another mechanical approach, more specific to microfluidic systems, consists of the intrinsic design of cell membrane piercing protrusions, that extend from the surface of the channel inside which the cells are forced through and ruptured by shearing forces, as patented by Wilding *et al.* [49] and schematized in Fig. (**3**).

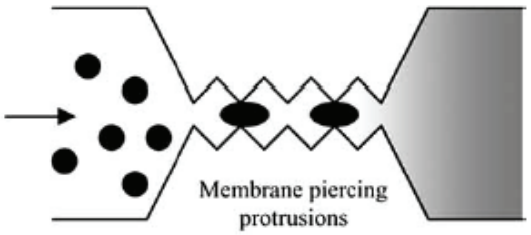

Fig. (3). Mechanical cell lysis in a specially designed microfluidic channel. The cells (black circles) are forced through a thin channel designed with membrane piercing protrusions. The protrusions disrupt the cellular membranes and the intracellular medium containing the nucleic acid material is released in the downstream compartment.

1.2.2.3. Thermal and Electrical Cell Lysis

Other methods, which are particularly attractive for NA analysis on microfluidic chips, are based on the thermal or electrical disruption of cellular membranes. Heating the cells at a high temperature, for instance, can be compatible with the subsequent on-chip NA amplification, using the same integrated heating element [50]. Elevated temperature in the solution can be achieved, for example, by radiating microwaves from a monolithic microwave integrated circuit (MMIC) [51], or can be induced at a precise location inside a microchannel by an external laser beam [52]. Likewise, electrolysis, also called irreversible electroporation, necessitates only microfabricated electrodes that can be also used for fluid handling and subsequent NA separation by capillary electrophoresis [53-55]. In particular, Motorola patented in 2004 a microfluidic device featuring embedded metal conductors to perform both cell lysis and NA amplification on a single chip [56]. The same company also released a patent on a multilayered microfluidic DNA analysis system in which cell lysis is performed by subjecting the cells to pulses of high electric field strength [57]. Similar to ultrasonication, the major drawback of both the thermal and electrical approaches is associated with the formation of bubbles inside the microfluidic system due to the elevation of the temperature. The generation of joule heating can however be minimized by applying electrical pulses instead of a continuous current. Techniques such as the local electrogeneration of hydroxide ions can also help reduce the high

field strength and voltage required for breaking the cells [58].

In recent years, many approaches have been described for microfluidic cell lysis. The chosen technique mostly depends on the type of cells or organisms from which the NAs have to be extracted and its compatibility with the subsequent steps of the analysis. Moreover, different methods can be combined to achieve the differential lysis of a specific cell type as proposed in the microfluidic differential extraction cartridge developed by Microfluidic Systems [59].

1.2.2.4. Nucleic Acid Extraction and Purification

Following the cell lysis, the next step in NA analysis is the extraction and purification of the NA material from the cell lysate. On a macro-scale, NA extraction is commonly completed by using various chemicals, precipitation and centrifugation. However, these conventional methods are time consuming, difficult to automate and to scale down to small sample volumes. In particular, the centrifugation and precipitation processes often involve the use of large-scale apparatus, such as that disclosed by Osanai *et al*. [60]. From this point of view, the solid phase extraction (SPE) method is expected to become mainstream in the future where downsizing is required. Various techniques of SPE involving the use of magnetic particles, filters, silica gels and beads, and micro- and nanoengineered surfaces have been developed. Novel devices utilizing these methods are discussed next.

1.2.2.5. Filters

Several microfluidic-based extraction devices that employ filters in lateral-flow devices [61-66] and in vertical-columns [67-70] have been described. While vertical column-based devices have the advantage of high throughput due to the high-level integration of columns, their fabrication does not benefit from microfabrication-batch process, hence only lateral-flow devices are considered in this section. In lateral-flow devices, a suitable sample extraction matrix comprises filters to block the impurities resulting from the cell lysis process while permeating the NA material [61,62]. Alternatively, a filter paper can be employed to temporarily entrap the NAs present in the sample, while washing the undesired contaminants [63,64]. Here, the NAs entrapped within the matrix may be eluted and then transported into the next channel for further processing. Affymetrix patented a system where the extraction device comprises a deformable porous material for NA binding and pneumatic ports for fluid transport [64]. As such, it overcomes the fluidic problems encountered with high surface area packed systems. However, as the filter is added after the micro-fluidic channel formation, it does not have the advantages of batch fabrication that arise from a monolithic design.

Although most of the reported inventions use external filters inserted into the microfluidic chamber at the assembly level, efforts have been made to monolithically integrate filtering functions at the fabrication level and thus simplify the system assembly. For instance, Microtechnology Ct Man presented a monolithic integration of a polymeric filter produced by ablation or stamping in microchannels, which also allows for precise control of pore size during fabrication [65]. Alternatively, Nanostream incorporated filter-holding structures to easily achieve fitting and tight seal of the filter element [66]. While on-chip filter-based extraction method has been demonstrated, unresolved issues concerning lateral-flow saturation at the filter and the resultant slow assay time have led to the development of other SPE methods.

1.2.2.6. Magnetic Beads

The use of magnetic beads is an alternative extraction method, where the target NA molecules can be captured by complementary binding with molecular probes immobilized on the surface of the beads. Subsequently, the beads are collected within a channel using an applied magnetic field and washed with an elution buffer. The NA strands, dissociated from the surface of the magnetic beads, are retrieved along with the buffer.

Several inventions have been reported utilizing this method; they vary on the arrangement and the number of external magnets and microchannels. For instance, a single magnetic field for collection of magnetic particles was shown by Yang *et al.* [71] and Kusumoto *et al*. [72]. In the latter invention, a multi-channel network is implemented to increase throughput. To enable more efficient mixing of the sample with magnetic beads, Kreuwel *et al*. from Biomerieux presented a microfluidic device utilizing two separate magnetic fields applied simultaneously in different directions [73]. In further attempts to improve the efficiency of target capture, Canon disclosed a patent application where an aggregate of magnetic particles is formed thus facilitating the capture without the need to apply a large magnetic field [74]. Nelson *et al.* from Aclara Biosciences patented an extraction-separation device consisting of a network of channels and electrodes that control the fluid flow electro-kinetically, while the magnetic bead collection inside the SPE channel is carried out with a single magnet [75].

1.2.2.7. Silica Beads and Gels

Several microfluidic inventions tailored to the extraction by silica-beads have been disclosed in patents and patent applications. Norchip demonstrated the use of packed silica beads on a PDMS microfluidic platform for NA extraction [42]. In the presence of chelating agents, the NAs bind to the packed silica particles. After washing, the NAs can be released with an elution buffer. To enhance the extraction, the device uses several electrodes adjacent to the packed silica beads-channel to reversibly bind and pre-concentrate the eluted NAs on-chip. A different invention disclosed in a patent application by Quake's group uses a densely packed channel network with a set of control valves instead of electric fields to trap and release the affinity-beads [43]. However, a disadvantage of the packed beads NA-extraction method is that the free beads are not strongly linked to the channel, thus they can be accidentally exhausted with the flow of solution.

As an alternative, sol-gel methods for improving NA extraction have been developed. Landers *et al*. used immobilized beads in a gel matrix to alleviate the problem of free beads in the solution flow [76]. A different invention, utilizing gel-extraction method in the form of microfluidic disk, was developed by Gyros [77]. This device relies on centrifugal forces for fluid transport and integrates other necessary components for NA analysis.

1.2.2.8. Micro- and Nano-engineered Surfaces

Engineered surfaces employ different micro- [78-82] and nano- [83] fabricated structures to improve the NA extraction yield. They may be used to capture affinity beads [81-83] or be coupled with a specific surface chemistry [78-80] to increase NA binding capacity and retention. For instance, Microfluidic Systems has a patent pending on a handheld portable extraction device that incorporates pillars configured in a gradient of silica-on-silicon structures, as represented in Fig. (**4**) [79]. In addition to increasing the extraction efficiency, the gradient acts as a filter to block physical debris present within the sample. By positioning the pillars less densely near the input port, they block more effectively the debris without becoming clogged. With the debris removed, the fluidic sample passing the more densely configured pillars is better prepared for NA extraction and collection. A similar invention utilizing pillars etched in silicon substrate to capture and retain NA affinity beads was also disclosed [82]. In this device, pillars of different heights and widths are etched to form a filter that traps the beads onto which NAs are subsequently immobilized. An advantage of the micropillar chip for NA purification and concentration, besides providing increased binding surface area, lies in the ability to produce multiplexed channels containing compact arrays of micropillar on a small footprint for high throughput purification.

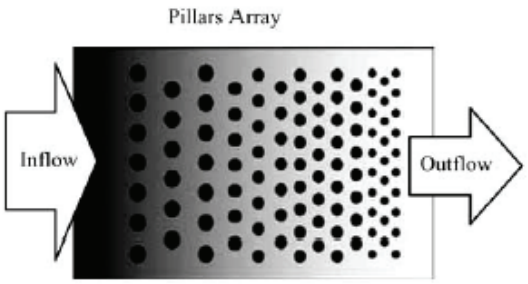

Fig. (4). Gradient of increasing density of pillars on substrate for nucleic acid extraction and purification.

However, to fabricate pillars in a silicon substrate, expensive DRIE (Dry Reactive Ion Etching) equipment and complex fabrication methodology are required. To simplify the fabrication process, smooth-walled silica channel with electrically controlled fluid-flow [84], or thermally grown silicon-dioxide on porous silicon substrate with an appropriate surface chemistry for enhanced NA absorption [85] have also been demonstrated. Further developments in this arena have led to novel devices with improved surface chemistries that employ dendrimers on glass or polymer channels [86] and minor groove binders for simultaneous detection on glass channels [87].

1.3. Microfluidics for Nucleic Acid Amplification

Polymerase Chain Reaction (PCR) is the most commonly used method for NA amplification. It is a three-step amplification process requiring three temperature transitions. The process starts with a *denaturation* step, during which the hydrogen bonds of a double stranded NA (*template*) are broken to form single stranded NAs. The process occurs at temperatures between 94°C and 96°C. In the *annealing* step, the temperature is lowered to 50-65°C, allowing primers which limit the NA region to be replicated to bind to the single stranded template. The temperature is then raised to 70-75°C to allow the enzymatic replication of the template by a DNA polymerase in the *extension* step. Several repeats of this three-step thermocycle result in millions of copies of the NA template.

The miniaturization of the PCR system brings particular advantages to the amplification process. Specifically, it offers a significant thermodynamic advantage as small device dimensions and reduced sample volume exhibit less inertia to temperature change. Conventional PCR thermocyclers achieve heating and cooling rate in the range of 2-10°C per second, while miniaturized thermocyclers can reach rate of 15-40°C per second. This thermal advantage remains the key driving force in the development of microfluidic PCR allowing for rapid amplification. Yet, the thermal requirement for PCR constrains the design of microfluidic chambers and channels for optimal heat flow and isolation, as it limits the fabrication to thermally stable materials.

As the first PCR patent issued in 1983 to Cetus, is set to expire in 2006, an extensive catalogue of patents exists describing integrated PCR systems on microfluidic platforms. Since Northrup *et al.* in 1993 first introduced on-chip PCR devices [88], they and many other inventors have successfully patented systems that can be categorized into *well-based PCR*, *flow-through PCR* and *thermal convection PCR*, shown in Fig. (**5**). Various heating principles, relying on both contact and non-contact techniques have also been described. The general operation of the PCR starts from extracted NA samples from upstream processing to which primers and reagents are added. After mixing, the homogeneous solution can be thermally cycled for amplification.

1.3.1. Well-based PCR

Early microfluidic PCR systems consisted of reaction chambers or wells, where the PCR reagents (NA template, primers, and polymerase) are kept stationary and the temperature is cycled between the three PCR temperature ranges. The amplified NAs are recovered from the chambers for post processing upon completion of the reaction.

Northrup A. and co-workers at the University of California patented various well-based PCR designs starting from 1996 [89-91]. These patents describe microfabricated reactors that incorporate reagent agitators and mixers, heaters, pumps, and later, optical or electromechanical sensors to the PCR chamber. The inventions focus on the design of silicon chambers that combine a critical ratio of silicon and silicon nitride to ensure uniform heating. Wilding and Kricka also patented and disclosed similar approaches to silicon PCR reaction chambers in 1996 [92,93] and 2005 [94]. They describe chambers designed with high surface to volume ratio to facilitate thermal regulation. The thermal cycling occurs in successive chambers set at different

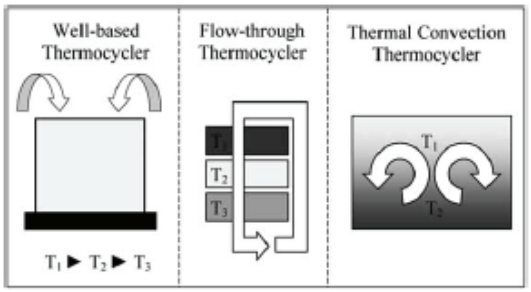

Fig. (5). Schematic of 3 different strategies for nucleic acid amplification on-chip. T_1, T_2 and T_3 represent 3 specific temperatures required for nucleic acid amplification by Polymerase Chain Reaction (PCR).

temperatures. The latter patent application describes a chamber design for use in conjunction with the collection and analysis of cell samples. A multi-chamber thermocycling device patent was also granted to Biometra Biomedizinische Analytik and the Institüt für Physikalische Hochtechnologie, which incorporates a heat sink on the substrate and heating elements constructed in the chamber wall [95].

In another direct adaptation of the semi-conductor fabrication technology, a patent by Tamiya *et al.* presents a rapid implementation of an array of hydrophilic microwells etched into a hydrophobic substrate via anisotropic bulk etching [96]. Recently, other materials have been considered for chamber fabrication. Briscoe *et al.* implemented a PCR device, using ceramic multilayer technology, embedding conductive and isolation layers to provide thermal control [97]. Similarly, Agilent Technologies patented a micro-reactor device in polymer materials [98]. Furthermore, the work at Fluidigm on elastomeric materials has led to the disclosure of a device for PCR with *N x M* reaction cells connected to samples and reagent inlets [99]. The approach is currently used for genetic analysis in their commercial system Biomark™.

1.3.2. Flow-Through PCR

Generally, a well or stationary approach to PCR limits its efficiency due to the time required for uniform temperature transition in the reaction chamber. An alternative approach consists of a dynamic, continuous sample flow system, where solutions are moved through successive zones of constant temperatures. The small sample volume allows the solution to reach the temperature equilibrium quickly, while the transition from temperature zones is only limited by the flow rate. In an early description of this technique in 1999 [100] and patented in 2005 [101], Koehler *et al.* show a microfluidic device constituting of three substrate platelets maintained at different temperatures. A fluidic path meanders through each zone successively, each passage equivalent to a PCR cycle. A similar concept was patented by the French Commissariat Energy Atomique in 2000 [102]. In 2001, Micronics described a PCR device where the samples and PCR reagent are mixed through a diffusion process in the PCR channel [103]. Later, Franzan J. from Bruker Daltonik patented an improved method of the temperature zone technique for very fast NA replication by simply dividing the PCR reaction solution into fine capillary arrays in each temperature zone [104]. The close proximity to the heating source and small volume further reduce the thermal inertia, allowing for a 3-step PCR thermocycle in only a few seconds.

The meander design limits the PCR reaction to a given number of cycles, defined by the number of loops. An alternative method consists of the circular path approach. The patent for a microfluidic continuous flow PCR device was granted to the California Institute of Technology [105]. The device includes a rotary channel featuring multiple temperature regions along the circular path. Agilent Technology also published a similar approach, but instead of channels, the PCR chamber is compartmentalized into 3 portions arranged in a cyclic manner [106]. The PCR solution flows from portion to portion during the duplication process in a continuous fashion. A linear version of the continuous flow rotary concept also exists. Auroux *et al.* with the Imperial College of London described a sample-shutting PCR device in which the sample is passed back and forth over the three thermal zones in a straight channel [107].

In a different implementation of the continuous flow PCR technique, the samples and reagents for NA amplification are manipulated as microdroplets. The discrete microdroplets are moved on a silicon based chip via electrowetting through different temperature zones for the thermal cycling and propelled into channels for post-processing [108].

1.3.3. Thermal Convection PCR

In 2003, Benett *et al.* from the University of California were granted a patent for a PCR microfluidic device based on thermal convection [109]. By creating a chamber reaction with different temperature zones and utilizing the differential temperature to create a convection current, rapid amplification can be realized with a simple design employing minimal pumping mechanisms and electronic control components.

1.3.4. Thermal Control and Novel PCR Approaches

In the description of PCR microfluidic systems, the design of an integrated heater, temperature sensor and control components are central. Variations of popular techniques using resistive elements made of platinum or chromium are often implemented [110]. Peltier-assisted thermocycling was also disclosed by the University of California [111]. A few patents are worth noting as they describe approaches to increase the heating/cooling efficiency in order to rapidly provide stable and uniform temperature zones. To improve thermal control, Aclara Technology described the incorporation of heat transfer films in the structure of the microfluidic channel [112]. Li D. and Erickson D. also disclosed a patent for a low power micro-channel reactor that incorporates in-channel heating elements instead of the conventional in-wall approach [113]. In conjunction with a capillary PCR method, Lee *et al.* disclosed a device in which a conductive polymer that emits heat under an applied current is molded around and in-between capillaries for fast heating [114]. In other patents, the focus is on novel non-contact techniques for temperature

control. IR/UV heating and air cooling for multiplexed microfluidic PCR devices have also been disclosed [115-117]. The integration of parallel microfluidic channels and reservoirs into a PCR microfluidic system to transport and carryout exothermal and endothermal chemical reactions was also described. Such a system was disclosed by Micronics [118]. Stichting Voor De Technische Waternschappen published a similar concept in which one of its embodiments uses the evaporation of acetone for cooling and the dissolution of sulphuric acid in water to generate heat [119].

Alternative PCR methods are considered in other patents. Techniques such as isothermal NA amplification (e.g. NASBA, SDA, etc [120,121]) was described using microfluidic devices. In many instances, devices designed for a 3-step PCR are well suited for these methods. Burns *et al*., at the University of Michigan, for example, disclosed a microfabricated device dedicated to low temperature isothermal NA amplification [122].

Improved handling of the PCR products were also proposed with the use of microcarriers or microspheres on which the NA template is immobilized. In 1995, Hitachi patented a capillary PCR device to amplify trace amount of NA on microspheres [123]. In 2005, Mathies *et al*. with the University of California, described an on-chip genomic analysis system using microspheres to move the NAs through a matrix thermocycling reaction chambers to a detection area, incorporating an optical scanner for the detection of the microcarriers [124].

Interestingly, Goel recently disclosed a novel approach to PCR without thermocycling, referred to as Nano-PCR [125]. Denaturation, annealing and extension of the NAs can be induced by a mechanical, hydrodynamic or electromagnetic stress of different intensities in a NA strand, analogous to changing the temperature. The disclosed microfluidic device incorporates microchannels in a linear or rotary configuration, treated for the anchoring of the NAs, in which hydrodynamic flow provides tension to denature, anneal and extend the NA strands.

1.4. Microfluidics for Electrophoresis and Nucleic Acid Separation

Traditionally, efficient electrophoretic separations are performed in either slab-gel or capillary configurations. While slab-gel electrophoresis exhibits higher resolution, capillary electrophoresis (CE) is more suited for high throughput sequencing and genotyping, since it does not require casting of a new gel prior to each separation experiment. Although significant advances have been made in electrophoretic analysis in silica capillaries over the past decade, the difficulty in assembling very large numbers of capillary arrays that would enable large-scale screening redirected the research focus on the development of microfabricated electrophoresis systems [126].

Generally, in CE microchips, the substrate defines at least one elongate capillary channel which extends between opposed cathode and anode ports and contains the electrophoretic medium. A typical chip-based electrophoretic system with cross-injection and separation channel is shown in Fig. (**6A**). When a biological fluidic sample is deposited in the sample port, electrical potential is applied to direct a portion of the fluid sample first into the elongate microchannel and then towards the opposed anode port The different chemical species within the sample migrate at distinct rates towards the oppositely charged end of the capillary; the rate of migration is dependent on the electrophoretic mobility of the chemical substance in the separation medium (polymeric solution or gel such as polyacrylamide and agarose gels). As a result of their distinct rates of migration, the various chemical components become separated as they progress along the electrophoresis channel and, thus, can be separately detected. The design and construction of electrophoretic microfabricated systems however pose challenges such as achieving high-resolution separation within a compact footprint, which requires optimization of electrokinetic manipulations, channel geometry and sieving media.

1.4.1.1. Capillary Gel Matrix Electrophoresis

Electrophoresis in planar chips was first patented by Salvatore from Du Pont in 1990 using a simple straight channel geometry etched in silicon substrate [127]. Following this invention, Manz from Ciba Geigy fabricated both silicon and glass microfluidic chips to demonstrate the use of the electrophoretic functions [128,129]. In the latter patent, channel length was increased using a closed-loop arrangement with multiple cross-injections to make the device more suitable for NA separation. However, the regular cross-injection method could alter the original sample composition in the separation channel due to sample leakage at the intersection by diffusion. Hence, another electrokinetic injection method using a disjointed sample and drain channel in a shape of a double-T to inject a well-defined sample plug was patented (Fig. **6B**) [130,131]. Another effort by Manz and Effenhauser was directed toward increasing the separation efficiency by integrating two separation paths in microfabricated devices having the shape of a double-T piece (Fig. **6C**) [131]. To increase throughput of microfabricated CE chips, Manz and Zhang have used a cross-injection scheme for sample loading in a multichannel electrophoretic separation device fabricated in glass and PDMS substrates comprising of eight separation paths [132]. Burns *et al*. have also addressed sample injection issue by patenting a novel electrode-driven injection scheme and precise interface gel casting techniques to achieve sample focusing [133]. By fabricating an array of on-chip electrodes to apply the electric field in the sample-loading region, the NAs are forced to migrate and are collected at an anode located just outside the gel interface. Next, the collected NAs are released and enter the gel as a narrow well-defined band, thus enhancing sample injection and enabling low-voltage operation. Another electrically assisted injector-concentrator CE-device has been described by Swierkowski S.P [134]. In this patent, sample injection and pre-concentration is achieved with a single input port, a feature desirable in highly packed array systems.

Simultaneously, other efforts have been directed towards developing polymer-based chips suitable to capillary electrophoresis. Aclara Biosciences has used a double-T injection scheme for a chip fabricated by hot-embossing

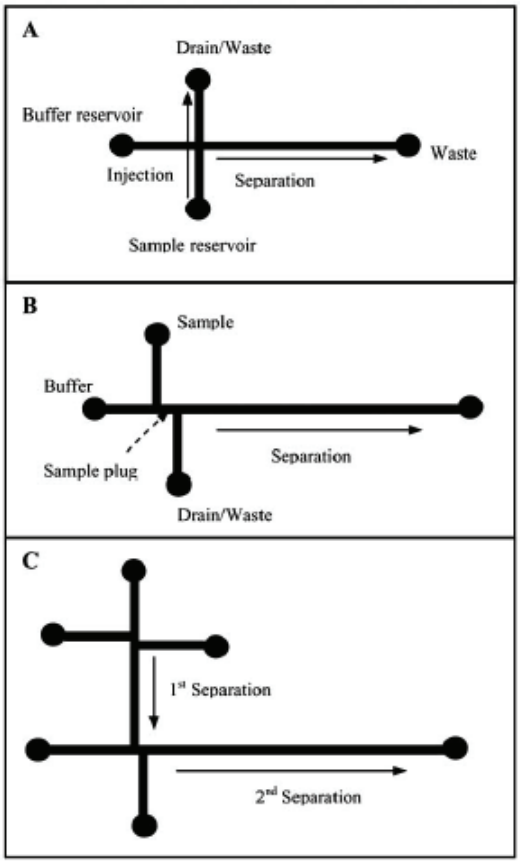

Fig. (6). Designs for microfluidic capillary electrophoresis-based nucleic acid separation. (**A**) Typical cross-section design (**B**) Sample injection through double-T design (**C**) CE chip integrating two separation paths.

PMMA [135] and Zeonor [136]. In particular, the use of a Zeonor substrate alleviates the problems related to complex polymer surface chemistries that tend to aggravate sample adsorption to the capillary walls and generate non-uniform electroosmotic flow resulting in reduced separation resolution.

In order to increase the length of the separation channels while maintaining throughput, Liu S. from Molecular Dynamics developed a microfabricated capillary electrophoretic DNA sequencing device that consists of an array of sixteen 7cm long channels that are fanned out on a 10cm diameter wafer [137]. Each channel has its own cathode, sample and waste wells and they all converge on a common high-voltage anode. An average of 457 bases per channel can be acquired in 15min with 99% accuracy [138]. Another high-throughput microfabricated CE system was presented by Davidson J. and Balch J. [139], which uses a high density array of microchannels with extended read lengths enabled by the channel geometry. To increase the effective length of the separation channels while minimally impacting the packing density, they use sinusoidally-shaped microchannels, and microchannels etched on both sides of the substrate, connected by a via. Similarly, Mathies *et al.* provided a capillary array electrophoresis microplate with an array of 96 radially configured separation channels [140]. The necessary separation length is provided by four hyperturns in the center of the device, which minimizes the geometric band dispersion introduced by turns in the separation path. This device is able to acquire 41,000 bases in 24 min with 99% accuracy [141].

In terms of integrated CE-detection systems, Motorola patented a capillary electrophoresis device in which an optical waveguide system transmits excitation radiation from a source port into each one of the electrophoresis channels, while a detector optical system images the fluorescence radiation onto a CCD or photodiode array, enabling individual monitoring of each channel [142]. An alternative CE-detection platform that fully integrates electrochemical detection and high voltage electrodes with a portable power supply was disclosed by Keyton *et al.* [143].

Finally, one of the recent inventions disclosed by Lee and Devoe demonstrates an automated, high-throughput, 2-dimensional DNA gel electrophoresis system. They patented a 2-dimensional plastic microfluidic network capable of rapidly and accurately resolving DNA fragments based on their differences in size and in sequence [144]. Increased throughput is achieved by rapid size-based separations in the first dimension, followed by simultaneous transfer of the size-separated DNA fragments together with the parallel sequence-dependent separations in the second dimension.

1.4.1.2. Nano-Electrophoresis

Many devices rely on sieving gel matrices for electrophoretic NA separation. Alternative methods utilizing nanostructured materials are also being explored for rapid microchannel electrophoretic separation. For instance, Yager *et al.* from Visible Genetics have demonstrated a dense separation chip comprising of 50 channels on a 1cm wide substrate [145]. The device uses an extended series of microelectrodes (i.e. multiple anodes and cathodes in each channel to permit greater control of the electrophoretic process) to move a NA sample through a homogeneous separation medium to a desired location for detection or further reaction. When a voltage is applied across two or more of the microelectrodes, the charged molecules are induced to move and separate according to the electric field density, the type of solvent film, the charge, the shape and the size of the molecule. Additionally, they patented a novel separation matrix that overcomes problems associated with gel, such as the need for hydration and the randomness of the structure [146]. The separation matrix comprises a solid support with a plurality of nanofabricated posts and pores that form an obstacle course for the NA strands.

Another interesting invention that relies on *entropic recoil* for length-based separation of NA molecules was developed by Craighead's group. [147]. The 3-dimensional microfluidic device is formed by placing a polymer

membrane, consisting of thick (1.5-3um) and thin (75-100nm) regions, between two micropatterned plastic chips. Size-dependent trapping of NA occurs at the onset of each constriction. The separation is achieved by moving the NA sample with short electric pulses through the porous membrane. Short NA molecules pass completely through the membrane, while longer NA molecules are only partially moved into the holes. By switching off the voltage, longer NA molecules recoil out of the holes, resulting in the separation of the NA molecules by length. The membrane may be a filter or artificial gel produced using *electron beam lithography* to define an array of entropic traps (holes, pillars, etc) [148,149].

Further developments in microfabricated capillary electrophoresis systems have been directed towards device optimization, such as new low-viscosity polymer sieving matrices [150] and novel designs of electrical circuitry for delivery of uniform electric fields in two dimensions [151]. Other optimizations include sample pre-concentration methods for enhanced electrophoretic separation, using semi-permeable porous silicate membranes [152] and nanofabricated obstacles [153].

2. TOWARD INTEGRATED MICROFLUIDIC NUCLEIC ACID ANALYSIS

In the previous sections, primary functional components necessary to perform microfluidic NA analysis have been reported. Many inventors described adaptations of standard laboratory approaches onto a miniaturized format, while others presented innovative microfluidic-oriented techniques. With the recent development in microfabricated valves and pumps for liquid handling, the next step lies in the integration of individual components into a self-sufficient device capable of delivering application-specific information.

In this regard, the following section discusses inventions incorporating some level of sample preparation, processing and detection. In some applications, the integration of sample preparation with NA separation by electrophoresis, followed by laser induced fluorescent detection or mass spectrometry, is sufficient. However, such systems are limited to applications where the detection can be carried out with only a small amount of genetic material. By reviewing inventions that incorporate PCR amplification in the processing of the samples, the following discussion is focused on the challenges in implementing more complex integrated systems (Fig. (**7**)).

The integration is necessarily application specific, as it determines which functional components are to be included. For example, a microfluidic platform for NA-based diagnosis requires sample preparation to extract the NAs from a blood sample, an amplification step, and a real-time detection via a sequence-specific molecular probe. This is opposed to an application in drug discovery, where the post-treatment variation in expression profiles of numerous genes is recorded following the non-specific amplification of the total NAs and the hybridization on a microarray chip.

Although theoretically straightforward, the integration of individual functional components has encountered many practical issues as the technological requirements for each component may be conflicting. Additional limitations to microfluidics, ranging from micro-to-macro interface compatibility to the resistance of end-users (both psychological and economical), must also be considered in order to understand the challenges in bringing such devices to market.

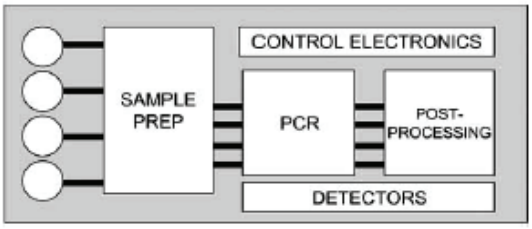

Fig. (7). Schematic of an integrated lab-on-a-chip device containing individual functional microfluidic components for sample preparation, nucleic acid amplification and post-processing. The detection system and the control electronics should ideally be integrated on-chip.

2.1. Integration of Functional Components

2.1.1. Sample Preparation and Detection

The inclusion of sample preparation is an important first step toward integration. Many devices described in the earlier sections for cell sorting, cell lysis, and NA extraction can be readily integrated onto a single substrate. Subsequently, the products of these processes can be carried to an amplification step, as described by Norchip [42]. This invention features a lab-on-a-chip platform for NA amplification displaying chambers for performing cell lysis and NA extraction. Similarly, Micronics described an integrated sample preparation and amplification system with a lateral flow strip for the visual detection of the PCR product [154]. Also, as reported in section 1.2.2.3, thermal and electrical cell lysis have been integrated with a subsequent NA amplification step in several inventions [50,56,57].

2.1.2. Electrophoresis

An extension to the above integration is the incorporation of controls and components for the purification and processing of the PCR products. In recent years, Mathies *et al.* have disclosed many examples of the integration of PCR with capillary electrophoresis and detection. For instance, they developed a PCR-CE glass chip that achieves the enzymatic digestion and the affinity capture of DNA for detection, patented by Affymetrix in 2001 [155]. In a more recent invention, another device incorporating sample preparation, PCR amplification, CE separation and detection was disclosed [156]. Here, the detection is done using a 4-color rotary confocal scanner described in a different patent [157]. Mathies *et al.* also released a patent application for an integrated capillary electrophoresis-electrochemical detection system fabricated in borosilicate glass substrate to detect DNA restriction fragments and size PCR products [158]. Furthermore, they described in several patent applications a microfabricated electrophoretic platform for sequencing that includes sample desalting, PCR template removal, precon-

centration and CE analysis [159-161]. The device comprises a four layer stack of PDMS and glass to form a membrane used to modulate the fluid flow and allow for less interfacing components to control very large number of valves.

Other integrated devices have been developed by Caliper Technologies and are currently being commercialized. In particular, the company presented a microfluidic DNA sequencing device that integrates sample preparation, mixing, amplification, size separation and detection [162-164]. In the latter system, the CE device allows size-separation of DNA in 75 sec separation time. In a different Caliper Technologies invention, simultaneous NA separation of a sample in 32 channels with minimal leakage was demonstrated [165].

Gyros also patented a device for sample purification, amplification and separation by CE using their centrifugal force disk approach [77]. Cardy and Allen expand on the electrophoresis or chromatographic approach by developing a lateral flow device for the detection of a specific NA sequence [63]. The device consists of linearly positioned zones containing reagents required to carry out the reactions for NA extraction, amplification, and detection.

2.1.3. Real-time PCR Detection

The use of intercalators the likes of SYBR® Green or ethidium bromide, and more recently sequence-specific fluorogenic probes, such as TaqMan®, enables real-time detection of the NA products during the replication process. The amplification kinetics are measured, from which the initial concentrations of target NA fragments can be calculated. Sequence specific probes also eliminate the need for electrophoresis separation and further detection. Real-time techniques are well-suited for microfluidic PCR as many implementations feature materials that are transparent at optically relevant wavelengths. As an example of a successful platform, Cepheid now commercializes a real-time PCR apparatus (GeneXpert® System) with fully integrated sample preparation. Its patented approach consists of a fabricated reaction chamber with optically transmissive walls through which the excitation and detection are carried out [166]. Another example of integrated real-time PCR is given by Oh *et al*. [167]. Alternatively, access ports can also be incorporated in the microfabricated substrate for the insertion of an optical system. Such a system, for instance, was patented by Benett *et al*. at the University of California [168].

2.1.4. DNA Array and Hybridization Detection

Nucleic acid assays using hybridization are also widely used in gene-expression analysis. The integration of large DNA arrays to microfluidic PCR has been developed; as exemplified by Lipshutz *et al.* in an Affymetrix's 1999 patent [169]. The device features several chambers for performing sample preparation and amplification connected to a hybridization chamber that includes a DNA array. Olympus Optical also realized the integration of a DNA array to a PCR chip that features electrophoresis for extraction and an elliptically polarized light system for detection of DNA hybridization [170]. Quake S.R. and Chou H.P. presented a modified approach to the DNA hybridization detection in which the DNA probes are immobilized on a closed loop channel (*active flux microfluidic*) [171]. The samples, with or without previous amplification, can be moved into the loop and exposed repeatedly to the probes. In a microfluidic device by Blackburn G., microchannels are sectioned into regions in which DNA probes are bound to a porous polymer or beads [172]. The hybridization is detected optically by fluorescence. Similarly, Mathies *et al.* described a miniature device featuring multiple functional components with NA probes immobilized on the substrate of the chambers. After hybridization, the substrate is removed for measurements under a microscope [156].

In other systems, electrical detection methods have been implemented. Miles *et al*. used impedance measurements for the detection of the end-products of PCR amplification [173]. For sequencing, Ouchi *et al.* from the Tokyo Shibaura Electric Company, patented a detection system in which a DNA array features electrical probes for the electrochemical measurement of hybridization [174].

2.2. Challenges of Component Integration

One major limitation impeding the integration of individual components lies in the intrinsic properties of the material chosen for the fabrication. The choice of material must meet all design requirements in terms of cost effectiveness, ease of fabrication, chemical functionality, thermal stability and optical transparency. More often than not, a compromise must be made to satisfy all the requirements of an integrated functional device. Simplicity in the design of an integration system is crucial. The development of novel methods of analysis or processing protocols may alleviate integration challenges by removing certain steps in the sequence of NA analysis. Specifically, new techniques, such as isothermal or non-thermal amplifications (discussed in section 1.3.4) avoid the need to design heating/cooling elements and thermal sensors. In this case, the formation of air bubbles in microchannels due to heating is also bypassed, along with the limitations related to the thermal stability of the material.

The majority of inventions described previously are *microscale* devices that need coupling to *macroscale* equipment. In order to achieve a higher degree of system portability and functionality required for on-field applications, it is desirable to decrease the reliance on external instruments. For instance, fluorescence lasers, lamps and microscopes used for detection can be replaced with arrays of optical or electrochemical detectors that are more suitable to miniaturization. Rapid and automatic dispensing and handling of small sample volumes is also needed to reduce the level of human intervention, which in particular requires improved *micro-to-macro* interface with innovative hardware interconnection technologies. In this regard, integrated microfluidic devices on CD, or *lab-on-a-CD*, are advantageous due to their versatility in handling fluids, their simple rotational motor requirements and inexpensive fabrication methods [175]. Additionally, the CD format is already adapted to miniaturized optical detection platforms used to image CDs at the micron resolution and soon at the submicron resolution with the advent of DVD and HD-DVD technologies. Several companies such as Gyros, Burstein Technologies and Abaxis are currently commercializing CD-based systems. However, an appropriate technological

solution is not necessarily commensurate with a commercial success. Tecan, for example, has discontinued the development of its LabCD technology as it foresaw difficulties in achieving "significant economical competitiveness and substantial market share in the required time-frame" (Thomas Bachmann, CEO of Tecan Group Ltd).

Several additional non-technological barriers can impede the introduction of microfluidic products to the market. One of them is the reluctance of some instrument-supplier companies to incur additional costs and loss of profit due to the commercialization of a new technology that is intended to replace the equipment they are currently marketing and for which great costs were already incurred. Additional impediments include the reluctance of end-users to adopt new technologies (due to the costs associated with equipment replacement and laboratory personnel training) and the general uneasiness of the public toward micro/nanotechnologies applications in life-science.

3. CURRENT & FUTURE DEVELOPMENTS

3.1. Trends for Integration

In developing the systems described in the earlier sections, inventors have managed to circumvent the issues related to the integration of individual functional components with some success. Many of these devices employ electromagnetic fields for liquid handling by electroosmosis, cell sorting by DEP, electrolysis, NA electrophoretic separation and for heating in PCR. This approach allows the implementation of the device using fewer materials, thus minimizing the cost and number of fabrication steps. However, as for most current technologies, such integration necessitates a certain level of trade-off in performance of each functional component.

Additionally, microsized particles and beads, either made of silica, polymers or magnetic materials, have been successfully incorporated in microchips at different steps of the analysis. Microbeads dramatically increase the surface area available for the capture of cells or NA; they are compatible with a subsequent amplification step, and can also be used for detection purposes [176]. Hence, microbeads represent a valuable approach in the integration of individual components.

3.2. Nanoengineering

Recent advancements in nanotechnology have opened new avenues for the development of nanodevices that promise to overcome some of the limitations in miniaturized NA analysis systems. For instance, nanostructures and nanomaterials have been explored for NA separation in microchip electrophoretic devices as an alternative to polymer sieving matrices (see section 1.4.2). Densely spaced nanofabricated structures (e.g. nanopillars) or nanopacking medium (e.g. nanosphere solution inside a microchannel) can replace the viscous polymers that are often unsuitable for separation of long DNA and are difficult to inject into narrow channels. These nanostructures can be produced in highly parallel fashion in each separation channel as to maintain throughput. Additionally, surface functionalization using self-assembled monolayers of capturing biomolecules can provide pre-concentration and highly specific separation of target NA molecule [177].

Although these nanoengineered systems offer advantages of high speed, potentially increased sensitivity and specificity due to their unique material properties and processing capabilities, they still require costly and complex fabrication processes. Nevertheless, the proliferation of nanotechnology in genomic analysis is certainly expected [178].

3.3. Main Contributors and Intellectual Property Market

Among the major contributors to the development of microfluidic NA analysis technologies, many academic researchers have played a critical role in the pioneering work, including Manz, Northrup, Quake, Toner, Wilding. and Kricka Other contributors to the wider field of microfluidics, such as Whitesides G.M., Madou M. and Delamarche E., have developed alternative fabrication methods, microfluidic components (valves, pumps, etc.), and surface chemistries, enabling the more recent progress in microfluidics for NA analysis [179]. Many of them have licensed their inventions to start-up and affiliated companies, presented in Table (**1**).

The development of platforms for microfluidic NA analysis has also been carried out by small and large companies, seeking to find a niche in an increasingly crowded microfluidic market. Table (**2**) lists the companies holding patents and patent applications related to

Table 1. Major Academic Researchers Identified Contributing to the Development of Intellectual Property in the Field of Microfluidic Nucleic Acid Analysis

Name	Academic affiliation	Company affiliation
Manz Andreas	Imperial College (UK), Institute for Analytical Sciences (Germany)	Ciba Geigy (now Novartis)
Northrup Allen	University of California (USA)	Cepheid , Microfldiic Systems
Quake Stephen	Stanford University, California Institute of Technology (USA)	Fluidigm
Wilding Peter	University of Pennsylvania (USA)	Aviva Biosciences, Chemcore (now Caliper Technologies)
Kricka Larry	University of Pennsylvania (USA)	Chemcore (now Caliper Technologies)

Table 2. Major Companies Identified Contributing to the Development of Intellectual Property in the Field of Microfluidic Nucleic Acid Analysis and Sorted by Categories*

Microfluidic
Aclara Biosciences
AVIVA Biosciences
Caliper Life Sciences (formely Caliper Technologies)
Cepheid
Fluidigm (formely Mycometrix)
Gyros
Handylab
Microfluidic Systems
Micronics
Nanogen
Nanostream
Norchip
Life Sciences
Becton Dickinson
Biomerieux
Bruker Daltonik
Ciba Geigy (now Novartis)
Evotec
Diversified with Life Sciences
3M Innovative Properties
Agilent technologies
Du Pont
Hitachi
Electronics
Canon
Motorola
Olympus Optical
ST Microelectronics
Tokyo Shibaura Electronic

***Microfluidic**: companies specialized in the development and commercialization of microfluidic products; **Life Sciences**: companies specialized in life sciences such as biotechnology, pharmacology, etc.; **Diversified with Life Sciences**: companies not specialized in Life Sciences but with a significant Life Sciences department; **Electronics**: companies specialized in electronics and microelectronics.

microfluidic NA analysis technologies. The listed companies are classified into four distinct groups according to their field of expertise.

Several companies, well established in their field of competency, such as Canon and ST Microelectronics, have applied their technological strengths to the field of molecular biology. Their interest is driven by the capacity of their technology to provide solutions to unmet application areas. In many cases, their competencies in microfabrication, electronic design, optical system components and packaging are essential in the development of microfluidic integrated platforms. For companies already well established in the life sciences providing instrumentations and laboratory equipments, microfluidic technology offers a particularly enticing opportunity. Mindful of the significant cost in replacing existing equipments and the consumer reluctance to accept new technology, they are able to leverage benefits of miniaturization by integrating microfluidic with their pre-existing technology.

A large contingent of companies currently working toward providing integrated NA analysis systems are smaller companies highly specialized in microfluidic technology, as listed in Table (**3**). Many originate from academia while other from larger companies (e.g. Gyros from Amersham Biosciences). Their competitiveness and success lies in providing the advantage of microfluidics to current laboratory equipment in terms of cost and performance, as well as in bringing portability and user-friendliness for new devices in point-of-care diagnosis or on-field instrumen-tations, where traditional technologies cannot provide viable solutions. As a group, these microfluidic companies, however, represent a small segment of the overall intellectual property market, with less than 1% of the share (Fig. (**8A**)). It should be noted that the numbers in this analysis must be taken qualitatively, as the comparison is based on a keyword search against a worldwide patent and patent application database rather than a company size, sales or market value. Nonetheless, these numbers highlight the major role that the smaller companies play as developers and innovators in the field of microfluidics, holding over 80% of the granted and pending patents worldwide, as shown in Fig. (**8B**).

The microfluidic market remains young and in constant evolution and the introduction of commercial products featuring microfluidic systems are on the rise. Many companies have been created in the late 90s or early 2000s, and have since merged or have established partnerships with larger companies. Increasingly, collaborations between companies with complementary competencies are becoming more common, as exemplified by ST Microelectronics joint development with Mobidiag for microfluidic lab-on-chip for NA-based diagnosis.

Geographically, Japan and Europe are important players in microfluidics; however the great majority of the companies identified in this review, involved in microfluidic NA analysis, are American. Thus, considering the US patent market as indicative of worldwide trends, one can observe a year to year growth of microfluidic granted patents and patent applications disclosed by NA analysis-orientated microfluidic companies (Fig. (**9**)). The growth in the late 1990 to 2003 stems from the rapid introduction of novel technologies and materials, and increased public awareness. In recent years, a stabilization of the number of granted patents is observed, pointing to a maturing microfluidic technology. In view of the number of recent patent applications and the lengthy process of patents prosecution,

Table 3. Description of Major Identified Companies Specialized in Microfluidics and Active in the Field of Nucleic Acid Analysis*

Name	Creation date	HQ Location	Number of patent		Commercialized product
			USG	USA	
Caliper	1995	Hopkinton, MA	222	128	LabChip
Nanogen	1991	San Diego, CA	76	41	NanoChip
Nanostream	1999	Pasadena, CA	36	44	Brio Cartridge
Cepheid	1996	Sunnyvale, CA	27	42	GeneXpert, SmartCycler
Gyros	2000	Uppsala, Sweden	21	21	Gyrolab Bioaffy
Aclara Biosciences	1995	San Francisco, CA	16	58	LabCard
Fluidigm	1999	San Francisco, CA	12	34	Topaz, BioMark
AVIVA Biosciences	1999	San Diego, CA	12	0	SealChip
Micronics	1996	Redmond, WA	9	9	Microflow, Microcytometer
Handylab	1999	Ann Arbour, MI	4	3	Integrated cartridge
Norchip	1998	Klokkarstua, Norway	0	1	NucliSens
Microfluidic Systems	2001	Pleasanton, CA	0	3	Biolyser

*USG: number of US granted patent; USA: number of US patent application since 2002.

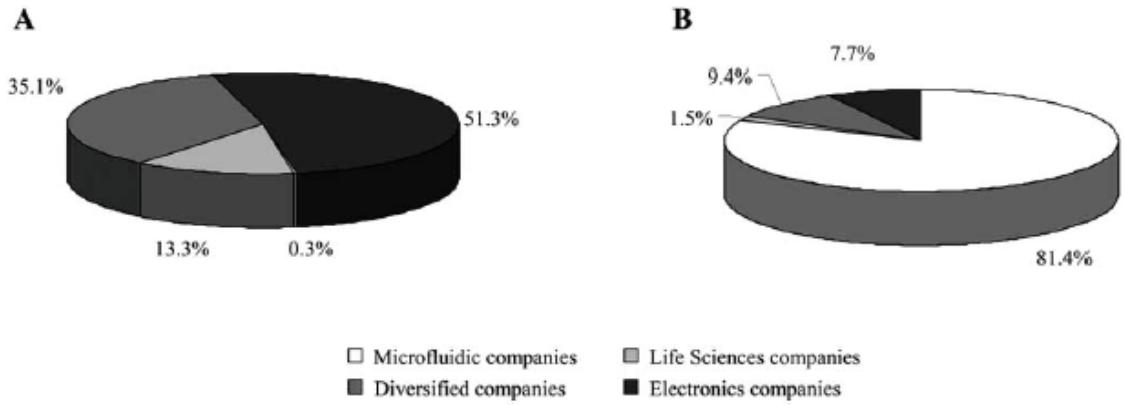

Fig. (8). Pie charts representing the distribution of intellectual property by company category. The search includes worldwide patents and patent applications of the companies listed in table 2 without any time limitation. (**A**) General intellectual property. (**B**) Intellectual property in the field of microfluidics as defined by the presence of the words "microfluidic", "microchannel" or "microfabricated channel" in the title or abstract of the document.

one can expect the current trend to continue in the coming years.

CONCLUSION

In this paper, recently disclosed patents and patent applications of microfluidic devices in key subject areas of NA analysis have been presented. As evident from this review, the major focus has been on the development of individual components for sample preparation, NA amplification, separation, and detection schemes on-chip, and great success has been reached in the miniaturization of each of these areas. However, to take full advantage of miniaturization technology for on-field applications, the ability to achieve full integration among different system components is essential in order to construct self-contained lab-on-a-chip NA analysis system. In this regard, the technical challenges (fabrication materials and micro-to-macro interconnects) along with non-scientific issues related to the introduction of new technology to the market, still need to be overcome. The more recent trends have therefore focused on the use of electromagnetic fields, bead and particles proven to be compatible with individual steps of NA analysis. Additionally, exploration of nanoengineered surfaces promises to solve some of the material-related

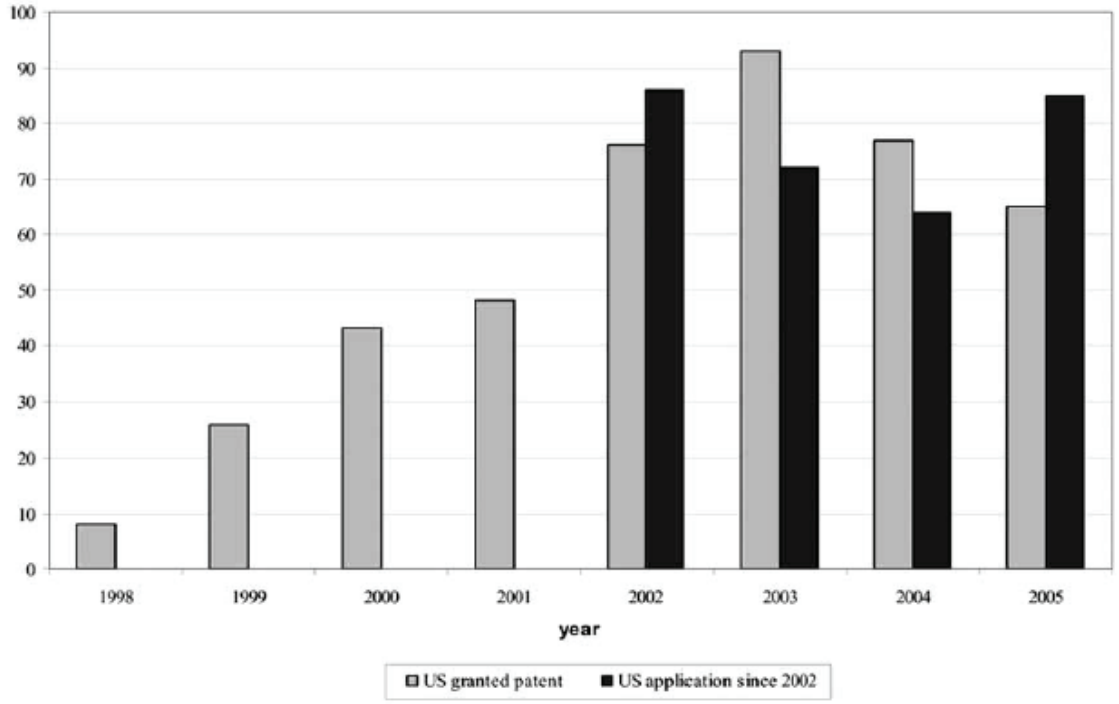

Fig. (9). Annual total number of US patents and patent applications (since 2002) of the companies specialized in microfluidics listed in tables 2 and 3.

challenges. Despite this work, the progress toward integrating many or all functions of an assay on-chip is difficult, since the conditions needed for successful completion of all steps of NA analysis, from cell sorting to detection, are not necessarily compatible. Nonetheless, several companies identified in this review are marketing commercial products which exhibit a certain level of integration. A continued collaboration between researchers with different expertises is needed in this highly multidisciplinary field, to enable rapid technological innovations that will overcome the integration challenges and allow the commercialization of self-contained lab-on-a-chip nucleic acid systems.

REFERENCES

* Patents of Special Interest

[1] Schulte TH, Bardell RL, Weigl BH. Microfluidic technologies in clinical diagnostics. Clin Chim Acta 2002; 321(1-2): 1-10.

[2] Ahn CH, Choi JW, Beaucage G, *et al*. Disposable smart lab on a chip for point-of-care clinical diagnostics. Proceedings of the IEEE 2004; 92(1): 154-73.

[3] Beebe DJ, Mensing GA, Walker GM. Physics and applications of microfluidics in biology. Annu Rev Biomed Eng 2002; 4: 261-286.

[4] Fiorini GS, Chiu DT. Disposable microfluidic devices: fabrication, function, and application. Biotechniques 2005; 38(3): 429-46.

[5] Duffy DC, McDonald JC, Schueller OJA, Whitesides GM. Rapid Prototyping of Microfluidic Systems in Poly(dimethylsiloxane). Anal Chem 1998; 70: 4974-84.

[6] Pallandre A, de Lambert B, Attia R, Jonas AM, Viovy JL. Surface treatment and characterization: Perspectives to electrophoresis and lab-on-chips Electrophoresis. 2006; 27(3): 584-610.

[7] Makamba H, Kim JH, Lim K, Park N, Hahn JH. Surface modification of poly(dimethylsiloxane) microchannels. Electrophoresis 2003; 24(21): 3607-19.

[8] Delamarche E, Donzel C, Kamounah FS, Wolf H, Geissler M, Stutz R. Microcontact Printing Using Poly(dimethylsiloxane) Stamps Hydrophilized by Poly(ethyle oxide) silanes. Langmuir 2003; 19: 8749-58.

[9] Auroux PA, Koc Y, deMello A, Manz A, Day PJ. Miniaturised nucleic acid analysis. Lab Chip 2004; 4(6): 534-46.

[10] Sun Y, Kwok YC. Polymeric microfluidic system for DNA analysis. Analytica Chemica Acta 2006; 556: 80-96.

[11] Mogensen KB, Klank H, Kutter JP. Recent developments in detection for microfluidic systems. Electrophoresis 2004; 25(21-22): 3498-12.

[12] Wada, H., Kopf-Sill, A., Alajoki, M., Parce, J., Wang, B., Chow, A., Brow, R.: WO020070080 (**2002**).

[13] Weigl, B., Bardell, R., Hayenga, J.: WO03078972 (**2003**).

[14] Bardell, R., Weigl, B.H., Battrell, F.C.: US20046674525 (**2004**).

[15] Foster, J.: US20056838056 (**2005**).

[16] Leary, J., Frederickson, C.: WO03060486 (**2003**).

[17] Brody, J.: US5726404 (**1998**).

[18] Quake, S., Fu, A., Arnold, F., Spence, C.F.: WO9961888 (**1999**).

*[19] Spence, C.F., Fu, A.Y., Quake, S.R., Arnold, F.H.: US20036540895 (**2003**).

[20] Liu, A.Q., Liang, X.J., Zhang, X.M., Sun, Y., Droge, P.: WO05108963 (**2005**).

[21] Schnelle, T., Mueller, T.: WO05075958 (**2005**).

[22] Schnelle, T., Pfennig, A., Mueller, T.: WO05075957 (**2005**).

[23] Cosman, M., Kapur, R., Carvalho, B., Barber, T., Balis, U., Toner, M., Huang, L.: WO05084374 (**2005**).

[24] Whitesides, G.: WO02093125 (**2002**).
[25] Ahn, C., Cho, H., Choi, J.W.: WO0187458 (**2001**).
[26] Toner, M., Truskey, G., Kapur, R.: WO04029221 (**2004**).
[27] Sethu, P., Toner, M.: WO04113877 (**2004**).
[28] Yamanishi, D., Hujsak, P., Yang, Z., Xu, J., Wang, X., Wu, L., Huang, M., Tao, G., Cheng, J.: WO03031938 (**2003**).
[29] Wilding, P., Kricka, L.J.: US5726026 (**1998**).
[30] Austin, R.H., Volkmuth, W.D., Rathburn, L.C.: US5427663 (**1995**).
[31] Takayama, S., Huh, D., Grotberg, J.: WO02084276 (**2000**).
[32] Shevkoplyas, S., Munn, L., Bitensky, M., Yoshida, T., Sun, C.: WO06031385 (**2006**).
[33] Betts, W., Hawkes, J.: US5569367 (**1996**).
[34] Ager, C., Dames, A., Purvis, D., Safford, N.: US20016310309 (**2001**).
[35] Soh, H.T., Wang, J., Kim, U., Hu, X., Qian, J., Meinhart, C.: WO06058245 (**2006**).
[36] Cheng, J., Sheldon, E., Wu, L., O'Connell, J.: WO9938612 (**1999**).
[37] Iliescu, C., Xu, G., Tay, F.: WO06004558 (**2006**).
[38] Gruber, L., Bradley, K., Lopes, W., Lancelot, R., Plewa, J., Grier, D.: WO04012133 (**2004**).
[39] Anderson, A., Gruber, L., Mueth, D., Plewa, J., Shireman, J., Rosenbaum, N.: WO05023391 (**2005**).
[40] Kayyem, J.F.: US20056942771 (**2005**).
[41] Parthasarathy, R.V., Ericson, K., Bedingham, W.: WO05068626 (**2005**).
[42] Schonfeld, F., Von Germar, F., Karlsen, F., Lichtenberg, J., Verpoorte, S.: WO05073691 (**2005**).
*[43] Hong, J., Studer, V., Anderson, W., Quake, S., Leadbetter, J.: WO04040001 (**2004**).
[44] Irimia, D., Toner, M.: WO05010147 (**2005**).
[45] Marmottant P, Hilgenfeldt S. Controlled vesicle deformation and lysis by single oscillating bubbles. Nature 2003; 423(6936): 153-56.
[46] Pourahmadi, F., McMillan, W., Ching, J., Chang, R., Christel, L., Kovacs, G., Northrup, M., Petersen, K.: WO9933559 (**1999**).
[47] Taylor, M., Belgrader, P., Pourahmadi, F., McMillan, W., Chang, R., Sakai, S., Ching, J., Petersen, K., Northrup, M.: EP1180135 (**2002**).
[48] Yuan, B., Northrup, A., Pourahmadi, F.: WO06060566 (**2006**).
*[49] Wilding, P., Kricka, L.J., Zemel, J.N.: US5635358 (**1997**).
[50] Wu, B., Handique, K., Parunak, G., Kehrer, A., Ganesan, K.: WO05011867 (**2005**).
[51] Barenburg, B.F., Burdon, J., Chan, Y.T., Dai, X., Gallagher, S., Grodzinski, P., Marrero, R., Nair, V., Rhine, D., Smekal, T.: US20036605454 (**2003**).
[52] Baeumner, A.J., Dhawan, M.D.: US20046815209 (**2004**).
[53] Culbertson, C.T., Jacobson, S.C., McClain, M.A., Ramsey, J.M.: US20046783647 (**2004**).
[54] Lee, H.J., Kim, J.H., Yoo, C.E., Lim, H.K., Hwang, K.Y., Ma, S.M., Min, J.H.: JP2006166916 (**2006**).
[55] Albritton, N., Li, G.-P., Bachman, M., Sims, C., Han, F.: WO03093791 (**2003**).
*[56] Rhine, D.B., Smekal, T.: US20046787339 (**2004**).
[57] Briscoe, C.G., Yu, H., Grodzinski, P., Marrero, R., Burdon, J.W., Huang, R.F.: US20036544734 (**2003**).
[58] Di Carlo D, Ionescu-Zanetti C, Zhang Y, Hung P, Lee LP. On-chip cell lysis by local hydroxide generation. Lab Chip 2005; 5(2): 171-78.
[59] Belgrader, P., Yuan, B., Aflatooni, N.: WO05028635 (**2005**).
[60] Osanai, T., Yamamoto, E., Tomaru, K., Fujimoto, J., Watanabe, K., Matsuki, T., Miyamoto, Y.: US2004248130 (**2004**).
[61] Oikawa, Y.: JP2005261389 (**2005**).
[62] Nakayama, H., Inuzuka, H., Tawara, S.: JP2003202347 (**2003**).
[63] Cardy, D., Allen, G.: US2006160078 (**2006**).
[64] Anderson, R.C., Lipshutz, R.J., Rava, R.P., Fodor, S.P.A.: US20016168948 (**2001**).
[65] Atkin, M.: WO04074169 (**2004**).
[66] Karp, C.D.: US20046811695 (**2004**).
[67] Gjerde, D., Hanna, C.: WO0400708 (**2004**).
[68] Kozwich, D., Gerdes, J.: WO0012675 (**2000**).
[69] Fujimoto, K., Torisawa, N.: US2005161377 (**2005**).
[70] Fujishiro, M., Togashi, A., Tani, Y., Ishii, T.: US5824224 (**1998**).
[71] Yang, M., Chen, X., Zhao, J.: CN1634965 (**2005**).
[72] Kusumoto, M., Nishiya, Y., Kishimoto, M., Umebayashi, N.: WO05008209 (**2005**).
[73] Kreuwel, H., Verwimp, E., Beerling, B., Spee, F.: BV: WO06010584 (**2006**).
[74] Okamoto, H., Canon K.K.: JP200604262 (**2006**).
[75] Nelson, R.J., Hooper, H.H., Hauser, A.K., Singh, S., Williams, S.J., Sassi, A.P.: US20026344326 (**2002**).
[76] Landers, J., Norris, P., Power, M., Ferrance, J., Shrinivasan, S., Wolfe, K., Breadmore, M.: WO03104774 (**2003**).
[77] Tooke, N., Anderson, P., Gyros A.B.: US20056884395 (**2005**).
[78] Pourahmadi, F., McMillan, W.A., Ching, J., Chang, R., Christel, L.A., Kovacs, G.T.A.: US20026440725 (**2002**).
[79] Yuan, B., Aflatooni, N.: WO06029387 (**2006**).
[80] Samper, V., Hongmiao, J., Yu, C., Kiat, H., Lim, T.: WO05066343 (**2005**).
[81] Harrison, D., Oleschuk, R., Shultz-Lockyear, L., Skinner, C., Li, P.: WO0138865 (**2001**).
[82] Anderson, H., Stemme, G., Van Der Wijngaart, W.: AB: WO0185341 (**2001**).
[83] Yamaguchi, Y.: JP2005130726 (**2005**).
[84] Ikeda, N., Kato, S., Hatsuzawa, T.: JP2006078475 (**2006**).
[85] Long, A., Gill, P., Cox, T.: WO04071662 (**2004**).
[86] Kazuhisa, F., Saya, S., Tadashi, M., Haruko, T.: US2005130191 (**2005**).
[87] Reed, M.W., Weigl, B.H., Bardell, R.L.: US2006166223 (**2006**).
[88] Northrup MA, Ching MT, White RM, Watson RT. DNA amplification with a microfabricated reaction chamber. Transducers 1993; 93: 924.
[89] Northrup, M.A., Mariella, J., Carrano, A.V., Balch, J.W. : US5589136 (**1996**).
[90] Northrup, M.A., White, R.M.: US5639423 (**1997**).
[91] Northrup, M.A.: US20036602473 (**2003**).
[92] Wilding, P., Kricka, L.J.: US5587128 (**1996**).
[93] Wilding, P., Kricka, L.J.: US5498392 (**1996**).
[94] Wilding, P., Kricka, L.J.: US20056953676 (**2005**).
[95] Baier, V., Bodner, U., Dillner, U., Koehler, J., Hler, J., Poser, S., Schimkat, D.: US5939312 (**1999**).
[96] Tamiya, E., Yokoyama, K., Murakami, Y., Sakaguchi, T., Morita, S., Nagai, S., Idegami, K.: JP2000236876 (**2000**).
[97] Briscoe, C., Burdon, J., Chan, T., Barenburg, B., Grodzinski, P., Hawkins, G., Huang, R.F., Kahn, P., Marcero, R., McGarry, M., Tuggle, T., Yu, H.: US2004043479 (**2004**).
[98] Tso, J., Swedberg, S.A., Wolber, P.K.: US20036613560 (**2003**).
[99] Goodsaid, F., Unger, M., Huang, J., Quan, E., Grossman, R., Lam, P., Chou, H.P., Kimball, J., Pieprzyk, M., Facer, G.: WO05107938 (**2005**).
[100] Kohler, J., Mokansky, A., Poser, S., Schulz, T.: WO9941015 (**1999**).
[101] Kohler, J., Mokansky, A., Poser, S., Schulz, T.: US20056896855 (**2005**).
[102] Caillat, P., Fouillet, Y., Vauchier, C., Clerc, J.F.: FR2795426 (**2002**).
[103] Weigl, B.H.: WO0189692 (**2001**).
[104] Franzen, J.: US20016180372 (**2001**).
*[105] Enzelberger, M.M., Liu, J., Quake, S.R.: US20056960437 (**2005**).
[106] Gottwald, E., Preckel, T.: WO05094981 (**2005**).
[107] Auroux, P.-A., Manz, A., Day, P. : WO04073863 (**2004**).
[108] Burns, M.A., Mastrangelo, C.H., Sammarco, T.S., Man, F.P., Webster, J.R., Johnson, B.N., Foerster, B., Jones, D., Fields, Y., Kaiser, A.: US6057149 (**2000**).
[109] Benett, W.J., Richards, J.B., Milanovich, F.P.: US20036586233 (**2003**).
[110] Zhang C, Xu J, Ma W, Zheng W. PCR microfluidic devices for DNA amplification. Biotechnol Adv 2006; 24(3): 243-84.
[111] Northrup, M.A., Beeman, B.V., Benett, W.J., Hadley, D.R., Landre, P., Lehew, S., Krulevitch, P.: WO9850147 (**1998**).
[112] Smith, T., Bjornson, T., Ricco, A.: WO0131053 (**2001**).
[113] Li, D., Erickson, D.: WO03006161 (**2003**).
[114] Lee, M.A., Bird, H.: US20016312886 (**2001**).
[115] Northrup, M.A., Mariella, R., Koo, J., Davidson, J.: WO9641864 (**1996**).
[116] Landers, J.P., Huehmer, A., Oda, R.P., Craighead, J.R.: US20016210882 (**2001**).
[117] Landers, J.P.: WO04033099 (**2004**).

[118] Breidford, W., Lancaster, C.A., Hayenga, J., Bardell, R., Tonn, J., Weigl, B.H.: WO04108287 (**2004**).
[119] Guijt, R., Dodge, A.: WO04040645 (**2004**).
[120] Jing C, Shoffner MA, Mitchelson KR, Kricka LJ, Wilding P. Analysis of ligase chain reaction products amplified in a silicon-glass chip using capillary electrophoresis. Journal of Chromatography A 1996; 732(1): 151-58.
[121] Anja G, Lars S, Frank K, Henrik R, Eivind H, Trine Nm, Reidun S. Real-time nucleic acid sequence-based amplification in nanoliter volumes. Anal Chem 2004; 76(1): 9-14.
[122] Burns, M.A., Denuzzio, J., Burke, D., Johnson, B.N.: WO9822625 (**1998**).
[123] Kuno, N., Uchida, N., Harada, Y.: JP07107962 (**1995**).
[124] Mathies, R.A., Blazej, R., Liu, C., Kumaresan, P., Yeung, S.: WO05118867 (**2005**).
*[125] Goel, A.: WO06076022 (**2006**).
[126] Ugaz VM, Elms RD, Lo RC, Shaikh FA, Burns MA. Microfabricated electrophoresis systems for DNA sequencing and genotyping applications: current technology and future directions. Philos Transact A Math Phys Eng Sci 2004; 362(1818): 1105-29.
[127] Pace, S.J.: US4908112 (**1990**).
[128] Manz, A.: US5180480 (**1992**).
[129] Manz, A.: US5296114 (**1994**).
[130] Manz, A., Harrison, D.J., Effenhauser, C.S., Zeptosens AG: US20016280589 (**2001**).
[131] Manz, A., Effenhauser, C.S: US5599432 (**1997**).
[132] Manz, A., Zhang, C.X.: US2003150766 (**2003**).
[133] Burns, M., Brahmasandra, S., Ugaz, V.: US20037005050 (**2003**).
[134] Swierkowski, S.P.: US20036558523 (**2003**).
[135] Soane, D.S., Soane, Z.M., Hooper, H.H., Amigo, M.G.A.: US20006054034 (**2000**).
[136] Lackritz, H.S., Cruzado, I., Tan, H.R.: WO0208744 (**2002**).
*[137] Liu, S.R.: WO0168898 (**2001**).
[138] Liu S, Ren H, Gao Q, Roach DJ, Loder RT, Armstrong TM, *et al* Automated parallel DNA sequencing on multiple channel microchips. Proc Natl Acad Sci USA 2000; 97: 5369-5374.
[139] Davidson, J., Balch, J.: US6153076 (**1999**).
*[140] Simpson, P.C., Mathies, R.A., Woolley, A.T.: US20046749734 (**2004**).
[141] Paegel BM High throughput DNA sequencing with microfabricated 96-lane capillary array electrophoresis bioprocessor. Proc Natl Acad Sci USA 2002; 99: 574-79.
[142] Foley, B., Sawyer, J., Briscoe, C.: US20016592733 (**2001**).
[143] Keyton, R., Baldwin, R., Naber, J., Walsh, K., Edelen, J., Jackson, D., Roussel, T., Crain, M.: WO03066514 (**2003**).
[144] Lee, C.S., Devoe, D.: US2006054504 (**2006**).
[145] Yager, T.D., Waterhouse, P., Izmailov, A.M., Maruzzo, B.C., Stevens, J.K., Larson, M.T.: US20016261430 (**2001**).
[146] Yager, T.D., Waterhouse, P., Izmailov, A.M., Maruzzo, B.C., Stevens, J.K., Larson, M.T.: US20006110339 (**2000**).
*[147] Turner, S.W., Kameoka, J., Park, H.Y., Craighead, H.G.: US2003180711 (**2003**).
[148] Craighead, H.G., Turner, S.W.: US2004209392 (**2004**).
[149] Han, J., Craighead, H.G.: US2004035701 **2004**).
[150] Baba Y., Kataoka, K., Tabuchi, M., Nagasaki, Y., Kuwahara C .: US2006040396 (**2006**).
[151] Huang, L.R., Sturm, J.C., Austin, R.: WO03035228 (**2003**).
[152] Jacobson, S.C., Ramsey, J.M., Culbertson, C.T., Whitten, W.B., Foote, R.S.: US20046685809 (**2004**).
[153] Huang, L., Sturm, J.C.: WO04037374 (**2004**).
[154] Battrell, C.F., Shen, M., Weigl, B.H., Houkal, J.M., Lancaster, C.A., Breidford, W.: US20040013732 (**2004**).
[155] Mathies, R.A., Simpson, P.C., Wiliams, S.J.: US6261431 (**2001**).
[156] Mathies, R.A., Lagally, E.T.: US2005019902 (**2005**).
[157] Mathies, R.A., Scherer, J.R., Wexler, D.: US6100535 (**1999**).
[158] Mathies, R.A., Emrich, C., Singhal, P., Ertl, P.: WO2005103672 (**2005**).
[159] Mathies, R.A., Grover, W.H., Paegel, B., Skelley, A., Liu, C.N., Lagally, E., Blazej, R.: US2006073484 (**2006**).
[160] Mathies, R.A., Grover, W.H., Paegel, B.M., Skelley, A., Lagally, E.T., Liu, C.N., Blazej, R.: US2006287572 (**2006**).
[161] Mathies, R.A., Grover, W.H., Paegel, B., Skelley, A., Lagally, E., Liu, C.N., Blazej, R.: US2004209354 (**2004**).
[162] Knapp, M., Parce, J.W., Bousse, L.J., Kopf-Sill, A.R.: EP0972082 (**2000**).
[163] Knapp, M., Parce, J.W., Bousse, L.J., Kopf-Sill, A.R.: US2003104466 (**2003**).
[164] Ausserer, W., Bousse, L.J., Dubrow, R., Sundberg, S., Chow, A., Wang, B.: WO0210732 (**2002**).
[165] Parce, J.W., Kopf-Sill, A.R., Bousse, L.J.: US2003003026 (**2003**).
*[166] Chang, R., Christel, L., Kovacs, G., McMillan, W., Northrup, M.A., Petersen, K., Pourahmadi, F., Young, S., Yuan, R., Dority, D.B.: US20036565815 (**2003**).
[167] Oh, K.W., Kim, J.-T., Namkoong, K., Park, C.S., Cho, Y.K.: US2005164281 (**2005**).
[168] Benett, W.J., Richards, J.B., Stratton, P.L., Hadley, D.R., Milanovich, F.P., Belgrader, P., Meyer, P.L.: US20046699713 (**2004**).
[169] Lipshutz, R.J., Rava, R.P., Anderson, R.C., Fodor, S.P.A.: US5856174 (**1999**).
[170] Makino, T. Co Ltd: JP2001149097 (**2001**).
[171] Quake, S.R., Chou, H.P.: US20046767706 (**2004**).
[172] Blackburn, G.: US20056875619 (**2005**).
[173] Miles, R.R., Belgrader, P., Fuller, C.K.: US2006136466 (**2006**).
[174] Ouchi, S., Okada, J., Hongo, S.: JP2004061427 (**2004**).
[175] Madou M, Zoval J, Jia G, Kido H, Kim J, Kim N. Lab on a CD. Annu Rev Biomed Eng 2006; 8: 601-28.
[176] Pamme N. Magnetism and microfluidics. Lab Chip 2006; 6(1): 24-38.
[177] Lin YW, Huang MF, Chang HT. Nanomaterials and chip-based nanostructures for capillary electrophoretic separations of DNA. Electrophoresis 2005; 26(2): 320-30.
[178] Mohamadi MR, Mahmoudian L, Kaji N, Tokeshi M, Chuman H, Baba Y. Nanotechnology for genomics & proteomics. Nanotoday 2006, 1(1): 38-45.
[179] Kamholz AE. Proliferation of microfluidics in literature and intellectual property. Lab Chip 2004; 4(2): 16N-20N.

Appendix B
Curriculum Vitae

- Languages and skills -

- **Languages** – French, English (fluent), German (intermediate)
- **Adaptability** – worked in several highly multidisciplinary and international environments
- **Communication skills** – published 4 technical papers in peer-reviewed journals; gave oral and poster presentations at 3 international conferences
- **Collaborative skills** – Acted for 4 years as a link between an academic and a governmental institution
- **Leadership and management skills** – Involved in several student associations and a research center

- Education -

2004-08 **Doctor of Philosophy in Biomedical Engineering**
McGill University, Montreal, QC, Canada (Collaboration with National Research Council – IMI)
- Development of a microfluidic immunoassay (ELISA) for the rapid quantification of low picomolar concentrations of protein biomarkers
- Photolithography techniques, rapid prototyping in PDMS, fabrication of microfluidic valves in PDMS
- Fluorescence microscopy, contact angle measurement, Fourier Transform IR Spectroscopy, Atomic Force Microscopy

2000-03 **Master of Engineering in Biotechnology**
Ecole Supérieure de Biotechnologie de Strasbourg (ESBS), Strasbourg, France
- Main focus on molecular and cellular biology, immunology, virology, microbiology with applications to biotechnology and pharmacology
- Advances courses in bioinformatics, biophysics and organic chemistry
- Introductory classes to management, economics, intellectual property
- European school with exchange programs in Basel (6 weeks), Freiburg (6 weeks) and Karlsruhe (2 weeks)

1998-2000 **DEUG in Biology – 2 year university degree (honor student)**
Université Louis Pasteur, Strasbourg, France
- Undergrad courses in diverse domains of biology

- Work Experience -

2003 **Research Biologist – Master's thesis project (8 months)**
Liver Research Centre, LRC, Brown University, Providence, RI, USA
- Study of the variation in expression of Frizzled genes during hepatocarcinogenesis and the role of β-catenin in the Frizzled signalling pathway
- Real-Time PCR, Cloning, protein purification, Western blot
- Cell culture, cell transfection by electroporation and lentiviral infection, motility assay (ALMI)

2001-02 **Research Assistant in Biology – Intern (4 months)**
- Transfection of F9 cells and selection of stable clones. FRET analysis of HP1s/TIF1α interactions in-vivo
  Institute of Genetic and Molecular and Cellular Biology IGBMC, Strasbourg, France
- Structural mutagenesis of a poly-(ADP ribosyl)-polymerase (PARP)
  National Center for Scientific Research CNRS, department of "Cancerogenesis and Molecular and Structural Mutagenesis", Strasbourg, France
- Generation of a tagged-WASp expression vector for efficient Western-blot analysis
  Department of Immunology, San Diego State University, San-Diego, CA, USA

- Extracurricular Activities -

2005-07	**Student representative at the Center for Biorecognition and Biosensors**: Led the organization of bi-annual thematic workshops for students, a 3-day workshop on microfluidics for faculties, participated in the annual General Assembly.
2005-07	**Member of the McGill biomedical engineering students' society**: Organized recreational and fundraising activities.
2000-01	**Member of the ESBS student association**: Coordinated a 1-week ski trip and other student activities.
1989-97	**Member of the French Scouts** including 3 years as a group leader

- Miscellaneous -

- **Informatics** – MS Office, AutoCAD, Adobe Photoshop and Illustrator
- **Travels** – San Diego, CA (2 months), Providence, RI (8 months), Montreal, Canada (4 years), Germany/Switzerland (4 months), Morocco (3 years), Israel (3 months)
- **Sports** – tennis, handball, martial arts, roller-skating, alpine skiing
- **Certificates** – first aid, driving license

- Publications and Conferences -

- **Herrmann M**, Veres T and Tabrizian M. "Rapid quantification of picomolar concentrations of TNF-alpha in serum using the Dual Network microfluidic ELISA platform". *Anal. Chem. In press.*
- **Herrmann M**, Roy E, Veres T and Tabrizian M. "Microfluidic ELISA on non-passivated PDMS chip using magnetic bead transfer inside dual networks of channels". *Lab Chip* 2007; 7(11):1546-1552.
- Malic L*, **Herrmann M***, Hoa XD* and Tabrizian M. "Current state of intellectual property in microfluidic nucleic acid analysis". *Recent Patents on Engineering* 2007; 1:71-88. (*equal contribution)
- **Herrmann M**, Veres T and Tabrizian M. "Enzymatically-generated fluorescent detection in micro-channels with internal magnetic mixing for the development of parallel microfluidic ELISA". *Lab Chip* 2006; 6(4):555-560.
- Merle P, Kim M, **Herrmann M**, Gupte A, Lefrancois L, Califano S *et al.* "Oncogenic role of the frizzled-7/beta-catenin pathway in hepatocellular carcinoma". *J Hepatol* 2005; 43(5):854-862.
- Merle P, de la Monte S, Kim M, **Herrmann M**, Tanaka S, Von Dem BA *et al.* "Functional consequences of frizzled-7 receptor overexpression in human hepatocellular carcinoma". *Gastroenterology* 2004; 127(4):1110-1122.
- **MicroTAS 2007**, Paris, France. Poster "Microfluidic ELISA using magnetic beads and pressure valves to reduce ASSAY noise"
- **NanoBio Europe 2006**, Grenoble, France. Oral presentation "Utilization of magnetic micro-beads in a stop-flow microfluidic ELISA"
- **NSTI 2006**, Boston, MA. Poster "Surface modification and characterization of a cyclic olefin copolymer for magnetic bead-based stop-flow microfluidic ELISA"
- **AASLD 2003**, Boston, MA. Presidential poster of distinction